UNIVERSITY OF
LIVERPOOL

Early Colon Cancer Model:

Analysis of Cited1 *in vivo* and *in vitro*

Thesis submitted in accordance with the requirements of the University of Liverpool for the degree of Doctor in Philosophy by

Fei Song

August 2009

Declaration

This thesis is the result of my own work, unless otherwise stated, and is based upon results from experiments performed as a Ph D. student between December 2005 and October 2008 in the University of Liverpool, with occasional collaborative experiments in the University of Cardiff.

Neither this thesis nor any part of it has been submitted in support of an application of another degree or qualification in another University or institute of learning.

Fei Song

August 2009

Acknowledgements

This work was funded by North West Cancer Research Fund (NWCRF). I have appreciated the help from my supervisors, Prof. Alastair Watson, Dr. John Jenkins, Prof. Alan Clarke (University of Cardiff); and the very kind and supportive teaching from Dr. Andrea Davies during the early time of this project.

I would thank the Clarke group from University of Cardiff for their supervision and help throughout this project: Dr. Toby Phesse, Dr. Valerine Meniel, Dr. Karen Reed, Mark Bishop (genotyping) and Derek Scarborough (histology).

I would also thank Dr. Helen Kalirai for the patient samples from Cancer Tissue Bank Research Centre, Liverpool; Dr. Andrea Jorgensen for the patient sample size calculation from Centre for Medical Statistics and Health Evaluation, Liverpool; Dr. Carrie Duckworth (Gastroenterology Research Unit, Liverpool) for showing me the mitotic and apoptotic scoring technique using WinCrypt package. Thanks to my advisory panel Prof Mark Pritchard and Dr Lugang Yu for their timely advice and technical discussion. Thanks to Dr Shioda (Massachusetts General Hospital Cancer Center, Charlestown, Massachusetts, USA) for providing the Cited1 antibody.

Last but not least, I would thank Dr. Owen Sansom (Beatson Institute for Cancer Research, Glasgow) for the nice preliminary work on *Apc* knock-out model and Wnt targets identification during the early time of this project.

Dedication

致谢

我的博士论文即将接近尾声，在此，非常感谢远在北京的爸爸妈妈对于我选择在英国学习深造的一贯鼓励和支持，包括慷慨的经济支持以及不断的精神鼓励。劳累的时候，拨通越洋电话，总是有智慧的和安慰的话语。我想，虽然你们可能看不太懂用英文写的论文，但是看到这样厚厚的四年的工作成果 ，也会很为我高兴和自豪的。你们经常说，一个阶段的结束就是下一阶段的开始。革命尚未成功，同志还需努力。

Abbreviations

α - alpha (Greek alphabet)

A- adenosine

ACF - aberrant crypt foci

ANOVA – analysis of variance

AOM - azoxymethane

APC/Apc (human/murine) - adenomatosis polyposis coli

β - beta (Greek alphabet)

BrdU - bromodeoxyuridine

BSA -bovine serum albumin

C - cytosine

CD44 – Clusters of differentiation molecule 44 (Indian blood group)

cDNA - complementary DNA

CIN - chromosome instability

CITED/Cited1 (human/murine) - CBP/p300-interacting transactivators with glutamic acid [E]/aspartic acid [D]-rich carboxyl-terminal domain 1

CRC - colorectal cancer

Ct - threshold cycle

DAB - 3, 3'-diaminobenzidine

DEPC - diethypyrocarbonate

DMH - dimethylhydrazine

DNA - deoxyribonucleic acid

DNase - deoxyribonuclease

dNTP - deoxynucleotide-5'-triphosphase

DPX - distrene plasticiser and xylene

Dsh – dishevelled, dsh homolog family of proteins

EDTA - Ethylene diamine tetraacetic acid)

EGR2 - early growth response 2

ErbB2- v-erb-b2 erythroblastic leukemia viral oncogene homolog 2, neuro/glioblastoma derived oncogene homolog (avian)

FAP - familial adenomatous polyposis

FCS - foetal calf serum

FWD - forward primer

Fzd – frizzled homolog family of proteins

G - guanine

Gsk3β - glycogen synthase kinase 3 beta

HBSS -Hank's buffered salt solution

HNPCC - hereditary nonpolyposis colorectal cancer

HRP - horseradish peroxidase

IDLs - insertion-deletion loops

JNK - Jun N-terminal kinase

LEF/Lef1 - lymphoid enhancer binding factor 1

LOH - loss of heterozygosity

Lrp5/6 – low density lipoprotein receptor-related protein 5/6

MCR - mutation cluster region

Mad - MAX dimerization protein 1

MAPKs - mitogen activated protein kinases

Max - MYC associated factor X

MGMT - DNA methyltranferase

Min - multiple intestinal neoplasia

Miz1 - Myc-interacting Zinc finger protein-1

MMR - mismatch repair

MSI - microsatellite instability

MTH1 - mutT human homolog 1

Myc - v-myc myelocytomatosis viral oncogene homolog (avian)

OGG1 - 8-oxoguanine DNA glycosylase

PAGE - polyacrylamide gel electrophoresis

PBS - phosphate buffered saline

PCR - polymerase chain reaction

PI3K - phosphoinositide 3' kinase

REV- reverse primer

RIPA - radioimmunoprecipitation assay

Rn - normalized reporter signal

RNA - ribonucleic acid

RNAi - RNA interference

RNase - ribonuclease

SDS - sodium dodecyl sulfate

siRNA - small interference RNA

Smad - the combination of mothers against decapentaplegic (MAD) in *Drosophila* and SMA protein in *Caenorhabditis elegans*

SRB - sulforhodamine B

T - thymine

TBS - Tris-buffered saline

TCF/Tcf - Tcf family of transcription factors

TEMED - tetramethylethylenediamine

TGF-β - transforming growth factor β type I

Tm - melting temperature

TNM - Tumour, Node, Metastasis system

Tris - tris(hydroxymethyl)methylamine

TSG - tumour suppressor gene

UICC - International Union Against Cancer

VEGF - vascular endothelial growth factor

Wnt – wingless related family of proteins

WT - wild type

Abstract

Background: Inactivation of *APC* gene is recognised as one of the first important genetic changes in the pathogenesis of colorectal cancer. Inactivation of APC stabilises β-catenin, which translocates into the nucleus, activating TCF/LEF1 with subsequent transactivation of many target genes through the Wnt signalling pathway. A Cre-*lox*P mouse model has been previously developed, wherein an inducible loss of Apc within the intestinal epithelium causes immediate activation of the Wnt signalling pathway, failure in cell migration and differentiation, perturbation of the normal crypt/villus homeostasis, induction of cell death and proliferation (Sansom et al., 2007). Loss of c-Myc, following losing Apc, completely rescues the phenotypes of altered differentiation, migration, proliferation and apoptosis (Sansom et al., 2007). Microarray analysis of the two unique mouse models have identified a cohort of c-Myc-dependent Wnt regulated gene alterations for which there has been little previous association with neoplasia.

Objectives: We aimed to validate the Cre-*lox*P-*Apc* mouse model in human using colorectal cancer tissues. We were also interested in underlying mechanisms of the identified gene *CITED/Cited1* that may give us an insight into colorectal carcinogenesis.

Results: Homologous human candidate genes were detected by Taqman real-time PCR analysis using colorectal cancer tissues with matched neighbouring normal mucosa. Eight (out of twelve) homologous human genes were significantly up-regulated, which demonstrated how transferable the candidate genes identified in the mouse model are to the study of human colorectal cancer. One of the Myc-dependent Wnt targets *CITED1* is up-regulated (2.74-fold, n=40, $p<0.001$) in human colorectal cancer. The effects of *CITED/Cited1* deficiency on colorectal carcinogenesis were investigated both *in vitro* and *in vivo*. In HT29 and HCT116 human colorectal cancer cell lines, reduction in expression of *CITED1* (siRNA treatment) significantly increases cell death and reduces cell proliferation. Losing *Cited1* leads to a significantly increased life span of Min mice with reduced number of adenomas in small intestine and large intestine. Loss of *Cited1* does not alter β-catenin translocation in Min adenomas. When using Cre-*lox*P-*Apc* early colorectal cancer mouse model, comparing *Apc/Cited1* double null mice to *Apc* null mice, crypt-villus architecture was more severely altered with an elongated crypt-like zone in the small intestine, as well as increased proliferation and elevated apoptosis. In *Apc/Cited1* double null mice, β-catenin also translocates into nucleus as observed in the *Apc* null mice.

Conclusions: Detected up-regulation of known Wnt targets again validates the process in human colorectal cancer. *CITED/Cited1* a previously unrecognised component of colorectal carcinogenesis was identified as a novel Wnt target in human colorectal cancer in the *in vitro* and *in vivo* studies. Data of immuno-histochemistry assay suggests that losing Cited1 is not sufficient to inhibit Wnt signalling activity at the point of nuclear β-catenin translocation. However, the more defined underlying molecular mechanisms of *CITED1* involved with colorectal carcinogenesis need further investigation.

Chapter 1 Introduction

1.1 Epidemiological Studies of Colorectal Cancer

Colorectal cancer (CRC) is widespread in western countries and has a high rate of mortality and morbidity (Huls et al., 2003; Parkin et al., 1999). Colorectal cancer is the fourth most frequent malignant neoplasm throughout the world (Watson, 2006; Weitz et al., 2005). Every year, about 1 million people develop colorectal cancer and half of the CRC patients have advanced disease at initial presentation (Weitz et al., 2005). In the UK, there were 16,007 deaths from colorectal cancer in 2007 (Cancer Stats CRUK 2007, accessed in August 2007, http://info.cancerresearchuk.org/cancerstats/types/bowel/mortality/). The percentage of colorectal cancer patient 5-year survivals reaches only 50%, which also depends on the grade - Dukes A, 100% survival following surgery (Soreide et al., 2006; Watson, 2006).

The risk of developing CRC is influenced by both genetic and environmental factors (Strate and Syngal, 2005). The lifetime colorectal cancer risk in general population is 5%, this figure will also increase dramatically along with age (Fodde, 2002). Although not directly inherited, first-degree relatives of patients who have a single colorectal carcinoma have a threefold greater risk of developing colorectal carcinoma than the average population (Weitz et al., 2005). The risk of colorectal cancer also seems to be linked to diet: a diet high in fat and red meat, low in dietary fibre increase the risk significantly (Weitz et al., 2005). In 2002, the incidence of

colorectal cancer was 34,889 with an age-standardised rate of 54.4 in men and 35.3 in women, which shows that gender is a risk factor (Weitz et al., 2005).

Colorectal cancer is a multi-step disease, which develops through a number of well characterised stages based on the degree of invasion (Watson, 2006). The histological changes help to define the parameters for treatment of the different stages. Staging assesses the grade of the disease, which embraces factors, including the size of the growth, degree of invasion, local and distant spread and the histological differentiation of the cells (Greene, 2006). The Modified Duke's Staging is typically used, but more recently, the International Union Against Cancer (UICC) or the Tumour, Node, Metastasis (TNM) systems have replaced it (Dukes and Bussey, 1958; Greene, 2006) (Figure 1.1; Table 1.1).

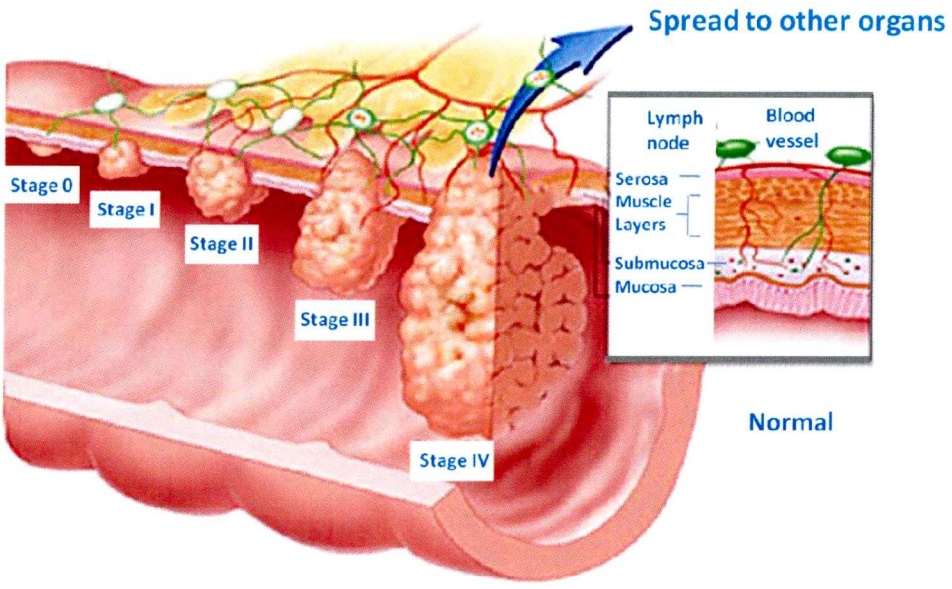

Figure 1.1 Diagram of staging of colorectal cancer. Adapted from http://visuals.nci.nih.gov/preview.cfm?imageid=7181&fileformat=jpg accessed in August 2009

Table 1.1 Staging of Colorectal Cancer (modified from the information on www.cancer.org, accessed in August 2009)

UICC/TNM		*Modified Dukes'*
Stage 0	Carcinoma in situ	
Stage I	Tumour invades submucosa (T1) Tumour invades muscularis propria (T2) No nodal involvement, no distant metastasis	A
Stage II	Tumour invades beyond muscularis propria (T3) Tumour invades into other organs (T4) No nodal involvement, no distant metastasis	B
Stage III	1-3 Regional lymph nodes involved – any T (N1) 4 or more regional lymph nodes involved (N2) No distant metastasis any T	C
Stage IV	Distant Metastasis (M1) Any T, any N stage	D

1.2 Molecular Pathogenesis of Colorectal Cancer

It is well known that colorectal cancer, like neoplasms of other organs or systems, is the result of the accumulation of genetic and epigenetic alterations underlying the progress of carcinogenesis (Bodmer, 2006; Grady and Markowitz, 2002) (Figure 1.2). The loss of genomic stability is a key event in this process and serves to create an environment for the occurrence of alterations in tumour suppressor genes, oncogenes and DNA repair genes (Grady and Markowitz, 2002). Although most cancer-causing mutations are somatic (Bodmer, 2006), there are a number of cancers that have a hereditary component (mutations affecting germline), which are heritable which contributes to the initiation of carcinogenesis (Benito and Diaz-Rubio, 2006).

Colorectal cancer arises as the cumulative effect of multiple mutations within the cells, allowing it to escape from growth and regulatory control mechanisms (Grady and Markowitz, 2002). The majority of colorectal cancers have chromosomal instability (CIN), referring to an increased rate of losing and gaining whole or part of chromosomes during cell division (Michor, 2005; Takayama et al., 2006). It is a step-wise progression of mutations that facilitates the histological alterations from normal mucosa to adenoma to carcinoma (Fearnhead et al., 2002). This adenoma to carcinoma sequence, associated with an increasing level of nuclear β-catenin and a gradual series of histological transitions that was addressed firstly by Fearon and Vogelstein in 1990, involving the accumulation of mutation in a number of genes and consequent progression (Fearon and Vogelstein, 1990; Giles et al., 2003; Pinto

and Clevers, 2005b). Tumour suppressor genes (TSGs) *APC* (chromosome, 5q), *Smad4* (18q) and *p53* (17q) and oncogene *K-ras* (12q) are the main targets of these genetic alterations (Fodde, 2002).

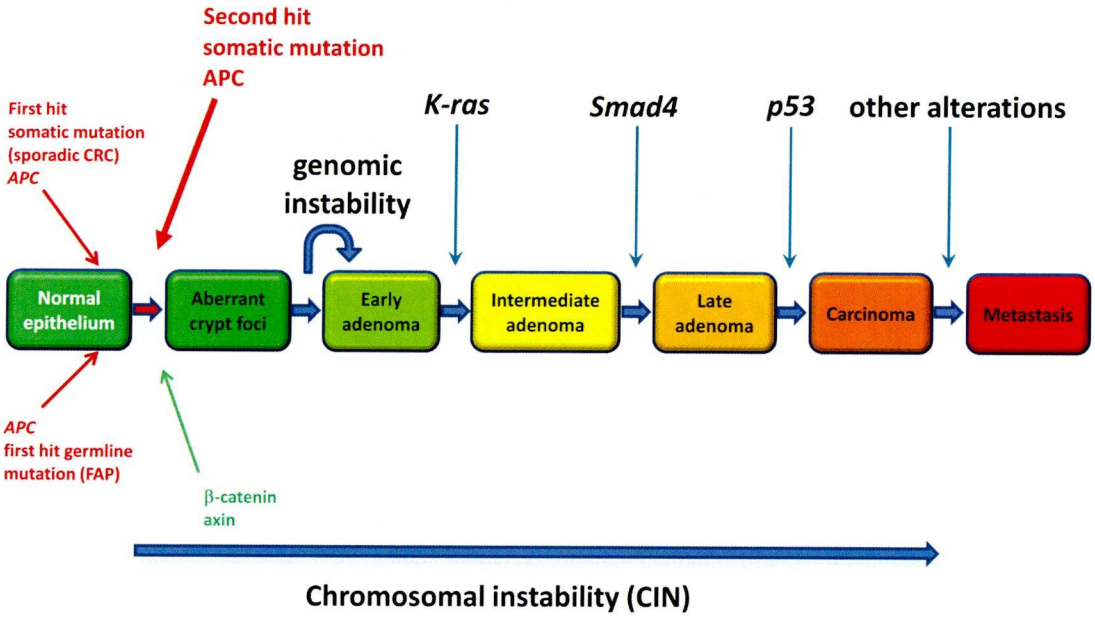

Figure 1.2 Multiple genetic alterations in the adenoma to carcinoma sequence for colorectal cancer. (Adapted from Pinto and Clevers, 2005)

CIN pathway is characterised by the initial allelic losses on these chromosomes leading to increased genetic instability to drive tumour progression (Nowak et al., 2002). CIN pathway is the model typically represented in familial adenomatous polyposis (FAP), which happens as two hits in the *APC* gene, followed by the mutation of *K-Ras*, subsequently mutations of *p53* and subsequently the deletion on chromosome 18q (Takayama et al., 2006).

1.3 Hereditary Colorectal Cancer

In human colorectal cancer, the hereditary syndromes include familial adenomatous polyposis (FAP) and hereditary nonpolyposis colorectal cancer (HNPCC) (Gryfe et al., 1997; Sancho et al., 2004). Both of the hereditary colorectal cancer syndromes are autosomal dominantly inherited diseases with respectively almost 100% and 80% lifetime risk of developing colorectal cancer, respectively (Fearnhead et al., 2002; Hisamuddin and Yang, 2004; Lynch and de la Chapelle, 2003; Sancho et al., 2004). The presence of hundreds to thousands of adenomatous colorectal polyps makes FAP remarkably different to HNPCC, however both conditions result in a high family risk (Lynch and de la Chapelle, 2003). Recent studies demonstrated that approximately 5% of the incidence of colorectal cancer could be attributed to recognizable heritable germline mutations (Cruz-Correa and Giardiello, 2002; Jeter et al., 2006).

1.3.1 Familial Adenomatous Polyposis (FAP) and FAP-like Syndromes

1.3.1.1 FAP Syndrome

FAP is rare, occurring at the frequency of 1 in 8000 within the population (Bodmer, 2006; Powell et al., 1993), and accounts for less than 1% of all colorectal cancer cases seen in practice (Burt et al., 1990). However, it is a distinctively classical and dominantly inherited syndrome, both clinically and genetically (Bodmer, 2006; Lipton and Tomlinson, 2006). FAP affects both sexes equally and in the majority of cases, it is inherited with a very high penetrance (Varesco, 2004). FAP was first described as a disease with clear familial inheritance in 1925 (Fearnhead et al., 2001;

Lockhart-Mummery, 1952). However, cases with no family history are recorded in nearly 30% of FAP patients, which suggests the presence of a *de novo* genetic event (Varesco, 2004). The *APC* gene responsible for FAP is involved in somatic as well as germline mutations in cancers predicted by Knudson, who also hypothesised the 'two-hit' theory in human cancers (Knudson, 1971). Although *APC* gene mutation was found in a large number of sporadic cases (Gregorieff and Clevers, 2005; Groden et al., 1991; Nagase and Nakamura, 1993), germline mutations of the *APC* gene are pre-dominantly responsible for FAP, in which CRC tumours typically display with the progressive development of numerous adenomatous colorectal polyps at very early stage (Gryfe et al., 1997; Sancho et al., 2004; Su et al., 1992).

1.3.1.2 FAP-like Syndromes

In 2003, it was first reported that 'APC-negative' FAP patients may carry biallelic germline mutations in the human MutY homologue (*MYH*) gene (Lipton and Tomlinson, 2004; Sieber et al., 2003; Strate and Syngal, 2005; Varesco, 2004), which encodes DNA glycosylase MYH, acting together with MTH1 and OGG1 as part of the base excision repair machinery to repair oxidative DNA damage, which is also frequently deleted in several human cancers (Knudsen et al., 2003; Yamaguchi et al., 2002). Inactivation of both copies of *MYH* gene readily mispairs with adenine (A) leading to G:C to T:A transversion mutations in the daughter strand (Al-Tassan et al., 2002; Lipton and Tomlinson, 2006; Strate and Syngal, 2005). Recent reviewed studies indicated that, beside *APC* mutations, mutations in *MYH* gene may be found

in a subset of individuals with FAP at the percentage of about 7.5-20%, which are frequently associated with a milder attenuated familial adenomatous polyposis (AFAP) phenotype (Galiatsatos and Foulkes, 2006; Jeter et al., 2006; Lipton and Tomlinson, 2006), in whom no germline *APC* mutation is detectable and showing a family history compatible with recessive inheritance, carrying biallelic *MYH* mutations (Galiatsatos and Foulkes, 2006; Varesco, 2004). AFAP is a phenotypic variant of FAP characteristically displaying 100 or fewer colorectal adenomas and delay in onset of adenomatosis and colorectal cancer (Galiatsatos and Foulkes, 2006; Knudsen et al., 2003). In addition, another two variants of FAP syndromes, Gardner syndrome, which is characterised by the association of colorectal polyps with osteomas as well as soft tissues tumours (desmoids and thyroid tumours) and Turcot syndrome, which is characterised by the association of colorectal polyps with the development of primary central nervous system (CNS) malignancies also exist (Gardner, 1962; Strate and Syngal, 2005; Turcot et al., 1959; Varesco, 2004). However, characteristic mutations of HNPCC in the mismatch repair (MMR) protein hMLH1 and hMSH2 are also found in a subset of patients with Turcot syndrome (Hamilton et al., 1995).

1.3.2 Hereditary Nonpolyposis Colorectal Cancer (HNPCC) Syndromes

Hereditary Nonpolyposis Colorectal Cancer (HNPCC) syndrome, also referred to as Lynch Syndrome, develops adenomas at a normal rate but progress more rapidly through the stages of carcinogenesis (Ahlquist, 1995; Hisamuddin and Yang, 2004). HNPCC is caused by the germline mutations of mismatch repair (MMR) gene with the hallmark of microsatellite instability (MSI) in tumours (Lynch and de la Chapelle, 1999; Thibodeau et al., 1993). MSI also displays in approximately 15% of sporadic CRC patients (Sancho et al., 2004; Soreide et al., 2006).

1.3.2.1 Mismatch repair (MMR) system

Microsatellites commonly present as short, tandemly repeated, nucleotide sequences in great number throughout genome (Sancho et al., 2004; Soreide et al., 2006). Microsatellite instability (MSI) showing the length variation of microsatellites with gained or lost repeated units on the germline allele is commonly associated with DNA mismatch repair (MMR) deficiency (Peltomaki, 2001a; Soreide et al., 2006). The mismatch repair (MMR) system is highly conserved across different species, from bacteria, yeast to human (Marti et al., 2002; Peltomaki, 2001b; Prolla et al., 1996) (Table 2). In humans, as a group of TSGs (tumour suppressor genes), at least six different MMR genes encode MMR proteins (hMSH2, hMLH1, hMSH3, hMSH6, hPMS1 and hPMS2) required for the complete MMR mechanism, which is responsible for the recognition and repair of base-base mispairs and single strand insertion-deletion loops (IDLs), arising in the genome during DNA replication

(Narayan and Roy, 2003; Peltomaki, 2001a; Prolla et al., 1996) (Table 1.2). MMR system initiates by heterodimer hMSH2-hMSH6 (hMutSα) and heterodimer hMSH2-hMSH3 (hMutSβ) binding to the mutated sites, which are required for the correction of base-base mispairs and IDLs, respectively (Marti et al., 2002; Palombo et al., 1996). Subsequently, heterodimer hMLH1-hPMS2 (MutLα) is recruited by hMutSα and hMutSβ to the mismatch recognition complex, which along with other proteins which are involved in incision, excision, resynthesis and ligation of DNA (Helleman et al., 2006; Jacob and Praz, 2002; Narayan and Roy, 2003) (Figure 1.3).

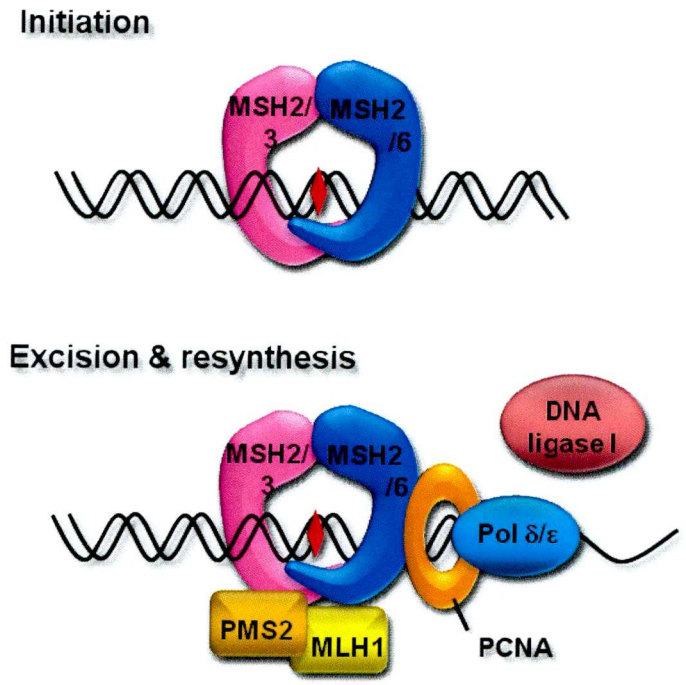

Figure 1.3 Diagram of MMR system. Modified from Helleman et al., 2006. See text for details.

E. coli	*S. cerevisiae*	*H. sapiens*	Function
MutS	*Msh2*	*MSH2* *	Recognizes the mismatch
	Msh6	*MSH6* *	Forms a complex with *Msh2* (*MSH2*)
	Msh3	*MSH3*	Forms a complex with *Msh2* (*MSH2*)
	Msh1	Not identified	Functions in mitochondrial MMR
	Msh4	*MSH4*	Required for meiotic recombination
	Msh5	*MSH5*	Required for meiotic recombination
MutL	*Mlh1*	*MLH1* *	Couples mismatch recognition and subsequent repair
	Pms1	*PMS2* *	Forms a complex with *Mlh1* (*MLH1*)
	Mlh2	*PMS1* *	Forms a complex with *Mlh1* (*MLH1*)
	Mlh3	*MLH3*	Forms a complex with *Mlh1* (*MLH1*)

* Mutated in the germline in HNPCC families.

Table 1.2 DNA mismatch repair gene homolog in bacteria, yeast and humans.
(Adapted from Peltomaki, 2001)

1.3.2.2 Microsatellite Instability (MSI)

Defects in the mismatch repair mechanisms resulting from MMR gene germline mutations lead to MSI, serving as the 'mutator phenotype' marker of HNPCC (Peltomaki, 1997; Soreide et al., 2006). In humans, germline mutations in any of the five MMR genes (*hMSH2*, *hMLH1*, *hMSH6*, *hPMS2* and *hPMS1*), can cause HNPCC (Buermeyer et al., 1999; Lynch and de la Chapelle, 2003; Peltomaki, 2001b) (Table 1.3). Notably, alterations of *hMSH2* and *hMLH1* genes have been suggested to cause early onset of colorectal cancer patients (Montera et al., 2000). Mutations of these two genes also account for approximately 85%-90% of all MMR germline mutations (Hisamuddin and Yang, 2004; Soreide et al., 2006). Furthermore, mutation rates in cell lines from tumour cells of HNPCC are 100-1000 fold as compared with normal cells (Eshleman and Markowitz, 1995; Narayan and Roy, 2003; Peltomaki, 2001b). The important consequence of mutations in MMR genes is that the lack of MMR proteins leads to failure of correction of nucleotide

mismatches and promotes mutations in other genes as the downstream target of MSI (Soreide et al., 2006; Takayama et al., 2006) (Table 3).

Gene	DNA repetitive sequence (nucleitides)	Incidence of mutations (%)		Function of the gene products
		HNPCC	Sporadic MSI positive tumour	
TGFβRII	$(A)_{10}$ (709-718)	75-83	80-90	Inhibition of cell growth
BAX	$(G)_8$ (114-121)	50-55	11-50	Induction of apoptosis
IGFIIR	$(G)_8$ (4089-4096)	13	9	Growth promotion
hMSH6	$(C)_8$ (3049-3056)	33	25-36	Mismatch repair enzyme
hMSH3	$(A)_8$ (1141-1148)	50-58	35-46	Mismatch repair enzyme
PTEN	$(A)_6$ (795-800)	—	18.8	Inhibition of cell growth
E2F-4	$(CAG)_{13}$ (918-956)	71	42-57	Progression of cell-cycle

Table 1. 3 Target genes of MSI in colorectal cancer. (Adapted from Takayama et al., 2006)

In the MSI positive tumours, frequent frameshift mutations have been identified in TSGs (*TGFβRII*, *IGFIIR*, *BAX*, *PTEN*), DNA MMR genes (*hMSH6* and *hMSH3*) and cell-cycle-regulatory gene (*E2F-4*) (Bertholon et al., 2006; Buermeyer et al., 1999; Narayan and Roy, 2003; Takayama et al., 2006). Interestingly, loss of MMR also appears to accelerate tumourigenesis in an *APC* deficient background (Huang et al., 1996; Prolla et al., 1996).

1.4 Sporadic Colorectal Cancer

Mutations in both *APC* and *MMR* genes are the cause of a large number of sporadic CRC (Narayan and Roy, 2003). Inactivating somatic mutations of *APC* have been reported to occur in about 70-80% of sporadic colorectal cancers (Fearnhead et al., 2001; Grady and Markowitz, 2002; Luchtenborg et al., 2004), the majority of which occur in the mutation cluster region (MCR) region (Luchtenborg et al., 2004). However, the frequency of MMR deficiency caused MSI in sporadic colorectal cancers is uncommon, about 10-15%, which is not as high as in HNPCC cases (Benito and Diaz-Rubio, 2006; Saletti et al., 2001). Taken together, genetic instability is a critical stage in human colorectal cancer initiation, promotion and progression in either familial or non-familial form (Grady and Markowitz, 2002), which provides the possibility to investigate the molecular mechanism of colorectal cancer pathogenesis.

1.5 APC and Wnt signalling pathway

Inactivation of both alleles of *APC* gene marks one of the earliest events in colorectal tumorigenesis (Gryfe et al., 1997), which has developed into the concept of *APC* as a 'cellular gatekeeper' protecting against tumorigenesis in the colon (Clarke, 2005).

The APC plays multiple intracellular roles with different functional domains in the processes of cell adhesion and migration, signal transduction, microtubule assembly and chromosome segregation (Fodde, 2002; Fodde et al., 2001) (Figure 1.4). The human *APC* gene (NM_000038) locates within 5q21-22 in the length of 10719 bp spanning 21 exons (Ashton-Rickardt et al., 1989; Thliveris et al., 1996), which encodes the APC tumour suppressor protein of 2843 amino acids (Nathke, 2004; Watson, 2006).

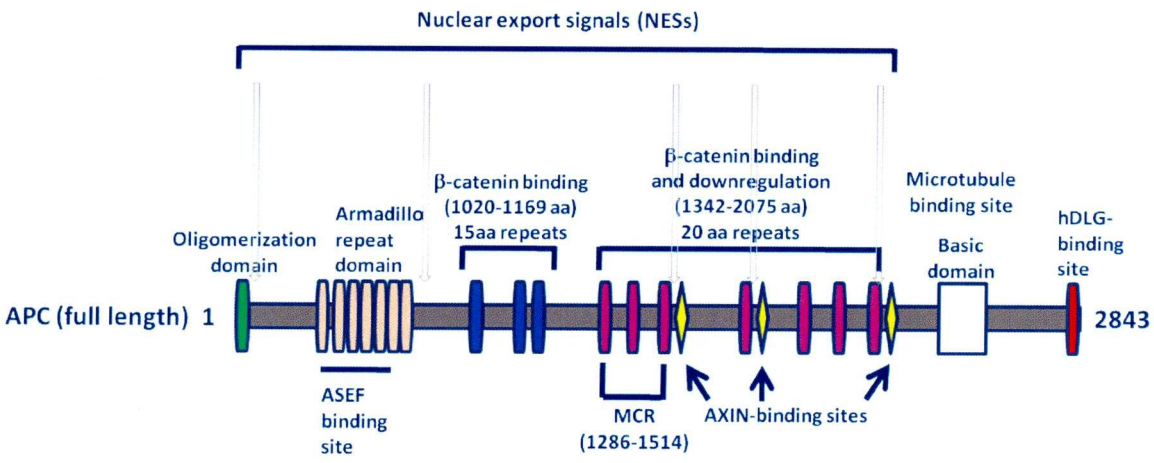

Figure 1. 4 Structure features of APC protein. (Adapted from Narayan and Roy, 2003)

The N-terminus and middle region of APC are the most highly conserved regions in the sequences of APC proteins from different species (Nathke, 2004). At the N-terminal site, the APC protein contains an oligomerization domain, which allows APC to form homodimers (Su et al., 1993) and Armadillo repeats domain, which binds to APC-stimulated guanine nucleotide exchange factor (ASEF) for Rho family proteins to regulate the actin cytoskeletal network (Kawasaki et al., 2000; Narayan and Roy, 2003; Nathke, 2004). The N-terminal region also contains nuclear export signals (NES) that are required for shuttling of APC between the nucleus and cytoplasm (Henderson and Fagotto, 2002). APC is capable of binding β-catenin through its 15 amino acid repeats domain. In the central region of APC, seven motifs of 20 amino acids were identified, which not only bind β-catenin but also down-regulate β-catenin by phosphorylation through interacting with axin and GSK3β (glycogen synthase kinase 3β), which are, apart from APC, the other two essential components in the Wnt signalling pathway (Rubinfeld et al., 1996; Yost et al., 1996). The first 20 amino acid repeats overlap with the 5' end of MCR, which presents a majority of APC mutation in severe polyposis (Nagase et al., 1992; Narayan and Roy, 2003). At the C-terminal site, APC contains motifs that mediate interactions with a number of structural proteins (Nathke, 2004), including the microtubule binding domain and tumour suppressor protein DLG binding domain (Narayan and Roy, 2003).

1.5.1 APC mutations

Mutations in *APC* gene are not only responsible for familial adenomatous polyposis (FAP), but also play a rate-limiting role in the majority of sporadic colorectal cancers and adenomas, 60% to 80% (Fodde, 2002; Narayan and Roy, 2003). Widely recognised as the initial event in the step-wise CRC development, once *APC* gene is mutated, the truncated APC protein has been demonstrated to be able to trigger abnormal mitosis by losing the ability to bind the microtubules and maintain the attachment of microtubules at kinetochores, resulting in the defect of segregation of chromosomes (Fodde et al., 2001; Kaplan et al., 2001; Narayan and Roy, 2003). However, the mechanism by which CIN generated in colon cancer cells is still not completely clear.

Almost all mutations in *APC* gene truncate the protein to take the form of allelic loss (loss of heterozygosity, LOH) (Sieber et al., 2006). Both truncating germline and somatic mutations occur in FAP and also in most of the sporadic colorectal cancers (Lamlum et al., 1999; Miyaki et al., 1995). Truncating germline mutations have been found to be responsible for 70-90% of FAP cases and families (Lipton and Tomlinson, 2006). The majority of mutations in patients result in truncations of the *APC* gene due to frameshifts (68%), nonsense (30%) and large deletion (2%) (Beroud and Soussi, 1996; Powell et al., 1993).

The two most frequent germline mutated 'hotspots' are at positions of codons 1061 and 1309 (Beroud and Soussi, 1996; Fearnhead et al., 2001). Inactivation mutations in APC have also been reported in 60-70% of sporadic colorectal cancer patients, the majority of which occur in the MCR, which spans from codons 1286 to 1513 (Luchtenborg et al., 2004; Nakamura, 1993).

In the case of human colorectal cancer, the mutations in *APC* gene are extremely complicated and might not result in simple loss of protein function (Lamlum et al., 1999; Rowan et al., 2000). According to the two-hit model, the position of the germline mutation in *APC* gene might affect the position or type of the second hit in FAP polyps (Lamlum et al., 1999). Several studies of colorectal adenomas from FAP patients have shown that somatic *APC* mutations are dependent on the position of the germline *APC* mutation (Crabtree et al., 2003; Lamlum et al., 1999; Sieber et al., 2006). The second mutation in *APC* gene represents the rate-limiting step for tumour initiation (Rowan et al., 2000). FAP patients with germline mutation in *APC* gene within a small region (codons 1194-1392) mainly show allelic loss in their colorectal adenomas and other FAP patients the 'second hit' tend to occur by truncating mutation in the MCR region (Lamlum et al., 1999). Moreover, mutations near codon 1300 are associated with LOH of the wild-type allele with particular severe disease and other tumours tend to have two protein truncating mutations (Crabtree et al., 2003; Debinski et al., 1996; Miyoshi et al., 1992; Nugent et al., 1994). However, when the first mutation does not hit the MCR region, the second event will be a

further mutation in MCR (Bodmer, 2006; Fearnhead et al., 2001). In fact, CRC patients with mutations outside of the MCR region have a milder phenotype (Narayan and Roy, 2003). The interdependent relationship of first hit and second hit of the *APC* gene mutation in a selective way is able to play its roles in β-catenin regulation through Wnt signalling pathway or some other Wnt-independent roles in the cellular regulations of cell adhesion and apoptosis (Nathke, 2004; Rubinfeld et al., 1996; Sieber et al., 2006).

1.5.2 APC regulates β-catenin via Wnt signalling pathway

The Wnt signalling pathway is important in organ development, cellular proliferation, morphology and motility (Cadigan and Nusse, 1997; Miller and Moon, 1996). Over 90% of colorectal cancers have a mutation that activates this pathway (Doucas et al., 2005).

Wnt was termed by the contraction of the *Drosophila* segment polarity gene *Wingless* and murine proto-oncogene *Int-1*, which were shown to share a common origin (Clevers, 2004; Pinto and Clevers, 2005b; Rijsewijk et al., 1987). *Wnt* genes encode 19 cysteine-rich glycoproteins with a highly conversed domain throughout metazoans (Giles et al., 2003; Gregorieff and Clevers, 2005; Nelson and Nusse, 2004; Watson, 2006). These Wnt proteins have also been implicated in the growth of the gastrointestinal tract (Nelson and Nusse, 2004; Watson, 2006).

The canonical Wnt signalling pathway is β-catenin-dependant, which is different from the non-canonical signalling pathway (Logan and Nusse, 2004; Reya and Clevers, 2005) (Figure 1.5). In the absence of Wnt signals, β-catenin binds the multiprotein degradation complex, in which Axin acts as the scaffold of the complex consisting of APC, GSK-3β and β-catenin in the cytosol (Giles et al., 2003; Pinto and Clevers, 2005a). β-catenin is then phosphorylated at the N-terminus of Ser-45,

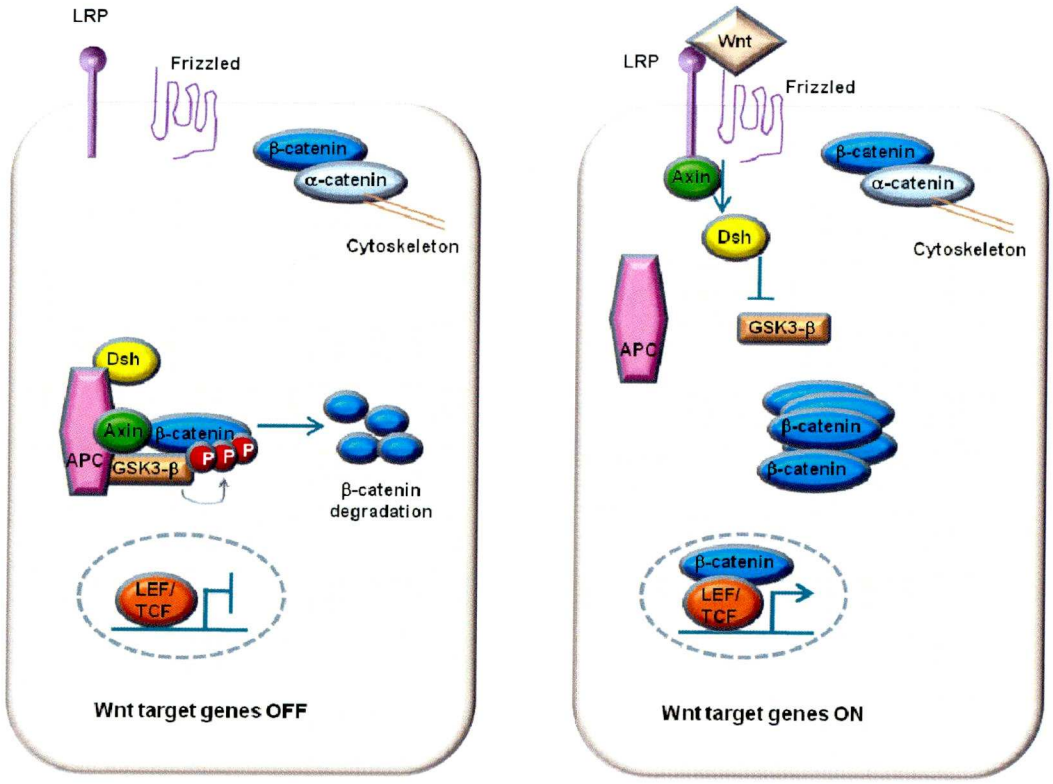

the conversed amino-terminal serine and threonine residues, by serine/threonine kinases, casein kinases and GSK-3β resulting in ubiquitination and proteasomal degradation (Bienz and Clevers, 2000; Hauck et al., 2005; Pinto and Clevers, 2005b; Watson, 2006).

When the Wnt signalling pathway is stimulated, the co-receptor, which consists of seven-span transmembrane protein Frizzled (Fzd) (Dale, 1998; Giles et al., 2003) and the single-span transmembrane protein LRP5/6 that belong to the low-density lipoprotein receptor-related protein family (He et al., 2004; Wehrli et al., 2000), is activated by Wnt ligands. Associated with Dishevelled (Dsh), this complex causes the recruitment of Axin to the membrane, causing the inhibition of APC degradation complex activity in cytosol (Gregorieff and Clevers, 2005). β-catenin is then released from the inhibited degradation complex without phosphorylation (Giles et al., 2003). Consequently, the accumulated β-catenin in a non-phosphorylated form translocates from cytosol into the nucleus, which targets the T-cell factor/lymphoid enhancing factor (TCF/LEF)-driven gene transcription (Figure.1.3) (Bienz and Clevers, 2000; Sansom et al., 2004; Watson, 2006). Therefore, APC regulates the level of β-catenin and targets downstream gene expression via the Wnt signalling pathway (Narayan and Roy, 2003).

1.5.3 Nuclear β–catenin mirrors the status of Wnt signalling pathway

The dynamic transformation of β-catenin between membrane-bound junction pools (connects E-cadherin with β-catenin to actin cytoskeleton) and free cytosolic pools (Wnt signalling pathway) balance the adhesion and transcription in cells as a dual functional protein (Bienz and Clevers, 2000; Doucas et al., 2005) (Figure 1.6). Translocation of accumulated stabilized β-catenin from cytosol into the nucleus is

independent of nuclear import machinery (Behrens, 2005; Yokoya et al., 1999). In the nucleus, in the absence of Wnt signalling, TCF/LEF complex, which belongs to high mobility group (HMG) proteins, acts as the transcriptional repressor by binding of negative regulators (Bienz and Clevers, 2000).

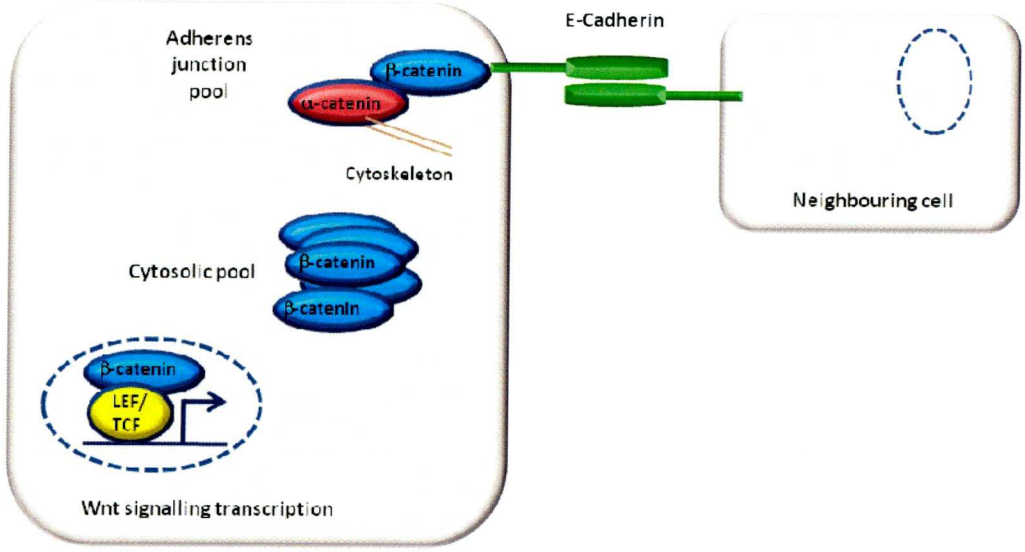

Figure 1.6 Diagram of dual role of β-catenin in the cadherin-catenin adhesion complex and within the Wnt signaling pathway. See text for details. http://zlp.charite.de/typo3temp/pics/15f06ee641.gif, accessed in August 2009.

β-catenin has at least two separate transcriptional activation domains (TADs) with the lack of a DNA binding domain, however, TCF/LEF factors provide the DNA binding specificity (Doucas et al., 2005; Fearnhead et al., 2001). The TATA-binding protein (Pontin52) is thought to mediate the contact between β-catenin and TCF/LEF complex and the basal transcription machinery (Bauer et al., 1998; Kolligs et al., 2002). Once in the nucleus, β-catenin binds to the TCF/LEF complex and serves as

a co-activator to trigger transcription of Wnt target genes (Behrens et al., 1996; Bienz and Clevers, 2000).

The importance of β-catenin in tumorigenesis has been shown in both animal models (azoxymethane stimulation and oligonucleotides inhibition) and human studies (Doucas et al., 2005; Green et al., 2001; Yamada et al., 2001). In human colorectal tumours, over 70 β-catenin mutations have been reported, most of which are mis-sense mutations (Doucas et al., 2005). Moreover, APC and β-catenin mutations are mutually exclusive (Behrens, 2005; Sparks et al., 1998) and both result in the stabilization and accumulation of nuclear β-catenin, which is detectable in even smallest neoplastic lesion of the colonic adenoma-carcinoma sequence (Hao et al., 2001; Pinto and Clevers, 2005b). However, small adenomas with β-catenin mutations do not appear to be as likely to progress to larger adenomas and invasive carcinomas as observed for APC mutations (Pinto and Clevers, 2005b). Also, about 75% of human colorectal cancer tumours have increased nuclear expression of β-catenin (Doucas et al., 2005) and the cells at the invasive front rather than those in the tumour centre tend to show high levels of nuclear β-catenin (Bienz and Clevers, 2000; Brabletz et al., 1998). Therefore, translocation of β-catenin into nucleus plays a critical role in colorectal cancer progression and is able to mirror the status of Wnt signalling pathway.

1.5.4 Identified β-catenin/TCF pathway target genes

The overactive status of the Wnt signalling pathway resulting from either the presence of Wnt signals or the mutations of any components of this pathway triggers the inappropriate transcription of downstream target genes (Doucas et al., 2005), *c-Myc*, *Cyclin D1*, *Axin2* and *CD44* are some of the known target genes (Cho et al., 2006).

Both c-Myc and Cyclin D1 promoters contain TCF/LEF-binding sites and increased nuclear β-catenin is followed by constitutively increased protein expression levels of both c-Myc and Cyclin D1 (Bondi et al., 2004; Morin, 1999), which is believed to enhance the tumorigenesis by their effect on cell-cycle progression (Behrens, 2005; Bondi et al., 2004). c-Myc, encoded by the corresponding proto-oncogene, has been known to be overexpressed in colorectal cancers (Kolligs et al., 2002; Pinto et al., 2003; Watson, 2006), which is able to prevent apoptosis and contributes to tumorigenesis by deregulation of cell growth and proliferation (Barker et al., 2006; Bondi et al., 2004; Doucas et al., 2005). Cyclin D1 regulates the G1/S transition phase of the cell cycle with cyclin-dependent kinases (Cdk4 and Cdk6) and links this pathway to colorectal carcinogenesis (Kolligs et al., 2002; Shtutman et al., 1999; Tetsu and McCormick, 1999). Up-regulation is more important for tumour progression than initiation (Sansom et al., 2005).

Axin2 has been identified as a β-catenin/TCF-regulated gene, which negatively regulates the signalling (Kolligs et al., 2002). High levels of *Axin2* gene expression have been detected in most human colon cancer cell lines (Salahshor and Woodgett, 2005) and observed in the APC deficient Min mice (Lustig et al., 2002). In response to increased β-catenin concentrations in cells and subsequent increased cell proliferation and carcinogenesis, Axin2 is upregulated and thus serves to limit the duration and intensity of the Wnt signals (Yan et al., 2001). Therefore, up-regulation of Axin2 may constitute a negative feedback loop that controls Wnt signalling activity with a role in tumour suppression (Hughes and Brady, 2006).

As downstream target of the β-catenin/TCF signalling pathway, CD44 overexpression is an early event in the colorectal adenoma-carcinoma sequence (Wielenga et al., 1999). CD44 is a cell–surface glycoprotein encoded by a single gene with alterative splicing and extensive post-translational modifications (Kuncova et al., 2005; Yamada et al., 2003), and plays a crucial role in cell migration, inflammation and immune responses (Mishra et al., 2005). The CD44 high molecular weight splice variants have been found to be over-expressed in colorectal cancer cell lines and carcinomas (Fernandez et al., 2004; Yasuda et al., 2002), which may play a role in the generation and turnover of epithelial cells (Kim et al., 1994; Wielenga et al., 1993; Wielenga et al., 1999).

1.6 Smads and TGF-β signalling pathway

TGF-β (Transforming growth factor β type I) is a ubiquitous cytokine and was originally termed by its ability of transforming normal fibroblasts in culture (Bachman and Park, 2005). The TGF-β/Smad signalling pathway is composed of the type I TGF-β receptor (TGFBR1), type II TGF-β receptor (TGFBR2) and Smad proteins (Takayama et al., 2006). The TGF-β family include 3 isoforms of TGFB1, TGFB2 and TGFB3 in mammals (Bachman and Park 2005) and TGFB1 is the most abundant and ubiquitously expressed isoform (Xu and Pasche, 2007).

TGF-β signalling pathway is activated by TGF-β signals binding to TGFBR2 (Chung, 2000). TGFBR2 then recruits TGFBR1, which is activated by phosphorylation on specific serine and threonine residues to stimulate the kinase activity of TGFBR1 (Chung, 2000; Xu and Pasche, 2007). Activated TGFBR1 phosphorylates downstream transcriptional factors Smad2/3 which then bind to Smad4 (Chung, 2000; Xu and Pasche, 2007). The Smad complexes translocate into the nucleus and interact with other transcriptional factors in a cell-specific manner to regulate the transcriptional induction or repression of a diverse programme of genes (Elliott and Blobe, 2005; Xu and Pasche, 2007) (Figure 1.7).

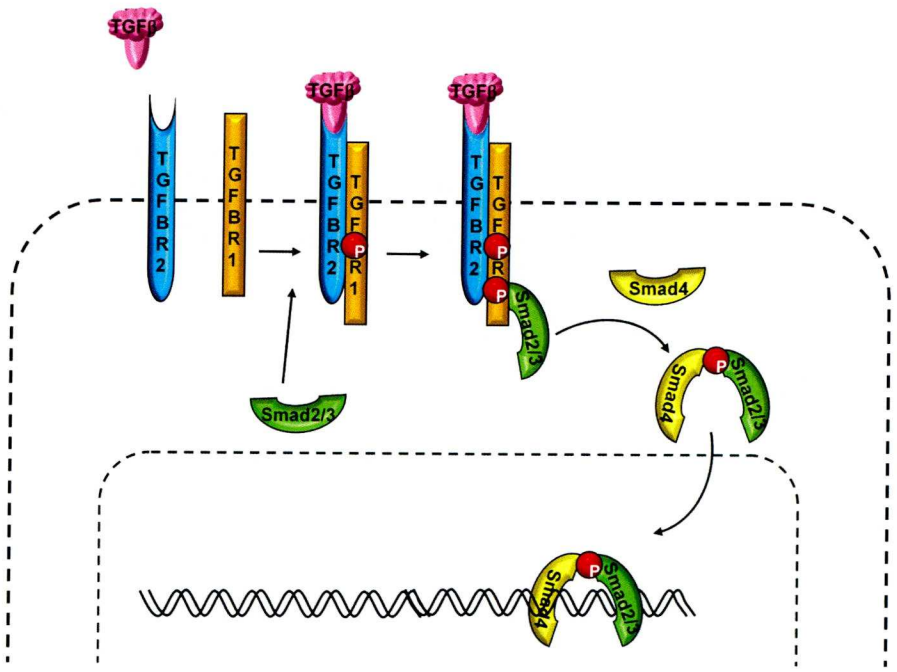

Figure1.7 TGF-β signalling pathway (Adapted from Xu and Pasche, 2007).
See text for details.

TGF-β signals initiate not only the Smads-mediated signalling transduction but also other pathways, including mitogen activated protein kinases (MAPKs), phosphoinositide 3' kinase (PI3K), small GTPases of the Ras superfamily (Moustakas and Heldin, 2005; Pardali and Moustakas, 2007). However, these pathways often regulate Smad-mediated responses and also induce Smad-independent responses (Derynck and Zhang, 2003; Xu and Pasche, 2007).

The TGF-β signalling pathway plays a central but paradoxical role in the initiation and progression of colorectal cancer development (Bachman and Park, 2005; Xu and Pasche, 2007). TGF-β receptors (TGFBR1 and TGFBR2) and Smad protein have been demonstrated to function as tumour suppressors by the finding of somatic

mutation of these genes in certain gastrointestinal cancers (Bachman and Park, 2005), however Smad4 is more frequently mutated in colorectal cancer than Smad2 and Smad3 (Kawabata et al., 1999; Xu and Pasche, 2007). Some of the downstream targets of TGF-β signalling are the cell-cycle checkpoint genes, including p21 (CDKN1A), p27 (CDKN1B) and p15 (CDKN2B), and their activation leads to the cellular growth arrest (Massague et al., 2000). Inactivation of TGFBR2, Smad3 and Smad4 in the *in vivo* models has been reported to induce intestinal tumourigenesis (Munoz et al., 2006; Sodir et al., 2006; Takaku et al., 1998). Therefore, TGF-β pathway acts as a tumour suppressor in the normal intestinal epithelium and early tumours, including colonic adenomas (Massague et al., 2000; Munoz et al., 2006; Siegel et al., 2003a; Sodir et al., 2006; Takaku et al., 1998). However, during the late stages of colorectal carcinogenesis, many colorectal cancers escape the tumour-suppressor effect of TGF-β and are resistant to TGF-β-induced growth inhibitor (Bachman and Park, 2005; Xu and Pasche, 2007). Therefore, TGF-β pathway also acts as a tumour promoter enhancing metastatic behaviour, immune evasion and angiogenesis (Bierie and Moses, 2006; Takahashi et al., 2000; Thomas et al., 2005). It is noticing that a body of studies on mouse models suggests that TGF-β and Wnt pathways can cooperate to regulate differentiation by controlling gene expression pattern to promote colorectal tumourigenesis (Attisano and Labbe, 2004; Xu and Pasche, 2007).

1.7 K-Ras

K-Ras is mutated in approximately 50% of human colorectal cancers (Malumbres and Barbacid, 2003). The majority of K-Ras mutations occur as an activating point mutation in codons of 12 and 13 (exon2) and 61 (exon3) (Capella et al., 1991; Takayama et al., 2006; Toyooka et al., 2003).

Mutant K-Ras can act as an initiator of tumorigenesis (Smakman et al., 2005) and it also associates with tumour progression and metastasis (Oudejans et al., 1999). Mutation of K-Ras on its own is not sufficient to induce metastasis in the intestinal epithelium (Janssen et al., 2002; Smakman et al., 2005; Tuveson et al., 2004); however, K-Ras mediated signalling pathways may contribute to the potential metastasis of tumour cells (Campbell and Der, 2004; Smakman et al., 2005). The effector pathways activated by K-Ras include RAF/MAPK, JNK (Jun N-terminal kinase), and PI3K, which can lead to promoted cell growth (Campbell and Der, 2004; Smakman et al., 2005); (Takayama et al., 2006). K-Ras mutations are associated with up-regulations of its downstream targets, such as DNA methyltranferase (MGMT) and vascular endothelial growth factor (VEGF) (Chung, 2000; Okada et al., 1998; Patra, 2008; Takayama et al., 2006).

K-Ras also cooperates with TGF-β signalling to induce de-differentiation and potential metastasis formation in carcinoma cells (Smakman et al., 2005), which was found in the study of using murine C26 colorectal carcinoma cell line with interfered

mutant K-Ras or a negative TGF-β receptor (Oft et al., 1998; Oliveira et al., 2007). An *in vivo* study showed that conditional expressed mutant *K-Ras* allele does not alter the intestinal homeostasis or the immediate phenotypes associated with Apc deficiency (Sansom et al. 2006). However, the effect of this K-Ras mutation in the intestine can only be observed over the long term with accelerated tumourigenesis followed by invasion (Sansom et al., 2006). A more recent study investigated the K-Ras splice variants in the adenomas of Apc Min mouse (K-Ras 4A and 4B), which shows that K-Ras 4A deficiency does not affect Min mouse survival, tumour burden and histopathology and the level K-Ras 4B increased in the adenomas with no activating K-Ras mutation (Patek et al., 2008).

1.8 TP53 (p53)

TP53 is the most commonly mutated tumour suppressor gene in various kinds of malignant tumours (Takayama et al., 2006). *TP53* mutations are also identified in more than 50% of colorectal tumours (Chung, 2000; Takayama et al., 2006), with higher frequencies in distal colon and rectal tumours and lower frequencies in proximal tumours (Iacopetta, 2003). Most mutations occur in highly conserved areas of exons 5-8 (Chung, 2000; Iacopetta, 2003). Approximately 80% of *TP53* mutations are missense mutations (GC to AT), which occur mainly in 5 hot spots codons (175, 245, 248, 273 and 282) (Beroud and Soussi, 1996; Takayama et al., 2006). *TP53* mutations are generally considered to occur at the time of the transition from adenoma to cancer as a late event (Fearon and Vogelstein, 1990; Takayama et al., 2006) and typically accompanied by deletions of the remaining wild type allele on chromosome 17q (Chung, 2000).

The *TP53* tumour suppressor gene encoded protein p53 is a sequence-specific transcriptional activator that plays diverse and complex roles in the regulation of cell cycle progression and apoptosis (Chung, 2000; Ko and Prives, 1996; Prives, 1998). p53 protein normally induces G1 cell-cycle arrest to facilitate DNA repair during replication, or induce apoptosis (Chung, 2000). p53 is also postulated to be involved as a critical negative regulator of the Wnt signalling pathway, suggesting that p53 should also have a role in the tumour initiation process (Clarke, 2007; Reed et al., 2008). However, p53 deficient Apc Min mice have variably been reported to have no

effect on or to modify adenoma formation (Clarke, 2007; Clarke et al., 1995; Halberg et al., 2000). A more recent *in vivo* study investigated the consequences of p53 deficiency on the phenotypes observed immediately following Apc loss (Reed et al., 2008). It was found that p53 modulates the Wnt transcriptome in the mouse intestine; however, this activity is not sufficient to modulate the immediate phenotype of Apc loss (Reed et al., 2008). This study supported the association of p53 mutation with only the later stages of colorectal disease (Kinzler and Vogelstein, 1996; Reed et al., 2008).

1.9 C-Myc

The role of *Myc* gene family (including *C-Myc*, *L-Myc*, *N-Myc*, *B-Myc* and *S-Myc*) in the biology of normal and cancer cells has been intensively studied (Eilers and Eisenman, 2008; Ignatenko et al., 2006). The *C-Myc* oncogene is over-expressed in many types of human cancer, including colorectal cancer (Ignatenko et al., 2006). *C-Myc* has been found to be over-expressed in both adenomas of FAP and in sporadic colorectal cancers (D'Orazio et al., 2002; Ignatenko et al., 2006; Smith et al., 1993). In colorectal cancer, *C-Myc* transcription is activated by the β-catenin/TCF complex and is inhibited by APC (He et al., 1998; Ignatenko et al., 2006).

The proto-oncogene *c-Myc* encodes a transcription factor that is widely expressed in proliferation embryonic and mature cells and possesses a potent transforming and trans-activation ability (Ignatenko et al., 2006; Xu et al., 1993). Myc is a basic helix-loop-helix zipper (bHLHZ) protein (Ayer and Eisenman, 1993; Eilers and Eisenman, 2008). Myc participates with the DNA binding proteins MAX (MYC associated factor X) and MAD (MAX dimerization protein 1) to regulate specific gene transcription and predominantly associated with gene activations (Eilers and Eisenman, 2008; Grandori et al., 2000). Myc heterodimerizes with the small bHLHZ protein MAX and binds the E-box (enhancer box) sequence CACGTG (Eilers and Eisenman, 2008; Ignatenko et al., 2006). Myc has also been associated with transcriptional repression (Eilers and Eisenman, 2008). Heterodimerization of MAX and MAD and its binding to E-boxes block most functions of the Myc-MAX dimers

(Ayer et al., 1993; Ignatenko et al., 2006). Another mechanism involves with specific binding and inhibition of the transcriptional activator MIZ-1 (Myc-interacting zinc finger protein-1) (Eilers and Eisenman, 2008; Kleine-Kohlbrecher et al., 2006).

Myc has been shown to be essential for intestinal crypt formation and Myc deletion induces rapid loss of intestinal crypts (Bettess et al., 2005; Muncan et al., 2006; Wilkins and Sansom, 2008). Myc has also been demonstrated to be a Wnt pathway downstream target in the mouse small intestine from an *in vivo* study with inducible *Apc* homozygous knock out (Sansom et al., 2004). Additionally, Myc is a critical mediator of the phenotypes of Apc loss in the intestine in both genomic and functional roles (Sansom et al., 2007; Wilkins and Sansom, 2008). An independent study using Apc Min mouse model showed that inactivation of Myc suppresses Apc-dependent intestinal tumourigenesis in adult Min mice, although not having apparent effect on normal intestinal mucosa (Ignatenko et al., 2006). Therefore, Myc plays very important roles in both initiation of tumourigenesis and tumour formation in the intestine.

1.10 Colorectal cancer mouse models

1.10.1 Carcinogen induced Model

Spontaneous formation of colorectal cancer in mice occurs with an extremely low incidence, which makes it impossible to perform experimental studies on CRC development using a natured population (Corpet and Pierre, 2005). In order to increase the incidence of CRC, mice models were developed using carcinogens (Takahashi and Wakabayashi, 2004). Carcinogen-induced CRC development in mice is largely dose, duration and frequency, routing and timing dependent (Heijstek et al., 2005). The most frequently used carcinogens are dimethylhydrazine (DMH) and its metabolite azoxymethane (AOM), causing onset of aberrant crypt foci (ACF) with DNA point mutation from G to A on codon 12 of *K-Ras* (Takahashi et al., 2000; Zaidi et al., 1995). Intrarectal administration of DMH induces mild hyperplasia and prenoeplastic lesions in the colon after 34 weeks and repeated intramuscular injections of AOM resulted in 80% incidence of CRC after 12 weeks (Heijstek et al., 2005). β-catenin gene mutations and altered protein cellular localization are frequently observed in colon tumours of AOM-induced mice, indicating the essential role of the activated Wnt signalling in the mechanism of AOM-induced colon tumours in mice as in human (Takahashi et al., 2000). *K-Ras* mutations are relatively frequent (Vivona et al., 1993), but *p53* is rarely observed (Takahashi and Wakabayashi, 2004). The reduced expression of APC protein in AOM-induced mice tumours has also been reported (Maltzman et al., 1997).

1.10.2 Apc Truncated Mouse Models

The Apc^{Min} germline mutation in mice, similar to that in patients with FAP and sporadic cancers, was found with multiple intestinal neoplasia (Moser *et al.*, 1990), carrying the truncated mutation of a premature translational stop codon at amino acid 850 in the APC protein (Su et al., 1992). The Min mouse model mimics the rapid development of adenomatous polyps that affect FAP patients (Corpet and Pierre, 2005). Several APC constructed mutations were also generated, $Apc^{\Delta 716}$ contains truncating mutation at codon 716 (Oshima et al., 1997); Apc^{1638N} and Apc^{1638T} at codon 1638 (Fodde et al., 1994; Smits et al., 1999). Mice carrying the Apc^{1638T} mutation can survive to adulthood without developing tumours, but this mutation is sufficient to induce β-catenin signalling (Smits et al. 1999). Like in humans, Wnt/β-catenin pathway also plays an important role in carcinogenesis in these mutant mice (Corpet and Pierre, 2005). However, most of the $Apc^{+/-}$ mutant mice develop polyps, but mainly in the small intestine and only a few polyps formed in the colon (Fodde et al., 1994; Heijstek et al., 2005; Taketo, 2006a). Moreover, ACF and adenocarcinomas are seldom observed in these models (Corpet and Pierre, 2005) and they do not progress into invasive or metastatic adenocarcinomas at a significant frequency (Taketo, 2006b).

1.10.3 Genetically targeted mutations, the Cre-*lox*P System

Conditional mouse models have been generated, in which the expression of the gene of interest can be regulated in a spatial and temporal specific manner by using genetically engineered constructs (Heijstek et al., 2005). The Cre-*lox*P system is one of the most widely used conditional knock-out control systems (Kuhn and Torres, 2002) (Figure 1.8). When cells that have *lox*P sites in their genome and also express Cre, the protein springs into action, catalyzing the reciprocal recombination event between the *lox*P sites (Ghosh and Van Duyne, 2002). The double stranded DNA is cut at both *lox*P sites by the Cre protein and then ligated back together (Ghosh and Van Duyne, 2002). As a result, any piece of DNA or the gene in between the *lox*P sites is excised and subsequently 'floxed'out and therefore the Cre-*lox*P system provide a method to produce a mouse model that no longer has a target gene (Utomo et al., 1999).

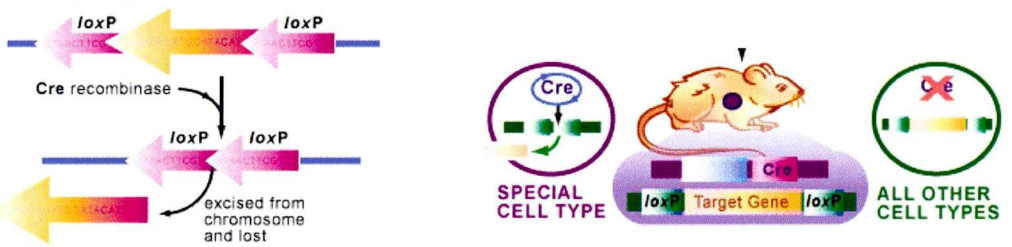

Figure1.8 Cre-LoxP system. http://www.scq.ubc.ca/targeting-your-dna-with-the-crelox-system/ accessed in August 2009.

In the animal model, mice containing a transgenic construct in which the gene of interest in flanked by two *lox*P sites are crossed with mice carrying a Cre recombinase gene under the control of a tissue-specific or inducible promotor element (Maddison and Clarke, 2005). Once the Cre recombinase is activated, the *lox*P sites recombine and excise the gene of interest (Maddison and Clarke, 2005).

1.10.3.1 Apc and β-catenin K/O Mouse Model

Although a body of studies has investigated a range of Apc heterozygous mutants, the primary consequences of *APC* loss in the gut are unknown, because homozygous loss of *APC* is embryonically lethal. Sansom generated an $Apc^{fl/fl}$ mice model using a novel inducible Ahcre transgenic line in conjunction with a *lox*P-flanked *Apc* allele at codon 580 (Sansom et al., 2004; Shibata et al., 1997) (Figure 1.9). In this study, to investigate the phenotype of conditional deletion of *Apc*, mice bearing a *lox*-flanked *Apc* allele were crossed onto a novel inducible Cre transgenic background, which uses the Cyp1A1 (cytochrome P4501A1) promoter to deliver inducible Cre expression in the intestine, resulting in virtually 100% recombination within the intestinal epithelium (Sansom et al., 2004). Loss of APC activates Wnt signalling pathway through the nuclear accumulation of β-catenin with the coincident alteration of differentiation, migration, proliferation and apoptosis and this study firstly confirmed a series of Wnt targets in an *in vivo* setting (Sansom et al., 2004).

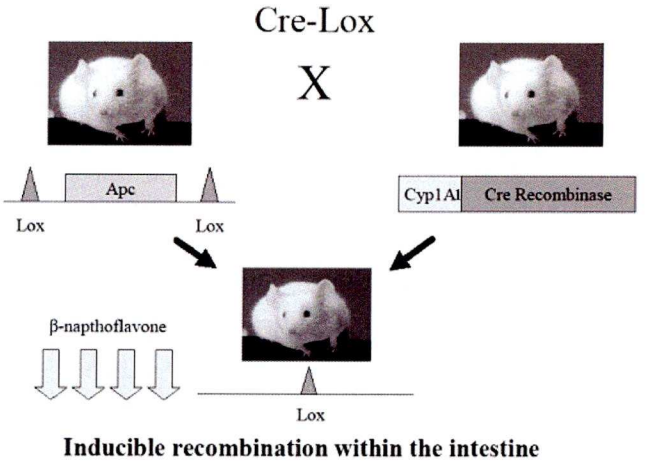

Figure 1.9 Inducible Cre-*Lox*P-*Apc* K/O mouse model
(Kindly provided by Prof A. Clarke). See text for details.

The central mediator of Wnt signalling, specific deletion of β-catenin was also shown to be induced, showing its requirement for maintenance of intestinal cell proliferation and the implication in goblet cell differentiation (Ireland et al., 2004).

1.10.3.2 Myc K/O Mouse Model

It was known that Myc was involved in the CRC process and the Clarke group demonstrated that Myc is an immediately activated Wnt target in mouse intestine. Because *c-Myc* inactivation is lethal in homozygotes between 9.5 and 10.5 days of gestation (Davis et al., 1993; Ignatenko et al., 2006), the Cre-*lox*P inducible system was employed. It has been surprisingly shown that the loss of c-Myc, following loss of APC, completely rescues the phenotypes of altered differentiation, migration, proliferation and apoptosis, demonstrating that c-Myc is the critical mediator for the majority of Wnt pathway targeted genes and activates following loss of APC (Sansom et al., 2007). The role of c-Myc (c-Myc mutant) has also been studied in the mouse

intestine as both a single and double (with APC) conditional mutation (Sansom et al., 2007). In APC and c-Myc double K/O mice, loss of c-Myc rescued the perturbed phenotypes which occur upon deletion of APC (Sansom et al., 2007). Interestingly, this rescue occurred despite high levels of nuclear β-catenin (Sansom et al., 2007). To study the role of the genes behind the phenotypes observed, expression array studies were carried out on both the single (*c-Myc* or *Apc*) and double (*c-Myc* and *Apc*) mutants, which identified a set of genes (59%, 24/46) whose expression reverted to the normal, non-mutated levels and a set whose expression was still altered in the double (*c-Myc* and *Apc*) mutant (Sansom et al., 2007). The former set (c-*Myc* dependent) tends to be more important in imposing Apc-dependent phenotype in the mouse model and the later (*c-Myc* independent) with non-specific gene expression may not be involved with the phenotypic changes from the immediate loss of Apc (Sansom et al., 2007). Therefore, these genes (c-*Myc* dependent) are responsible for the phenotype of Apc loss in mice.

1.10.3.3 *K-Ras* K/O Model

K-Ras is mutated in about 50% of human colorectal cancers (Malumbres and Barbacid, 2003). Ras proteins are activated by binding GTP and regulate cell cycle progression, apoptosis, and cell migration and are capable of transforming cells (Malumbres and Barbacid, 2003). After deleting APC, *K-Ras* was not identified to be over-expressed in mouse intestine accompanied with the immediate phenotypic changes (Sansom et al., 2004). The Clarke group has used a conditional transgenic knock in strategy to switch

on the oncogenic K-Ras^{v12} allele in the intestine of mice (Guerra et al., 2003; Johnson et al., 2001). It has been shown that K-Ras^{v12} expression does not impose a 'crypt progenitor' phenotype, importantly that nor does it perturb the Wnt signalling pathway (Sansom et al., 2006). However, K-Ras accelerates tumour formation when expressed in the context of APC heterozygosity (Sansom et al., 2006). 81% of the animals were systematic for the disease, in double mutants, at day 165 as compared to 10% for the single APC mutation, with a Chi-Square p value of 0.0001 (Sansom et al., 2006).

1.11 Cited1

Cited1 is one of the genes identified to be a Myc-dependent Wnt signalling downstream target (Sansom et al., 2007). Cited1 (CBP/p300-interacting transactivators with glutamic acid [E]/aspartic acid [D]-rich carboxyl-terminal domain 1) was originally identified as melanocyte-specific nuclear protein from a murine melanoma cell line (Shioda et al., 1996). Formerly known as *Msg1* (melanocyte-specific gene 1), *Cited1* locates on X-chromosome (Fenner et al., 1998). Cited1 is the founding member of family of transcriptional cofactors, which also contains another 3 members: Cited2 (formerly Mrg1, Msg1-related gene 1), Cited3 (not present in mammals) and Cited4 (formerly Mrg2, Msg1-related gene 2) (Plisov et al., 2005; Rodriguez et al., 2004). The *Cited* encoded proteins have approximately 200 amino acid residues and share a conserved carboxy-teminal transcription activation domain (CR2 domain of approximately 50 amino acids) (Plisov et al., 2005; Shioda et al., 1997).

Cited1 is a non-DNA binding transcriptional co-factor having 2 known functional domains SID (Smad4 Interacting Domain) and CR2 (Conserved Region 2) (Lovvorn et al., 2007a) and the bi-function of activating or repressing transcription is dependant on cellular context (Plisov et al., 2005). It has been shown to activate estrogen and TGF-β dependent transcription *in vitro*, and is able to bind to β-catenin to inhibit Wnt-induced transcription and axis formation during *Xenopus* development (Heasman, 1997; Plisov et al., 2005; Yahata et al., 2000). Both activation and

inhibition of transcription are dependent on the CBP/p300 binding domain CR2 (Freedman et al., 2003; Yahata et al., 2000).

During vertebrate development Cited1 is expressed in progenitors of the heart, limb, axial skeleton, kidney, and placenta (Rodriguez et al., 2004). It is implicated as a key co-ordinator during renal epithelial morphogenesis, regulating cellular responses to TGF-β and Wnt signalling (Plisov et al., 2005). In adults, Cited1 is expressed in the mammary gland and heart, as well as melanocytes, melanoma cells, and papillary thyroid carcinoma (Li et al., 1998; Nair et al., 2001; Scognamiglio et al., 2006).

Little is known about the role of Cited1 in cancers but it has been implicated in several types of cancers. Increased expression has been observed in melanoma, thyroid, breast cancers (Li et al., 1998; McBryan et al., 2007; Prasad et al., 2004). Over-expression of Cited1 in a human Wilms tumour cell line led to a significant increase in proliferation, whereas mutation of the CR2 domain of Cited1 resulted in a reduction of proliferation (Lovvorn et al., 2007a). *In vivo* injection of CR2 mutant Cited1 Wilms tumour cells into immuno deficient mice also led to a reduction in proliferation and tumourigenesis (Lovvorn et al., 2007a). Cited1 has also been linked to mammary cancer, as it is up-regulated in mammary tumours and associates with EGR2 (early growth response 2) to regulate expression of the oncogene *ErbB2* (v-erb-b2 erythroblastic leukemia viral oncogene homolog 2, neuro/glioblastoma derived oncogene homolog (avian)) (Dillon et al., 2007).

1.12 Objectives

The microarray gene analysis on the Cre-*lox*P-*Apc* mutant and *Apc Myc* double mutant mouse models have identified a large number of Wnt regulated gene alterations, for the majority of which, there has been little previous association with neoplasia. We proposed to apply these findings from the mouse models to the human disease to determine the prevalence of altered gene expression in human colorectal cancer through mRNA analysis of the match paired samples from CRC patients. In the human study, *CITED1* was identified as a previously unrecognised Wnt target. We were interested in the underlying mechanisms of *CITED1*, which may give us an insight into colorectal carcinogenesis.

1.13 Aims

1 — To validate the observed gene array alterations in Cre-*lox*P-*Apc* mouse model using human colorectal cancers and to identify the novel Wnt target genes (from the early stage mouse model) involved with colorectal carcinogenesis.

2 — To investigate the effects of reduced *CITED1* mRNA expression on colorectal carcinogenesis and the alterations of Wnt signalling activity using siRNA treatment of colon cancer cell lines (cell survival and proliferation).

3 — To investigate the role of *Cited1* loss in the intestinal tumourigenesis using the Min mouse model and to investigate the underlying molecular mechanism of *Cited1* in regulation of Wnt signalling and in other involved pathways (e.g. TGF-β).

4 — To investigate the early effects of loss of *Cited1* in the intestine using *Cited1* K/O and Cre-*lox*P-*Apc* mouse models and to investigate the underlying molecular mechanism of Cited1 in Wnt signalling pathway regulation.

Chapter 2 Materials and Methods

2.1 Patient tissue collections and genetic material extraction

Patient tissue samples were obtained from Cancer Tissue Bank Research Centre, which were surgically removed tissue for the research with informed patient consent. Total RNA, genomic DNA and protein samples were extracted from colorectal cancer tissues and adjacent uninvolved colonic mucosa from the random numbered patients. Uninvolved colonic mucosa was generally 5-10cm away from the malignant tissue, depending on the availability of non-malignant tissues (size and type of specimen).

2.2 Animal work

All experiments were performed according to UK Home Office regulations. The procedures involved with animal breeding, drug injection and tissue collection & preparation were performed by Dr Phesse and Dr Meniel in Cardiff. Tissue sections for histology staining and immuno-histochemistry were prepared by Derek Scarborough.

2.2.1 Transgenic mouse strains

The animals were housed at the experimental animal facility under a 12 hour light:dark cycle with standard rodent chow and water in the University of Cardiff. Mice breeding were carried out by Dr Phesse and Dr Meniel in the University of Cardiff.

Min Mice

Min mice carrying the heterozygous Apc were bred routinely in the animal house in the University of Cardiff (Moser et al., 1990).

***Apc*Flox Mice**

Conditional *Apc* knock-out mice were generated in Prof Clarke's group, bearing inducible AhCre transgenic line with *lox*P-flanked *Apc* allele. Injections of β-napthoflavone at 8-10 weeks age (see details 2.2.3) induced the conditional gene targeting Cre-*lox*P system resulted in virtually 100% intestinal recombination (Sansom et al., 2004).

***Cited1* K/O Min Mice**

Cited1 null mutant mice were obtained from Dr. Dunwoodie, University of New South Wales, Australia (Rodriguez et al., 2004). *Cited1* null mutant mice had previously been backcrossed for 6 generations onto a C57Bl/6 background and these animals were crossed with $Apc^{Min/+}$ mice on the same C57Bl/6 background to produce three cohorts, $Apc^{Min/+}$ $Cited1^{+/+}$, $Apc^{Min/+}$ $Cited1^{+/-}$ and $Apc^{Min/+}$ $Cited1^{Y/-}$. Mice were aged and culled upon signs of intestinal neoplasia (white feet, rectal bleeding and lack of activity).

Cited1 K/O ApcFlox Mice

$Apc^{Min/+}$ $Cited1^{Y/-}$ were then used to cross onto AhCre Apcflox background to produce $Cited1^{+/+}$ $Apc^{+/+}$, $Cited1^{+/+}$ $Apc^{fl/fl}$, $Cited1^{Y/-}$ $Apc^{fl/fl}$ and $Cited1^{Y/-}$ $Apc^{+/+}$ cohorts. Mice from all four cohorts carry the Cre promoter to be comparable controls. Cre-*lox*P was induced as previously stated for ApcFlox mice.

2.2.2 Genotyping

Genotyping work was carried out by Mark Bishop in University of Cardiff. A small (3-5mm) section of mouse tail tip was taken from the new born pups. 500µl of cell lysis solution (Gentra) and 10µl of proteinase K 20mg/ml (Roche) were added to each tube containing mouse tail and tubes were shaked overnight at 37°C. The tubes were allowed to cool to room temp before adding 200µl of protein precipitation solution (Gentra) to each tube. The tubes were inverted and then spun in micro-centrifuge at 10,000 *g* for 10 minutes. The supernatant was removed into clean tubes containing 500 µl of isopropanol. The tubes were inverted and spun again at 10,000 *g* for 15 minutes. The supernatant was poured off and the tubes were left upside down to dry for 1 hour. 500µl of nuclease-free water was added to each sample. 2µl of the resulting DNA suspension was used in the following genotyping PCR protocols. The Genotyping protocols were provided by Mark Bishop.

APC Min mouse

Apc Min mutation was characterised by PCR reactions on genomic DNA extracted from mouse tail. The following primers were used: min1 5'-TCT CGT TCT GAG AAA GAC AGA AGC T-3', min2 5'-TGA TAC TTC TTC CAA AGC TTT GGC TAT-3'. PCRs were performed to the following conditions: 1 cycle at 94°C for 2 minutes; 30 cycles at 94°C for 1 minute, 60°C for 1 minute, 72°C for 1 minute; 1 cycle at 72°C for 5 minutes. 20 µl PCR product were then digested with 2.5µls of buffer E (Promega) and 1.5µls of HIND III (10 Unit/µl) (Promega) for 2 hours at 37°C, then run on 4% gel. The fragment size generated were ~300bp for wild type and ~330bp for min.

Cre-*lox*P flanked *Apc* mutation detection

Frame-shift mutation of *Apc* gene were characterised by PCR reactions on genomic DNA extracted from mouse tail. The following primers were used: P3 5'-GTT CTG TAT CAT GGA AAG ATA GGT GGT C-3', P4 5'-CAC TCA AAA CGC TTT TGA GGG TTG ATT C-3', P5 5'GAG TAC GGG GTC TCT GTC TCA GTG AA-3'. PCRs were performed to the following conditions: 1 cycle at 95°C for 3 minutes; 30 cycles at 95°C for 30 seconds, 60°C for 30 seconds; 72°C for 1 minute; 1 cycle at 72°C for 5 minutes using Pic Taq polymerase. Amplification products were run out on 2% agarose gels. P3 and P4 were used to amplify the wild type or the mutant *Apc*, for which mutant allele gave product at the size of 314 bp and 226bp for wild type allele. P3

and P5 were used to detect the recombined *Apc* allele after inducing Cre-*lox*P, which gave product at size of 250bp.

Cre recombination reporter assay

Cre and Cre-mediated recombination reporter Laz were genotyped. The following primers were used: for Cre FWD 5'-TGA CCG TAC ACC AAA ATT TG-3'; REV 5'-ATT GCC CCT GTT TCA CTA TC-3': for LacZ, FWD 5'-CTG GCG TTA CCC AAC TTA AT-3'; REV 5'-ATA ACT GCC GTC ACT CCA AC-3'. PCRs were performed to the following conditions: 1 cycle at 95°C for 3 minutes; 30 cycles at 95°C for 30 seconds, 55°C for 30 seconds, 72°C for 1 minute; 1 cycle at 72°C for 5 minutes by using Go Taq polymerase. Amplification products were run out on 2% agarose gels.

***Cited1* K/O genotyping**

Cited1 global knock-out mice on both *Apc* Min and *Apc*flox background were genotyped. The PCR primers used to distinguish between the wild type *Cited1* allele and Cited1neo alleles were FWD 5'-TTA CTT GCA GAC CAA CAG GC-3'; REV 5'-TGC TTC TTT GAC CCA TTT CC-3' and GFP-REV 5'-TGT TGC ATC ACC TTC ACC CT-3'. PCRs were performed to the following conditions: 1 cycle at 94°C for 2.5 minutes; 35 cycles at 94°C for 30 seconds, 60°C for 30 seconds, 72°C for 1minute; 1 cycle at 72°C for 5 minutes by using Go Taq polymerase. Amplification

products were run out on 2% agarose gels. The fragment sizes generated were 367 bp for the wild type *Cited1* allele and 206 bp for the *Cited1* neo-allele.

2.2.3 Animal treatment

Injections of β-napthoflavone and bromodeoxyuridine were carried out by Dr Meniel in the University of Cardiff.

Cre recombination induction

ApcFlox mice and Cited1ApcFlox mice were given 4 daily intraperitoneal (IP) injections of β-napthoflavone at 80 mg/kg to induced Cre recombination, and harvested 4 days later. If we assume mouse is with the weight of 25g, 0.2 ml of 10mg/ml β-napthoflavone was injected into one mouse to give final concentration.

Bromodeoxyuridine (BrdU) *in vivo* labelling

4 days after first injection of β-napthoflavone, 2 hours before the cull, mice were given an intraperitoneal (IP) injection of BrdU (Amersham Biosciences) at 1 ml per 100g body weight.

2.2.4 Tissue Retrieval

2.2.4.1 Sample preparation for RNA and protein extraction

Mouse tissue sample preparation was carried out by Dr Phesse and Dr Meniel in the University of Cardiff. The small intestine was removed up to the appendix (pulling on the stomach so the intestine would not be damaged) and flushed through with water (through placement of a syringe in one end). The large intestine was then removed to the anus and also flushed.

Cited1 null/*Apc* Min

Three cm of the small intestine located 7 cm from the stomach was placed in RNAlater (after removing any mesentery and ensuring that no Peyer's patches were present). The tissue was then homogenized in Trizol reagent and RNA extracted using standard phenol-chloroform methodologies (Chomczynski, 1993)

Epithelial cell harvesting from *Cited1* null/*Apc* flox mice

Seven-10 cm of the small intestine located 10 cm from the stomach was removed from the culled mouse for epithelial extraction. The section was flushed with water and then flushed once with PBS. One end of the section was tied off using suture. The intestine was then inverted over the curved end of a glass spiral, starting at the tied end. The straight end of the spiral was inserted into a vibrator. The inverted intestine on the glass spiral was placed into a tube containing HBSS (Hank's buffered salt solution)/EDTA (ethylene diamine tetraacetic acid) (2 ml 0.5M EDTA

pH8.0 per 100ml HBSS (Gibco), pre-warmed in water bath at 37°C), leaving the tube in water bath. After 15 minutes incubation (with vibration) in HBSS/EDTA, the intestine was taken out of the tube and transferred into another tube of pre-warmed HBSS/EDTA for further 15 minutes incubation with vibration. Tubes (0-15 minutes and 15-30 minutes fractions) were then spun down at 1,000 *g* for 15 minutes. The pellets were washed once with 10ml of PBS and then spun down again. For RNA extraction, pellet was resuspended in 1ml Trizol and stored at -80°C for following standard phenol-chloroform procedures. For protein, pellet was resuspended in 5 ml of PBS and spun down again at 1,000 *g* for 15 minutes. Pellets were then snap frozen in liquid nitrogen and stored at -80°C for following protein extraction procedures.

2.2.4.2 Preparation of samples for paraffin embedding

Tissue preparation and fixation were carried out by Dr Phesse and Dr Meniel in the University of Cardiff. Prepared tissue embedding in paraffin was carried out by Derek Scarborough in the University of Cardiff.

Gut rolls:

The intestine was placed onto one piece of Whatman 3MM filter paper and openedt up with the villi facing upwards. Samples were then wound into 'swiss rolls' (picked up with forceps at one end and then wound around and a needle placed through).

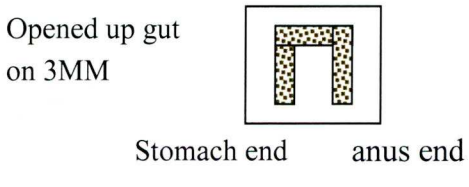

Gut parcels:

Murine intestine was removed and flushed with water, then cut into 3 x 1.5cm pieces. The 3 sections were arranged in a pyramid shape on 3M surgical tape and rolled into a bundle. The surgical tape prevented the gut from falling apart.

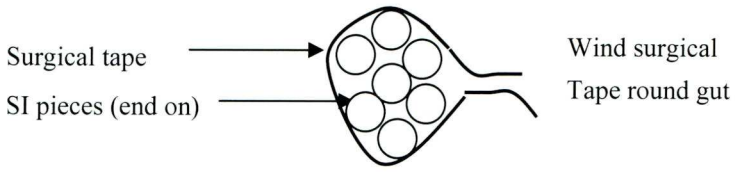

Tissue fixation

Opened up intestine was fixed for at least 3 hours to overnight in methacarn (4 parts methanol, 2 parts chloroform, 1 part acetic acid) in a glass dish before rolling up. Gut rolls were then stored in 70% ethanol or formalin prior to staining. For antibodies working better in formalin, gut rolls and parcels were fixed in ice cold 10% formalin (4% formaldehyde) for 12-24 hours and then embedded in paraffin as normal.

2.2.5 Histology staining

Histology staining was carried out by Derek Scarborough in the University of Cardiff. For all procedures, used sections were obtained from formalin-fixed, paraffin-embedded samples at a thickness of 5-10μm. Sections must not be allowed to dry out at any point in the procedure. Xylene and ethanol rehydration/ dehydration steps were carried out in a fume hood. Incubations are carried out in a humidified slide box, at room temperature unless otherwise stated. Standard steps of rehydration, dehydration, clearing and mounting are as below.

Rehydration

Wash slides 2 x 10 minutes in xylene

Wash 2 x 5 minutes in 100% ethanol

Wash 1 x 5 minutes in 95% ethanol

Wash 1 x 5 minutes in 75% ethanol

Wash in tap water 1x 2 minutes.

Dehydration

Wash slides 1 x 5 minutes in 75% ethanol

Wash 1 x 5 minutes in 95% ethanol

Wash 2 x 5 minutes in 100% ethanol

Wash 2 x 10 minutes in xylene

Mounting

Stained slides were mounted in DPX (distrene plasticiser and xylene) (Sigma). Place the coverslip on a flat surface and apply a small amount of DPX, making sure there are no bubbles. Slides were picked up and gently placed section side down onto a coated coverslip. the assembly was turned over and gently pressed down onto the coverslip with a blunt pencil until the DPX spread out to cover the whole section and the whole of the underneath of the coverslip. Slides were left on a level surface to dry for 48 hours.

Haematoxylin and Eosin staining

Slides were rehydrated as normal and then immersed in haematoxylin for 1 minute. Slides were rinsed in tap water with a continuous flow-through for 5 minutes and then immersed in eosin for 30 seconds. Slides were rinsed again in tap water for 5 minutes. Stained slides were then dehydrated, cleared and mounted as normal.

2.3 Tissue Culture

2.3.1 Maintenance of cell lines

The human colon adenocarcinoma cell line HT29 was provided by Dr. B. J. Campbell in Henry Wellcome Laboratory, Liverpool and HCT116 was obtained from John Hopkins Medical Institute, MD, USA. Cell lines were grown as monolayers (37°C in 5% CO2) in DMEM (HT29) and McCoy's 5A media (HCT116) supplemented with fœtal calf serum (FCS) (10% v/v) (Gibco), penicillin/streptomycin (50U/50μg per ml, Sigma), and L-glutamine (2 mM final conc., Sigma). Media were all supplied by Sigma. The cells were maintained by sub-culturing at 70-80% confluence using trypsin (50 μg/ml) (Sigma). HT29 carries mutant APC with wild type β-catenin and HCT116 carries wild type APC with mutant β-catenin (Din et al., 2004).

2.3.2 Sulforhodamine B cell growth assay

Cells from each treatment were seeded at a density of 1,000-3,000 cells per well (2,000 for HT29 cells and 1,000 for HCT116) in 96 well flat-bottomed plates and allowed to adhere overnight. Plates were then fixed from day 1 to day 7 post seeding. In the hood, cells were fixed with 100 μl per well of 3:1 methanol:glacial acetic acid for 5 minutes and washed gently with ddH_2O. Move out of hood, cells were then stained with 0.4% (w/v) sulforhodamine B (SRB) in 1% (v/v) glacial acetic acid for 30 minutes (100 μl per well), washed 3 times gently with 1% (v/v) glacial acetic acid and left to air dry for overnight. The dye was then solubilised by the addition of 100μl per well of 10 mM Tris-HCl pH 10.5, left for 5 minutes and the plates gently

agitated to disperse the dye. Plates were subsequently read at $A_{570\,nm}$ (absorbance at 570 nm) using a Tecan Sunrise absorbance microplate reader (Tecan, Reading,UK) and data analysed using XRead Plus v4.30 software.

2.3.3 Clonogenic cell survival assay

Cells from each treatment were seeded at a density of 1,000 cells (HCT116) per well or 2,000 cells (HT29) per well of 6-well plate in 2ml complete media. The cells were grown in complete media and incubated at 37°C for 10 days (HCT116) or 11 days (HT29). The media was discarded and the colonies fixed with 70% methanol (1ml) at room temperature for 5 minutes. The fixative was discarded and the cells stained with crystal violet solution (0.2%w/v in 70% methanol) (Sigma) for 5 minutes. The stain was removed by pipetting and the colonies washed gently (to avoid colony loss), by pipette, with tap water. The plates were air-dried overnight before colony counting (a colony was classed as a plaque of 50 or more cells). Colony counting was carried out independently by the author of this thesis and by another person (blinded to the experiment) to avoid experimenter/observer bias.

2.3.4 Harvesting cells for RNA extraction

The media was removed from the cultured cells, and the cells were washed once with PBS. The cells were trypsinized for 5-10 minutes in the incubator. Sufficient volume of media (5 ml for T25 flask, 2 ml for 6-well plate, 1 ml for 12-well plate) was then added into suspended cells and transferred to a 15 ml centrifuge tubes. The

cells were pelleted at 1,000 rpm for 5 minutes at 4°C using a IEC Multi-RF centrifuge (Thermo Electron Corporation). The supernatant media was removed by pipetting. 10ml of PBS was then used to wash the cell pellet and removed by centrifugation. Cell pellet were resuspended in lysis buffer (RLT buffer) provided in the RNeasy Kit (Qiagen) (2.6.1). The samples were stored at -80°C until processed for RNA extraction.

2.4 RNA work on human samples from tissue bank

2.4.1 RNA precipitation in sodium acetate

Ten μg of total RNA samples were supplied in 40 μl of ethanol at -80°C. One tenth volume (4μl) of 3M sodium acetate (Sigma), pH5.2, which is made up with DEPC (diethypyrocarbonate) treated water, was added into the total RNA samples, which were then incubated overnight at -80°C. On the following day, the incubated samples were centrifuged at 11,000 *g* at 4°C for 10 minutes. Ethanol was removed and RNA pellets were resuspended in 20μl of DEPC treated water at the concentration of 0.5μg/μl.

2.4.2 DNase digestion on human tissue total RNA samples

Since these total RNA samples provided by Cancer Tissue Bank Research Centre were not treated with DNase, DNase digestions were required to eliminate the genomic DNA contamination when the Taqman probe is designed from the 3' coding end rather than going through the exon/intron boundary of the nucleotide sequences of candidate genes, which is possible to amplify the contaminated genomic DNA in the RNA samples. DNase digestion on the patient RNA samples were performed by using TURBO DNA-*free*™ kit (Ambion). 2.5μg of total RNA sample (5μl of each aliquote) was treated with DNase in the reaction size of 25μl. 1μl of TURBO DNase (2U/μl), 2.5μl of 10X TURBO DNase buffer and 16.5μl of Nuclease-free water were added into the digestion reaction together with 5μl of total RNA, which was mixed gently and incubated at 37°C for 30 minutes. Then 2.5μl of DNase inactivation reagent was added into the above digestion reaction system.

After being incubated at room temperature for 2 minutes with occasionally mixing, the digestion reaction system was centrifuged at 10,000 *g* for 1.5 minutes. The supernatant that contains RNA was transferred into fresh tubes, which were stored at -20°C and ready to be used for 5 reactions of the following first strand cDNA synthesis.

2.4.3 First strand cDNA synthesis (Reverse iT ™, ABgene)

RNA with or without DNase digestion, which depends on the way of probe designing, was used to synthesize the first strand cDNA by using Reverse-iT™ 1st Strand Synthesis Kit (ABgene). For each 20 µl reverse transcription reaction, the following components were mixed firstly:

1 µl of RNA template (0.5 µg/µl)

1 µl of anchored oligo dT (500 ng/µl)

10 µl of RNase free water to make the reaction up to 12 µl

This 12 µl reaction system was heated at 70°C for 5 minutes and then placed on ice. Other components were added in when the reaction mixture was cooled down on ice.

4 µl of 5X first strand synthesis buffer

1 µl of DTT (100 mM)

2 µl of dNTPs (5 mM each)

1 µl of Reverse-iT™ RTase Blend (50 U/µl)

The final reaction system was incubated at 47°C for 50 minutes and 75°C for 10 minutes. The synthesised cDNA can be used to perform the real-time PCR amplification or stored at -20°C.

2.5 RNA work on mouse samples

2.5.1 RNA extraction in Trizol

Frozen mouse tissue samples in Trizol were defrosted on ice and then transferred into Lysing Matrix D tubes containing ceramic beads (MP Biomedicals). Samples were homogenised for 20 seconds each time (twice) on the homogenizer (Precellys 24). The homogenized samples were incubated on ice for 5 minutes to permit the complete dissociation of nucleoprotein complexes. Tubes were then spun at 10,000 *g* for 10 minutes at 4 °C and supernatant was transferred into clean tubes. 200 µl of chloroform was added into each tube and shaken vigorously for 15 seconds and incubated on ice for 10 minutes. Tubes were spun again for 15 minutes at 4 °C. The top clear aqueous phase (RNA) was carefully transferred into clean tubes (making sure no interphase material is transferred). RNA sample in each tube was then precipitated by mixing with 600 µl of isopropanol. Mixture was incubated from 2-3 hours to overnight at 4°C. Tubes were spun at 10,000 *g* for 15 minutes at 4°C. Supernatant was then carefully removed without touching the pellet. Pellet was washed with 500 µl of cold 75% ethanol. Supernatant was removed and pellet was air-dried for 5-10 minutes. 100 µl of RNase-free water was used to dissolve pellet by 10 minutes incubation at 65°C on heating block. 2-5 µl of RNA was run on 2% w/v

agarose gel to check sample quality. RNA samples were then quantified using nanodrop spectrophotometer.

2.5.2 RNA quantification (Nanodrop)

With the sampling arm open, 2 µl of RNA sample (or RNase free water as the reference) was added onto the lower measurement pedestal. The sampling arm was then closed and the operating software was used to initiate a spectral measurement. Sample concentrations were then calculated by the software.

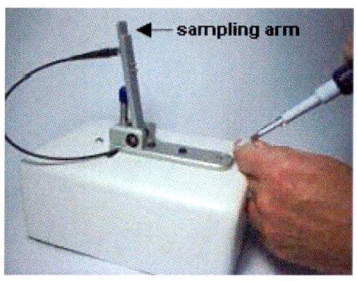

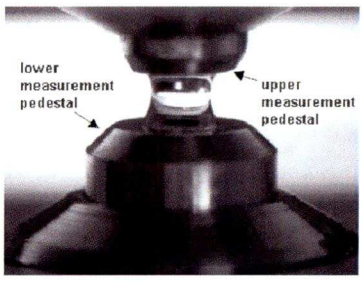

http://www.molcardiology.com/index.php?option=com_content&view=article&id=55:working-with-nanodropr-nd-1000-spectrophotometer&catid=46:micrornas-extraction&Itemid=56

2.5.3 DNase Digestion (Promega)

For 50 µl reaction system, 5 µl of RQ1 buffer and 10 µl of RQ1 enzyme were added onto 10 µg of total RNA in required volume of RNase-free water to make up to be 50 µl. The mixture was heated at 30°C for 30 minutes on heating block. Afterwards, 5 µl of stop solution was added into the 50 µl reaction and heated at 65 °C for 10 minutes. The DNased RNA samples were ready to be used in following experimentations.

2.5.4 First strand cDNA synthesis (Invitrogen)

For 25 µl reverse transcription reaction

4 µl of 100 ng/µl Random Hexamers

4 µl of 5X First-Strand Buffer

2 µl of 0.1M DTT

0.8 µl of 25mM dNTP

7.5 µl of DNase treated RNA template

5.7 µl of ddH2O

Mixture was heated in water bath at 65°C for 5 minutes then put back on ice. 1µl of SSII (superscript II reverse transcriptase) was then added into the mixture. Tubes were heated on PCR machine, 25°C for 10 minutes; 42°C for 1 hour; 70°C for 15 minutes and hold at 4°C. 200 µl of ddH2O was added into 25 µl of cDNA to make it to be at working concentration.

2.6 RNA work on human cell samples

2.6.1 RNA extraction with DNase treatment (QIAgen)

Cells were harvested as a cell pellet and lysed in 350 µl of RLT buffer (2.3.4). Lysate was homogenized using QIAshredder spin column by full speed centrifugation for 2 minutes at 4°C. One volume of ethanol was added into the homogenized lysate and mixed well. Mixture was then spun down in RNeasy spin column at 10,000 *g* for 15 seconds at 4°C to let total RNA bind onto the spin column. Spin column was washed twice with 350 µl of RW1 buffer by centrifugation at 10,000 *g* for 15 seconds at 4°C. Genomic DNA contamination was eliminated using RNase-Free DNase Set. Total RNA binding on the spin column was treated with 10 µl of DNase I stock solution by 25 minutes incubation at room temperature in between the two RW1 washes. Total RNA on spin column was then washed with 500 µl of RPE buffer (at 10,000 *g* for 15 seconds at 4°C). A long centrifugation (at 10,000 *g* for 2 minutes at 4°C) was used to dry the spin column membrane to ensure no residual ethanol remains. Total RNA samples were then eluted in 30µl of RNase-free water by centrifugation at 10,000 *g* 1 minute at 4°C. DNase treated total RNA samples from human cells were then stored at -80°C for following experimentations.

2.6.2 RNA quantification (Spectrophotometer)

RNA (5 µl) was added to RNase-free water (995 µl) and the sample analysed at A_{260nm} and A_{280nm} using the UV/VIS Spectrophotometer (UVP). RNase-free water alone was used as the reference. An absorbance of 1 is equal to 40 µg of RNA, therefore the concentration was calculated using the following formula:

RNA conc. (μg/ml) = A_{260nm} x 40 x dilution factor

The purity of RNA was calculated by the absorbance ratio A_{260nm}/A_{280nm}; where pure RNA exhibits a ratio of 1.9-2.1.

2.6.3 First strand cDNA synthesis (Verso ™, ABgene)

Quantified DNase treated total RNA was used to synthesize the first strand cDNA using Verso™ cDNA Kit (ABgene). For each 20 μl reverse transcription reaction, the following components were mixed:

4 μl of 5X cDNA synthesis buffer

2 μl of dNTP mix (5 mM each)

1 μl of anchored oligo dT (500 ng/μl)

1 μl of Verso™ reverse transcriptase

1 μl of RNA template (0.5 μg/μl)

11 μl of RNase free water to make the reaction up to 20 μl

Reactions were performed to the following conditions: 1 cycle at 42°C for 30 minutes and 1 cycle at 95°C for 2 minutes. The synthesised cDNA can be stored at -20°C for the real-time PCR amplification.

2.7 Real-time quantitative PCR

2.7.1 Taqman real-time quantitative PCR

2.7.1.1 Taqman Reaction Principle

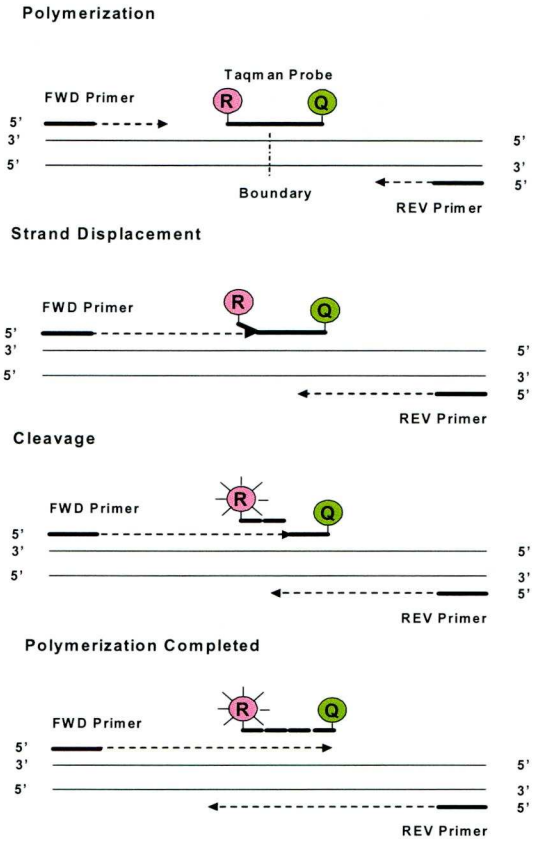

In the Taqman real-time PCR reaction, the 3' end of the Taqman probe is always blocked, so it is not extended during the PCR reaction. When both dyes are attached to the probe, reporter dye emission is quenched due to fluorescence energy transfer from the reporter (FAM) to the quencher (TAMRA). During each extension cycle, the probe is displaced at the 5' end by the DNA polymerase. The 5' exonuclease activity of the polymerase cleaves the probe, releasing the reporter dye from the probe. Once separated from the quencher, the reporter dye emits its characteristic fluorescence. The whole process repeats in every cycle. The fluorescence intensity of

the reporter dye, as a result increases. The amount of fluorescence measured is proportional to the amount of PCR product made.

2.7.1.2 Primers and Taqman probe designing

Taqman primers and probes were designed by using the Primer Express program (Applied Biosystems), which should be specific to the candidate genes on NCBI Nucleotide-BLAST search. When the primers and probes being designed, the G/C content should be between 30% and 80%, which can be done automatically by the Primer Express program when the item of 'limit G/C content' is chosen. In all the designing of primers and probes, Tm (melting temperature) of the primer sets should be 10°C lower than the Tm of the probe that should be 70 °C.

2.7.1.3 Primers and probe optimisation

Before performing the Taqman real-time PCR assays on the RNA samples of human colon cancer tissues from Cancer Tissue Bank Research Centre, the designed and synthesised primers and probes (Eurogentec) were required to be optimised on the RNA samples of colon cancer cell lines. HCT116 colon cancer cell RNA samples were provided by Dr. Andrea Davies, which was used to optimise the sets of primers and probes.

The Taqman real-time PCR reactions were set up by using the qPCR Core Kit (Eurogentec), which components will be listed in the following part of Taqman real-

time PCR amplification. The ABI PRISM 7700 real-time PCR machine was used to run and record the reactions, and to analysis the data of qPCR reactions. The optimisation protocol was provided by Applied Biosystems. For the primer optimisation, probes were firstly used at the concentration of 200nM for all combinations of primers at the final concentrations in nM.

50 FWD / 50 REV	**50 FWD / 300 REV**	**50 FWD / 900 REV**
300 FWD / 50 REV	**300 FWD / 300 REV**	**300 FWD / 900 REV**
900 FWD / 50 REV	**900 FWD / 300 REV**	**900 FWD / 900 REV**

Secondly, probes were optimised with the above optimised primers at the final concentration in nM.

25	**50**	**75**	**100**	**125**	**150**	**175**	**200**	**225**

For all the optimisation experiments, each reaction was set up in triplicate, and the combination which gives the both lowest Ct (threshold cycle) value and highest Rn (normalized reporter signal) value was chosen to precede the following experimentation. All the sets of primers and probes of candidate genes in the optimised concentrations (in nM) were tested by using a series of increasing cDNA concentrations. A serial dilution of cDNA template of 0.25 µl, 0.5 µl and 1 µl were used to assess the efficiencies of both the target gene and reference gene amplifications being approximately equal.

2.7.1.4 PCR Amplification reaction

The expression levels of candidate genes were determined by performing Taqman real-time PCR amplification on the first strand cDNA template from the DNase treated or untreated total RNA samples of patients. Each reaction was set up in triplicate.

For each 25 µl real-time PCR reaction, the components are listed below:

2.5 µl of 10X reaction buffer

2.5 µl of 50mM $MgCl_2$

1 µl of 5mM dNTP Mix

0.5 µl of optimised primers

0.5 µl of optimised probe

0.5 µl of cDNA template from reverse transcription

0.125 µl of HotGoldStar PCR enzyme (5U/µl)

17.325 µl of molecular water (Sigma)

The thermal amplification conditions are as below:

1 cycle at 50°C for 2 minutes (enzyme activation); 1 cycle at 95°C for 10 minutes (cDNA and primers denaturation); 40 cycles at 95°C for 15 seconds and at 60°C for 1 minute (amplification).

Primers and probe optimisations of candidate genes on HCT116 colon cancer cell line and genomic DNA control test after DNase digestions were also performed by applying the same amplification reaction system.

2.7.2 SYBR Green real-time quantitative PCR

2.7.2.1 SYBR Green Reaction Principle

The SYBR Green I dye binds onto double-stranded DNA. During the extension phase, the dye binds to the newly synthesized DNA and exhibits enhanced fluorescence which increases proportionally to the amount of the amplicon (the target mRNA) present. The products detected by SYBR Green I can be analysed by a dissociation curve (or melting curve). As the reaction being heated, the point at which the double stranded DNA denatures (or melts) is observed as a drop in fluorescence as the SYBR Green I dissociates. Different length products and products of different sequences will melt at different temperature and be observed as distinct peaks.

2.7.2.2 Primers design (Primer3)

Primers for SYBR Green real-time qPCR were designed and optimised by Dr T. Phesse using Primer3 programme and manufactured in Sigma. Primers for detecting recombined Apc were kindly provided by Dr K. Reed.

m Myc Fwd 5'-TGA GCC CCT AGT GCT GCA T-3'

Rev 5'-AGC CCG ACT CCG ACC TCT T-3'

m Axin2 Fwd 5'-GCT CCA GAA GAT CAC AAA GAG C-3'

Rev 5'-AGC TTT GAG CCT TCA GCA TC-3'

m CD44 Fwd 5'-GGC AGA AGA AAA AGC TGG TG-3'

Rev 5'-TCT GGG GTC TCT GAT GGT TC-3'

m Her2 Fwd 5'-AAT GCC AGC CTC TCA TTC CT-3'

Rev 5'-CCA GGG CAT ACT TGT CCT CA-3'

m EGR2 Fwd 5'- GGG AGA TGG CAT GAT CAA CA-3'

Rev 5'-TGG AGA ATT TGC CCA TGT AA-3'

m βActin Fwd 5'-ACA GCT TCT TTG CAG CTC CTT-3'

Rev 5'-TGG TAA CAA TGC CAT GTT CAA T-3'

m ApcRec Fwd 5'-TTG ATG GAA TGT GCT TTG GAA-3'

Rev 5'-CAC AAG GCT TCC TGG TCT TT-3'

2.7.2.3 SYBR Green PCR Amplification - I

The SYBR real-time PCR reactions were set up by using the FINNZYMES master mix. The MJ Research Chromo 4 real-time PCR machine was used to run and record the reactions, and to analysis the data of qPCR reactions by Opticon Monitor 3 Software.

For each 28μl of SYBR green PCR reaction, the components are listed as below:

12.5 μl of SYBR Master Mix

6 μl of cDNA template from reverse transcription

2.5 μl of paired primers (10μM of each)

7 μl of ddH_20

The thermal amplification conditions are as below:

1 cycle at 95°C for 15 minutes; 40 cycles at 95°C for 30 seconds, 60°C for 30 seconds, 72°C for 30 seconds; 1 cycle from 53°C to 95°C for dissociation curve generation.

2.7.2.4 SYBR Green PCR Amplification- II

The SYBR Green real-time PCR reactions were set up by using the Eurogentec qPCR Core Kit for SYBR Green I, which components will be listed in the following part of real-time PCR amplification. The ABI PRISM 7700 real-time PCR machine was used to run and record the reactions, and to analysis the data of qPCR reactions. For each 25 μl real-time PCR reaction, the components are listed below:

2.5 μl of 10x Buffer

1.75 μl of 50mM MgCl2

1 μl of 5mM dNTP

0.125 μl of HotGoldStar polymerase (5U/μl)

0.75 μl of SYBR Green I

0.5 μl of template cDNA template from reverse transcription

0.5 μl of Paired Primers (10μM for each)

17.875 μl of ddH_2O

The thermal amplification conditions are as below:

1 cycle at 95°C for 10 minutes; 40 cycles at 95°C for15 seconds and 60°C for 1 minute.

Dissociation curve were generated separately on ABI PRISM 7700 real-time PCR machine: 1 cycle at 95 °C for 15 seconds; 1 cycle at 60 °C for 20 seconds; 1 cycle from 60 °C to 95 °C for 20 minutes; 1 cycle at 95 °C for 15 seconds.

2.8 Semi-quantitative PCR

2.8.1 PCR amplification

The PCR amplification cycles of the mouse β-actin gene were used to standardize the concentration of cDNA samples. When the amounts of the β-actin PCR products of all the samples were equal, cDNA concentration was halved and doubled in order to confirm that the chosen amplification cycles were within the exponential phase. The normalised volume of cDNA for each sample was then used to amplify *Cited1*, whose exponential amplification curve was also evaluated. Amplification products were run out on 2% w/v agarose gels. The density of each band was measured by densitometry and the tumour samples were normalised to the non-adenomatous tissue from the same mouse resulting in arbitrary density units for each tumour sample. The primers used were as below. The sequences of mouse β-actin primers were kindly provided by Dr T. Phesse and the mouse Cited1 primers were obtained from the published work of S. Boyle (Boyle et al., 2007).

mouse β-actin FWD 5'-ACA GCT TCT TTG CAG CTC CTT-3'

REV 5'-TGG TAA CAA TGC CAT GTT CAA T-3'

mouse Cited1 FWD 5'-GCA CTT GAT GTC AAG GGT GG-3',

REV 5'-GAG AGA CAG ATC CCG GAG AC-3'.

For each 50 μl β-actin PCR reaction, the components are listed below:

5 μl of 10X Buffer

5 μl of 25 mM $MgCl_2$

0.4 μl of 25 mM dNTP

0.1 μl of 10 μM Forward Primer

0.1 μl of 10 μM Reverse Primer

0.4 μl of Go Taq Polymerase (5 U/μl)

1 μl of cDNA template from reverse transcription

38 μl of H_2O

The thermal amplification conditions of mouse β-actin are as below:

1 cycle at 94°C for 2.5 minutes; 30 cycles at 94°C for 30 seconds, 60°C for 30 seconds, 72°C for 1 minute; 1 cycle of 72°C for 5 minutes; Hold at 4°C.

For each 20 μl *Cited1* PCR reaction, the components are listed below:

4 μl of 5X Phusion HF Buffer

0.4 μl of 10 mM dNTP

1 μl of 10 μM Forward Primer

1 μl of 10 μM Reverse Primer

1 μl of cDNA template from reverse transcription

0.2μl of Phusion Taq Polymerase (2 U /μl)

12.4 μl of H_2O

The thermal amplification conditions are as below:

1 cycle at 98°C for 1 minute; 28 cycles at 98°C for 10 seconds, 60°C for 30 seconds, 72°C for 30 seconds; 1 cycle at 72°C for 5 minutes; Hold at 4°C.

2.8.2 DNA agarose gel electrophoresis

PCR products were detected by performing DNA agarose gel electrophoresis. 2% Agarose gel was made up with 2 g of agarose (Sigma) in 100 ml of 1X TAE buffer (50X TAE buffer: 242g of Tris base (Sigma); 57.1 ml of acetic acid (Fisher Scientific) and 18.6g of EDTA (Sigma) in 1L of dH_2O, pH 8.5). 5µl of ethidium bromide (10 mg/ml) was added into the gel to stain the DNA samples. Five µl of Hyper Ladder IV (Bioline) and 10 µl of DNA sample (2 µl of 5X loading buffer and 8 µl of PCR product) were loaded onto the gel, which was running for 50 minutes at 100 volts. Samples in the gel were visualised by employing Quantity One™ program (BioRad) on FX scanner.

2.8.3 Densitometry

The density of bands from western blotting assay and agarose gel electrophoresis assay were measured using Quantity One™ software. The area of each band from the assays was measured individually. Band density of each sample was then normalised to the corresponding internal control (e.g. β-actin).

2.9 RNA interference (RNAi)

2.9.1 Principle of lipid-mediated siRNA transfection

Cationic lipid mediated transfection is one of the most common delivery methods and cationic lipid-based transfection reagents are suitable for transfecting into dividing cell cultures (De Paula et al., 2007; Gilmore et al., 2004). In cationic lipid mediated transfection, siRNA interact with the cell membrane in the form of an siRNA:lipid complex, a partly hydrophobic, partly hydrophilic, detergent-like structure held together by electrostatic forces between the positive charges lipids and negatively charged siRNAs (De Paula et al., 2007; Gilmore et al., 2004). Although the mechanistic details of this form of transfection are poorly understood, current models suggest that siRNA:lipid complexes enter cells by way of enhanced adsorptive endocytosis and allow escape of the nucleic acid from endosomal/lysosomal vesicles by membrane destabilisation (De Paula et al., 2007; Gilmore et al., 2004).

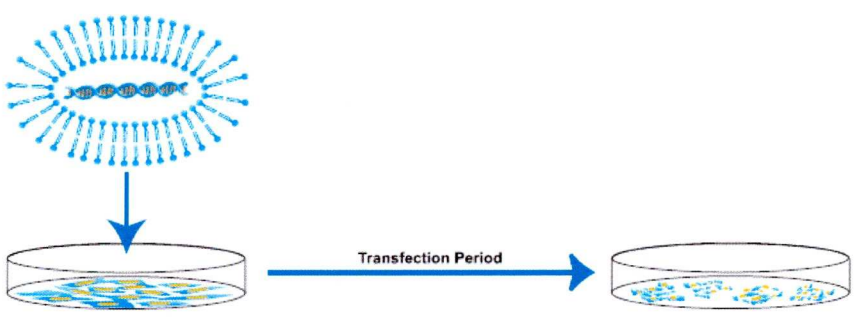

Adapted from RNA interference: Technical reference & Application guide

RNA interference

RNA interference technologies provide the possibility of a more rapid genetic manipulation *in vitro* and *in vivo* at the level of gene transcription and consequent protein translation (Kumar and Clarke, 2007; Martin and Caplen, 2007). RNA interference (RNAi) is a gene-silencing mechanism induced by double-stranded RNA (dsRNA) and can silence gene expression at both a transcriptional and post-transcriptional level, which involves in cellular antiviral responses, transposon expansion and post-transcriptional regulation of endogenous gene expression (Hannon, 2002; Martin and Caplen, 2007; McManus and Sharp, 2002; Tuschl, 2001; Zamore, 2001). The mechanism of gene silencing was first noted in plants in 1990 (Napoli et al., 1990). The major understandings of the mechanisms underlying RNAi were identified in *C. elegans* by dsRNA injection (Fire et al., 1998; Kumar and Clarke, 2007) and subsequently found to explain previous observations in plants and fungi (Martin and Caplen, 2007; Nakayashiki et al., 2006; Vaucheret, 2006).

The appearance of these dsRNAs (>30-50bp) induces a cascade of events involving the initial recognition of cytoplasmic RNase III-like protein Dicer (Kumar and Clarke, 2007; Martin and Caplen, 2007). Dicer is responsible for cleaving double-stranded molecules into small inhibitory or interfering RNA duplexes (siRNA) of 21-23 base pairs with characteristic 3' overhangs of 2nt (dinucleotide) (Bernstein et al., 2001; Elbashir et al., 2001; Martin and Caplen, 2007). Processed siRNA is then incorporated into RISC (RNA Induced Silencing Complex) in cytosol (De Paula et

al., 2007; Gilmore et al., 2004). Dicer is also involved in the early steps of RISC formation and may be required for siRNA entry into RISC (De Paula et al., 2007; Lee et al., 2004). The antisense RNA strand is then guided by RISC complex to the complementary sequence in target mRNA (Gilmore et al., 2004). In mammalian cells, the protein Argonaute 2 (Ago2) is the catalytic component of RISC that cleaves target mRNAs (De Paula et al., 2007; Liu et al., 2004; Meister et al., 2004). The RISC can undergo numerous cycles of mRNA cleavage that comprise the high efficiency of RNAi (De Paula et al., 2007; Elbashir et al., 2001; Meister and Tuschl, 2004). The target gene expression is then inhibited that subsequently reduce the level of the encoded protein translation. Therefore, RNA interference can be a powerful tool for investigating the gene-specific functions (Martin and Caplen, 2007).

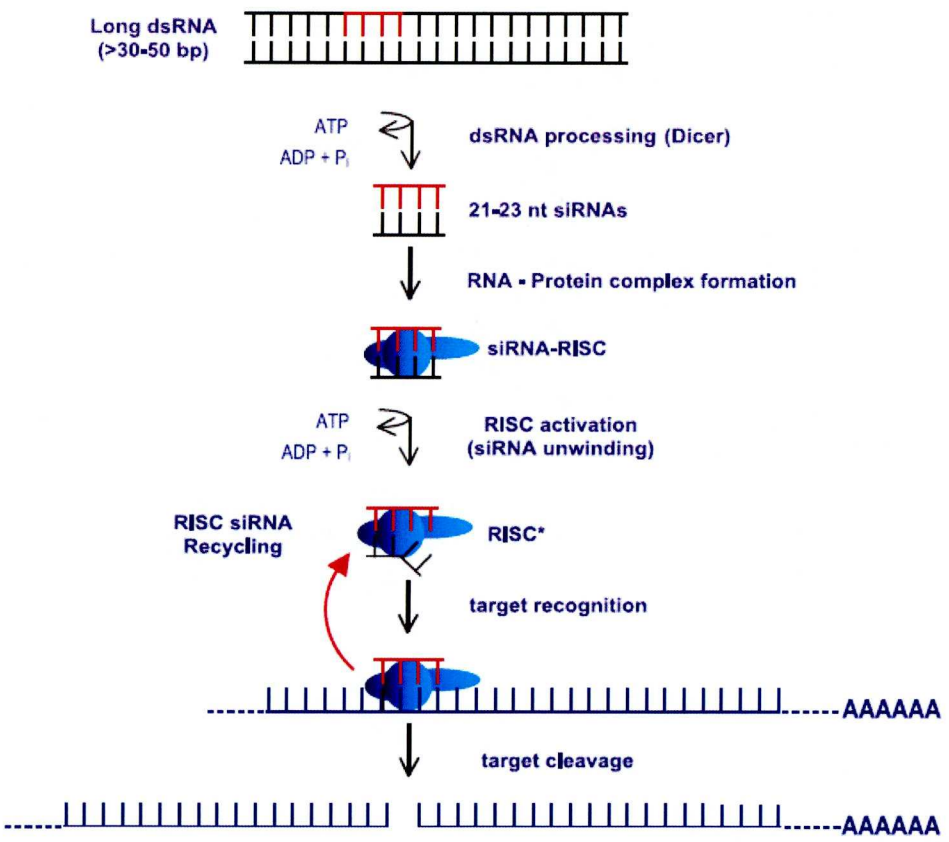

Schematic diagram of the mechanism of RNA interference. Adapted from RNA interference: Technical reference & Application guide. See text for details.

2.9.2 siRNA transfection optimisation

2.9.2.1 siRNA transfection optimisation in HCT116 cell line

The transfection protocol (DharmaFect 1) of HCT116 cells was optimised using the si*TOX* transfection control. si*TOX* is a cytotoxic, RNA-based reagent and triggers an apoptotic response within 24-72 hours once entering the cells. Matrices of siRNA:lipid concentrations and cell densities for use in 96-well plate format were employed for optimisation. HCT116 cells were seeded in 96-well plates. On the following day, si*TOX* (or non-target siRNA) were mixed with transfection lipid in a series of siRNA:lipid ratio, according to the manufacturers suggested guidelines. After an additional 24 or 48 hours incubation, cell surviving transfection with si*TOX* (or non-target siRNA) were then quantified for all cultures using AlamarBlue™ dye (BioSource, Inc.).

AlamarBlue™ assay incorporates an oxidation-reduction (REDOX) indicator based on detection of metabolic activity. The colour of the dye changed in response to chemical reduction of growth medium, resulting from cell growth. Plates were subsequently read at A_{570nm} (absorbance at 570nm) and A_{595nm} (absorbance at 595nm) using a Tecan Sunrise absorbance microplate reader (Tecan) and data analysed using XRead Plus v4.30 software.

To determine the percent reduction of AlamarBlue™ dye:

%Reduced = C_{RED} Test Well / C_{OX} Negative Control Well

$$= [(\epsilon_{OX})\ \lambda_2\ A\lambda_1 - (\epsilon_{OX})\ \lambda_1\ A\lambda_2 / (\epsilon_{RED})\ \lambda_1\ A'\lambda_2 - (\epsilon_{RED})\ \lambda_2\ A'\lambda_1] \times 100$$

The lowest concentration of the experimental siRNA that includes the greatest amount of silencing with the least amount of cell death is the desired concentration.

Optimisation of the conditions for inhibitory siRNA transfection of HCT116 cell line

It is important to optimise experimental conditions of lipid-mediated siRNA transfection to achieve effective silencing while minimizing toxicity. In this procedure, the viables are: transfection reagent (lipid) type, siRNA type, concentration, siRNA:lipid ratio, cell density, transfection incubation time for different cell lines. HCT116 cell line is not among the previously validated protocols from Dharmacon and there is no detailed protocol available in the literature. Therefore, a thorough optimisation of CITED1 siRNA transfection in HCT116 cell line was required. Due to the time limit, some of the siRNA knock-down optimisation was tested once as the preliminary experiment.

Selection of siRNA and transfection reagent (lipid)

A number of companies provide the pre-designed siRNA to known genes in human genome. We selected siRNA together with transfection reagent from Dharmacon. Human CITED1 siGENOME SMARTpool siRNA is a pool of 4 siRNA duplexes.

The standard negative control of siGENOME Non-Targeting siRNA Pool #2 was used in parallel. In addition, the transfection efficiency control si*TOX* was also used in the optimisation procedure. si*TOX* is a cytotoxic, RNA-based reagent and triggers an apoptotic response within 24-72 hours of entering the cells. It therefore is well suited for monitoring siRNA delivery and uptake. The precise mechanism of si*TOX* activity is not well understood, although it is thought to participate in a variety of pathways that likely converge to induce global cell death (company information).

Due to the cell type characteristics, different types of lipid (transfection reagent) may induce greater or less cell viability and transfection efficiencies. Whilst there is no detailed literature concerning which transfection reagent, a number mention that they have been successful using DharmaFECT1. Therefore, DharmaFECT1 was chosen to be the first choice in terms of the transfection reagent type.

Optimisation of siRNA:lipid ratio of siRNA transfection in HCT116 cell line in 96-well plate format by AlamarBlue assay

The ratio of siRNA: lipid was firstly optimised. Several possible cell densities and incubation time were included in the design, in order to ensure the best siRNA: lipid ratio can be detected in the provided conditions. The results of siRNA treatment of cultured cells in multi-well plate may differ from format to format, however the 96-well plate was initially used in the optimisation, because it allows siRNA:lipid ratio, cell density and transfection incubation time all to be tested on one plate. The resultant AlamarBlue^{TM} dye provided a measure of metabolic activity. The rate of

loss of colour in the medium is proportional to the metabolic activity, when added into culture medium. Therefore, AlamarBlue™ assay was used to detect cell viability.

Experimental design of the matrices of siRNA: lipid ratio in 96-well format

Several conditions were included therefore an explanation of the 96-well matrix is required. The layout of the experimental design on the 96-well plate format is shown as below (Figure 2.1 A).

The siRNA transfection controls and the AlamarBlue™ assay controls were both considered. A1, A2 and A3 are the wells with 100 µl of culture medium but with no cells, which is used as the negative control for the AlamarBlue™ assay (Figure 2.1 A). A4, A5 and A6 are the blank wells that are used to zero the plate reader when the absorbance of the AlamarBlue™ dye was measured (Figure 2.1 A).

siRNA transfection in all the wells was performed in the same way using DharmaFECT1. One hundred nM of siRNA was used with a series of lipid volumes. In this optimisation, there are 3 groups of siRNA treatment: no siRNA (water) (Figure 2.1B), si*TOX* positive control (Figure 4.5C) and non-target siRNA negative control (Figure 2.1D). In each group, the tested lipid volumes are 0.1 µl, 0.2 µl, 0.4 µl and 0.8 µl per 100 µl culture medium to cover the routine range of lipid dose in 96-well plate (Figure 2.1 B-D). Different cell densities are 5K, 10K, and 25K cells

per well, in duplicate. Two separate plates were used for 24 hours and 48 hours incubation time.

A

	1	2	3	4	5	6	7	8	9	10	11	12
A	NC	NC	NC				5k	5k	10k	10k	25k	25k
B	5K	5K	10K	10K	25K	25K	5k	5k	10k	10k	25k	25k
C	5K	5K	10K	10K	25K	25K	5k	5k	10k	10k	25k	25k
D	5K	5K	10K	10K	25K	25K	5K	5K	10K	10K	25K	25K
E	5K	5K	10K	10K	25K	25K	5k	5k	10k	10k	25k	25k
F	5K	5K	10K	10K	25K	25K	5k	5k	10k	10k	25k	25k
G	5K	5K	10K	10K	25K	25K	5k	5k	10k	10k	25k	25k
H	5k	5k	10k	10k	25k	25k	5k	5k	10k	10k	25k	25k

No siRNA (water) and a series of lipid volumes

B

No lipid	5K	5K	10K	10K	25K	25K
0.1μl	5K	5K	10K	10K	25K	25K
0.2μl	5K	5K	10K	10K	25K	25K
0.4μl	5K	5K	10K	10K	25K	25K
0.8μl	5K	5K	10K	10K	25K	25K

siTOX – single concentration with a series of lipid volumes

C

No lipid	5K	5K	10K	10K	25K	25K
0.1μl	5K	5K	10K	10K	25K	25K
0.2μl	5K	5K	10K	10K	25K	25K
0.4μl	5K	5K	10K	10K	25K	25K
0.8μl	5K	5K	10K	10K	25K	25K

siGENOME Non-target siRNA–single concentration with a series of lipid volumes

D

No lipid	5K	5K	10K	10K	25K	25K
0.1μl	5K	5K	10K	10K	25K	25K
0.2μl	5K	5K	10K	10K	25K	25K
0.4μl	5K	5K	10K	10K	25K	25K
0.8μl	5K	5K	10K	10K	25K	25K

Figure 2.1 The experimental design of siRNA: lipid ratio optimisation using AlamarBlue™ assay in HCT116 cells on the 96-well cell culture plate. Three different siRNA treatments were tested with a series of transfection lipid volumes. The area in green on the pate indicates the no siRNA control (B). The area in blue indicates the si*TOX* transfection efficiency control (C). The area in yellow indicates the siGENOME non-target siRNA control (D) Three cell densities of 5K, 10K and 25K were seeded into wells in duplicate, together with the controls of blank wells (A4-A6) and no cell wells (A1-A3).

Establishment of siRNA:lipid ratio

The criteria for this optimisation are to identify the lowest cell viability in si*TOX* treatment with minimal reduction of cell viability in the no siRNA control (water) and siGENOME non-target siRNA control. AlamarBlue™ assay detects the colour loss of the dye in medium, which in turn reflects the percentage of viable cells.

The absorbance of the dye was measured after 24 hours and 48 hours transfection incubation. Standard curve for each time point was generated from cells with no treatment on the plate in order to verify the incubation time for the validity of the assay. At each time point, the measurement of each well is normalised to the no treatment control.

At 24 hour time point, the assay is not sensitive at 5K cell density, because the standard curve does not show much colour loss of the dye after being added into medium (figure 2.2A). The valid dye incubation time is 75 minutes, when the dye colour loss was the quickest for both 10K and 25K cells. In figure 2.2C, transfection with 0.1μl of lipid induces the lowest level of cell viability in si*TOX* treatment and the much higher level of both no siRNA and non target siRNA controls. The difference between si*TOX* and the other 2 controls is the largest for 10K cells.

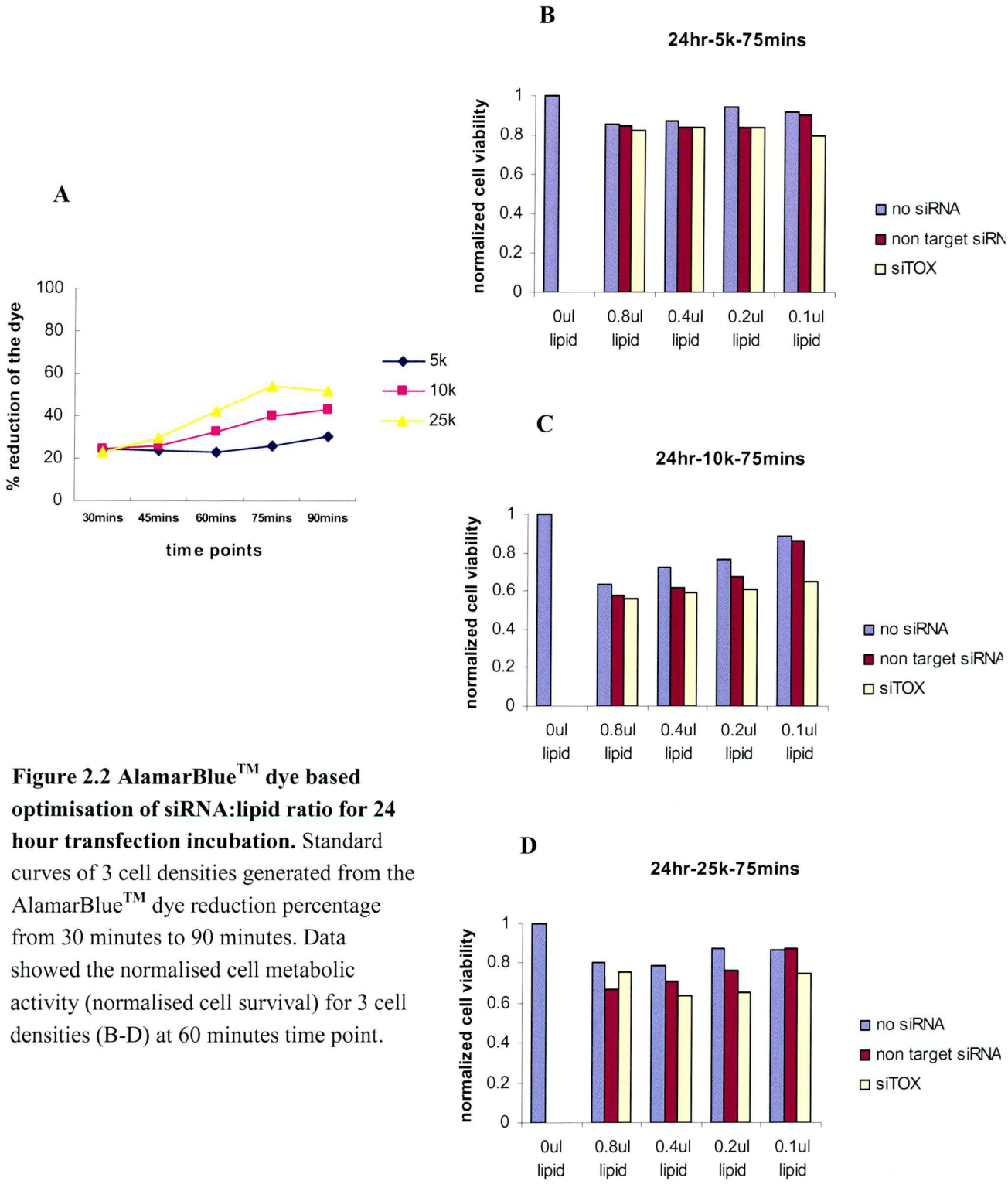

Figure 2.2 AlamarBlue™ dye based optimisation of siRNA:lipid ratio for 24 hour transfection incubation. Standard curves of 3 cell densities generated from the AlamarBlue™ dye reduction percentage from 30 minutes to 90 minutes. Data showed the normalised cell metabolic activity (normalised cell survival) for 3 cell densities (B-D) at 60 minutes time point.

The 48-hour transfection incubation results in a higher cell confluence at the end point than 24 hours, although cells were originally seeded at the same densities in 2 separate 96-well plates. At 48hour time point, the valid dye incubation time is 60 minutes considering all 3 cell densities. The cell viability difference is still large between si*TOX* and non-target siRNA control when being transfected with 0.1 μl of lipid in 10K cells. However, the lipid only control induced a higher toxicity to cells, which must merely result from the exploration to transfection lipid for a longer time.

Although there was limitation of AlamarBlue™ assay on cell numbers, I conclude from these experiments that the optimum lipid concentration is 0.1 μl per 100 μl transfection medium. This condition was used for all the following experiments of siRNA transfection in HCT116 cell line.

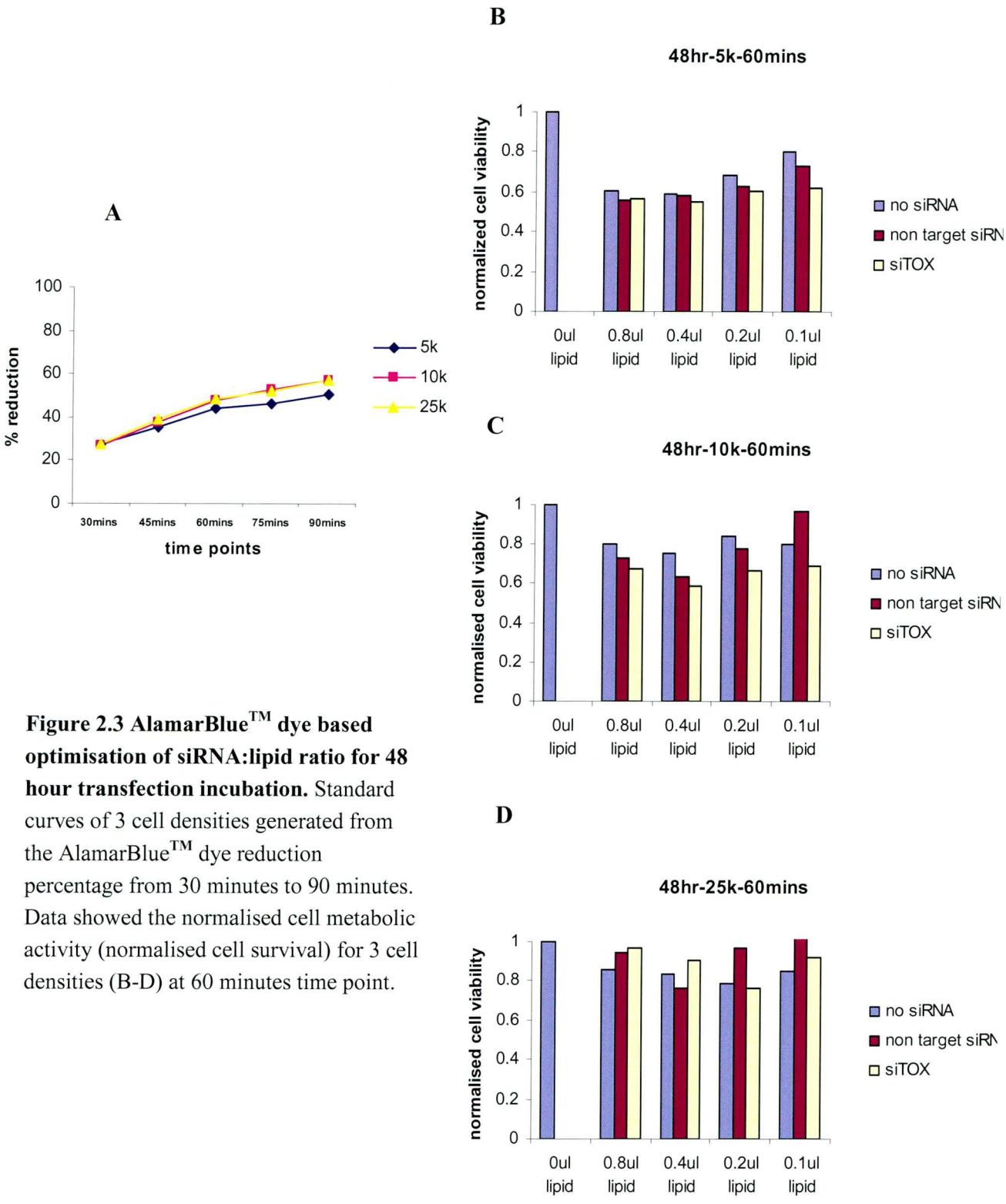

Figure 2.3 AlamarBlue™ dye based optimisation of siRNA:lipid ratio for 48 hour transfection incubation. Standard curves of 3 cell densities generated from the AlamarBlue™ dye reduction percentage from 30 minutes to 90 minutes. Data showed the normalised cell metabolic activity (normalised cell survival) for 3 cell densities (B-D) at 60 minutes time point.

Optimisation of cell density and incubation time of siRNA transfection in HCT116 cell line in 6-well plate format

In order to obtain sufficient material for detecting the gene silencing effect at mRNA level, siRNA transfection in HCT116 cells needed to be scaled up from 96-well to 6-well format. The established siRNA: lipid ratio was also scaled up based on the volume of transfection medium in 6-well format. For siRNA transfection, cell density and incubation time needed to be determined and therefore a 2 by 2 combination of experiments were performed in this format.

siRNA inhibitory effect was measured by qPCR. Clonogenic and SRB assays were then used to detect the cell growth post siRNA transfection. In these two assays, cell numbers have already been determined in the laboratory protocols.

Experimental design of optimisation of cell density and incubation time

Cell densities were scaled up based on the space of the well surface. The transfection conditions may vary over this transformation, because the parameters were scaled up based on volume or well space. Compared with the range from 5K to 10K, there is a greater cell density gap between 10K to 25K in 96-well format optimisation. Cell density of 15K needs to be considered to be a closer density to 10K in the following tests.

In the 6-well plate, cell densities were scaled up to 200K (equivalent to 10K in 96-well plate) and 300K (equivalent to 15K in 96-well plate) per well. Incubation time

of 24 hour and 48 hour was tested with the HCT116 cells. Therefore, 4 sets of experiments were performed in terms of different parameter combinations.

In each set of experiment, blank control (no treatment to cells), lipid only control (no siRNA), nontarget siRNA control and si*TOX* control were performed together with the target CITED1 siRNA test. For clonogenic and SRB assays, treatment conditions are as described above, 200K, 300K; it is important to note that from these different treatment populations only 1,000 cells per well were used.

Establishment of cell density and incubation time by CITED1 siRNA inhibitory effect on mRNA

The normalised *CITED1* mRNA expression levels were all dramatically reduced by CITED1 target siRNA treatment in 4 sets of experiments (figure 2.4 A-D). However, *CITED1* mRNA expressions were also reduced in the lipid only control and non-target control in 2 sets of 24 hour transfection experiments (figure 2.4 A-B). In 48 hour siRNA transfection, lipid only control increased the *CITED1* level for about 60%, although the non-target control is similar to the blank control in 200K cell density (figure 2.4 C). In figure 4.7 D, *CITED1* mRNA expression level in lipid only control and non-target siRNA control were both similar to the blank control and the dramatic inhibition of *CITED1* mRNA cellular expression by target siRNA. Therefore, the optimal siRNA transfection conditions in HCT116 cell line are 48 hour siRNA transfection in 300K cell density determined by mRNA expression inhibition.

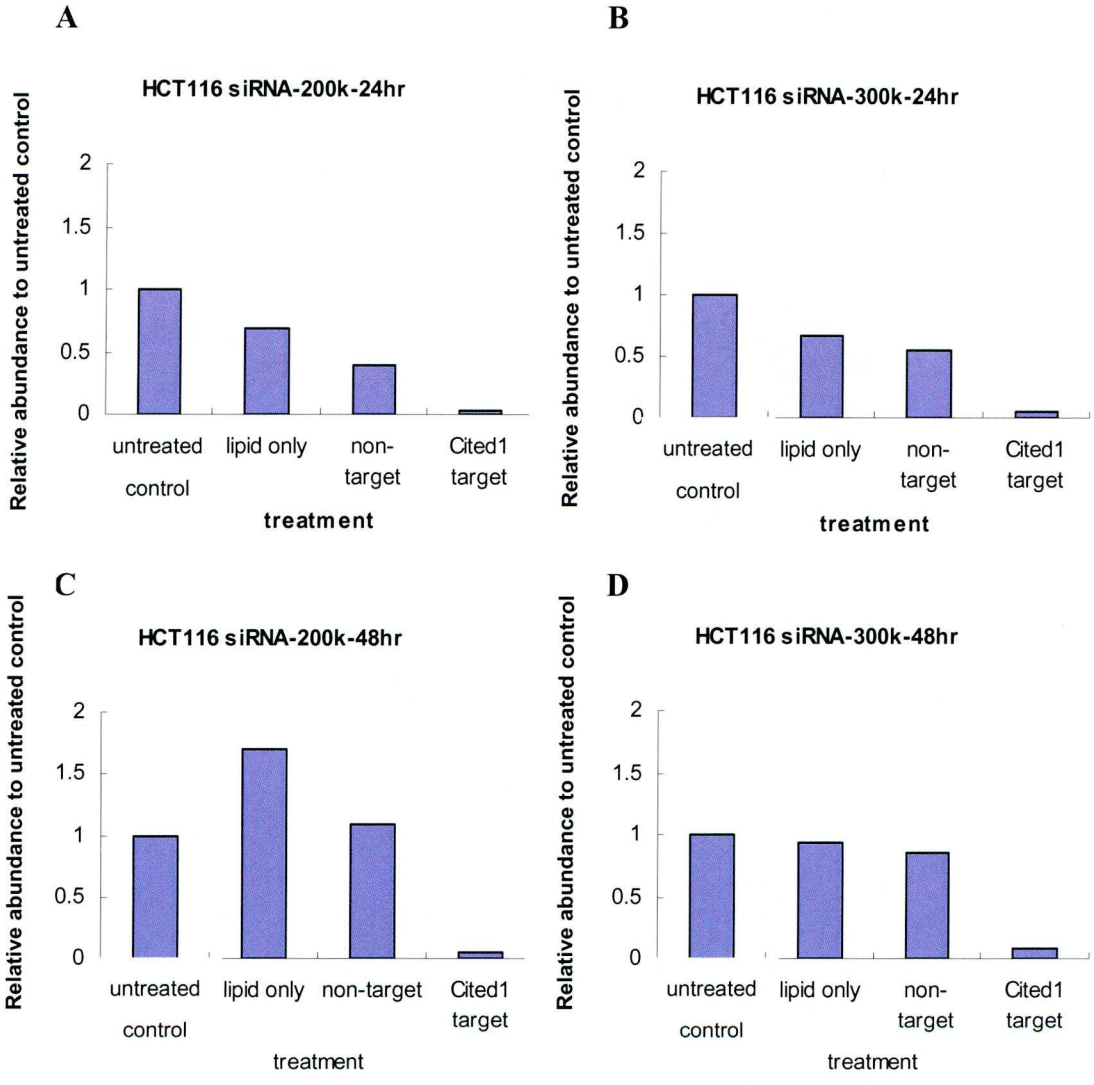

Figure 2.4 Effect of siRNA transfection on *CITED1* mRNA abundance in the preliminary tests on HCT116 cells in 6-well plate. Cell densities of 200K (A, C) and 300K (B, D) and incubation time of 24 (A, B) and 48 hours (C, D) were tested.

Confirmation of established cell density and incubation time by siRNA inhibitory effect on cell growth

The cell growth assays were used to confirm the established cell density and incubation time of siRNA transfection for HCT116 cell line. In SRB proliferation assay, the si*TOX* control showed a more prolonged low level of proliferation over 7 days after 48 hour transfection, which indicates a higher functional transfection efficiency (figure 2.5 C-D). After 48 hour transfection, the proliferation curve of target siRNA treatment in 300K cell density is slightly lower than 200K cell density (figure 2.5 C-D). Similarly, in clonogenic assay, si*TOX* induced a lower level of cell survival after 48 hour transfection by counting the colony forming units (2.5 C-D). Cell colonies of non-target control are slightly less in 200K cell density compared with the non-target control in 300K cell density after 48 hour transfection (figure 2.5 C-D). Therefore, 48 hour siRNA transfection in 300K cell density is confirmed to be the optimal conditions for HCT116 cell line.

Due to the time limitation, optimisation experiments were only performed once. Taken qPCR, SRB and clonogenic assay together, data consistently showed that 300K cells per well in 6-well plate and 48 hours transfection incubation were the best conditions for siRNA transfection in HCT116 cell line. So far, siRNA:lipid ratio, cell density and incubation time of this siRNA transfection experiment have been optimised.

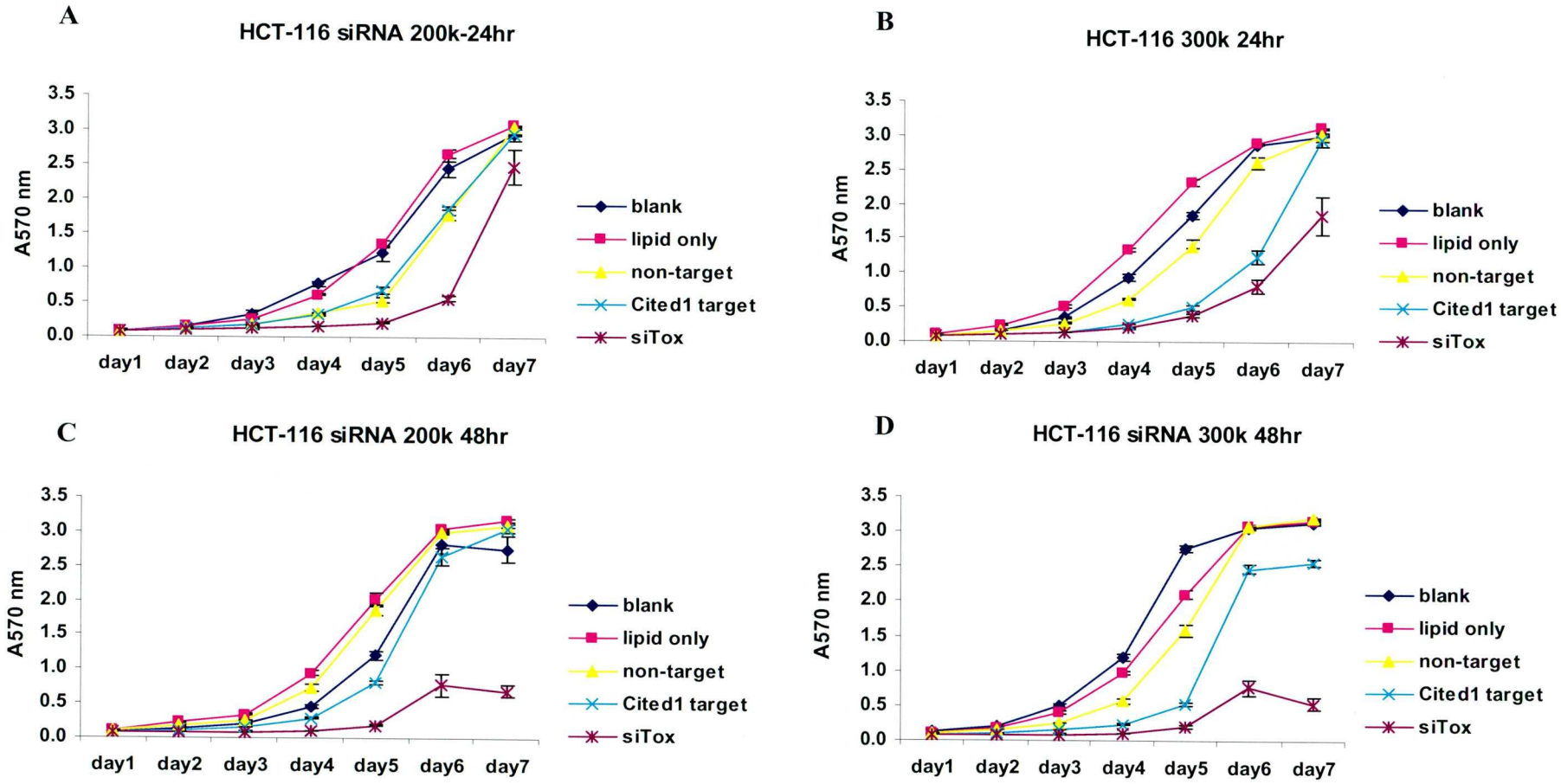

Figure 2.5 Cell viability (by SRB cell proliferation assay) was being measured in the preliminary test on HCT116 cells in 6-well plate. Cell densities of 200K (A, C) and 300K (B, D) and incubation time of 24 hours (A,B) and 48 hours (C, D) were tested. The error bars stand for the standard error of the mean (SEM).

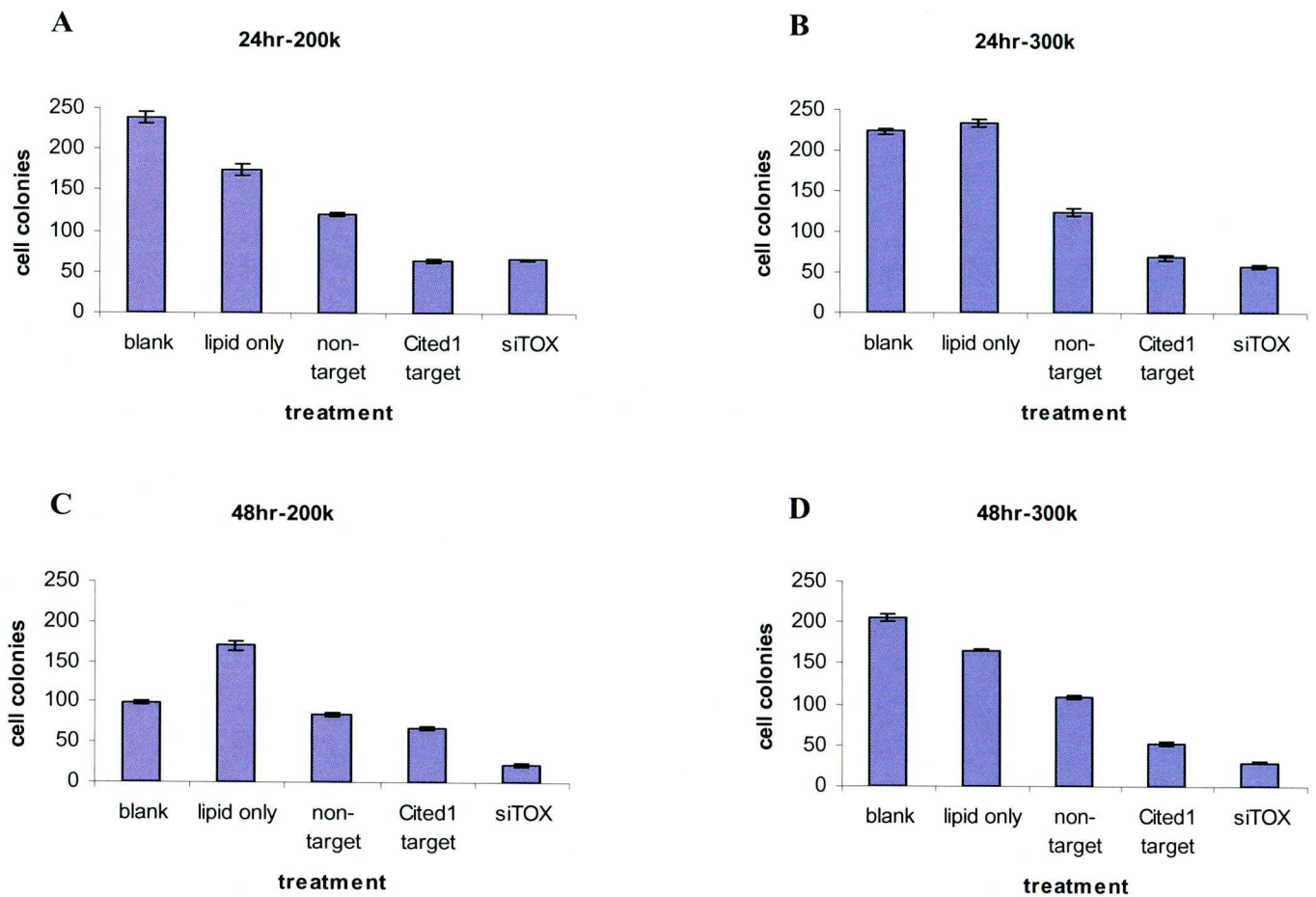

Figure 2.6 Cell viability (by clonogenic cell survival assay) was being measured in the preliminary test in HCT116 cells in 6-well plate. Cell densities of 200K (A, C) and 300K (B, D) and incubation time of 24 hours (A, B) and 48 hours (C, D) were tested.

Off target effect of non-target siRNA control

Knowing that CITED1 is a co-activator of transcriptional complex, it was interesting to detect whether knocking down CITED1 in HCT116 cells has an effect on expression of target gene transcriptions regulated by Wnt signalling. Axin2 (c-Myc dependent) and CD44 (c-Myc independent) have been identified as Wnt downstream targets.

When *CITED1* mRNA expression was inhibited, *Axin2* was dramatically over-expressed and CD44 expression level was slightly increased. However, in the non-target siRNA control, *Axin2* mRNA expression was decreased at 70% compared with the lipid only control, which indicates a strong off-target effect of this non-target siRNA on *Axin2* (Figure 4.11 A). This off-target effect was also observed in the other 3 sets of experiments (Figure 4.11 B-D). Therefore, this is not dependent on cell density or incubation time over the transfection.

Although there is no off target effect of non-target siRNA control on *CITED1* gene, in a perfect condition, the non-target siRNA will not have any effect on known genes. However, I found that non-target siRNA have an off target effect on one of the identified Wnt targets. Therefore this needed to be eliminated before we carried on the actual experiments on CITED1 inhibition.

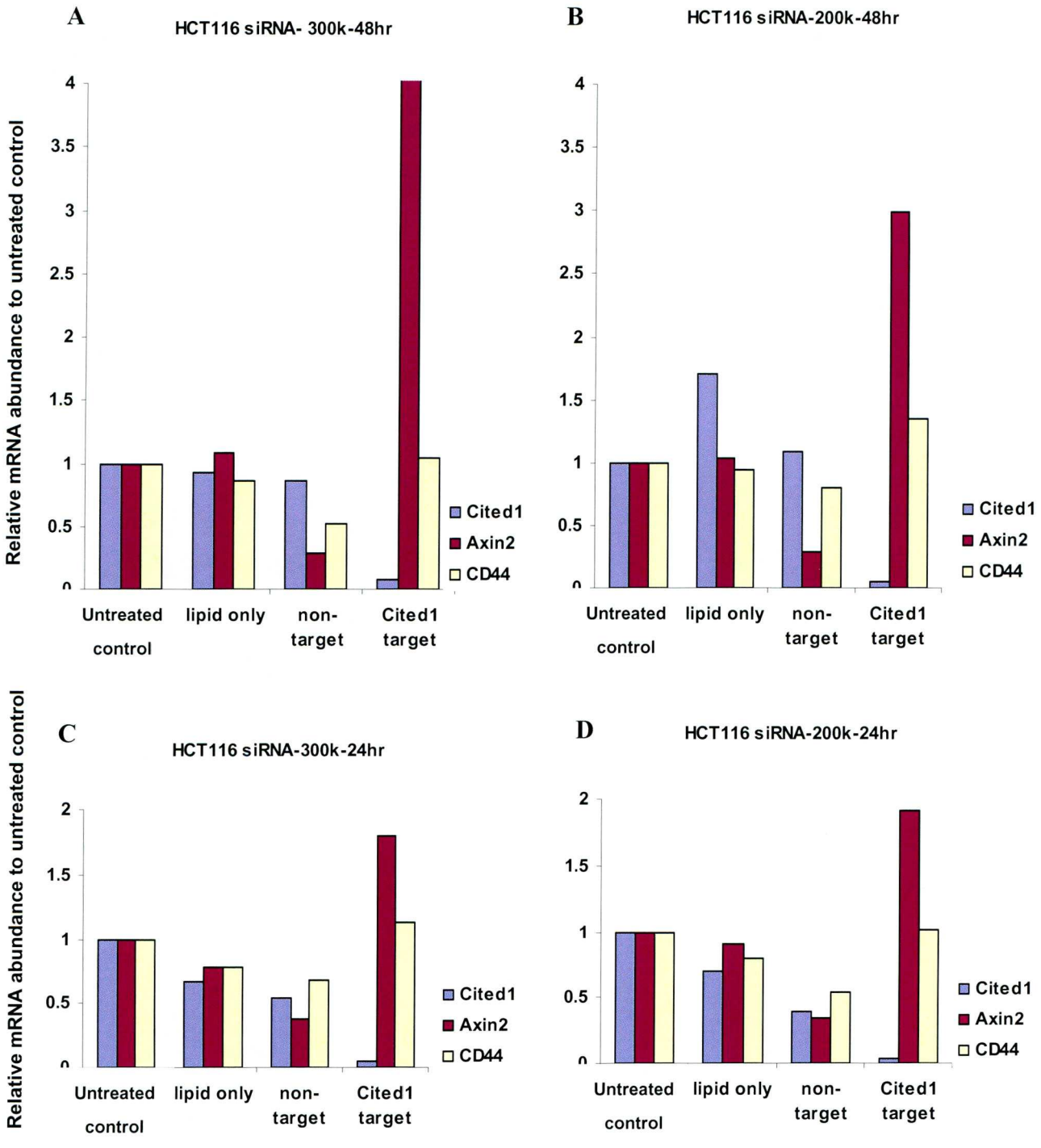

Figure 2.7 Off-target effect of siGENOME non-target siRNA control on Axin2 in HCT116 cell line.

Resolving off-target effect issues

Axin2 is a component of the Wnt signalling pathway in cytoplasm and closely related to the Wnt regulated nuclear transcription. The reduction of Axin2 in the siGENOME non-target control may result in an unexpected alteration of this pathway, which could be phenotype related. Therefore the siGENOME non-target control needs to be replaced with another siRNA product.

In order to reduce off-target effects and therefore to enhance siRNA specificity, I then selected ON-TARGETplus siRNA from Dharmacon. The new pair of siRNA has the only modification pattern that addresses off-target effects caused by both strands (Jackson et al., 2006). Sense strand is modified to prevent interaction with RISC and favors antisense strand uptake. Additional modification is applied on the antisense strand seed region to minimize seed-related off-targeting (personal communication with Dharmacon company).

The pair of ON-TARGETplus non-target and target siRNA was used instead of the siGENOME duplexes in the optimised conditions in HCT116 cells. qPCR data showed the inhibition of *CITED1* mRNA expression in target siRNA with no obvious off-target effect in non-target siRNA control (figure 4.12). Up to this step, the thorough optimisation of *CITED1* siRNA transfection in HCT116 cell line was accomplished. The optimised transfection conditions were then used in all the following cell assays in HCT116 cell line.

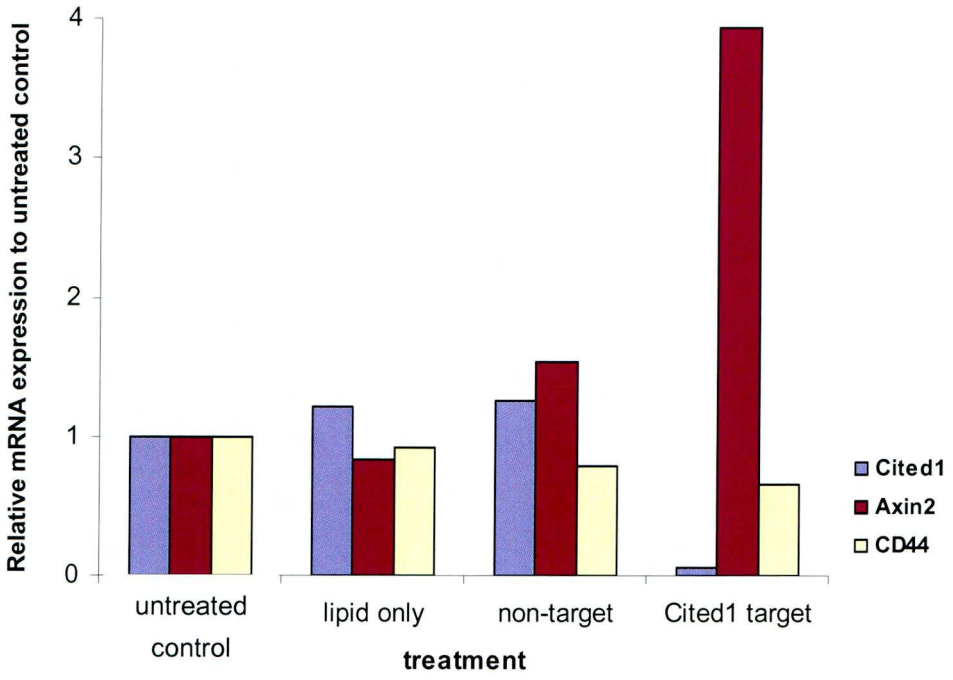

Figure 2.8 Reduction of *CITED1* using ON-TARGET plus siRNA pair at optimised conditions in HCT116 cell line.

2.9.2.2 siRNA transfection conditions in HT29 cell line

The optimised protocol (DharmaFect 2) of siRNA transfection in HT29 colon cancer cells was provided in a 96-well plate format from Dharmacon. In my experiments, 96-well plate was converted to 12-well plate format in the larger scale experiment.

2.9.3 Lipid-mediated siRNA delivery into cultured cells

Cultured colon cancer cells were used at low passage number. Lipid-mediated siRNA transfection was performed following the recommended procedure from. Cell density, type of lipid and siRNA, siRNA:lipid ratio, transfection incubation time differ among several colon cancer cell lines.

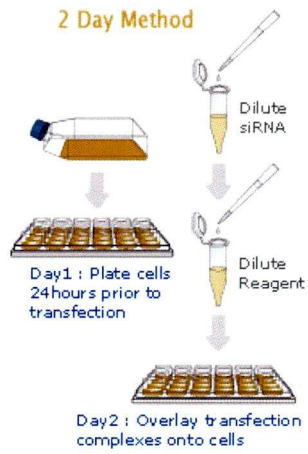

Taking HT29 cells as an example, cells were grown in T75 flask until 70-80% confluence in complete media. Twenty four hours prior to transfection, cells were trypsinized, counted and seeded in antibiotic-free media, at the density of 50,000 cells per well in 12-well plate. The following day, 5µl of 20µM siRNA was diluted in 95µl of antibiotic-free and serum-free media (Tube1) and 4µl of Dharmafect 4 transfection reagent was diluted in 96µl of antibiotic-free and serum-free media (Tube2). Both tubes were incubated for 5 minutes at room temperature by pipetting carefully up and down. Tube1 and Tube2 were then combined and incubated for a further 20 minutes at room temperature. Media in cultured cells were removed and replaced with 800µl of fresh antibiotic-free media

whilst siRNA lipid complex was being incubated. When the siRNA transfection lipid complex was ready, the mixture was added into the freshly changed medium. Cells were then incubated for 48 hours at 37°C with 5% CO_2 until being harvested.

Cell line	Multi-well plate Format	Cell Density	Type of lipid	Lipid Volume	siRNA Volume	Incubation Volume
HT29	12-well plate	50K per well	DharmaFect 4	4μl	5μl	1000μl
HCT116	6-well plate	300K per well	DharmaFect 1	4μl	10μl	2000μl

Blank (no-treatment), transfection reagent only (lipid only) and non-target siRNA controls were also performed in parallel. Lipid only control was used to detect the siRNA delivery into cells efficiently with minimal disruption of cellular function. Non-target siRNA control was a duplex which lacks sufficient homology with any known gene. Gene silencing effect on the target mRNA was detected by Taqman quantitative PCR.

2.10 Protein Analysis

2.10.1 Western Blotting

Protein Extraction from mouse tissue

Mouse tissues were harvested, snap frozen in liquid nitrogen and stored at -80 °C (2.2.4). 200µl of RIPA lysis buffer (for 100ml stock: 50mM Tris-HCl pH 7.5, 150mM sodium chloride, 1% Nonidet P40, 0.5% sodium deoxycholate and 0.1% SDS in ultrapure water; protease and phosphotase inhibitors were added just prior to use) was added to each tissue sample and then left in buffer to defrost. Once defrosted, sample tubes were transferred on ice. Tissue was homogenised on ice using Eppendorf homogenizer for 10 minutes and then the mixture of tissue and buffer was sheared by passing through 21G or 23G needle for 20 times. Tubes were spun down at 10,000 *g* for 10 minutes at 4°C. The supernatant of cell lysates was then quantified.

Protein Estimation and Sample Preparation:

Total protein estimations were performed using the Bradford Assay technique (Bradford 1976). 1 µl of lysate was mixed with ddH_2O (159 µl) and Bradford Assay Solution (BioRad) (40 µl) and loaded (final volume of 200 µl) into a 96-well plate. The plate was read at A_{595nm} absorbance using the Tecan Sunrise microplate reader (Tecan). Data was analysed using the XRead Plus v4.30 software. The absorbance readings of the unknown protein concentrations were interpolated against a BSA (bovine serum albumin) standard curve: - 0, 1, 2, 3, 5, 8 and 10 µl of BSA stock

solution (1 mg/ml). The protein samples were adjusted to a concentration of 10 μg protein/μl using RIPA Buffer.

Tewnty five μg total protein of sample lysate was mixed with 5X sample loading buffer (2% w/v SDS, 0.125M Tris-base HCl pH6.8, 0.001% w/v bromophenol blue, 10% v/v glycerol) with β-mercaptoethanol (one fourth volume of loading buffer), vortexed briefly, and heated at 95°C for 5 minutes. The samples were brought to room temperature and spun down briefly prior to gel loading.

SDS-Polyacrylamide Gel Electrophoresis (SDS-PAGE):

The denatured protein samples (prepared as above) were separated by SDS-PAGE (western blotting) using the MINI PROTEAN™ (BioRad) gel casts. A 12% resolving gel (10ml final volume) was prepared by combining ddH_2O (3.35 ml), 1.5M Tris-base HCl pH8.8 (2.5ml), 10% w/v SDS (100 μl), 30% acrylamide (4.0 ml) (Sigma), 10% w/v APS (ammonium persulphate) (50 μl) and TEMED (5 μl) (Sigma). The gel components were mixed thoroughly by inverting and poured immediately into the vertical gel cast. Saturated butanol (1:9 parts ddH_2O: butanol) (~500 μl) was overlaid (to prevent a meniscus forming) and allowed to set for ~45 minutes. The butanol was washed off thoroughly with water, and the excess water removed with blotting paper. A 4% stacking gel (10 ml final volume) was prepared by combining ddH_2O (6.1 ml), 0.5M Tris-base pH6.8 (2.5 ml), 10% w/v SDS (100 μl), 30% acrylamide (1.33 ml) (Sigma), 10% w/v APS (ammonium persulphate) (50

μl) and TEMED (10 μl) (Sigma). The gel components were mixed thoroughly by inverting and poured immediately over the resolving gel. The comb was inserted carefully avoiding trapping any bubbles at the bottom of the teeth. The stacking gel was allowed to set for 30 minutes. The comb was removed and the protein samples loaded into the wells and run at constant voltage (100 V) in Running Buffer (14.4 g glycine, 3.03 g Tris-base, 10 ml 10% w/v SDS, and make it up to 1 litre with ddH_2O).

Western Blotting:

The SDS-PAGE separated proteins were transferred to a Protran® nitrocellulose membrane (Shneiller & Shneider) using Transfer Buffer (14.4 g glycine, 3.03 g Tris-base, 200 ml MeOH and make it up with 1 litre of ddH_2O) for 1 hour at constant voltage (100 V). The membranes were stained with Ponceau S solution (5% w/v in glacial acetic acid) (Sigma) to verify success of protein transfer. The Ponceau S stain was washed off with either PBS or TBS buffer depending on the recommended antibody probing buffer. Membranes were blocked (5% w/v non-fat dried milk powder in either 0.1% TBS- or PBS-Tween 20 for 1 hour with constant agitation, to reduce background non-specific binding, prior to antibody probing.

Western Blot Analysis:

Primary antibodies were added to the membranes (p-mad,1:1000 in 0.1% TBS-Tween; β-actin, 1:2000 in PBS- Tween) and incubated with constant agitation for

either 1 hour at room temperature (β-actin), or overnight at 4°C (p-smad2). The membranes were washed three times (5 minutes each wash) with constant agitation using the appropriate wash buffer (PBS or TBS). The HRP-conjugated secondary antibody was incubated at room temperature for 1 hour with constant agitation. The membranes were washed three times (5 minutes each wash) with constant agitation using the appropriate wash buffer prior to developing.

The above described blots were developed using SuperSignal® West Dura Extended Duration Substrate (Pierce) and the images captured on the Fluor-S MultiImager System (BioRad) using the QuantityOne™ software (BioRad).

2.10.2 Immuno-histochemistry

Tissue sections for immuno-histochemistry were prepared as described in histology staining (2.2.5). Xylene and ethanol rehydration/ dehydration steps were carried out in the same way (2.2.5). Sections were all counterstained with haematoxylin. Immuno-histochemistry procedures for the following antigens differ between the rehydration and dehydration steps.

β-catenin (BD transduction Laboratories)

Endogenous peroxidase activity was blocked in peroxidase buffer with 1.5% hydrogen peroxide (83.2 g of citric acid, 215.2 g of disodium hydrogen phosphate 2-

hydrate, 20 g of sodium azide in 20 litres stock) for 30 minutes. Sections were then boiled in Tris EDTA buffer pH 8.0 (242 g Tris and 18.6 g EDTA in 1 litre stock) for 50 minutes. Once boiled, sections were slowly cooled down in solution. Sections were then blocked in 1% w/v BSA in PBS for 30 minutes and stained with 1:50 anti-β-catenin primary antibody (BD transduction Laboratories) in 1% w/v BSA in PBS at 4°C overnight. After washing 3 times in PBS, mouse HRP-labelled polymer (Envision plus Dako) was applied on sections for 1 hour. After washing another 3 times in PBS, peroxidase was then developed with DAB (Dako).

Phosphorylated Smad2 (Cell Signaling Technology)

Antigen was retrieved in 10 mM citric acid buffer pH 6.0 (Sigma) for 15 minutes (5 minutes each time, 3 times) in microwave. Sections were then allowed to cool for 30 minutes in solution. Endogenous peroxidase was blocked in 3% hydrogen peroxide solution (Sigma) in water for 20 minutes. After washing twice in water and once in TBS-Tween, sections were blocked in 5% v/v normal goat serum in 0.1% TBS-Tween for 40 minutes. 1:500 anti-p smad2 primary antibody in 5% v/v goat serum in 0.1% TBS-Tween was applied on sections overnight at 4°C. After washing 3 times in TBS-Tween, 1:200 HRP-conjugated goat anti-rabbit secondary antibody (Dako) in 5% v/v goat serum in 0.1% TBS-Tween was applied on sections for 1 hour followed by washing 3 times in TBS-Tween. ABC complex (Vector Labs) was applied on sections for 30 minutes. After washing twice in TBS-Tween, sections were then stained with DAB (0.07% w/v plus 0.3% hydrogen peroxide) (Sigma) for 5 minutes.

BrdU (BD transduction Laboratories)

Antigen was retrieved in 1X citrate buffer (Labvision 10X stock) in preheated solution at 99°C in water bath for 20 minutes. Sections were then cooled down in solution for 30 minutes. Endogenous peroxidase activity was then blocked in hydrogen peroxide solution (Envision plus, Dako) for 20 minutes. After washing 3 times in PBS, sections were blocked in 1% w/v BSA in PBS for 30 minutes and stained with 1:150 of anti-BrdU (BD transduction Laboratories) primary antibody in 1% BSA in PBS overnight at 4°C. After washing 3 times in PBS, sections were incubated with mouse HRP-labelled polymer (Envision plus, Dako) for 1 hour followed by washing 3 times in PBS. ABC complex (Vector Labs) solution was then applied on sections for 7 minutes. After washing 3 times in PBS, peroxidase was then developed with DAB (Dako).

Active caspase3 (R&D Systems)

Endogenous peroxidase activity was blocked in 0.3% hydrogen peroxide (Sigma) in methanol for 45 seconds with constant agitation in between 100% and 90% ethanol rehydration steps. After washing once in distilled water and twice in PBS, antigen was retrieved in 10 mM citric acid buffer, pH 6.0 (Sigma) for 20 minutes in microwave. Sections were left in the microwave heated solution for 10 minutes and then slowly rinsed in running tap water. After washing twice in PBS, sections were blocked with 10% v/v normal goat serum in 0.5% TBS-Tween for 45 minutes. The

solution was removed and sections were then incubated with 1:750 active caspase-3 (R&D Systems) in 10% v/v goat serum in 0.5% TBS-Tween overnight at 4 ^{o}C. After washing twice in TBS-Tween, sections were incubated with 1:200 biotin-labelled goat anti-rabbit secondary antibody (Dako) in 5% v/v goat serum in 0.5% TBS-Tween for 45 minutes. After washing twice more in TBS-Tween, ABC complex (Vector Labs) was applied on sections for 20 minutes followed by another twice washing in TBS-Tween. Sections were then briefly rinsed in PBS and stained with DAB (Dako) for 5 minutes.

2.11 Mouse small intestine crypt scoring

The effect of insults on the intestine was assessed by distribution of apoptotic and mitotic bodies in the crypt on histological sections. The Potten laboratory generated a computer model called "WinCrypts" (Merritt *et al.*, 1996). Here the cells were counted sequentially from the bottom of the crypt (cell position 1) towards the neck and along the villus. Each cell was assigned as BrdU negative (value "1"), BrdU positive (value "2"). The data was used to generate a graphical representation of the percentage population of apoptotic or mitotic cells (y-axis) versus their crypt location (x-axis).

2.12 Statistical Analysis

Comparison between the median of a single column of data against a hypothetical median was performed on relative fold changes of candidate gene expressions in human colorectal tumours using Wilcoxon Signed Rank Test (GraphPad PRISM for Windows v4). Pairwise comparison of treatment means of delta Ct, the cell survival and the proliferation data following siRNA treatment of human colon cancer cell lines were performed post Kruskal-Wallis non-parametric analysis of variancet (ANOVA) (StatsDirect v2.6.8). In the *in vivo Cited1* knock out studies, comparison of medians of delta Ct data sets and tumour burden between mouse cohorts were performed using Mann-Whitney U test (MiniTab for Windows v15). Comparison of median life span of murine cohorts was performed on survival percentage using Kaplan Meier method and analysed by Chi-square test (GraphPad PRISM for Windows v4). Comparison of maximum vertical distance of cell proliferation was performed on cumulative frequency between mouse cohorts using the Kolmogorov-Smirnov test (Sokal and Rohl, 1981). P values, where applicable, were assigned to indicate statistical significance ($P<0.05$ = * ; $P<0.01$ = ** ; $P<0.001$ = ***). Error bars indicate standard error of the mean (SEM).

Chapter 3 Gene validation from early colorectal cancer mouse models to the human disease

3.1 Introduction

Loss of APC in the Cre-*lox* regulated *APC* floxed mice model ($APC^{fl/fl}$) activated Wnt signalling pathway through the nuclear accumulation of β-catenin with the coincident alteration of crypt-villus architecture, differentiation, migration, proliferation and apoptosis (Sansom et al., 2004). In order to test whether the nuclear translocation of β-catenin following loss of *APC* activated the transcription of known and unknown Wnt target genes, microarray analysis were performed using the Affymetrix chips (Sansom et al., 2004). From these results of microarray analysis, a subset of dysregulated genes were also validated and confirmed by performing immunohistochemistry in the Apc-deficient tissue (Sansom et al., 2004). In this project, we aimed to determine whether genes that have previously been identified as dysreglated following deletion of *Apc* in mice, also showed altered expression in human colorectal cancers.

Top dysregulated target genes from the *Apc* conditional K/O mouse model

Following the preliminary work on the Cre-*lox*P *Apc* mice model in Clarke's group, we validated a subset of 21 candidate genes that were significantly up-regulated following loss of *Apc* in mice. These top 21 genes were the highest up-regulated as seen from the DNA microarray analysis, the majority of which were over-expressed at least 4-fold after losing *Apc* in mice. In murine tissues, these 21 genes had already

been validated by quantitative PCR and immuno-histochemistry to confirm the findings from the arrays. For some candidates on this list, their roles in intestinal tumourigenesis were already being studied by Clark's group in Cardiff. The table below shows the list of top 21 candidate genes that were significantly upregulated overlapping between day 4 and day 5 (Table 3.1).

Table 3.1 List of the top 21 up-regulated genes in Cre-*lox*P APC mouse model.

Gene Name	Accession ID Number (Mouse)
TROY	NM_013869
Fem1b	AF064448
Tiam1	U05245
Fzd6	NM_008056
CyclinD2	NM_009829
CD44	X66084
Axin2	NM_015732
Musashi	NM 008629
EphB2	AV221401
EphB3	BC014822
EphB4	NM_010144
Semac3	X85994
Sox17	AK004781
Fn14	NM_013749
HtrA1	NM_019564
Sox4	NM_009238
Mash2	NM_008554
MBD4	NM_010774
SPARC-Like	NM_010097
CITED1	NM_007709
MTAP	NM_024433

3.2 Bioinformatics: Gene list from mouse to human

In order to test whether these genes are also up-regulated in human colorectal cancer samples, the corresponding orthologue human genes were identified from the mouse gene, using the public databases (NCBI, ExPASy, MGI) (Table 3.2).

Taking Cited1 as an example, NM_007709 is the GenBank Accession ID number in *Mus musculus* as provided in the list of genes which were identified in Cre-*lox*P *Apc* mouse model. Mouse GenBank Accesion ID number was firstly being searched on MGI (Mouse Genome Informatics) database. The item of 'mammalian orthology' in MGI was then selected for obtaining the accession number of the orthologue genes in *Homo sapiens.* The corresponding human gene was then linked with the NCBI database through this human GenBank Accession number. The sequence of mRNA and the encoded protein in human was shown in the Evidence Viewer of NCBI. To ensure the accuracy of the orthologue human GenBank Accession number, human Cited1 protein was also searched in ExPaSy proteomics database. If the identical amino acid sequences were found in both UniProtKB from ExPaSy and Evidence Viewer from NCBI, this orthologue human GenBank Accesion number was assumed to be correct. The mRNA sequence shown in the Evidence Viewer of NCBI was then used to design the primers and probes for Taqman real-time PCR assay.

3.2.2 Array analysis on c-Myc and APC double conditional K/O mouse model

In APC and c-Myc double K/O mice, loss of c-Myc rescued the perturbed phenotypes which occur on deletion of APC (Sansom et al., 2007). Interestingly, this rescue occurred despite high level of nuclear β-catenin (Sansom et al., 2007). The c-Myc dependent genes overlapping with the top 21 genes were labelled in yellow boxes in the list (Table 3.3).

Table 3.2 Orthologue human genes from the list of top 21 upregulated mouse genes.

Full Gene Name	Official Symbol	Accession ID (Mouse)	Accession ID (Human)
Tumor necrosis factor receptor superfamily, member 19	TNFRSF19	NM_013869	AB040434
Fem-1 homolog b (C. elegans)	FEM1B	AF064448	NM_015322
T-cell lymphoma invasion and metastasis 1	TIAM1	U05245	NM_003253
Frizzled homolog 6 (Drosophila)	FZD6	NM_008056	AB012911
Cyclin D2	CCND2	NM_009829	AF518005
CD44 antigen (homing function and Indian blood group system)	CD44	X66084	M59040
Axin 2 (conductin, axil)	AXIN2	NM_015732	AF078165
Musashi homolog 1 (Drosophila)	MSI1	NM 008629	AB012851
EPH receptor B2	EPHB2	AV221401	NM_017449
EPH receptor B3	EPHB3	BC014822	NM_004443
EPH receptor B4	EPHB4	NM_010144	AY056047
Sema domain, immunoglobulin domain (Ig), short basic domain, secreted, (semaphorin) 3C	SEMA3C	X85994	AB000220
SRY (sex determining region Y)-box 17	SOX17	AK004781	AB073988
Tumor necrosis factor receptor superfamily, member 12A	TNFRSF12A	NM_013749	AB035480
HtrA serine peptidase 1	HTRA1	NM_019564	AF097709
SRY (sex determining region Y)-box 4	SOX4	NM_009238	AF070669
Achaete-scute complex-like 2 (Drosophila)	ASCL2	NM_008554	NM_005170
Methyl-CpG binding domain protein 4	MBD4	NM_010774	AF072250
SPARC-like 1 (mast9, hevin)	SPARCL1	NM_010097	X86693
Cbp/p300-interacting transactivator, with Glu/Asp-rich carboxy-terminal domain, 1	CITED1	NM_007709	U65092
Methylthioadenosine phosphorylase	MTAP	NM_024433	AB062485

Table 3.3 List of genes from APC c-Myc double K/O mouse model.
Genes in yellow boxes are c-Myc dependent downstream Wnt target genes.

Full Gene Name	Official Symbol	Accession ID (Mouse)	Accession ID (Human)
Tumor necrosis factor receptor superfamily, member 19	TNFRSF19	NM_013869	AB040434
Fem-1 homolog b (C. elegans)	FEM1B	AF064448	NM_015322
T-cell lymphoma invasion and metastasis 1	TIAM1	U05245	NM_003253
Frizzled homolog 6 (Drosophila)	FZD6	NM_008056	AB012911
Cyclin D2	CCND2	NM_009829	AF518005
CD44 antigen (homing function and Indian blood group system)	CD44	X66084	M59040
Axin 2 (conductin, axil)	AXIN2	NM_015732	AF078165
Musashi homolog 1 (Drosophila)	MSI1	NM 008629	AB012851
EPH receptor B2	EPHB2	AV221401	NM_017449
EPH receptor B3	EPHB3	BC014822	NM_004443
EPH receptor B4	EPHB4	NM_010144	AY056047
Sema domain, immunoglobulin domain (Ig), short basic domain, secreted, (semaphorin) 3C	SEMA3C	X85994	AB000220
SRY (sex determining region Y)-box 17	SOX17	AK004781	AB073988
Tumor necrosis factor receptor superfamily, member 12A	TNFRSF12A	NM_013749	AB035480
HtrA serine peptidase 1	HTRA1	NM_019564	AF097709
SRY (sex determining region Y)-box 4	SOX4	NM_009238	AF070669
Achaete-scute complex-like 2 (Drosophila)	ASCL2	NM_008554	NM_005170
Methyl-CpG binding domain protein 4	MBD4	NM_010774	AF072250
SPARC-like 1 (mast9, hevin)	SPARCL1	NM_010097	X86693
Cbp/p300-interacting transactivator, with Glu/Asp-rich carboxy-terminal domain, 1	CITED1	NM_007709	U65092
Methylthioadenosine phosphorylase	MTAP	NM_024433	AB062485

3.3 Taqman qPCR primers and probes designing and optimisation

Taqman qPCR technique was chosen to measure gene level alteration in human colorectal cancer samples, which provides the advantages of giving accurate gene expression levels from limited amount of patient cancer tissue samples. To the gene of interest, there are more specific signals released from the qPCR reactions with additional Taqman probes than simply adding SYBR Green I dye in the reactions.

The designing of primers and probes was carried out before the data from the double K/O (APC and c-Myc) mice were available. Wnt signalling pathway downstream targets, which were either c-Myc dependent or independent, were designed following the list of 21 genes. The Primer Express program (Applied Biosystems) was employed to design the primers and probes.

3.3.1 Taqman qPCR primers and probe designings

The criteria for a good qPCR primer set is that forward and reverse primers should bind to neighbouring exons respectively and Taqman probe should cross the intron/exon boundary to avoid false positive results arising from amplification of contaminating genomic DNA (intron) in the RNA samples. Figure below showed an example (human Cited1) of primers and probes designing in the 'intron spanning approach' (figure 3.1).

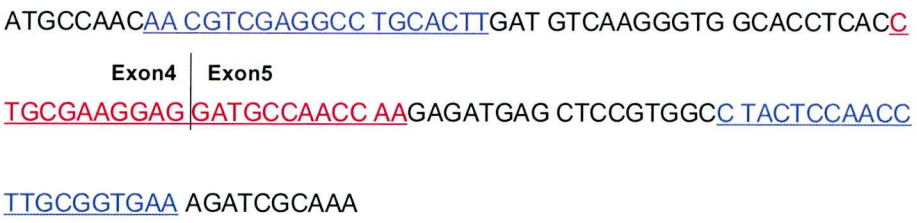

Figure 3.1 Diagram of an example of 'intron spanning approach' for primer and probe designing. The nucleotide sequence was the neighbouring sequences of exon4 and exon5 from human gene *Cited1*. The sequence was obtained from NCBI database. The underlined blue letters indicates the location of designed forward or reverse primers and the underlined red letters indicates the location of designed Taqman probe.

However, not all the sets of primers and probes for these 21 candidate genes can be designed via the 'intron spanning boundary' approach, especially when there was only one exon existing in the nucleotide sequence of the gene. In these cases, the sets of primers and probes were designed via another approach, from the 3' coding end of the nucleotide sequence. This also requires the DNase treatment to remove the possible existence of contaminating genomic DNA in the RNA samples. Figure below showed an example of the primers and probe designing (human *FEM1B*) in the '3' coding end approach' (figure 3.2).

Figure 3.2 Diagram of an example of '3' coding end approach' for primer and probe designing. Nucleotide sequence was the sequence of the close end of 3' coding from human gene *FEM1B*. The sequence was obtained from NCBI database. The underlined blue letters indicates the location of forward or reverse primers and the underlined red letters indicates the location of Taqman probe.

When the '3' coding end' primers and probes were being used, the genomic DNA control set of primers and probe are required to test the effectiveness of the DNase digestion on the RNA samples, giving no or, in most cases, acceptable low levels of signals from the genomic DNA. For this genomic DNA control set of primers and probe, primers should bind to the neighbouring intron and exon, respectively. This probe should be comprised of part of the exon and part of the intron, which would pick up the signals from the contaminating genomic DNA (intron) in the RNA samples. The nucleotide sequence of any known gene could be used to design the genomic DNA control set. Figure below showed the designing of genomic control primers and probe on human gene *Axin2* (figure 3.3).

ACCCCACCCA ACACGCTGGC TCAGCTGGAG GAGGCCTGTC GCAGGCTAGC

Exon9 | Intron9

TGAGGTGTCG AAGCCCCCAA AGCAGCGGTG AGTGGAAGTG AAGGGTCCTA

GGTTGAGGCA GGGATTGGGT TTGGGTGGAG ACCTGGTCTG

Figure 3.3 Diagram of the genomic DNA control for primer and probe designing. Nucleotide sequence was the neighbouring sequence of Exon9/Intron9 from the human gene *Axin2*. The sequence was obtained from Ensembl database. The underlined blue letters indicates the location of forward or reverse primers and the underlined red letters indicates the location of Taqman probe.

For all the primers and probes designed to the genes on the list using any approach, the primers and probes sequences were searched using the online database Nucleotide BLAST to ensure the specificity of the nucleotide sequence to the gene of interest. The primers and probes sequences that could possibly result in unspecific amplifications were redesigned until the possible unspecificity was eliminated.

3.3.2 Taqman qPCR primers and probe optimisations

The primers and probes needed to be optimised prior to performing Taqman qPCR reactions on human colorectal tumour samples (2.7.1.3). In order to preserve the precious human tissue samples, human cell line (HCT116) RNA was employed to optimize the primers and probes working conditions.

Various ratios of primers were used to establish the conditions. Taking CITED1 as the example, we are looking for the best ratio to produce an amplicon of approximately 100bp. The gel below shows the specific PCR products of the correct amplicon size (102bp) according to the designing (figure 3.4).

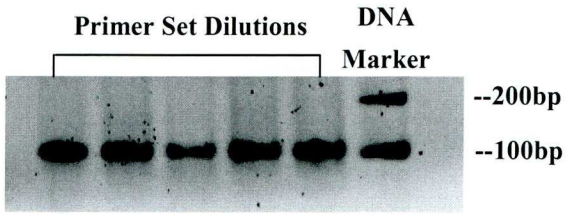

Figure 3.4 Human *Cited1* gene primers optimisation test on 2% w/v agarose gel.

Five lanes on the left hand side were the specific products of human *Cited1* PCR reactions showing the specific amplifications. The lane on the right hand side was the DNA marker (HyperLadder IV) to show the size of PCR products.

A similar process was repeated with additional Taqman probe to access the required concentrations of primers and probe. For both primers and probe, the relative low concentrations of primers and probe giving the relative high level of qPCR products with more steep exponential amplification curves were chosen to be the working concentrations.

After the primers and probe optimisation, a series of dilutions of cDNAs were used to ensure the efficiencies of both the target gene and reference gene. Again, taking the human gene *CITED1* as an example, doubling amount of cDNA sample were

analysed to ensure the values observed fall within the linear range of the exponential amplification. The data showed that two lines respectively indicating target gene *CITED1* and reference gene *β-actin* were approximately parallel (figure 3.5). Therefore, amplification efficiencies were equal for both target gene and reference gene. This set of primers together with its Taqman probe were then used on human colorectal tumours.

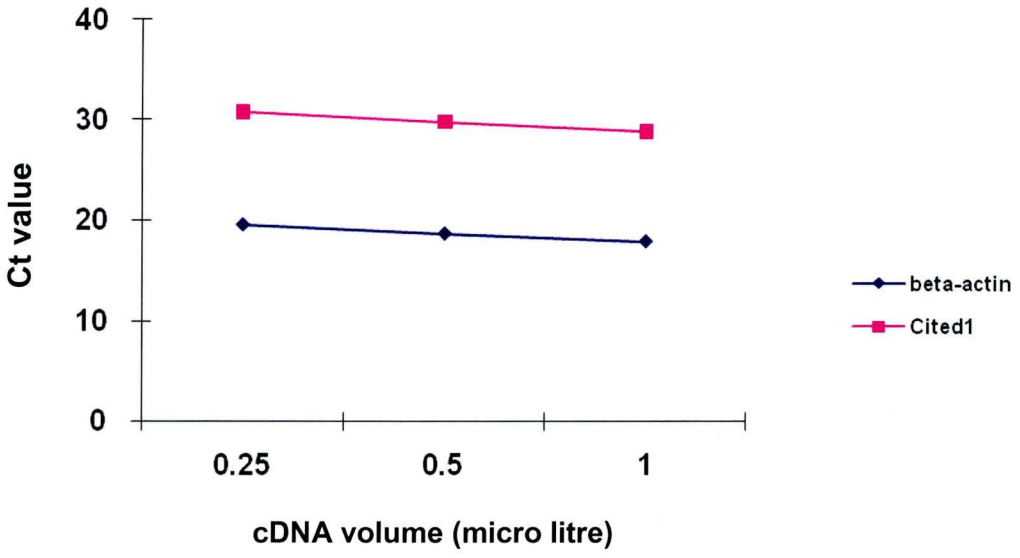

Figure 3.5 Equal amplification efficiencies of human Cited1 and human beta-actin genes. 2 paralleled straight lines of Ct values showed the equal amplification of target gene (*CITED1*) and reference gene (*β-actin*) along with the increased cDNA amount.

3.3.3 Optimised Taqman qPCR primers and probes

The optimised primers and probes of gene of interest are listed as below (Table 3.4). Genes in group I were designed using 'intron spanning approach'. Genes in group II were designed in '3' coding end approach'. *G-AXIN2* in group III was designed for detecting the level of genomic DNA in RNA samples when primers and probes from group II were being used.

Top II and *GPR49* genes were used as the positive controls. Top II is a known proliferation marker indicating the level of cell mitosis and proliferation (Barker et al., 2006). *GPR 49* has been shown to be a small intestine and colon stem cell marker in mice (Barker et al., 2007). They were both designed using the intron spanning approach. *β-ACTIN* was used as the internal reference gene to standardize the amount of the cDNA samples. Primers and probe for human gene *β-ACTIN* were kindly provided by Dr. A. Davies.

Table 3.4 List of Designed primers and probe. Sequences were all written from 5' to 3'.

h β-ACTIN	HQ	TCA AGA TCA TTG CTC CTC CTA GCG C
	FWD	GGC ACC CAG CAC AAT GAA G
	REV	GCC GAT CCA CAC GGA GTA CT
Group I		
h TopII	HQ	TTC GAA AGC AGT CAC AAG CAA GAA ATC CAA
	FWD	TGA TTC TGA CTC TAA TTT TGA GAA AAT TG
	REV	GGA GCC ACA GCT GAG TCA AAG

h GPR49

HQ	TTC CCC AGG CCC CTT CAA ACC C
FWD	AGA CCT GAA AGC CCT TCA TTC A
REV	GGT CCA CAC TCC AAT TCT GAT CA

h AXIN2

HQ	CAG CAA AAA GGG AAA TTA TAG GTA TTA CTT CAA AAA AGC A
FWD	TGA CCC TGG GCC ACT TTA AA
REV	ACC GCT CCA CAG GCA AC T

h CD44

HQ	TTC CAG AAT GGC TGA TCA TCT TGG CAT
FWD	AAC ACA ACC TCT GGT CCT ATA AGG A
REV	AAT CAA AGC CAA GGC CAA GA

h CITED1

HQ	CTG CGA AGG AGG ATG CCA ACC AA
FWD	AAC GTC GAG GCC TGC ACT T
REV	TTC ACC GCA AGG TTG GAG TAG

h EPHB2

HQ	ACG TCG TGT CTC AGA TGA TGA TGG AGG A
FWD	GCC GGC TTC ACC TCC TTT
REV	GAC CCC AAC CCG GAG AAT

h EPHB3

HQ	TCC TTC CTC CGG CTC AAC GAT GG
FWD	CCT CAC TGA GTT CAT GGA AAA CTG
REV	GCA ATG CCC CGC AAC A

h EPHB4

HQ	AGA TCT CTG CTG AGG ACC TGC TCC GAA
FWD	TGG CTT TGG CTC CTT CGA
REV	GGT GTC CCG CCA GAG TGA

h Fn14

HQ	CGC AGG AGA GAG AAG TTC ACC ACC CC
FWD	GCT GCT TTC TGG CTT TTT GG
REV	TCT CCG CCG GTC TCC TCT AT

h FZD6

HQ	CGC GGA GTG AAG GAA GGA TTA GTC CAA
FWD	CAG GCA GGC AGT GTA TCT GAA A
REV	CCA GGC CAG TGT CAG TAA TAT CAC

h MBD4

HQ	CAG ATG AAT ACC TGA CAA AGC AGT GGA AGT ATC C
FWD	CTC TAC GAT CTT CGG GCA AAA A
REV	TTA CCA ATC CCA TGA AGC TCA A

h MTAP

HQ	CCC CAA AAC GAG AGA GGT TCT TAT AGA GAC TGC
FWD	CCA ATG GCT GAG CCG TTT T
REV	GCA CCG GAG TCC TAG CTT CTT

h SEMA3C

HQ	ACA AAG ACA GGA GGA AAG AGG TTA AGC TGA ATG A
FWD	GCA TCT ATC AAG TGG CTG TTA CAG A
REV	CCC TGT GAA GTG GCT ATT ATT CG

h TIAM1

HQ	ACC TGG ACG TGG CCA TCA AGA CCA
FWD	CGG AGA GCG AGG AGC ACT AC
REV	TGA TGT GAC TGG CAA CCT TGT T

h MSI1

HQ	CCT GGC TAC ACC TAC CAG TTC CCC G
FWD	TAC GCC AGC CGG AGT TAT ACA
REV	GGG TCC GCT CTA CAC GGA AT

Group II

h FEM1B

HQ	ACC AAG ACC AGA TCC CCA GAA CTC TTG AAG A
FWD	GCA GTT CGG GCT AAT GAC ATT AAC
REV	TCC AGT CAC TTA ATG AAA TCC AAC AA

h TROY

HQ	TGC TGC AGA AGC TCG TTG ACA AGA CTG A
FWD	GCT GAA TGG GCA TAA CCA CTG T
REV	ACT TTA CTT GGT TGC TCT TGA AAT CCT

h ASCL2

HQ	ACC TGG ACC CCT GCC CCC ACT ATC T
FWD	GCT GGC AAA CGG AGA CCT ATT
REV	TTG GCC AGC ATG GAA AAC TC

h SOX4

HQ	TTA AAA TTC AAG GCC ACA AAA ACA ATG TTT GGG
FWD	CCT GTG CAA TAT GCC GTG TAG A
REV	ACT TGA CAT GAT TAG CTG GCA TGA

h SOX17

HQ	CTG ATC CGC CCC AGC CTG CA
FWD	TTA CTG CAA CTA TCC TGA CGT GTG A
REV	CTC CAG GAA GTG TGT AAC ACT GCT T

h HTRA1

HQ	CAG AGA CCC CGG GTG GGT GAG C
FWD	AGT CAG CAC CCA AAG GTC AAT G
REV	CAA CTT CGG CCG TTT GAG AA

h SPARCL1

HQ	TCC AGC ATC CTC CTC TGT TCT AAC CAC TTC A
FWD	TTG TTT TGA ACG AAG ATT TTA AAG AAC TC
REV	AAT ATA AAT CTA CAA GTA TCA CAG CTG CAT ATA TTT

h CCND2

HQ	TGG CAA AAA TGT TGT ATT GGC TAT GAT GGT G
FWD	TGA TCA GTG TAT GCG AAA AGG TTT
REV	CTC TTA AAA GGC AGC TGA CTA TAT CAT G

Group III

G-AXIN2

HQ	CCA AAG CAG CGG TGA GTG GAA GTG AA
FWD	CAG GCT AGC TGA GGT GTC GAA
REV	AAC CCA ATC CCT GCC TCA AC

Due to the time limitation and sample availability, MSI1, FEM1B, TROY, ASCL2, SOX4, SOX17, HTRA1, SPARCL1, CCND2 were not analysed in the human colorectal tissue samples.

3.4 Real time quantitative PCR data

This section describes how the data from the real-time PCR experiments was analysed. Reference: User Bulletin #2 of ABI PRISM 7700 Sequence Detection System (Dec. 1997). C_t value is the first significant increase in the amount of PCR product. It is inversely correlated to the logarithm of the initial amount of target template.

Normalisation of the target Ct to the internal reference Ct value:

ΔCt = target Ct - reference Ct

Relative comparison to normal tissue Ct:

$\Delta\Delta Ct$ = tumour tissue Ct – normal tissue Ct

The relative fold change = $2^{-\Delta\Delta Ct}$

In normal and tumour tissue samples, Ct values of the target gene are normalised to the reference gene used as the internal control, which gives the delta Ct. On the graph, delta Ct represents the distances from the curve of reference gene to the curve of target gene, respectively (Figure 3.6). Then the normalised Ct in tumour was compared to the normalised Ct in normal tissue, which gives the delta delta Ct value. This represents the distance difference in between the normal and in tumour samples. Finally, the relative fold change was calculated as 2 to the power of minus delta delta Ct, which shows the relative amount of mRNA message in tumour sample.

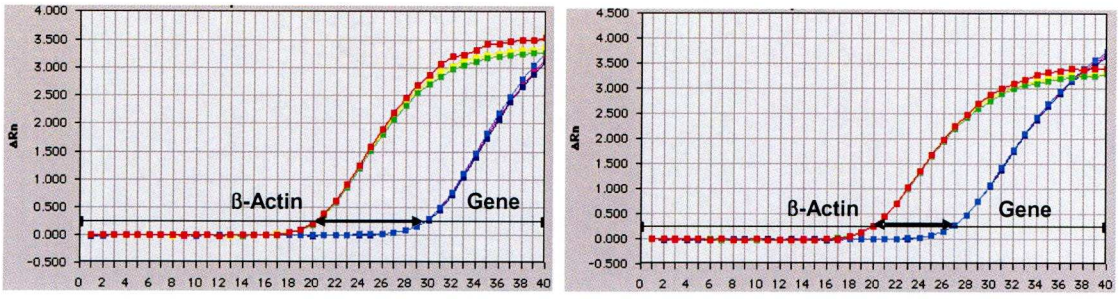

Normal Tumour

Figure 3.6 Example of an up-regulated gene in tumour tissue.

3.5 Candidate gene expressions in human colorectal cancer

To determine whether the changes observed in mouse model also alter in human colorectal cancer, the patient tissue samples for this project were obtained from Cancer Tissue Bank Research Centre (with informed patient consent). Match paired Total RNA samples were extracted from colorectal cancer tissues with adjacent uninvolved colonic mucosa. Taqman real-time PCR was used to amplify candidate gene expression in human colorectal tumours. The sample size calculations were performed by Dr. A. Jorgensen, giving a guide for the minimal patient number (n=10) needed to show statistical significance. The fold change for each gene was calculated separately for each pair of patient samples. The minimum required patient number (n=10) was initially used for each gene of interest. The candidate gene expression levels in fold change from patients are non-parametric data, the median value (rather than mean value) was used to carry out the data analysis for each candidate gene.

For the Taqman assay, a fold change of lower than 2 is considered to be no change. Therefore, after the first round of 10 pairs of patient samples, the genes that showed less than 2-fold (plus or minus) in tumour tissues were no longer considered to be candidate genes. These 4 human genes were *MTAP* (1.97-fold, n=10), *MBD4* (1.35 fold, n=10), *SEMA3C* (-1.31-fold, n=10) and *TIAM1* (-1.40-fold, n=10).

Data from the Taqman assay showed that 8 orthologous human candidate genes were over-expressed (figure 3.7). These genes were: *AXIN2* (4.55-fold, n=43), *CD44* (4.81-fold, n=16), *EPHB2* (2.31-fold, n=29), *EPHB3* (2.48-fold, n=26), *EPHB4* (2.22-fold, n=29), *FZD6* (2.42-fold, n=16), *Fn14* (5.48-fold, n=20) and *CITED1* (2.74-fold, n=40). For each group of data, the candidate gene (non-parametric data), the Wilcoxon Signed Rank Test was used to determine the statistical significance. Overexpression of all 8 genes observed showed statistical significance at $P<0.001$. In addition, 6 (in the yellow boxes) out of those 8 homologous human candidate genes were c-Myc dependent, as identified in the APC and c-Myc double K/O mouse model. The tumour sample positive controls, *Top II* (3.92-fold, n=10) and *GPR49* (5.83-fold, n=23) were also significantly over-expressed at $P<0.01$.

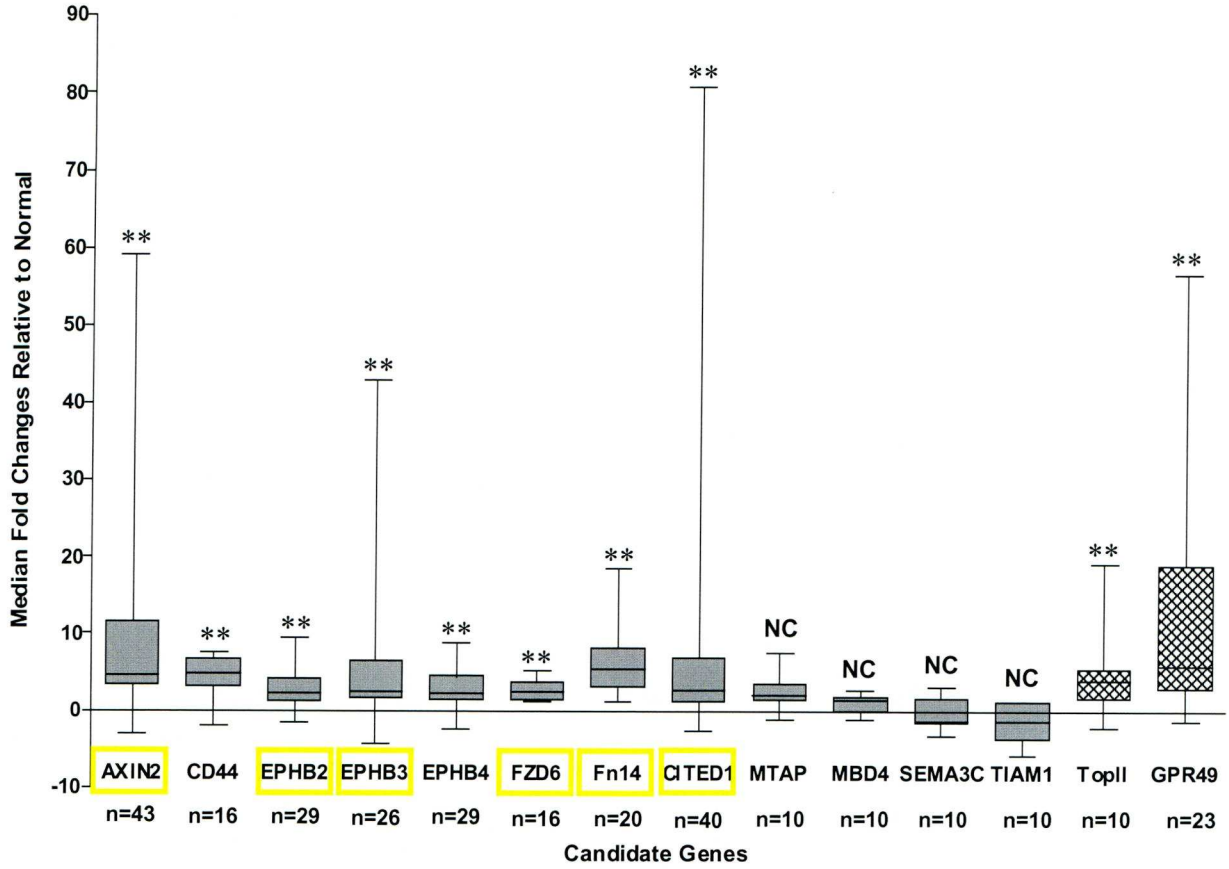

Figure 3.7 Candidate gene expression in human colorectal cancer. Data for altered gene expression levels in tumour tissues were presented as the fold changes relative to normal, which were shown in the graph as column of box-and whiskers plot showing the median values with the interquartile ranges and whiskers. In each column of the graph, the horizontal line across each box showed the median of that group of data for this candidate gene. Each box extends from 25th and 75th percentiles. Whiskers extend down to the lowest value and up to the highest. n= 'number' beneath each column indicated the patient number being employed for that group of data. 'NC' above each column indicated no change as altered by the Taqman assay. '**' above each column indicated the significance ($P<0.01$) from the statistical analysis. Genes covered by yellow boxes were c-Myc dependent Downstream Wnt target genes.

3.6 Discussion

3.6.1 Wnt signalling status in human colorectal tissues

The Wnt signalling pathway is switched on following loss of *Apc* in the Cre-*lox* mouse model. To validate these observations, it was necessary to clarify the Wnt signalling status in human colorectal tumours. One of the initial thoughts was detecting the mutations of *APC* in human colorectal tumours by employing the method of DNA sequencing. *APC* is a very large gene with a MCR (mutation clustered region) site in which the majority of APC mutations occur. Therefore we decided to sequence this specific site of *APC* gene. However, it was not easy to use this strategy to analyse *APC* mutations in patient samples and APC protein would also be truncated during the post-translational process. It is not possible to clarify the Wnt status by sequencing of the *APC* gene in human colorectal tumour tissues.

It has been reported that mutations in the *APC* tumour suppressor gene are present in approximately 85% of colorectal tumours (Anderson et al., 2002). Over 90% of colorectal cancer have a mutation from any components of Wnt signalling, which are able to activate this pathway (Doucas et al., 2005). APC and β-catenin are two central components of this pathway, their mutations have been reported to be mutually exclusive (Behrens, 2005; Sparks et al., 1998). Mutations in both APC and β-catenin result in the accumulation of nuclear β-catenin which is detectable in even the smallest neoplastic lesion of the colonic adenoma (Hao et al., 2001; Pinto and Clevers, 2005b). Therefore, we assume that the large majority of the human

colorectal tumour tissues obtained from our Cancer Tissue Bank Research Centre maintained the activated Wnt signalling.

3.6.2 Validation of the mouse model strategy

Data from Taqman real-time PCR analysis showed that 8 out of 12 detected genes from the mouse model were over-expressed in human colorectal tumours, which were also over-expressed from qPCR data in the Cre-*lox*-*Apc* mouse model. These observations demonstrated how transferable the candidate genes identified in the mouse model are to the study of human colorectal cancer. Six out of these eight over-expressed orthologue human genes have already been known to be Wnt targets. Elevated *AXIN2* and *CD44* gene as well as *EPHB2*, *EPHB3*, *EPHB4* and *FZD6* gene expressions and corresponding gene encoded protein functions have been well studied, which again validates the process in human colorectal cancer.

3.6.3 Previously known Wnt downstream target in colorectal cancer

Below is a summary of the previously known Wnt downstream targets we identified as up-regulated in both the mouse model and human colorectal samples.

AXIN2 was elevated in human colorectal tumours as reported previously (Yan et al., 2001) and is cMyc dependent Wnt target from the Sansom study (Sansom et al., 2007). Being a scaffold protein molecule in the APC degradation complex, AXIN2 promotes the phosphorylation and degradation of β-catenin (Jho et al., 2002) . In the case of mutant APC, TCF binding sites in the *AXIN2* promoter play a key role in the ability of β-catenin to activate *AXIN2* transcription (Leung et al., 2002). AXIN2 functions as a tumour suppressor and has been reported to be one of the negative effectors in the Wnt signalling pathway by inhibiting β-catenin abundance and functions (Leung et al., 2002; Salahshor and Woodgett, 2005). Over-expressed *AXIN2* also constitutes a negative feedback loop of Wnt signalling activity in colorectal cancer (Lustig et al., 2002).

CD44 is a family of cell–surface glycoproteins encoded by a single gene with alterative splicing and extensive posttranslational modifications (Kuncova et al., 2005; Yamada et al., 2003), and plays a crucial role in cell migration, inflammation and immune responses (Mishra et al., 2005). An early study reported that CD44 is downstream target of the Wnt signalling pathway, which was over-expressed in the adenomas of the Min mice and in human FAP (Wielenga et al., 1999). Over-

expression of CD44, both CD44s and CD44v forms, is an early event in the colorectal adenoma-carcinoma sequence and plays a role in the generation and turnover of epithelial cells (Wielenga et al., 1999). Another more recent study reported that deletion of CD44 in Min mice attenuated the intestinal tumourigenesis in Min mice with 50% reduction in number of intestinal adenomas (Zeilstra et al., 2008). However, in Clarke's early stage Cre-*lox* transgenic mice models, although elevated in intestinal epithelium was observed 4-5 days after losing APC (Sansom et al., 2004), it was unaffected by the additional loss of c-Myc within the same time frame (Sansom et al., 2007). Data from CD44 expression from this double K/O mouse model showed that CD44 is still altered in the rescued intestinal epithelium after losing both Apc and c-Myc, which demonstrated the insufficient role of CD44 in imposing the phenotype associated with Apc loss. Data of the Taqman assays showed the over-expression of *CD44* at mRNA level in human colorectal cancer tissues, which was consistent with other previous studies, although it may not associate with the onset of colorectal carcinogenesis from Cre-*lox* mice studies.

EphB receptors have been reported to control intestinal epithelial architecture through repulsive interactions with EphrinB ligands, which was inversely mediated by β-catenin and TCF (Batlle et al., 2005; Batlle et al., 2002; Sansom et al., 2004). Reduction of EphB activity accelerates tumorigenesis in the colon and rectum in Min mice, which demonstrated that EphB receptors suppress colorectal cancer progression (Batlle et al., 2005; Clevers and Batlle, 2006). Our human qPCR data

showed the elevated transcription of EphB receptors in the colorectal tumours as observed in *Apc* deficient intestinal epithelium. Essentially, EphB2 and EphB3 are c-Myc-dependent Wnt targets and their normal transcription levels are consistent with the normal localization of paneth cells in the double mutants (Sansom et al., 2007).

FZD6 has been reported to act as a negative regulator of the Wnt signalling cascade in colon cancer cell lines (Golan et al., 2004). Being c-Myc dependent downstream Wnt target, our data showed that *FZD6* was elevated in human colorectal tumours as observed in *Apc* deficient mouse intestinal epithelium.

3.6.3 Previously undiscovered Wnt targets in human colorectal cancer

The over-expression of ***Fn14*** and ***CITED1*** gene have not previously been detected as Wnt pathway targets in human colorectal cancer and therefore are the potential novel candidates for future investigation.

A member of TNF receptor superfamily, Fn14 is a small cell surface receptor of TWEAK (tumour necrosis factor-like weak inducer of apoptosis) (Wiley and Winkles, 2003). TWEAK binding to Fn14 receptor plays an important role in the ability of Fn14 to activate NF-κB pathway, which involves with a number of immune and inflammatory processes, as well as oncogenesis (Winkles et al., 2007). Fn14 has already been reported to be expressed at relative high levels in certain types of human tumours (Winkles et al., 2006; Winkles et al., 2007). A more recent study demonstrated a non-redundant role of Fn14/TWEAK in intestinal damage in mice

through a TWEAK/intestinal epithelial cell axis (Dohi et al., 2009). It firstly reported the role of Fn14/TWEAK in the intestine, which elucidated the potential contribution of this pathway to the maintenance of the intestinal homeostasis (Dohi et al., 2009). However, it has not been shown to be part of the Wnt signalling pathway in colorectal carcinogenesis.

CITED1 is involved in regulating a wide variety of CBP/p300-dependent transcriptional responses (Shi et al., 2006). CITED1 is over-expressed in renal development and acts as a bifunctional regulator of transcription, activating TGF-β family signals while repressing Wnt-β-catenin-dependent responses (Plisov et al., 2005; Shi et al., 2006). However, CITED1 has not been shown being regulated by the Wnt pathway in colorectal carcinogenesis.

In this project, we were establishing the importance of these Wnt target gene alterations in intestinal tumourigenesis using animal models. In the literature, there are *Fn14* and *Cited1* K/O mice available (Zhao *et al.*, 2007; Rodriguez *et al.*, 2004), which provided us the opportunities to investigate their roles *in vivo*. The role of Fn14 in intestinal tumourigenesis had been taken by another research group for further investigations. Therefore, we set out to investigate the role of CITED1 in intestinal tumourigenesis.

Chapter 4 Effects of CITED1 deficiency (siRNA knock down) on human colon cancer cell lines

4.1 Introduction

Cited1 was originally identified in murine melanoma cell line, which has been found to be associated with pigmentation (Shioda et al., 1996). It has been characterized as a non-DNA binding transcriptional co-regulator which is able to activate or repress transcription in association with other transcriptional factors depending on the cellular context (Labbe et al., 2007; Plisov et al., 2005). It is implicated in embryogenesis, in vertebrate development and carcinogenesis in breast, thyroid and Wilms' cancers (Dillon et al., 2007; Lovvorn et al., 2007b; Prasad et al., 2004). However, its role in colorectal carcinogenesis is still unknown.

From our previous data, *Cited1* was found to be one of the genes which were over-expressed in the inducible mouse intestinal epithelium specific Apc knock-out model (Sansom et al., 2004). In the Apc and c-Myc double knock-out mouse model, *Cited1* was identified as a c-Myc dependent Wnt target, which identifies it as a candidate in the pathway resulting in the phenotype of Apc loss (Sansom et al., 2007). We also found *CITED1* to be over-expressed in human colorectal cancer tissues compared with adjacent uninvolved colonic mucosa (See figure 3.7, Chapter 3). Therefore, we hypothesized that CITED1 is involved in colorectal carcinogenesis and its deficiency would inhibit the growth of colorectal cancer.

Before progressing to transgenic mouse models, we used human colon cancer cell lines to establish a potential role for CITED1 as part of the mechanism of precancerous phenotype.

4.2 Selection of human colon cancer cell lines

In order to establish the *in vitro* model for investigating the functional role of CITED1 in colonic carcinogenesis, suitable human colon cancer cell lines were selected. Due to the involvement of CITED1 mRNA transcription in the Wnt pathway, the major criteria for the cell line selection is a maintained activated Wnt signalling. HCT116 and HT29 are two widely used human colon cancer cell lines. HCT116 carries the mutant β-catenin with wild-type APC and HT29 carries the mutant APC with wild-type β-catenin (Din et al., 2004), both maintain an activated Wnt signalling pathway resulting from the mutations of the central components of this pathway.

One of the most efficient approaches of generating a reduced expression of a specific protein in cultured cell lines is RNA interference (RNAi) gene silencing technique. The transient transfection of small interference RNA (siRNA) duplexes induces the degradation of the mRNA and consequently loss of protein over a period of time (Wu et al., 2004). siRNA induced gene silencing is primarily an mRNA level event, therefore Taqman qPCR was chosen to detect the siRNA gene silencing effect.

Prior to the siRNA experimentation, the basal cellular expression levels of *CITED1* mRNA were detected by Taqman qPCR in HCT116 and HT29 cell lines. For both cell lines, mRNA samples were extracted from the cells which were randomly harvested 4 times. As shown in the figure 4.1, *CITED1* mRNA is detectable and expressed stably in both cell lines as normalised to the reference gene *beta-Actin*.

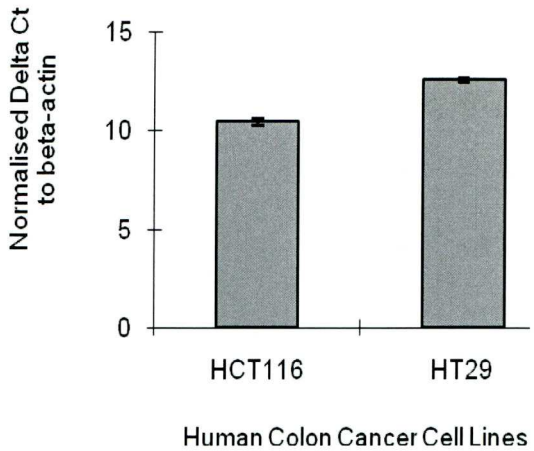

Figure 4.1 Basal expression levels of CITED1 in the studied human colon cancer lines. Grey bars show the normalised delta Ct values of CITED1 to beta-actin in HCT116 and HT29 cell lines. The error bars stand for the standard error of the mean (SEM) of the Ct value for each cell line (n=4).

Ideally, both mRNA and protein levels should be analysed whenever possible to detect the siRNA knock down effect. Unfortunately, there is no suitable CITED1 antibody for western blotting assay in this project.

A commercial CITED1 antibody from Genetex was firstly used on HepG2 whole cell lysate positive control. The predicted molecular mass for CITED1 is approximately 23 kDa (Shioda *et al.*, 1996); however, Genetex CITED1 antibody showed a band of a much larger size than 41 kDa, which was unlikely to be CITED1 (figure 4.2). Therefore, this antibody cannot be used to detect CITED1 protein.

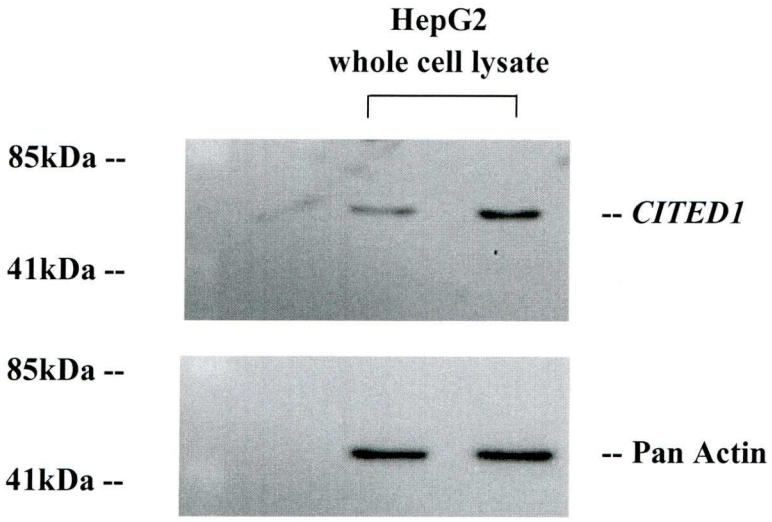

Figure 4.2 Western blotting of HepG2 whole cell lysate probed by Genetex CITED1 antibody. This antibody did not detect CITED1 antigen in samples. Pan-actin was used as an equal loading control.

Another antibody was then found in literature, which is not commercially available but has been reported to be good for western blotting (Howlin et al., 2006; Lovvorn et al., 2007b). We used this antibody on western blotting assay of HT29, HCT116 whole cell lysate samples and Min mouse small intestine tissue protein samples, together with HepG2 whole cell lysate positive control. The blotting band of

CITED1 was observed on the Min mouse small intestine tissue sample and it was of the correct molecular size (Figure 4.3). Unfortunately, this antibody was not able to visualise CITED1 antigen in any of these human cell lines samples (including HepG2 positive control) in our western blotting assay. Therefore, data is only available at mRNA level for siRNA inhibition experiments on human colon cancer cell lines, which is measured by qPCR.

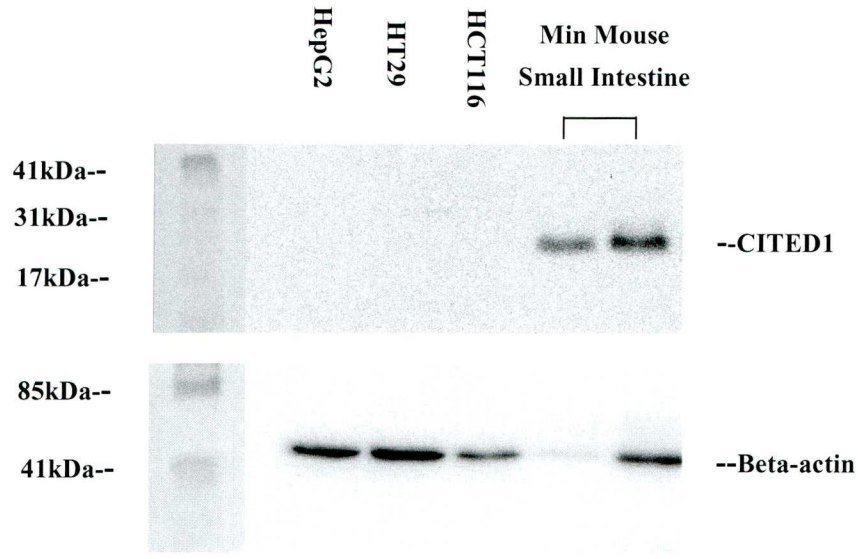

Figure 4.3 Western blotting of studied human cell line lysate and Min mouse small intestine protein using CITED1 antibody provided by Dr. Shioda. CITED1 antigen was only detected in Min mouse small intestine sample using this antibody. Beta-actin was used as an equal loading control. This is the representative data of 3 repeats.

4.3 siRNA inhibition of *CITED1* mRNA expression in human colon cancer cell lines

CITED1 down regulation is demonstrated by qPCR. Cellular expression of *CITED1* mRNA was reduced by siRNA transfection in HCT116 and HT29 human colon cancer cell lines, as detected by qPCR. All pairwise comparisons were analysed following Kruskal-Wallis non-parametric analysis of variance (ANOVA) and data showed a statistically significant reduction of CITED1 in both cell lines (Figure 4.4). In HCT116 cells, *CITED1* expression was significantly reduced by 95% in target siRNA compared with the non-target siRNA control ($P<0.01$, Kruskal-Wallis) (figure 4.4 A). This reduction was 80% in HT29 cells ($P<0.05$, Kruskal-Wallis) (figure 4.4 B). siRNA transfection experiments were all performed at the optimised conditions (as outlined above) to obtain the highest reduction in the mRNA of our gene of interest. The difference of knocking down effect in the HCT116 and HT29 cells may be a result of the different cellular context.

For both cell lines, *CITED1* mRNA expression in the lipid only control and non-target siRNA control stay at similar level to the blank control. This indicates that there is no off-target effect from either cellular toxicity of the transfection lipid or the non-target control siRNA. This is the final step in validating the down regulation of CITED1 mRNA in the two cell types. Therefore, the siRNA transfection experiments in HCT116 and HT29 human colon cancer cell lines have been proven to be valid for the following phenotypic studies.

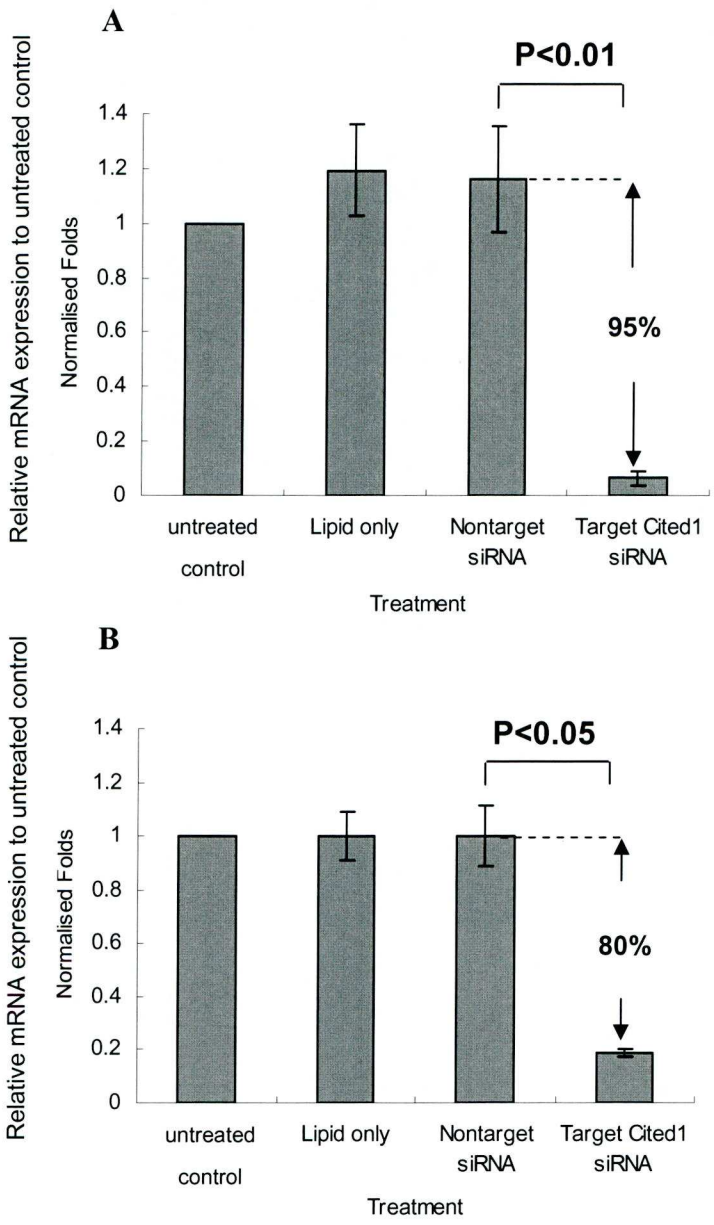

Figure 4.4 siRNA inhibition of CITED1 in HCT116 cell line (A) and HT29 cell line (B). Data are from a minimum of 3 experiments.

4.4 Effects of CITED1 deficiency on human colon cancer cell growth

As mentioned earlier in this chapter, high level of *Cited1(CITED1)* mRNA are present in both *Apc* knock-out mouse intestinal epithelium and human colorectal tumour tissues, we hypothesized that CITED1 is involved in colorectal carcinogenesis and its deficiency could possibly inhibit the growth of colorectal cancer.

4.4.1 Effect of CITED1 deficiency on cell survival

The clonogenic assay was used to measure the ability of the cancer cells to divide and grow following siRNA treatment. After 48 hours siRNA transfection, cell numbers for each treatment were counted and the same number of cells (1000 for HCT116 and 2000 for HT29) from each treatment were reseeded and re-grown with no further siRNA treatment until the visible colonies were observed.

For HCT116 cells, there was a small but statistically significant decrease in cell survival following targeted siRNA treatment compared with the other controls ($P<0.001$, Kruskal-Wallis) (figure 4.5 A). Similar results were also observed for HT29 cells ($P<0.01$, Kruskal-Wallis test) (figure 4.5 B). Therefore, data demonstrated a decreased cell survival following the knock down of CITED1.

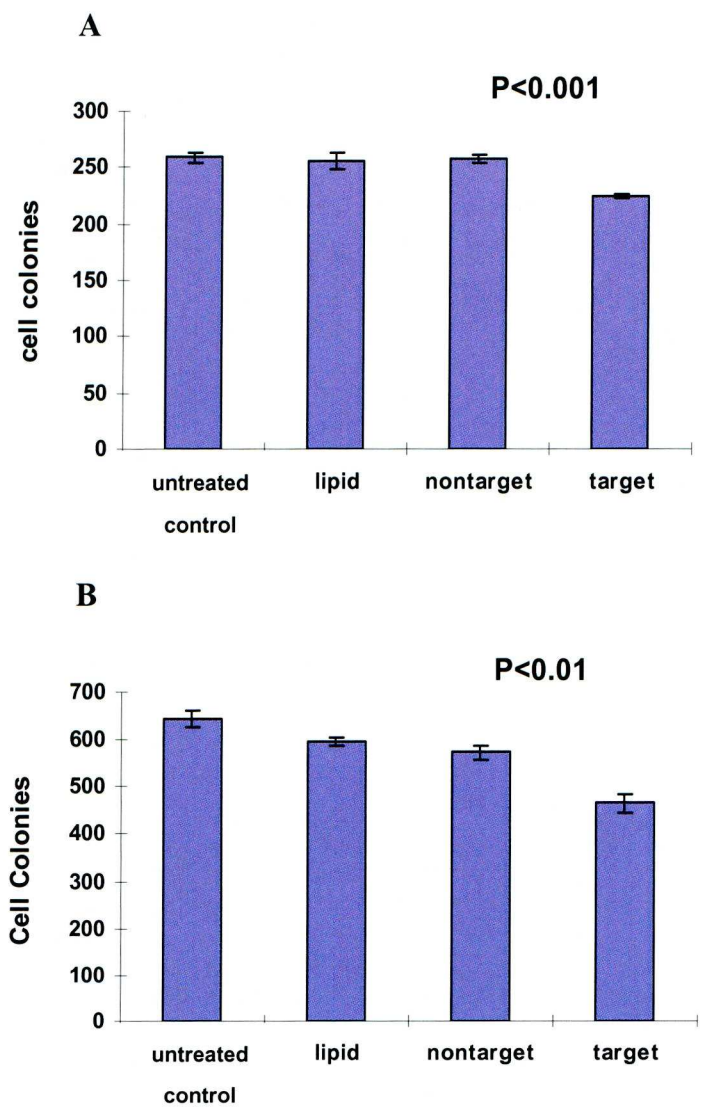

Figure 4.5 Reduction in CITED1 expression reduces clonogenic survival in HCT116 cell line (A) and HT29 cell line (B). This is the representative data from minimum of 3 experiments.

4.4.2 Effect of CITED1 deficiency on cell proliferation

The cell survival assay only measured the end point effect of cell growth. Therefore, we used the SRB assay to access cell proliferation over several days.

For both HCT116 and HT29 cell lines, cells were reseeded as described above and collected over 7 days post transfection. For both cell lines, there was a demonstratable reduction in cell proliferation following siRNA treatment. The reduction in cell proliferation was statistically significant from day 3 to day 5 for HCT116 cells ($P<0.05$, Kruskal-Wallis) and the largest reduction being observed on day 4 ($P<0.01$, Kruskal-Wallis) (figure 4.6 A). For HT29 cells, the reduction in cell proliferation was significant from day 2 to day 7 and the largest reduction was observed on day 5 ($P<0.01$, Kruskal-Wallis) (figure 4.6 B). One of the reasons for this cell proliferation difference between two cell lines could possibly be the different cell growth speed. HT29 cells generally grow slower than HCT116 cells in culture. Once the cells were reseeded after the 48 hour siRNA treatment, CITED1 deficient HCT116 cells would proliferate at a higher rate than CITED1 deficient HT29 cells. This could explain the later time point of the largest proliferation difference between target and non-target siRNA treatment in HT29 cell line.

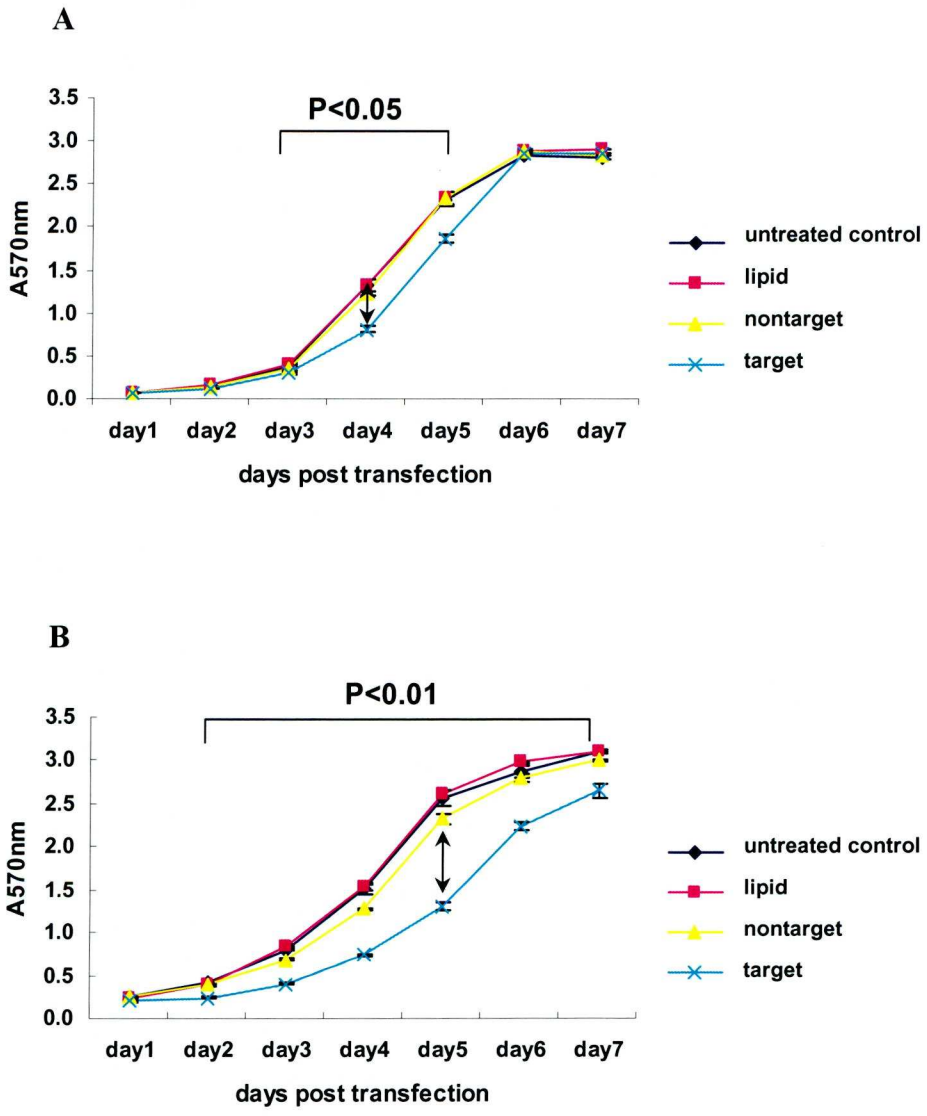

Figure 4.6 Reduction in CITED1 expression reduces proliferation (SRB assay) in HCT116 cell line (A) and HT29 cell line (B). This is the representative data from minimum of 3 experiments.

4.5 CITED1 deficiency does not turn Wnt signalling off

As stated earlier, CITED1 has been characterized as a non-DNA binding transcriptional co-regulator depending on the cellular context (Labbe et al., 2007; Plisov et al., 2005). Therefore, the question addressed here is whether or not CITED1 acts as a transcriptional co-regulator in this cellular context. Furthermore, does CITED1 deficiency cause the inhibition of downstream Wnt signalling?

Axin2 and CD44 are known Wnt regulated downstream targets, we used these to access the effect on the Wnt pathway following down regulation of CITED1. In HCT116 cells, *Axin2* was significantly three-fold over-expressed following siRNA knock down ($p<0.05$, Kruskal-Wallis test). However, *CD44* did not show much changes in cellular expression between target and non-target siRNA treatment ($P>0.05$, Kruskal-Wallis) (figure 4.7 A). In HT29 cells, *Axin2* and *CD44* were both significantly increased (both $P<0.05$; Kruskal-Wallis), although the changes are not as much as the level of *Axin2* in HCT116 cells (figure 4.7 B). So far, data showed that these two Wnt targets were not down-regulated with the deficiency of *CITED1* and therefore *CITED1* deficiency does not turn off the Wnt signalling in HCT116 and HT29 cell lines.

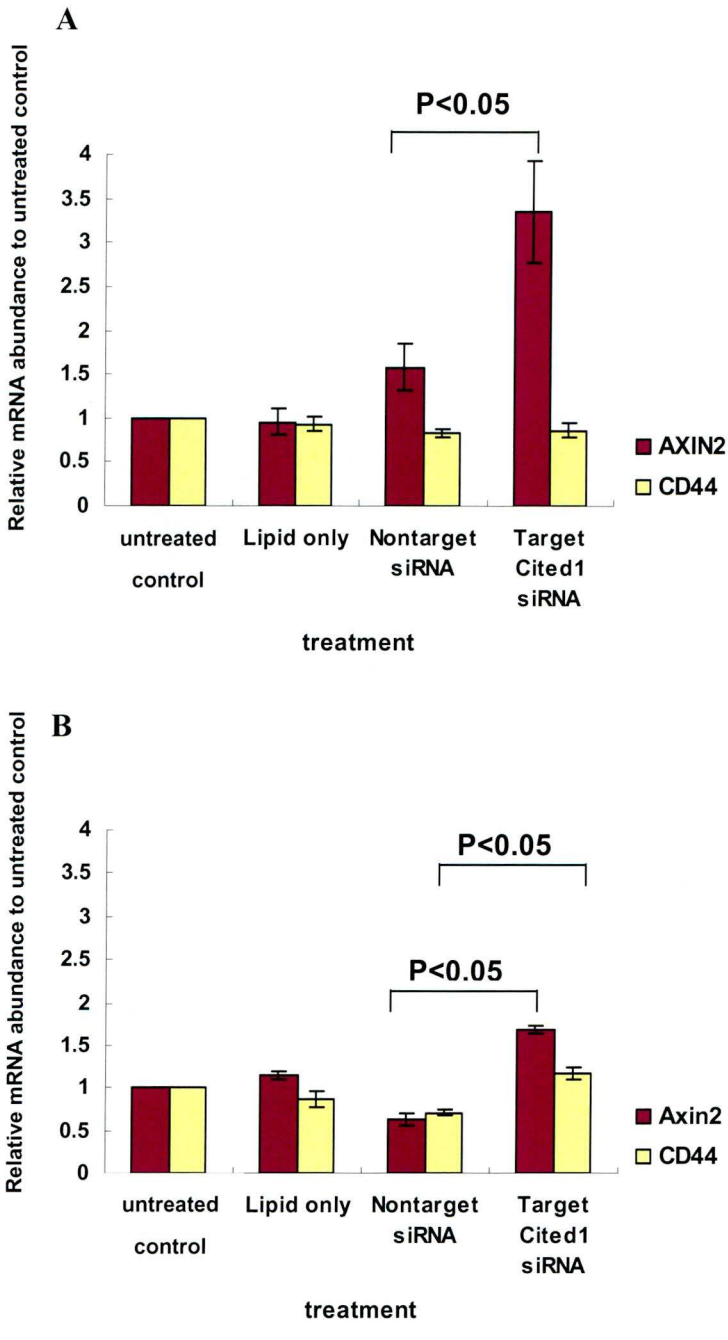

Figure 4.7 Detection of Wnt downstream target regulations with CITED1 deficiency in HCT116 cell line (A) and HT29 cell line (B). Data are from minimum of 3 experiments.

4.6 Discussion

4.6.1 Possible mechanism of cell growth reduction

In our *in vitro* model, cell survival and cell proliferation were significantly reduced following CITED1 knock down for both HCT116 and HT29 cells. There are several possible mechanisms behind the observed cell growth reduction. Unfortunately, no further mechanism studies were carried out because of the time limit.

Firstly, a smaller number of surviving cells following reduction in CITED1 expression are likely to be the result of a greater cell death. An essential step in clonogenic assay is that the same number of living cells was settling down and attached at the bottom of the cell culture wells to grow. The reduced number of cell colonies was therefore initially decided by the number of successfully attached living cells. However, the proportion of cells processed to cell death is presumably not large, because of the minor reduction of cell survival. Additionally, the ability of the attached cells to divide may also contribute to the result of clonogenic assay. Active-caspase 3 labelling would be an approach for determining if the cell death was due to apoptosis.

When the cell proliferation was being tracked by SRB assay on a daily course, the cell proliferation was obviously reduced following *CITED1* knock down (4.6.2). It is important to note that there was no further siRNA treatment during the SRB assay. Therefore this assay is measuring the effect of CITED1 deficiency on the starting

population of cells. The reduced proliferation may result from either a prolonged cell cycle or a cell cycle arrest. Cells would be arrested at certain phase of the whole cell cycle in the later case, which will result in an increased number of cells being blocked at one phase, and in turn will interfere the rate of cell proliferation. The cell cycle analysis can be detected by using flowcytometry assay on the cells pulse labelled with BrdU to track the cells went through the S-phase and propidium iodide (PI) for the DNA content.

4.6.2 Hypothetical molecular mechanism of CITED1

Following *CITED1* knockdown, *AXIN2* and *CD44* were not down-regulated, which indicates that *CITED1* deficiency does not turn off downstream Wnt signalling.

For both HCT116 and HT29 cell lines, *AXIN2* was dramatically up-regulated following *CITED1* knock down. As identified in Sansom's Nature paper (Sansom et al., 2007), CITED1 and Axin2 are both c-Myc dependent Wnt targets. In the context of knocking down *CITED1* in colon cancer cells, up-regulation of Axin2 may be one of the rapid compensatory effects induced by CITED1 efficiency on maintaining the activity of the downstream of c-Myc, because *CITED1* and *Axin2* expression levels were measured at the end point of siRNA transfection, where is the start point of the SRB cell proliferation assay. However, in function, Axin2 is primarily a repressor of the Wnt signalling pathway (Lustig et al., 2002), as well as being a target. In a slightly longer time frame (e.g. days post transfection) after the *CITED1* knock

down, the negative feedback loop of Axin2 onto the Wnt pathway may induce more inhibition. Therefore, the hypothetical functional relations between CITED1, Axin2, c-Myc and Wnt are that if CITED1 has a negative effect on Axin2. It then acts in a negative manner upstream of Wnt signalling, as shown in figure 4.17.

Due to the complexity of Axin2 being both repressor and target of Wnt signalling pathway, a series of TOP-FLASH reporter assay is needed to clarify the alterations of the activities of this pathway at different point from the top to the bottom. If possible, a comprehensive DNA microarray or PCR signalling pathway assay would be able to generate a full map of the related- pathway alterations following *CITED1* knock down in cell lines.

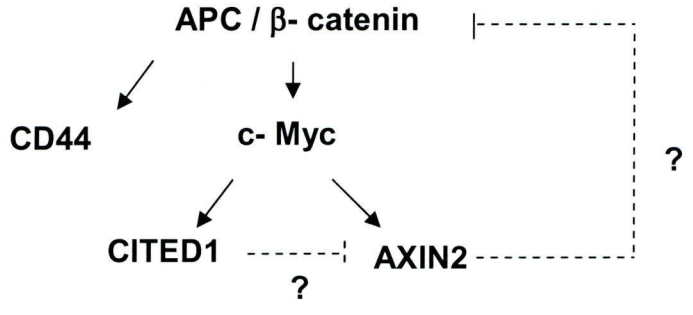

Figure 4.8 Hypothetical functional relations between CITED1, Axin2, c-Myc and the Wnt pathway.

Chapter 5 Effect of Cited1 loss on intestinal tumourigenesis in the Min mouse

5.1 Introduction

In chapter 4, the inhibitory effect of CITED1 on human colon cancer cell growth was demonstrated *in vitro*, although the underlying molecular mechanism was elusive. In this chapter, we use a transgenic mouse model to demonstrate the potential of Cited1's key role in the intestinal tumourigenesis and the underlying *in vivo* molecular mechanism.

5.2 Mouse models

Min (multiple intestinal neoplasia) mouse model carries a heterozygous truncating mutation of Apc and typically develops multiple intestinal polyps in the small intestine (Taketo and Edelmann, 2009). The min mouse model mimics the rapid development of adenomatous polyps that affect FAP patients, which is caused by germline mutation of APC in humans (Corpet and Pierre, 2005). In this project, Min mice on C57Black/6 background were used and provided a high penetrance of disease.

Cited1 is located on the X chromosome. *Cited1* global knock-out mice (also on C57Black/6 background) are available, which display placental deficiency resulting in developmental growth retardation from embryonic day 18.5 (E18.5) and a high death rate immediately during birth or after birth (Rodriguez et al., 2004). *Cited1*

null mice also display a mammary ductal outgrowth defect during (Howlin et al., 2006).

Given that Cited1 is over-expressed in the small intestine after Apc loss and in Min mouse intestinal adenomas, together with its role in human colon cancer cell lines, we asked whether deficiency of Cited1 could inhibit intestinal adenoma formation in Min mice.

Homozygous (*Cited1*$^{-/-}$ *Apc*$^{Min/+}$), heterozygous (*Cited1*$^{-/+}$ *Apc*$^{Min/+}$) and wild type (*Cited1*$^{+/+}$ *Apc*$^{Min/+}$) cohorts were generated by crossing Cited1 null mice with *Apc* Min mice. The mice used were all homozygous with respect to *Pla2g2a* (*phopholipase* A2) locus for Mom-1 (modifier of Min1), which is C57Black/6 background dependent.

Cited1 null mice are not born according to Mendelian ratios and pups that are born are significantly smaller than wild type litter mates. The intestine of Cited1 heterozygous females will be composed of mosaic areas of tissue that are essentially wild type or null for *Cited1*, which is due to random X chromosome inactivation during development leaving either the wild type or the mutant allele inactive (Figure 5.1). Due to the nature of the X-linked *Cited1* mutation, the males can only be homozygous mutants.

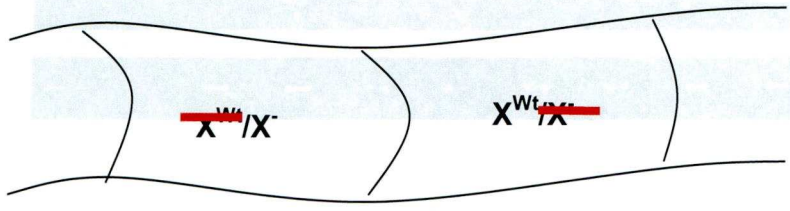

Figure 5.1 Due to random X chromosome inactivation, heterozygous females will have a mosaic expression pattern for Cited1 with large areas of homozygous and wild type tissue. This diagram is kindly provided by Dr. Phesse.

5.3 Characterization of Cited1 knock-out mice on Min background

5.3.1 Characterization of Cited1 mRNA expression in small intestine

The *Cited1* mRNA expression in 3 mice cohorts were analysed by semi-quantitative PCR and the data of the representative samples is shown in Figure 5.2A. Normal tissues and tissues of random adenoma polyps were taken from mouse small intestine of 3 cohorts. PCR products of *Cited1* and *β-actin* at exponential phase were separated on gel. The normal tissue and adenomas from the Cited1 homozygous null min mice (*Cited1*$^{-/-}$ *Apc*$^{Min/+}$) expressed no *Cited1* as expected and confirmed their status as genuine *Cited1* null animals. *Cited1* expression was almost undetectable in the normal tissue of both Cited1 heterozygous (*Cited1*$^{-/+}$*Apc*$^{Min/+}$) and wild type (*Cited1*$^{+/+}$*Apc*$^{Min/+}$) Min mice, but was up-regulated in adenomas of both cohorts when compared to normal tissue from the same mouse.

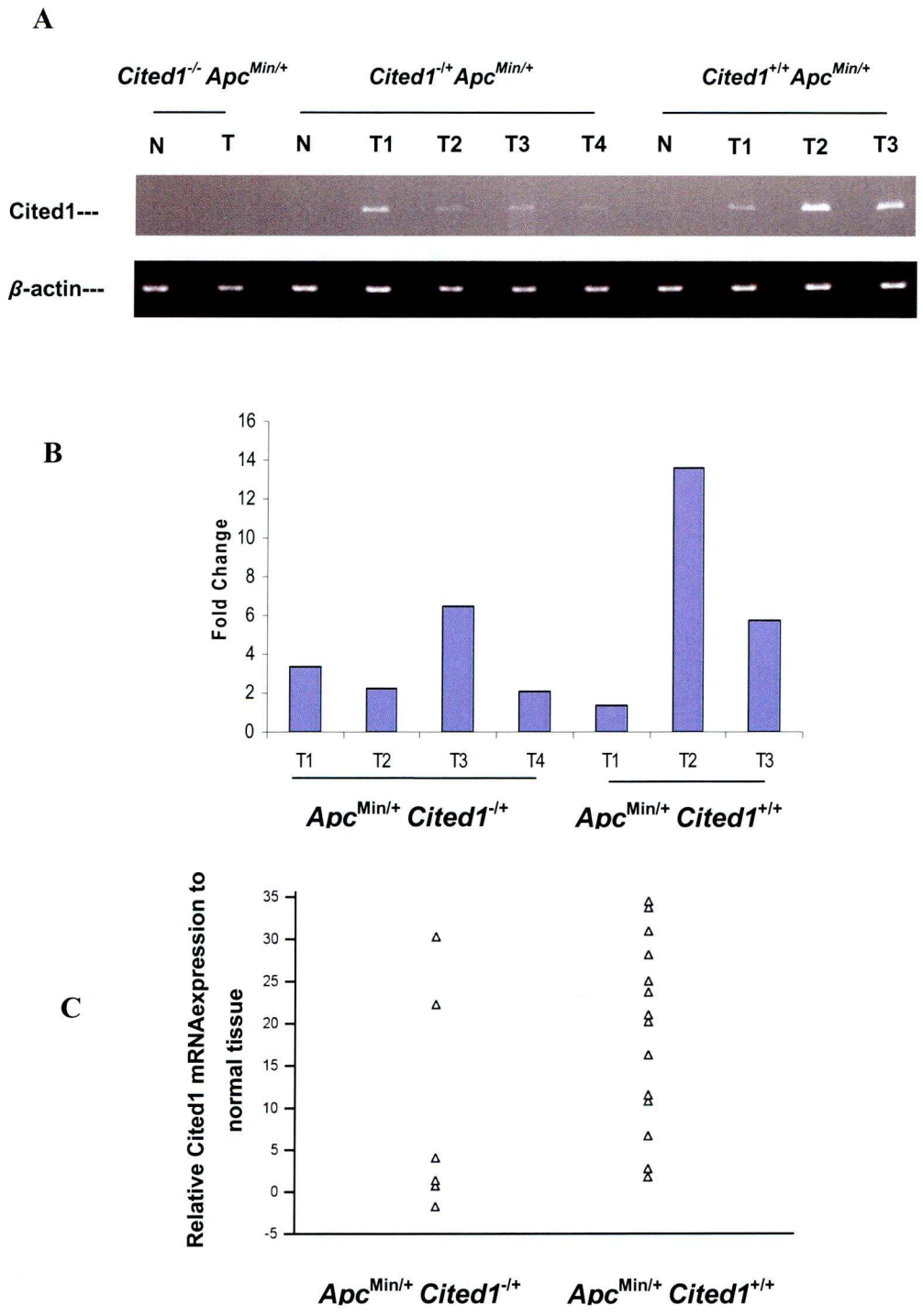

Figure 5.2 Analysis of Cited1 expression in 3 Min mice cohorts. (A) Representative gel showing Cited1 mRNA expression from semi-qPCR. (B) Relative fold changes of Cited1 mRNA in tumours in heterozygous and homozygous Cited1 null Min mice. (C) Cited1 mRNA expression levels in all analysed Min adenomas from heterozygous and homozygous Cited1 null Min mice. This is the representative data from 2 repeat experiments.

Similar results were observed in an independent SYBR Green quantitative PCR assay (Figure 5.2B), which confirmed the semi-quantitative data showing the *Cited1* status in the inter-cross-generated Min mice. There were no detectable amplification curves in the normal and adenoma tissues of the homozygous *Cited1* null Min mice showing no detectable *Cited1* mRNA, therefore the fold changes cannot be calculated. The fold changes of adenomas in heterozygous and wild type Cited1 Min mice were normalised to the normal tissues taken from the same mouse, which showed the *Cited1* mRNA over-expression in Min adenomas in heterozygous mutants and wild type Cited1 Min mice.

Densitometry of the semi-quantitative PCR gel of samples taken from all 9 mice (3 from each cohort) was used to analyse the *Cited1* expression levels (Figure 5.2C). Density data showed large majority of adenomas (12 out of 14) displayed dramatically up-regulated *Cited1* mRNA expression (larger than 5-fold) in Cited1 wild type cohorts, when compared to normal tissue from the same mouse. Highly expressed *Cited1* mRNA was in a smaller proportion (2 out of 6) of adenomas in the heterozygous mutants.

In Cited1 homozygous null mice, adenomas were present and these had undetectable level of Cited1 demonstrates that Cited1 is not essential for adenoma formation in Min mice. However, the adenomas displayed significantly up-regulated levels of

Cited1 in both Cited1 heterozygous and Cited1 wild type cohorts suggests that Cited1 plays an important role in intestinal tumourigenesis.

5.3.2 Characterization of Cited1 protein expression in small intestine

Western blotting analysis was used to measure protein levels of Cited1 expression in the 3 mouse cohorts. In chapter 4, two different Cited1 antibodies were tested. The commercial antibody from Genetex failed to show the correct band of Cited1 protein. However, the antibody (a kind gift from Dr. Shioda; in Methods) was able to detect Cited1 antigen in Min mouse samples at the correct size. This antibody was then used to characterise the *Cited1* knock out.

Paired normal and tumour tissue samples from heterozygous and homozygous *Cited1* null Min mice were analysed (Figure 5.3). As a point of note, these protein samples came from the same mice as the mRNA samples for semi-qPCR. In figure 5.3A, on the blot, the lower bands are assumed to be Cited1 because it is the correct size. However, what the upper bands are is unknown. It is observed that there are weaker bands of normal and tumour tissues from homozygous *Cited1* null Min mice compared with the normal and tumour tissues from the heterozygous cohort. However, the visible bands of homozygous *Cited1* null Min mice from western blotting conflicts with the semi-qPCR and qPCR data showing no detectable mRNA in *Cited1* homozygous KO /Min using specific primers. Due to the unique result of

using Cited1 primers as confirmed by the Blast nucleotide search, it is highly probable that this Cited1 antibody lacks specificity to mouse Cited1 antigen.

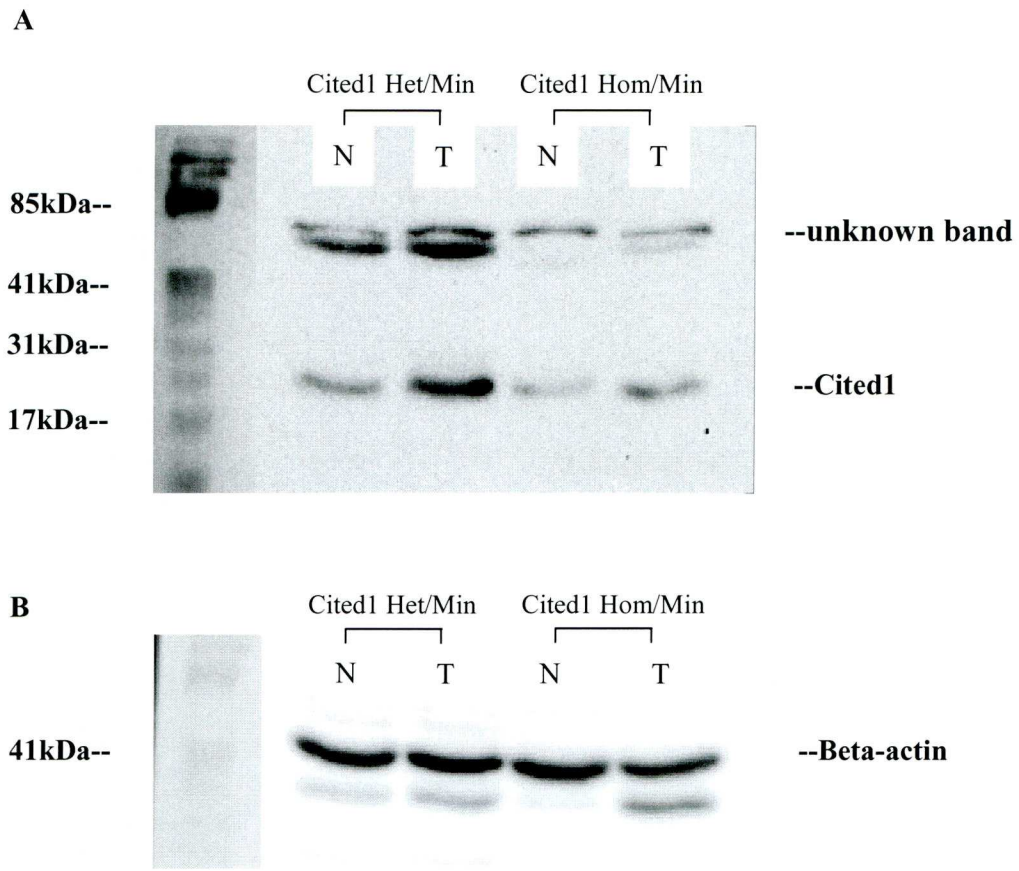

Figure 5.3 Cited1 protein expression levels detected by antibody provided by Dr. Shioda. (A) Blot of intestinal tissues probed by Cited1 antibody. (B) Blot shows the equal loading control of Beta-actin. N=normal, T=tumour; Het= heterozygous, Hom= homozygous. This is the representative data from 2 repeats.

In the Cited1 blotting of figure 5.3, two bands for each sample (both upper and lower) are very close to the size of light chain (25kD) and heavy chain (50kD) of mouse IgG immunoglobulin. Since this is an antibody generated from mouse and probed to a mouse antigen, it is likely that there is unspecific mouse IgG immunoglobulin in this antibody.

A mouse IgG immunoglobulin sample was then used together with Cited1 heterozygous and homozygous samples, light chain and heavy chain of mouse IgG are at the same position as the two bands probed by Cited1 antibody (Figure5.4). Again, bands of Cited1 homozygous are weaker than heterozygous, but still visible on the blotting (Figure 5.3 and Figure 5.4).

Taken all above data together, it suggests that Cited1 antibody provided by Dr. Shioda does not appear to be absolutely specific to Cited1 (partcularly given that bands could be detected in the homozygous *Cited1* animals), with the antibody potentially only showingCited1 when overexpressed. Data from semi-quantitative and quantitative PCR are more reliable than western blotting analysis in terms of characterisation of the Cited1 knock out Min mouse model to be genuine Cited1 null animals.

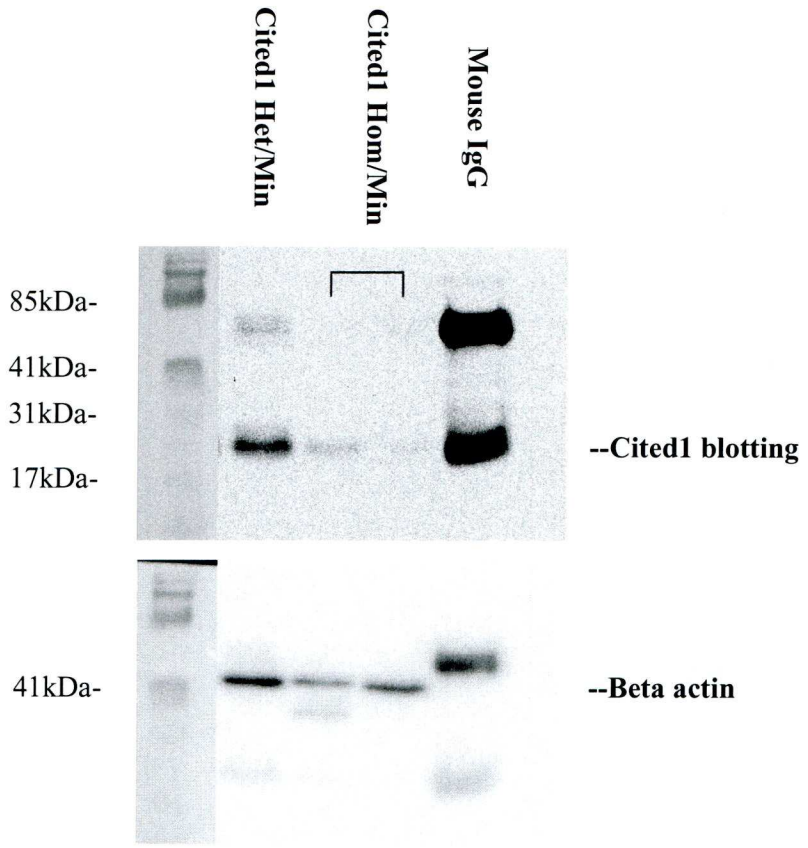

Figure 5.4 Test of Cited1 antibody with Mouse IgG immunoglobulin. Protein samples of mouse intestinal tissues (different from samples used in figure 5.3) were used with Mouse IgG antigen. Top blotting was probed by Cited1 antibody. Bottom blotting shows the loading control Beta-actin. No beta-actin was detected in Mouse IgG sample. The bands on the right panel of the bottom blotting were carried over from the previous western blotting. Het= heterozygous, Hom= homozygous. This is the representative data from 2 repeats.

5.4 Loss of Cited1 increased the life span of Min mice

The 3 cohorts were aged and culled upon signs of intestinal neoplasia. The median life span of wild type *Cited1* Min mice is 284.5 days (n=8). The median life span of heterozygous *Cited1* Min mice is 269 days (n=21). However, the median life span dramatically increased to 515 days for *Cited1* homozygous null Min mice (n=5) (Figure 5.7). 'Wild type' *Cited1* Min mice are naturally heterozygous for *Cited1* (Min *Cited1*$^{Y/+}$), as *Cited1* is located on the X chromosome. Additionally, due to the high penetrance of disease on C57Black/6 genetic background for the *Cited1* deficient induced placental defect, the homozygous mice survived to adulthood were all males (Min *Cited1*$^{Y/-}$). Accordingly, the statistical significance cannot be analysed as the heterozygous cohort is actually the mixture of 'wild type' male (Min *Cited1*$^{Y/+}$) and heterozygous female (Min *Cited1*$^{-/+}$). Therefore, it is necessary to separate female and male populations in cohorts for comparison due to the nature of the X-linked *Cited1* mutation.

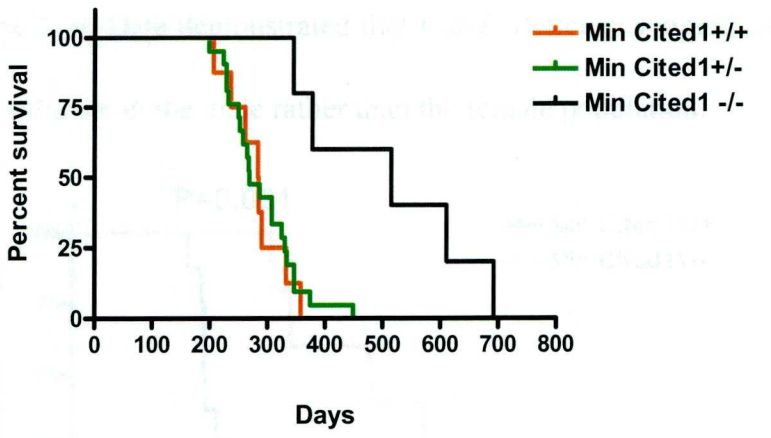

Figure 5.7 Kaplan Meier plot showing the survival percentage of 3 mice strains. (Data for this figure is kindly provided by Dr. Phesse)

In the female population, the median life span slightly increased from 284.5 days (Min *Cited1* $^{+/+}$, n=8) to 325 days (Min *Cited1* $^{+/-}$, n=13) after losing *Cited1* on one allele (Figure 5.8). However, the life span extension was not significant with P value of 0.237 (Kaplan-Meier; Chi squared =1.4, DF=1).

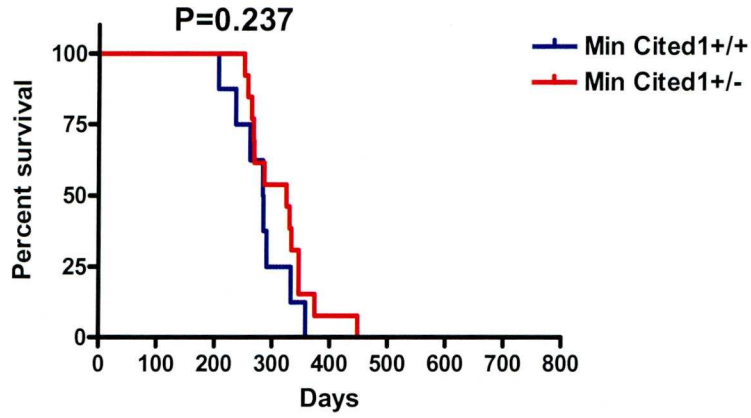

Figure 5.8 Survival percentages of wild type and heterozygous Cited1 female Min mice.

In the male population, the median life span of 'wild type' *Cited1* Min mice cohort was 230.5 days (Min *Cited1* $^{Y/+}$, n= 8), which was significantly increased to 515 days (Min *Cited1* $^{Y/-}$, n=5) with a P value of 0.001 (Kaplan-Meier; Chi squared =10.68, DF=1) (Figure 5.9). Data demonstrated that *Cited1* deficiency significantly increase life span of Min mice in the male rather than the female population.

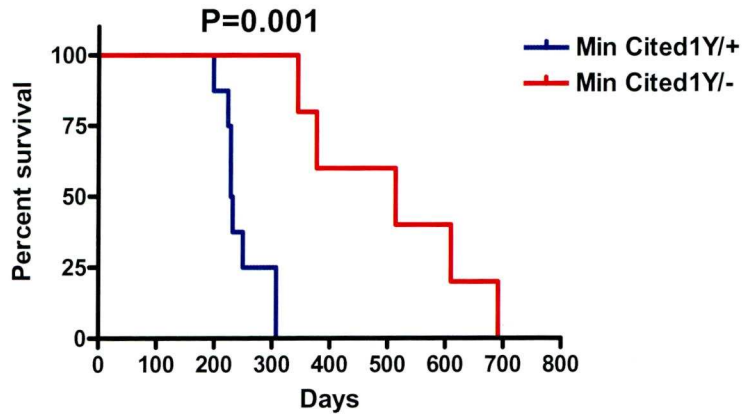

Figure 5.9 Survival percentages of heterozygous and homozygous Cited1 male Min mice.

It is interesting that the significant life span extension after losing Cited1 only happened to Min males, although the females theoretically lost *Cited1* on one X chromosome in heterozygous mutants. In mammalian females, most genes on one X chromosome are silenced by X inactivation through epigenetic system, however, some 'escape' X inactivation and are expressed from both active and 'inactive' Xs (Heard and Disteche, 2006). Due to the potential complication of variable expression of genes on the X chromosome, therefore the following tumour burden characterization only focuses on the Min males.

5.5 Tumour burden characterization in Cited1 knock-out Min mice

5.5.1 Loss of Cited1 reduced the tumour number in both small intestine and large intestine of male Min mice

The tumour number per mouse was used to analyse the initiation of tumourigenesis in male Min mice. Taking both small and large intestine into consideration, tumour numbers were significantly reduced in the *Cited1* homozygous null mice compared to the heterozygous mutants ($P<0.05$, Mann-Whitney) (Figure 5.10). The *Cited1* homozygous null mice still developed some adenomas in both the small and large intestine demonstrating that Cited1 is not essential for the formation of adenomas in the intestine of Min mice. However, the significant reduction of tumour number in homozygous null suggests that Cited1 expression is required for the increased development of adenomas in Min mouse intestine. In the heterozygous mice, tumours were predominant in small intestine and only a few in the large intestine. In homozygous null mice, there are several tumours in the small intestine and only one in the large intestine. Tumours that developed in the small intestine of homozygous nulls were less than one third as many as seen in the heterozygous mice. In the large intestine, the reduction of tumour number was even greater.

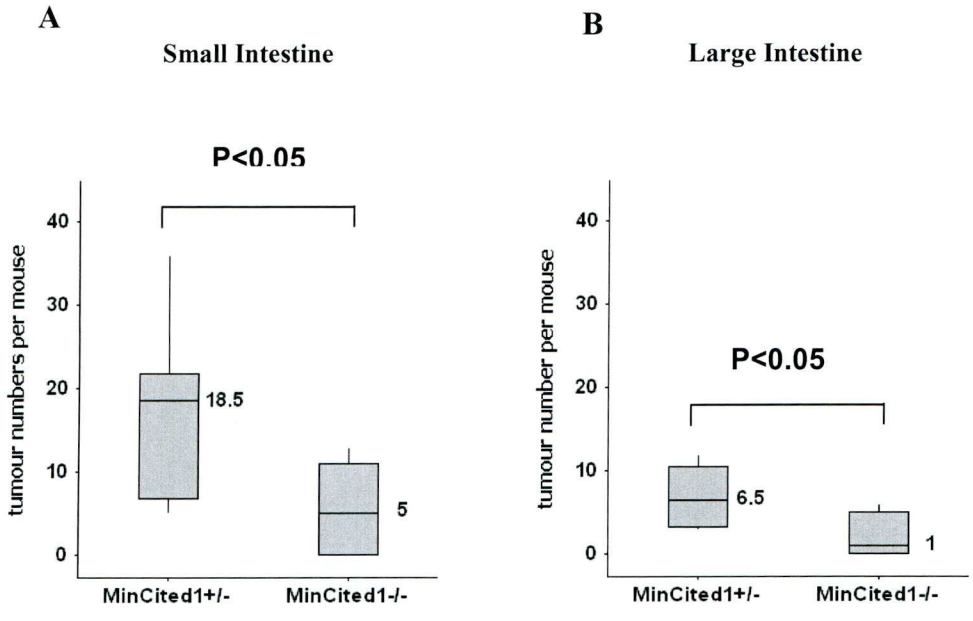

Figure 5.10 Tumour number in small and large intestine in Cited1 deficient Min males. (A) Tumour number counted in the small intestine. (B) Tumour number counted in the large intestine. (Data for this figure is kindly provided by Dr. Phesse)

5.5.2 Loss of Cited1 increased the tumour size in both small intestine and large intestine of male Min mice

The median tumour size (mm) was also analysed for heterozygous and homozygous null mutants. Tumour size was significantly increased in both small intestine ($P<0.001$, Mann-Whitney) and large intestine tissues ($P<0.05$, Mann-Whitney) (Figure 5.11). This increase is larger in small intestine than large intestine tissue. Presumably, this increase is because that the *Cited1* homozygous null mice live the longest and there was longer time frame to develop adenomas in a larger size.

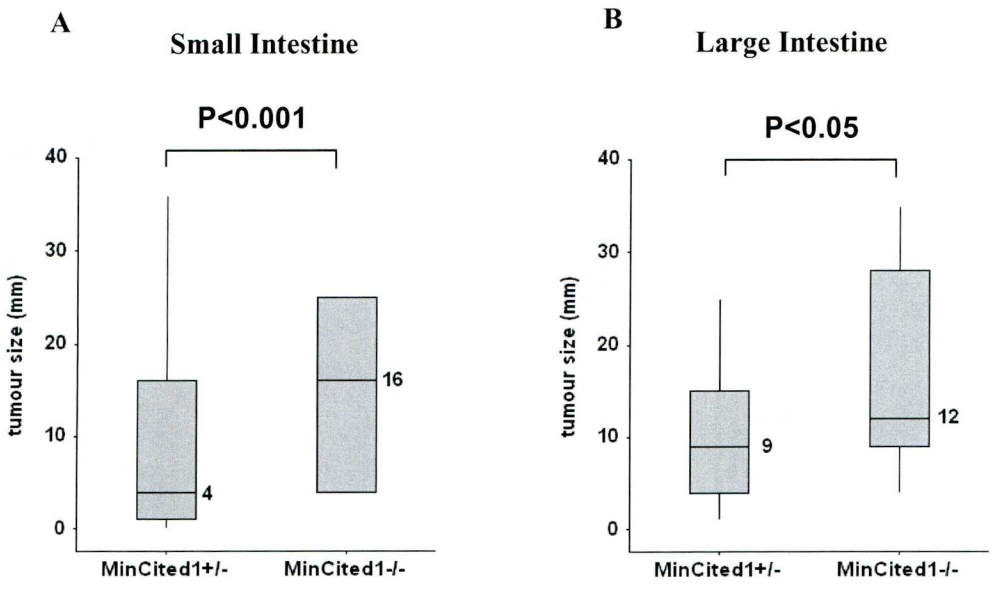

Figure 5.11 Tumour size in small and large intestine in Cited1 deficient Min males. (A) Tumour size measured in small intestine. (B) Tumour size measured in large intestine. (Data for this figure is kindly provided by Dr. Phesse)

Taken tumour number and tumour size data together, the life span of male Min mice was terminated by the tumour number rather than the absolute tumour size. Tumour number indicates the abundance of tumourigenesis events taking place in the tissues. Data was collected at the end points for different cohorts. To obtain the best comparison, the tumour size should be measured at the same time points of heterozygous and homozygous cohorts of male Min mice, which may provide more comparable data.

5.6 Loss of Cited1 does not switch off Wnt signalling status in mouse intestine

5.6.1 Loss of Cited1 does not alter β-catenin translocation in Min adenomas

Nuclear β-catenin translocation is critical for activated Wnt signalling pathway. β-catenin immuno-histochemistry was performed on small intestinal tissue sections for 3 cohorts of Cited1 deficient Min mice (Figure 5.12). β-catenin translocation from cytoplasm to nucleus was observed only in adenomatous tissue but from all 3 cohorts. There is no nuclear β-catenin translocation in normal (non-adenomatous) tissue in any of the 3 cohorts.

Data of immuno-histochemistry suggest that loss of Cited1 does not inhibit β-catenin translocation into the nucleus in Min adenomas. The development of the Min adenomas occurs in all 3 cohorts, regardless of the Cited1 status. It could be inferred that active Wnt signalling is required for almost all the adenoma development, however *Cited1* over-expression is only required for a proportion of adenomas in heterozygous and wild type *Cited1* Min mice, but not in homozygous null Min mice. Presumably, the reduced number of adenoma tumours from 'wild type' *Cited1* to *Cited1* null Min males was actually dependent on high level of Cited1 expression; therefore fewer adenomas developed when no Cited1 was present in the small intestine of Min males.

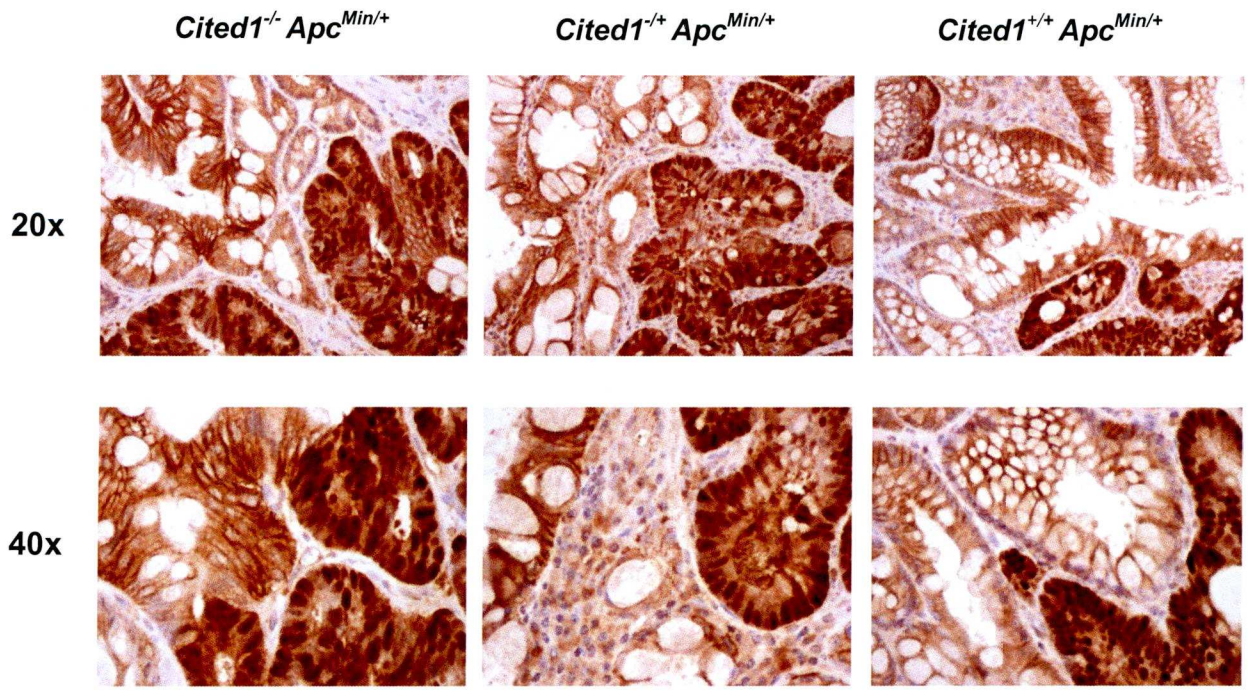

Figure 5.12 Immunohistochemistry of β-catenin of 3 Min cohorts. Images on the top row were taken under a lower amplification and the bottom row under a higher amplification. This is the representative data from 3 mice.

5.6.2 Loss of Cited1 does not switch off downstream Wnt signalling activity in Min normal tissues

Wnt downstream targets were then used to measure the alteration of Wnt signalling activity. *Cited1* deficient Min mice from 3 cohorts were terminated at different time points, due to signs of neoplasia, therefore using transformed adenomatous tissues from various development times with different Cited1 status will bring complications to the comparison. However, the normal tissues remain untransformed among 3 cohorts. Non-adenomas intestinal tissue of *Cited1* homozygous null Min mice must be more resistant to tumourigenesis, since a small number of adenomas were developed in the intestine of this cohort, in turn, resulted in a longer life span. Therefore, normal tissues of 3 cohorts were used to detect the alteration of Wnt signalling activity.

c-Myc, CD44 and Axin2 were used as reporters of Wnt signalling. Their mRNA expression levels in normal intestinal tissues of wild type, heterozygous and homozygous *Cited1* null Min mice were measured using quantitative PCR. Data were all normalised to wild type intestinal tissue. In the Cited1 homozygous null mutants, *Myc*, *CD44* and *Axin2* were all over-expressed compared with heterozygous *Cited1* Min mice (Figure 5.13).

Although it was only preliminary data from one mouse of each cohort, data suggests that the presents of Cited1 seems to be able to inhibit downstream Wnt signalling

activity. When losing Cited1, downstream Wnt signalling is more active on the Min background, under which condition Min mice survived for another ~250 days compared with heterozygous Cited1 Min. However, no nuclear β-catenin translocation was observed in the normal intestinal tissues from the 3 cohorts. Therefore, there must be some unknown molecular events happening, dependent on Cited1 status, lying between β-catenin and Wnt signalling regulated gene transcription. In normal tissue, this potential molecular mechanism will modulate Wnt signalling activity possibly inhibiting β-catenin translocation from cytoplasm into nucleus; however, downstream Wnt signalling is more active.

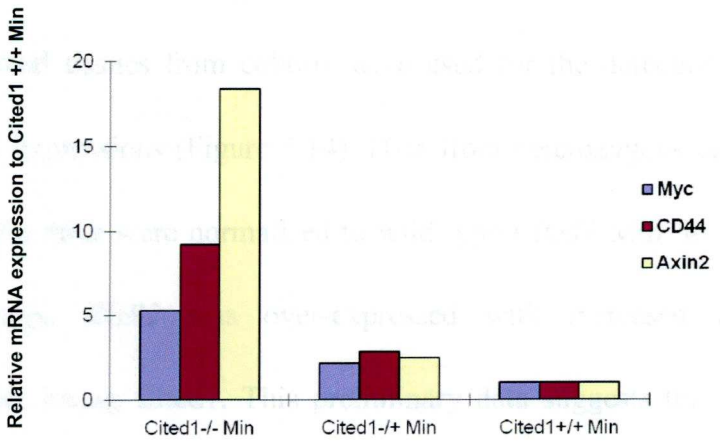

Figure 5.13 Wnt targets expression in Min normal tissues of 3 cohorts. Myc, CD44 and Axin2 were all dramatically overexpressed in homozygous Cited1 null min mouse non-transformed intestinal tissues. Due to the limited amout of sample, this experiment was carried out once on one mouse from each cohort. It is shown as preliminary data.

5.7 Is ErbB2 part of the underlying Cited1 mechanism for enhancing tumour formation?

5.7.1 Cited1 deficiency does not reduce *ErbB2* mRNA expression in the Min mouse intestine

ErbB2 has been demonstrated to be an oncogene in breast cancer (Ross and Fletcher, 1999). The importance of ErbB2 in mammary gland tumour development has been well demonstrated and it is the target of therapy in this disease (Ross et al., 2009). Cited1 has been reported to be a co-activator of the EGR2 transcription factor and is able to associate with EGR2 to activate ErbB2 expression during mammary tumour progression (Dillon et al., 2007). The research question is that whether *Cited1* deficiency is reducing *ErbB2* expression levels in Min mouse intestinal tissues and therefore inducing a longer life span of the homozygous *Cited1* null Min cohort.

Normal intestinal tissues from cohorts were used for the detection of *ErbB2* and *EGR2* mRNA expressions (Figure 5.14). Data from heterozygous and homozygous Cited1 null Min mice were normalised to wild type *Cited1* Min. In the Min mouse intestinal tissues, *EGR2* was over-expressed with increased *ErbB2* mRNA expression after losing Cited1. This preliminary data suggests that *ErbB2* mRNA remain expressed at a high level in the *Cited1* homozygous null Min mice which lived the longest. Therefore, *Cited1* deficiency does not reduce *ErbB2* expression in Min mouse intestine.

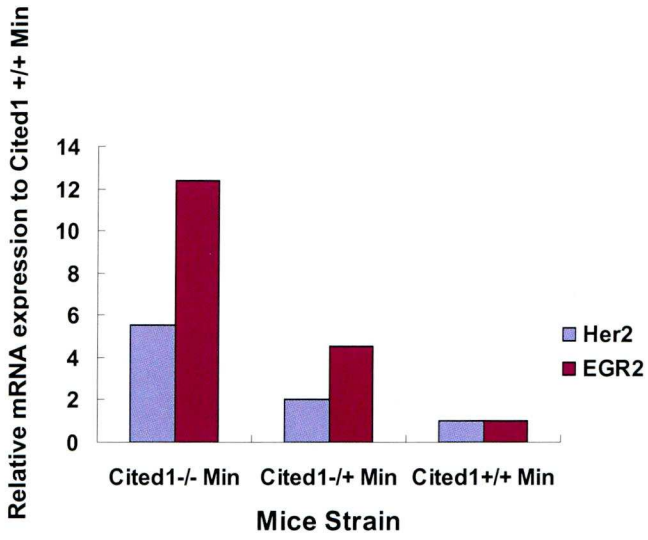

Figure 5.14 ErbB2 and EGR2 mRNA expression in Min normal tissue of 3 cohorts. ErbB2 and EGR2 were both over-expressed in homozygous Cited1 null Min mouse normal intestinal tissue. Due to the limited amout of sample, this experiment was carried out once on one mouse from each cohort. It is shown as preliminary data.

5.7.2 No ErbB2 over-expression in the initial stage of tumourigenesis

The involvement of ErbB2 in the initial stage of tumourigenesis needs to be clarified by detecting whether it is altered as one of the Wnt signalling regulated targets in the early *Apc* knock-out model. Intestinal epithelium of wild type and knock out *Apc* mice were used to detect *ErbB2* mRNA expression levels together with the controls of another 3 known Wnt targets (Axin2, CD44 and cMyc) (Figure 5.15). As expected, three Wnt targets were all over-expressed. However, the normalised fold change data showed that *ErbB2* mRNA expression level was slightly decreased less than 2-fold in the Apc knock-out mouse intestinal epithelium, which was considered to be no change. Therefore, ErbB2 mRNA is proposed to be uninvolved in the initial stage of intestinal tumourigenesis.

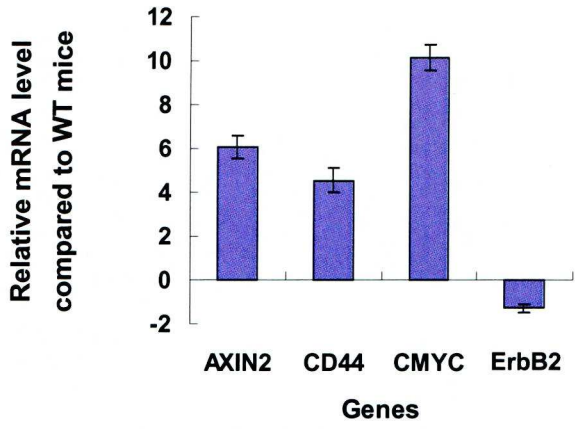

Figure 5.15 ErbB2 and Wnt targets expression in Apc knock out intestinal epithelial cells. Error bars indicate the standard error of the mean (SEM). n=3

Taken all together, ErbB2 is not an important target of the intestinal tumour progression in both Min mouse model and immediate Apc knock-out model.

5.8 The possible involvement of TGF-β pathway in the mechanism of the inhibitory role of Cited1 deficiency in intestinal tumourigenesis

In the TGF-β pathway, the TGF-β ligands bind to transmembrane TGF-β receptors which phosphorylate SMAD2/3 (Li et al., 2005). Phosphorylated SMAD2/3 then associates with SMAD4 forming a heterotrimeric complex (Li et al., 2005). This phosphorylated receptor complex of Smads translocate to the nucleus where it interacts with transcription factors to control gene expression (Figure 5.16) (Massague et al., 2000).

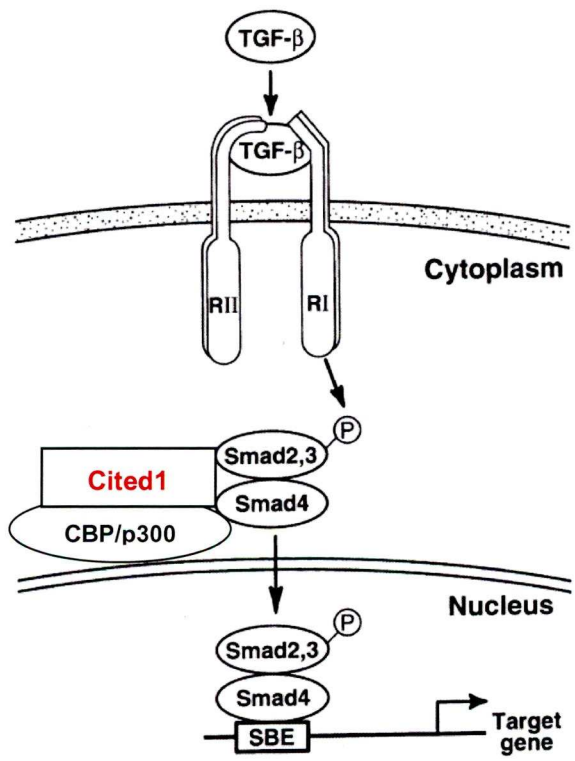

Figure 5.16 Schematic graph showing TGF-β signalling pathway. (Adapted from Li *et al.*, 2005) The hypothetical role of Cited1 through CBP/p300 in this pathway was added by the author of this thesis, but not included in the original paper.

In addition to this canonical pathway TGF-β also interacts with many other pathways regulating cellular growth, for example, RhoA, Cdc42, Ras, PI3 kinase, which causes the role of TGF-β in cancer to be both complex and highly dependent on cellular context (Barrios-Rodiles et al., 2005; Bierie and Moses, 2006). In early stages of tumourigenesis, including colonic adenomas, TGF-β acts as a tumour suppressor (Munoz et al., 2006; Siegel et al., 2003a; Sodir et al., 2006; Takaku et al., 1998). In more advanced lesions, TGF-β acts as a tumour promoter enhancing metastatic behaviour, immune evasion and angiogenesis (Muraoka-Cook et al., 2004; Thomas et al., 2005).

Non-DNA binding transcriptional co-regulator Cited1 has been reported to be able to bind to the CBP/p300 coactivators and DNA-binding Smad proteins, in turn enhancing the functional link between Smads and CBP/p300, and the Smad-mediated transcription (Yahata et al., 2000). The research question is whether Cited1 deficiency is altering the TGF-β signalling activity in Min mouse intestinal tissues and therefore induced a longer life span of the homozygous *Cited1* null Min cohort. The phosphorylated Smad2/3 translocation would indicate the TGF-β signalling pathway activation.

5.8.1 Loss of Cited1 does not prevent nuclear translocation of phosphorylated Smad2/3

In the images of immuno-histochemistry, phosphorylated Smad2/3 translocates into nucleus in both Min adenomas and the surrounding normal tissues in all 3 cohorts (Figure 5.17 top row). The condensed nuclear phosphorylated Smad2/3 were observed in all the intestinal epithelium cells as shown under higher amplifications in both tissue types (Figure 5.17, middle and bottom row). Immuno-histochemistry data suggests that loss of Cited1 does not prevent phosphorylated Smad2/3 translocation into nucleus in either normal or adenoma tissues of Min mouse intestine. Therefore, TGF-β signalling turns out to be active in normal and adenoma intestinal tissues in all 3 cohorts. The following question is whether Cited1 deficiency alters the degree of TGF-β signalling activity. However, it is difficult to determine the level of TGF-β signalling activity from immuno-histochemistry data of phosphorylated Smad2/3.

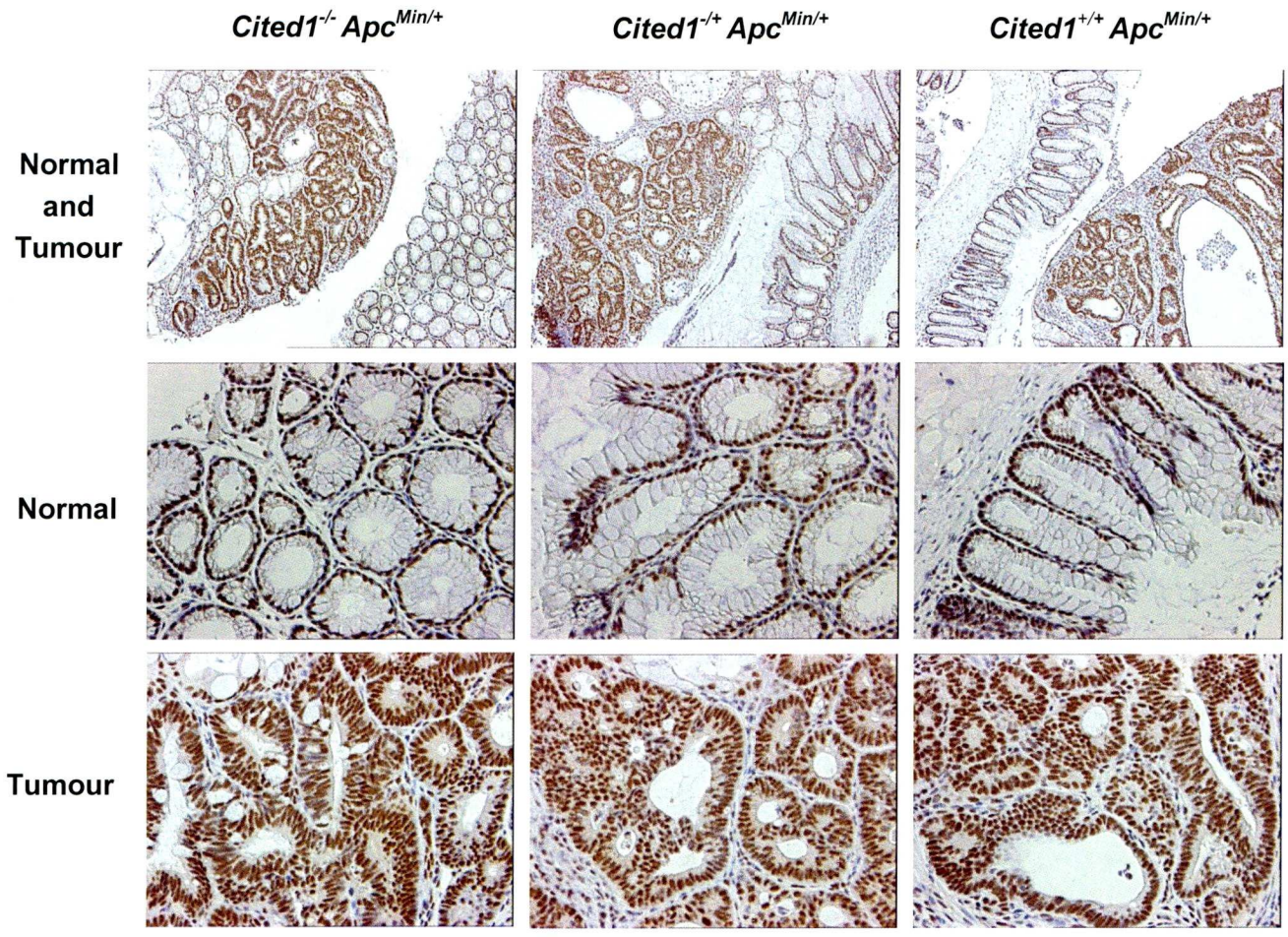

Figure 5.17 Immunohistochemistry of phophorylated Smad2/3 of Min mouse intestine in 3 cohorts. Top row shows the phosphorylated Smad2/3 location in both normal and tumour intestinal tissues. Middle and bottom row show the phosphorylated Smad2/3 in normal or tumour tissue under high amplification, respectively. This is the representative data from 3 mice.

5.8.2 Cited1 is not interacting with TGF-β signalling pathway

In order to clarify the activity of TGF-β signalling and then the involvement of Cited1 in this pathway in mouse intestinal tissue, levels of phosphorylated Smad2/3 were measured by western blotting and phosphorylated Smad2/3 expression were analysed by densitometry.

In the western blotting assay (figure 5.18), the top blot shows that the phosphorylated Smad2/3 protein expression is at a higher level in the tumours than in the normal tissue taken from the same mouse. However, the bottom blot shows the higher density of control beta-actin for the tumour samples in the heterozygous and homozygous *Cited1* null Min intestine. Thus, it is difficult to directly compare the phosphorylated Smad2/3 from the images of the blot. Additionally, the difference of phosphorylated Smad2/3 between normal and tumour tissues does not reflect the effect of *Cited1* deficiency on the mechanism and the life span changes. However, the comparable samples are normal tissues from wild type, heterozygous and homozygous *Cited1* mutants. Therefore, the densitometry was used to measure the normalised expression level of phosphorylated Smad2/3 in normal intestinal tissues.

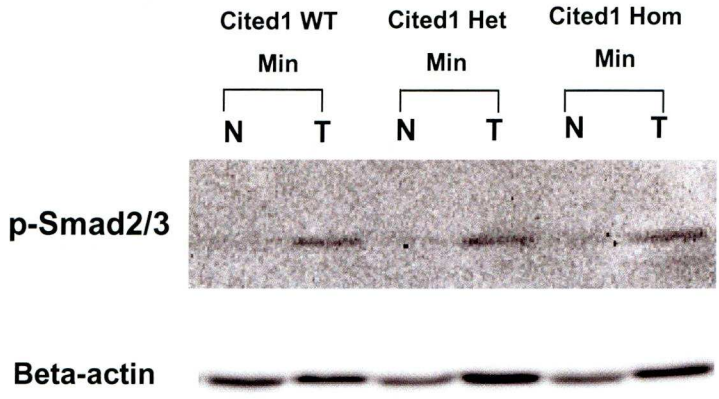

Figure 5.18 Western blotting of phosphorylated Smad2/3 in 3 mice cohorts. Top blotting shows the phosphorylated protein expression in intestinal tissues. Bottom blotting shows the loading control Beta-actin. N=normal, T=tumour; WT=wild type, Het= heterozygous, Hom= homozygous. Due to the limited amout of sample, this experiment was carried out once on one mouse from each cohort. It is shown as preliminary data.

Data from the densitometry on western blotting shows that the normalised level of phosphorylated Smad2/3 expression increased in heterozygous and homozygous *Cited1* mutants compared to wild type Min cohort (Figure 5.19). However, in the two *Cited1* deficient cohorts, normalised Smad2/3 expression levels are more or less the same. This indicates that activation of TGF-β pathway increased in normal tissues with both reduced and absent Cited1which level compared with the normal tissue with the wild type Cited1.

Taking the data of survival percentages into consideration, the significant extended life span was only observed in homozygous *Cited1* null Min cohort rather than heterozygous mutants, but not between wild type and heterozygous *Cited1* cohorts. Therefore, TGF-β signalling activity, indicated by the levels of phosphorylated

Smad2/3, does not consistently associate with the extended life span of *Cited1* deficient Min mice, as there is no difference in the levels of phosphorylated Smad2/3 expression between heterozygous and homozygous *Cited1* Min cohorts. Therefore, data suggests that Cited1 is not interacting with TGF-β signalling pathway in the context of *Apc* Min mouse intestinal Wnt pathway.

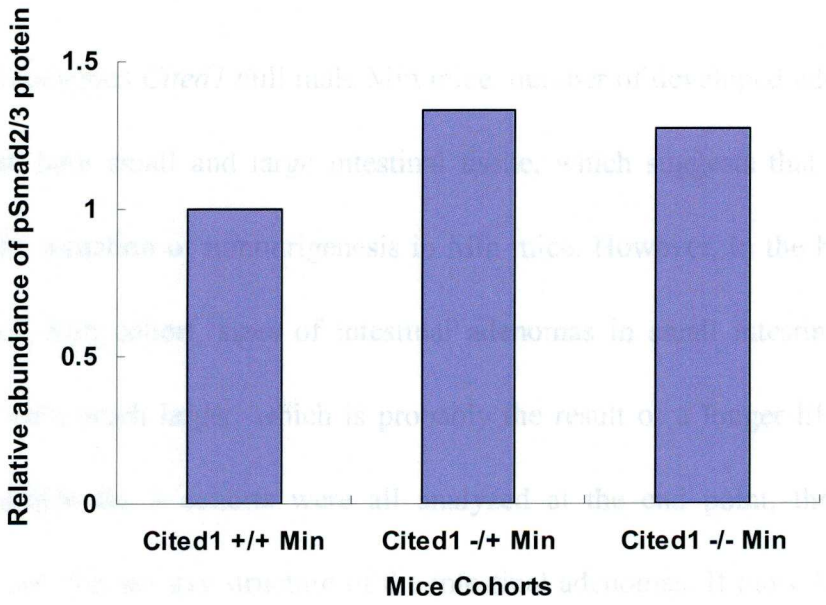

Figure 5.19 Phosphorylated Smad2/3 expression levels in Min mouse normal intestinal tissue of 3 cohorts normalised to β-actin levels.

5.9 Discussion

Cited1 was identified as one of the Apc/c-Myc dependent Wnt targets. When *Cited1* null mice were crossed with *Apc* Min mice, the Min carrying homozygous deficient *Cited1* have a significantly extended lifespan in the male population. This may be the result of *Cited1* being located on X chromosome. The mechanisms of random inactivation of one allele of X chromosomes and the fine tuning of the possible escape from the X-inactivation in female mammals made the data from the female Min mice too complex to interpret.

In the homozygous *Cited1* null male Min mice, number of developed adenomas was reduced in both small and large intestinal tissue, which suggests that Cited1 loss inhibits the initiation of tumourigenesis in Min mice. However, in the homozygous *Cited1* null Min cohort, sizes of intestinal adenomas in small intestine and large intestine were much larger, which is probably the result of a longer life span. The tumour burden for 3 cohorts were all analyzed at the end point, therefore data demonstrated the last day structure of the intestinal adenomas. If those homozygous *Cited1* null male Min mice were culled at the same time point as the 'wild type' *Cited1* males, the tumour size could possibly be the same or even smaller. However, there was no opportunity to perform the experiment for comparing samples collected at this time point.

In homozygous *Cited1* null Min cohort, *c-Myc*, *Axin2*, and *CD44* are all over-expressed compared with the heterozygous *Cited1* Min mice in normal tissues although we could not detect β-catenin in the nucleus. There may be a problem of methodology in tissue fixation when performing β-catenin immunohistochemistry. However, if β-catenin is not present in the nucleus of the normal tissue, whilst Cited1 deficiency enhanced the level of Wnt pathway regulated gene transcription, this suggests other pathways may contribute to this attenuated tumourigenesis. It could be at some point in downstream of β-catenin, but in upstream of gene transcription regulation (Figure 5.20).

We tested two hypotheses described above in normal tissues from the cohorts: the possible role of ErbB2 and TGF-β in the Wnt-Cited1 pathway. Cited1 associates with EGR2 to activate ErbB2 expression during mammary tumour progression (Dillon et al., 2007). However, in mouse normal intestinal tissue, *ErbB2* and *EGR2* mRNA were both up-regulated when no Cited1 was expressed. It has also been demonstrated that ErbB2 is probably not involved in the initial stage of intestinal tumourigenesis in this model as shown by its mRNA expression in the intestinal epithelium cells taken from an immediate *Apc* knock-out model. These data demonstrate that ErbB2 is not an important target in this model and its expression is not regulated by Cited1 as in the mammary gland (Figure 5.20).

The TGF-β signalling pathway is the other candidate, as Cited1 interacts with CBP/p300 and Smads to activate TGF-β signalling regulated transcription (Yahata et al., 2000). Phosphorylated Smad2/3 was used as an indicator of TGF-β signalling activity and did not show obvious changes at protein levels between heterozygous and homozygous *Cited1* null mutants. Ideally and for the future, a set of TGF-β pathway regulated genes should be analysed to measure the signalling activity. However, so far, there is little evidence demonstrating that TGF-β pathway may contribute to the attenuated intestinal tumourigenesis in Min mice in the context of knocking out *Cited1* (Figure 5.20).

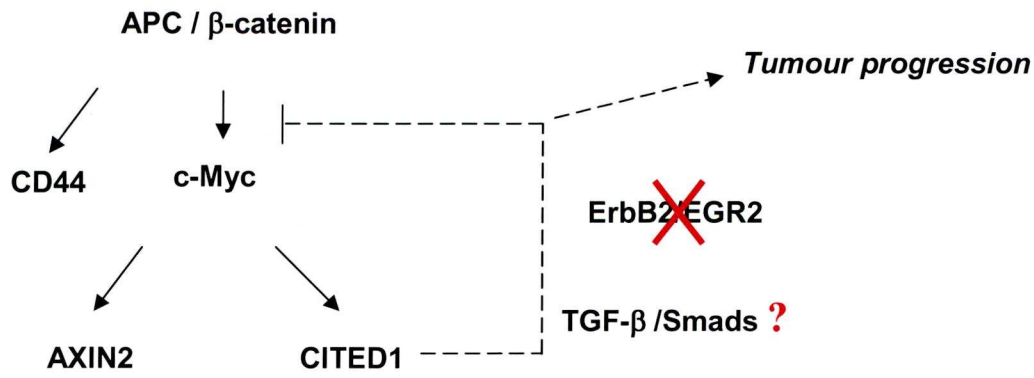

Figure 5.20 Hypothetical relations between Cited1, Wnt and tumour progression.

In the Min mouse model, *Cited1* deficiency does inhibit the intestinal tumour progression, which is consistent with the observation in the human colon cancer cell lines. Wnt pathway regulated gene transcriptions were elevated in both *in vitro* and *in vivo* models. However, the underlying molecular mechanism involved in this process is still illusive. The Min model has its limitations, whilst it has been good for studying life span. It has limitations when it comes to understanding the immediate events following Apc loss.

Chapter 6 Role of Cited1 loss in intestinal epithelium in the inducible Apc knock-out mice

6.1 Introduction

Chapter 5 demonstrates the involvement of Cited1 in mouse intestinal tumourigenesis. Cited1 deficiency significantly extended the Min mouse life span. However, the underlying mechanism linking Cited1 to the intestinal tumourigenesis is still unclear. A different model was required to investigate the early effects of loss of Cited1 in the intestine.

As stated in chapter 1 and chapter 3, there is a conditional Cre-*lox*P *Apc* knock-out model available. The primary consequences of Apc loss in the intestine has been investigated after inducing the Cre specific recombinase in the intestine of this model (Sansom et al., 2004). Additionally, Cited1 was found to be a Myc-dependent Wnt target, as it is over-expressed in this immediate model with *Apc* deletion and its over-expression reversed to be normal with the rescued phenotype after losing both Apc and Myc in mouse intestine (Sansom et al., 2007; Sansom et al., 2004). Taken all above together, the conditional *Apc* knock-out model is a better tool for investigating the primary phenotypic changes together with the underling molecular mechanisms in the intestine.

Since Cited1 deficiency extended the Min mice life span, the research question is whether knocking-out *Cited1* on the *Apc* flox background will rescue or attenuate the Apc loss imposed phenotypic changes.

6.2 Mouse models

Homozygous *Cited1* null Min mice were crossed onto the AhCre Apcflox background to produce *Cited1*$^{+/+}$ *Apc*$^{+/+}$ (wild type), *Cited1*$^{+/+}$ *Apc*$^{fl/fl}$ (Apc flox), *Cited1*$^{-/-}$ *Apc*$^{fl/fl}$ (Apc flox plus Cited1 null) and *Cited1*$^{-/-}$ *Apc*$^{+/+}$ (Cited1 null) cohorts. *Cited1* null mutants are global knockout to Cited1, rather than flox inducible mice. There are 3 mice in each cohort and mice from all 4 cohorts carry the AhCre^{+} to be comparable controls. All 12 mice were induced by injection of β-napthoflavone and were culled 4 days after the first injection.

6.3 Confirmation of *Apc* and *Cited1* knock-out status in mice

6.3.1 Confirmation of Apc recombination after inducing Cre recombinase

The Apc recombination after being induced by β-napthoflavone was detected by quantitative PCR using a pair of primers locating outside of the Cre-*lox*P-*Apc* construct. Here, qPCR is not used to measure *Apc* gene expression level, however it is detecting the amplification product size as PCR product from the recombined *Apc* allele is slightly smaller than the wild type allele after Cre-induced deletion.

According to the primer design (Dr. Zoe Burke, University of Bath), the PCR product of wild type band is a size of 383bp and the recombined band is a size of

168bp. As shown on the gel of qPCR products from 4 cohorts, Apc was successfully recombined in the *Apc* flox and *Apc* flox/*Cited1* null cohorts (Figure 6.1, sample 4-9). However, Apc remains wild type in the wild type cohort and Cited1 null cohort, although those mice were also injected by the inducing reagent β-napthoflavone (Figure 6.1, sample 1-3 and 10-12).

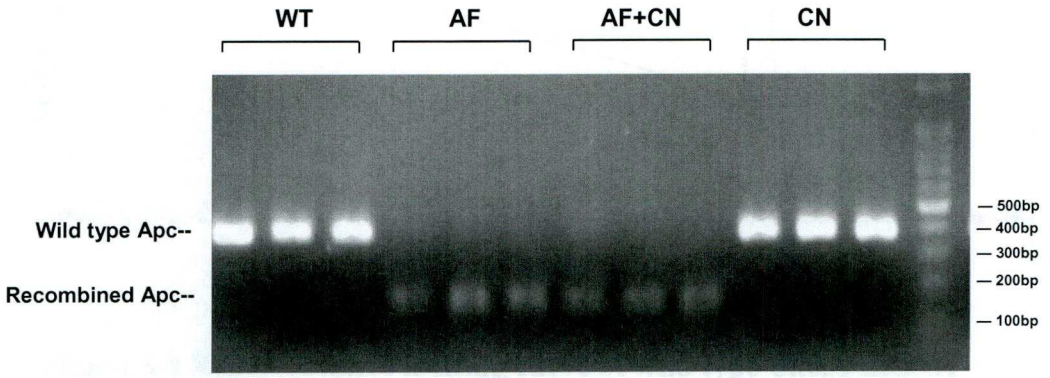

Figure 6.1 Confirmation of wild type and recombined *Apc* expression in small intestinal epithelial cells 4 days after the first injection of the cre-inducing agent β-napthoflavone. Primers were designed by Dr. Z. Burke and kindly provided by Dr. K. Reed. Gels show the amplified products from qPCR (of 40 cycles) on Apc after inducing cre recombinase. Bands of wild type *Apc* are at the size of 383bp and bands of recombined Apc are at 168bp. WT= wild type, AF=*Apc* flox/flox, AF+CN=*Apc* flox/flox and Cited1 null, CN=*Cited1* null. Three mice were being studied in each cohort. There are 3 mice in each cohort.

6.3.2 Confirmation of Cited1 status in mice

Quantitative PCR was used to confirm the Cited1 status as stated in chapter 5 (5.3.1). As expected, samples taken from wild type and *Apc* flox cohort generated melting curve with a single peak showing the detectable *Cited1* mRNA expression (figure 6.2).

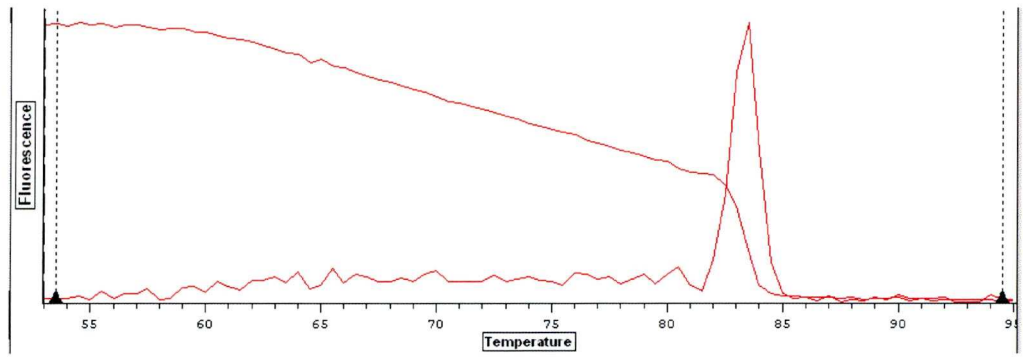

Figure 6.2 Representative melting curve of wild type *Cited1* mRNA expression in quantitative PCR from 3 mice.

However the delta Ct value is much lower for the Apc flox cohort than the wild type cohort indicating the up-regulation of *Cited1* mRNA expression after *Apc* deletion (figure 6.3) (a lower delta Ct value equates to increased amount of the allele being amplified within the sample, as fewer PCR cycles are required to reach a designed cut-off point for PCR product produced). This up-regulation is statistically significant ($P<0.04$, Mann-Whitney U test). Similar data has been demonstrated in previous work and it is used as the positive control in the context of this new colony.

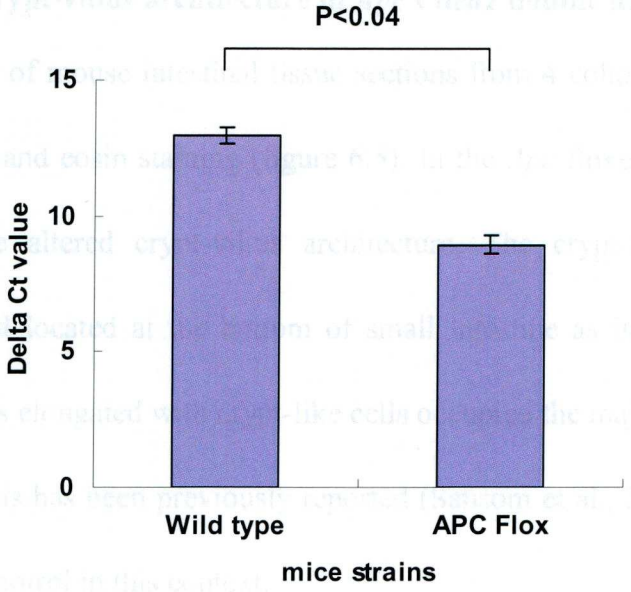

Figure 6.3 Decreased delta Ct value of Cited1 in Apc flox cohort indicates an up-regulation. Error bars indicate the standard error of the mean. There are 3 mice in each cohort.

In the double null and *Cited1* null cohorts, there was no melting curves with a single peak suggesting that *Cited1* mRNA in samples taken from these 2 cohorts is undetectable e.g. figure 6.4. The delta Ct values cannot be calculated as the samples within the wild type and *Apc* flox cohorts. Therefore, the melting curve data confirmed the Cited1 knock out status in the *Cited1* single null and *Cited1* null in addition of *Apc* loss.

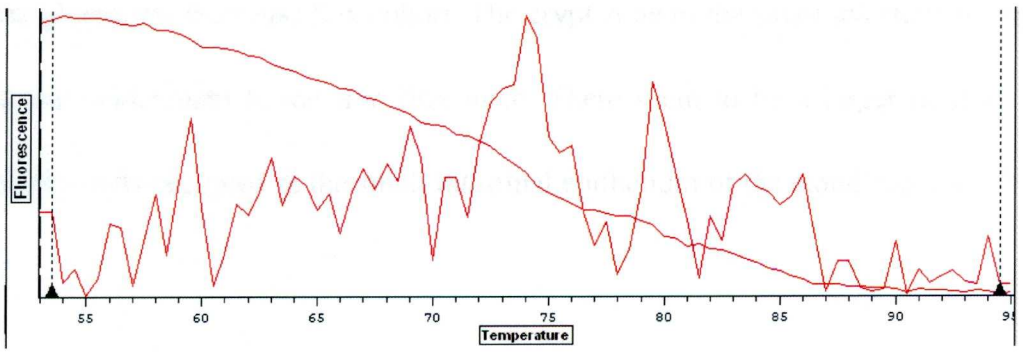

Figure 6.4 Representative melting curve of knocking out Cited1.

6.4 Altered crypt-villus architecture in *Apc Cited1* double null mice

The histology of mouse intestinal tissue sections from 4 cohorts were examined by haematoxylin and eosin staining (figure 6.5). In the *Apc* floxed mice, the important feature is the altered crypt-villus architecture. The crypt-zone was no longer condensed and located at the bottom of small intestine as in the wild type mice, however it was elongated with crypt-like cells occupied the majority of the crypt-like villus axis. This has been previously reported (Sansom et al., 2004) and it was used as a positive control in this context.

In the *Cited1* knock-out mice, the morphology of the stained sections did not show the obvious dramatic changes as in the Apc deleted sections. The crypt-villus architecture is more similar to the wild type control tissues. Data suggests that losing Cited1 alone is not sufficient to trigger large morphological alterations in mouse small intestine.

Intriguingly, when *Cited1* was knocked out in addition to inducing *Apc* deletion in mouse small intestine, the altered crypt-villus architecture showed an even more severe phonotype than *Apc* flox cohort. The crypt zone in the small intestine of these mice was wider than in the *Apc* flox mice. There seem to be a larger number of crypt-like cells occupied in the small intestinal epithelium of the elongated crypt-like zone.

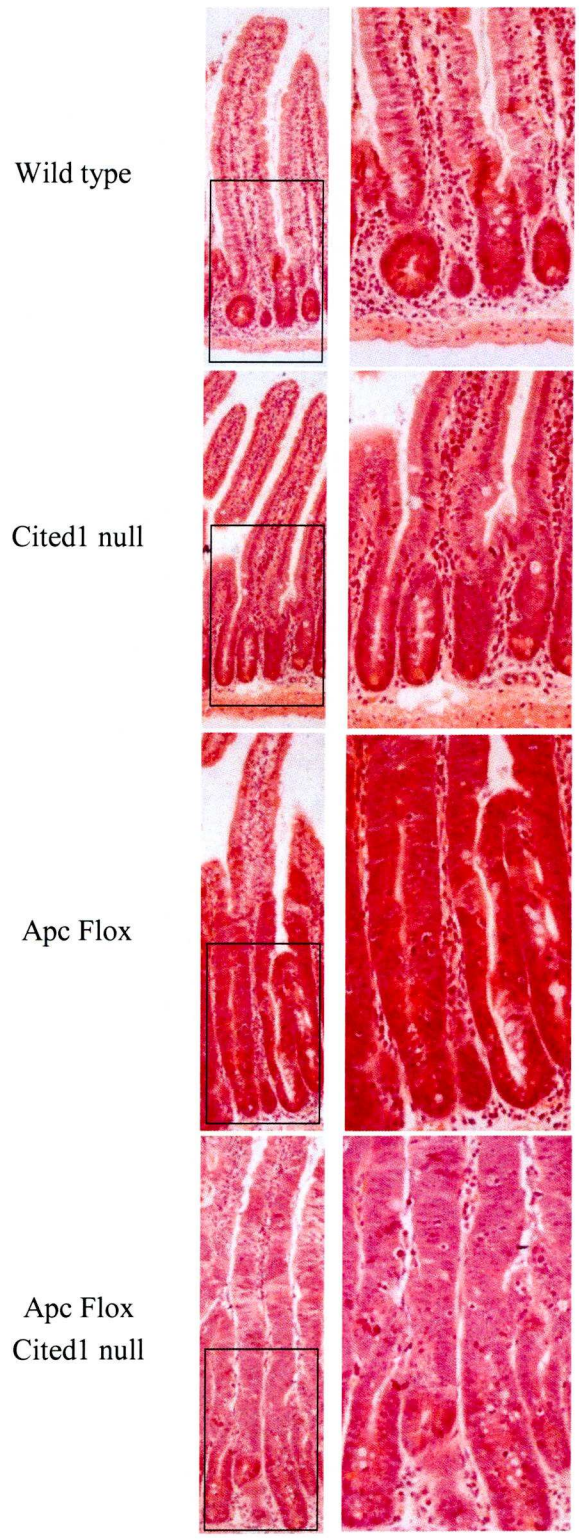

Figure 6.5 More altered crypt-villus architecture in double null mice 4 days after the first injection of the cre-inducing agent β-napthoflavone. WT= wild type, AF=Apc flox/flox, AF+CN=Apc flox/flox and Cited1 null, CN=Cited1 null. One representative image is shown for each cohort. There are 3 mice in each cohort.

This observation was the opposite of our expectations in light of the data from the *Cited1* deficient Min mouse model. This enhanced alteration of crypt-villus architecture in the double *Apc Cited1* null cohort may also be accompanied with altered patterns of proliferation, apoptosis and differentiation.

6.5 Increased proliferation in *Apc Cited1* double null mouse intestinal epithelium

In the previous study, the proliferation zone has been found to increase after losing Apc in mouse small intestine compared with the wild type control mice (Sansom et al., 2004). The proliferation pattern of *Apc Cited1* double null mice was examined following 2 hour BrdU labelling (mice were injected with BrdU and culled 2 hours after) and analysed by BrdU immuno-histochemistry. Tissues taken from wild type, *Apc* flox and *Cited1* null were also examined as the controls.

In the wild type and *Apc* flox mice, the patterns of proliferation were similar as shown previously in paper (Figure 6.6). In the *Cited1* null cohort, the BrdU staining did not show dramatic difference in proliferation from the wild type mice, although the BrdU positive cells were slightly spread as compared with the defined proliferation zone within the normal crypt. However, in the *Apc Cited1* double null mice, the image showed that the BrdU labelled proliferation zone were stretched wider as compared with the mice from *Apc* flox cohort. This pattern of proliferation was observed in the *Apc Cited1* double null cohort whilst also altered more in the

crypt-villus architecture with the elongated crypt-like zone in the mouse small intestine.

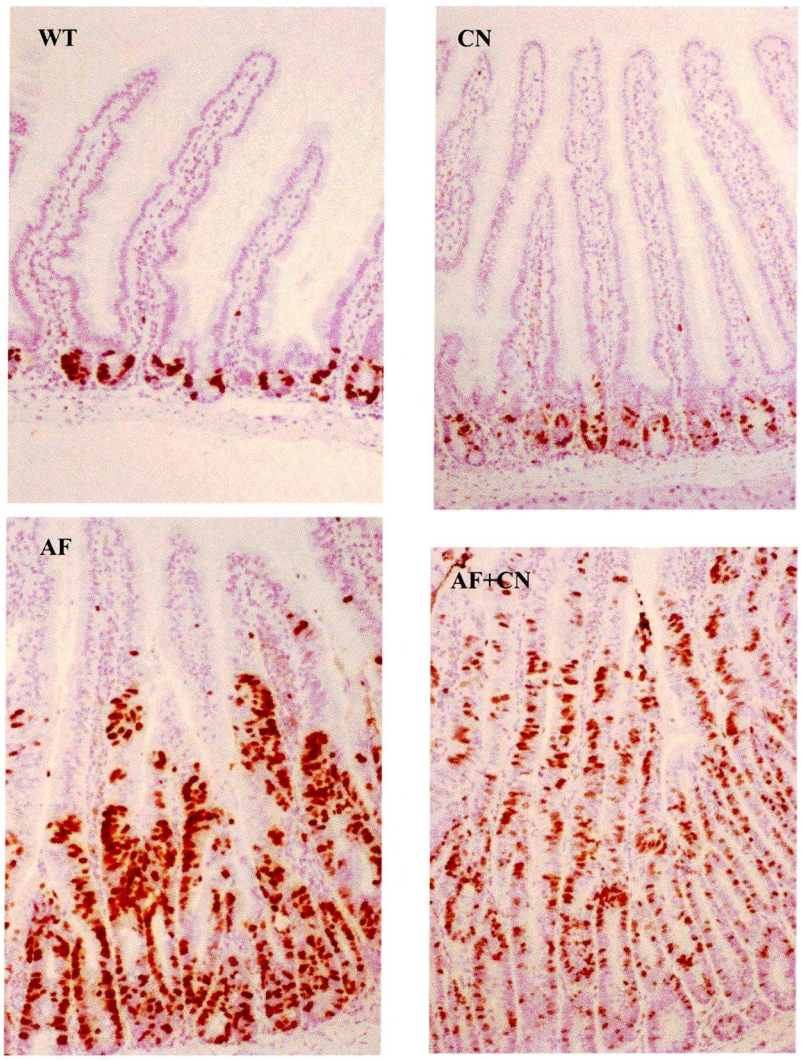

Figure 6.6 Increased proliferations in double null mice as compared to Apc flox/flox mice, detected by BrdU immuno-histochemistry staining in induced epithelium 2 hours after BrdU injection. WT= wild type, AF=*Apc* flox/flox, AF+CN=*Apc* flox/flox and *Cited1* null, CN=*Cited1* null. One representative image is shown for each cohort. There are 3 mice in each cohort.

The proportions of cells in S phase (BrdU positive cells) were then scored for their position along the crypt-villus axis. Tissue sections from 3 mice of each cohort were scored and 25 crypts (or 50 half crypts) were scored for each mouse using WinCrypt program (kindly provided by Prof. M. Pritchard (Gastroenterology Unit, Liverpool).

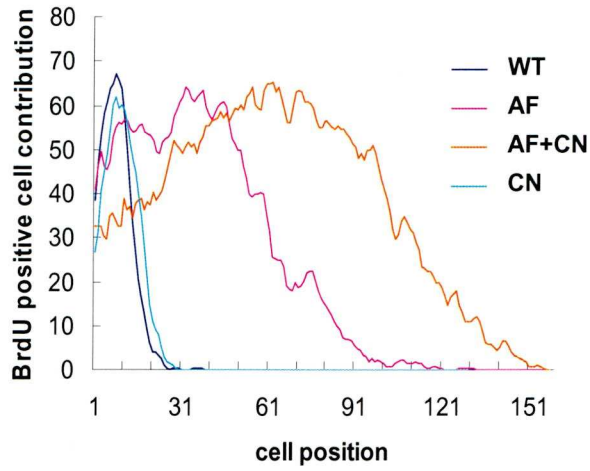

Figure 6.7 Position of BrdU positive cells within the crypt-villus axis from the mouse cohorts at 2 hours following BrdU injection. Position 0 represents the base of the crypt. Curve for each cohort is the mean value of 3 mice in the cohort. WT= wild type, AF=Apc flox/flox, AF+CN=Apc flox/flox and *Cited1* null, CN=*Cited1* null. Data agreed with the scoring result by a master project student in the University of Cardiff.

The BrdU positive cell percentage showed similar level of proliferation between wild type and *Cited1* null cohort (figure 6.7). The proliferation level was dramatically increased in the *Apc* flox mice compared with wild type mice, which was one of the phenotypes associated with early colorectal lesions (Sansom et al., 2004). This increased proliferation level was even higher in the *Apc Cited1* double

null mice. The cumulative frequency graph shows the trend of BrdU positive cells accumulation from the bottom of the crypts in 4 cohorts (figure 6.8). Wild type and *Cited1* null cohort showed similar trend, however this cumulative frequency significantly shifted to higher cell position in *Apc* flox cohort ($D>D_{0.05}$, Kolmogorov-Smirnov test) and even higher in double null cohort ($D>D_{0.05}$, Kolmogorov-Smirnov test).

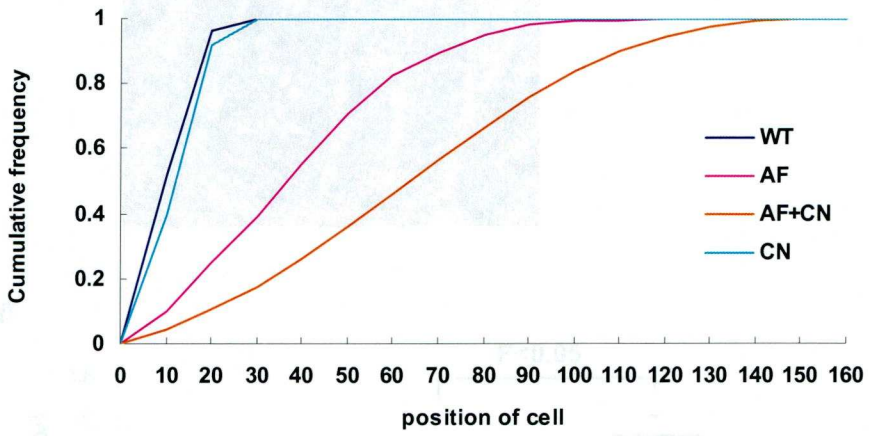

Figure 6.8 Graph showing the position of the BrdU-labelled cells 2 hours after being labelled. WT= wild type, AF=*Apc* flox/flox, AF+CN=*Apc* flox/flox and Cited1 null, CN=*Cited1* null. There are 3 mice in each cohort.

Taking the morphological changes together with the quantified proliferation index, data suggests that there were more cells traversing the S phase in the proliferation zone when crypt-like zone was elongated. Therefore, knocking out *Cited1* enhanced the proliferation in the *Apc* flox mice.

6.6 Increased apoptosis in *Apc Cited1* double null mouse intestinal epithelium

The intestinal crypts were scored for apoptotic bodies using haematoxylin and eosin stained sections. Figure 6.9A shows the representative apoptotic bodies. Tissue sections were taken from 3 mice from each cohort and 25 crypts (or 50 half crypts) were scored for each mouse.

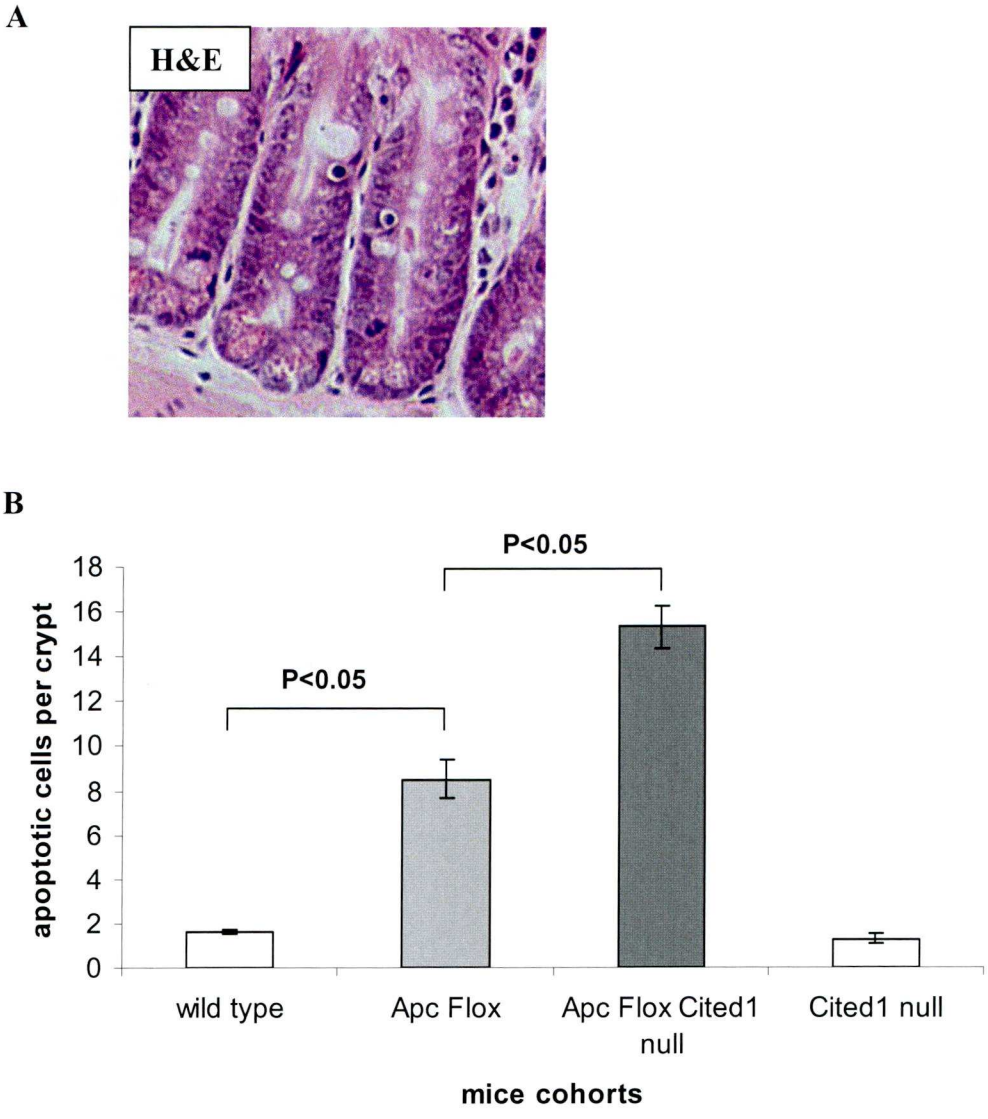

Figure 6.9 Increased apoptosis in the double null mouse small intestinal epithelium. (A) Representative image showing apoptotic bodies in haematoxylin and eosin staining. (B) Scored apoptotic bodies in 4 cohorts. Data of apoptosis level was confirmed by scoring an independent caspase 3 immunohistochemistry experiment by Dr V. Meniel. There are 3 mice in each cohort.

Tissues taken from wild type cohort shows basal level of apoptosis in the mouse small intestine after being injected of β-napthoflavone (figure 6.9B). All pairwise comparisons were performed following Kruskal-Wallis ANOVA. There was not much change in the number of apoptotic cells in the *Cited1* null cohort compared with the wild type mice (not significant). The level of apoptosis was significantly elevated in the Apc flox cohort as observed previously ($P<0.05$, Kruskal-Wallis) (Sansom et al., 2004). However, in the *Apc Cited1* double null cohort, a significant much larger number of cells underwent the apoptotic process ($P<0.05$, Kruskal-Wallis).

Active caspase 3 immuno-histochemistry was then used to confirm apoptosis as observed from haematoxylin and eosin staining in 4 cohorts. The condensed dark round cells labelled by the active caspase 3 antibody are cells going through apoptosis. Again, the image of immuno-histochemistry assay implies that the elevated apoptosis was enhanced by *Cited1* loss on the *Apc* flox background (figure 6.10).

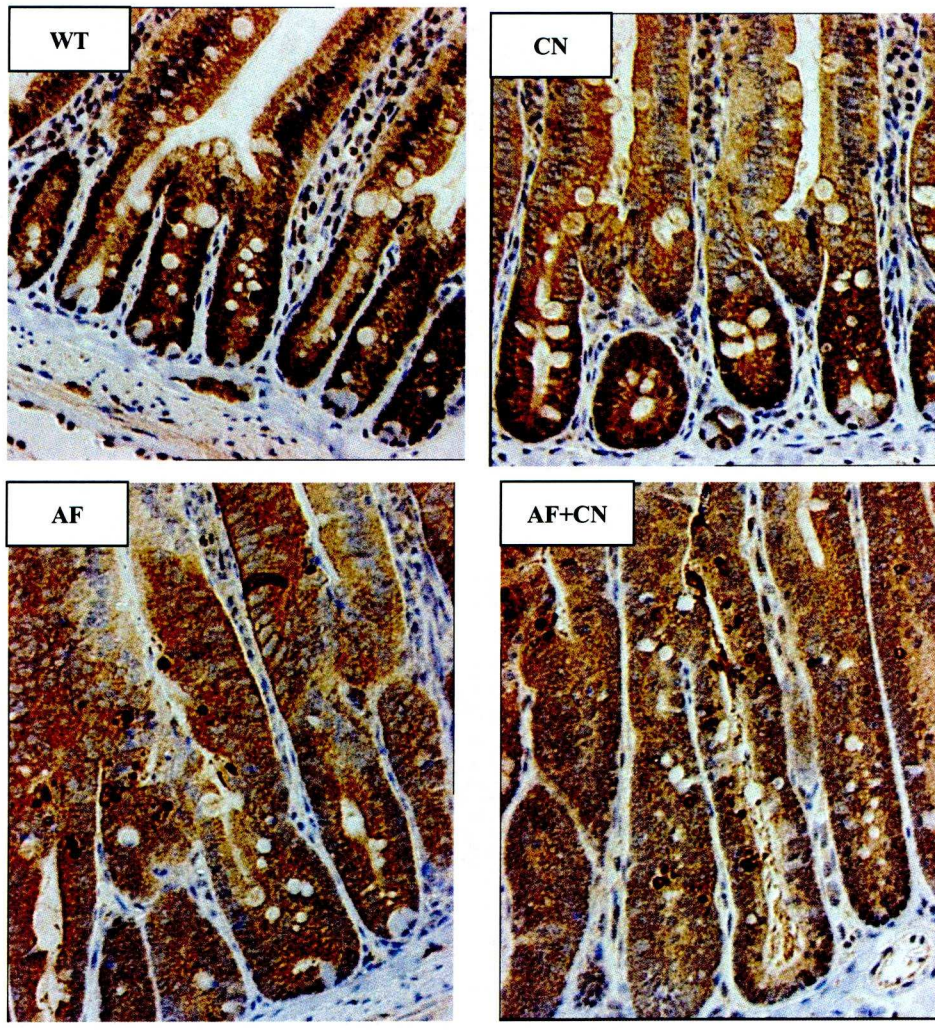

Figure 6.10 Increased apoptosis in double null mice as detected by active caspase3 immuno-histochemistry assay. WT= wild type, AF=Apc flox/flox, AF+CN=Apc flox/flox and Cited1 null, CN=Cited1 null. One representative image is shown for each cohort. There are 3 mice in each cohort.

6.7 Wnt signalling regulation in *Apc Cited1* double null mouse intestinal epithelium

In the *Apc* flox mice, the altered crypt-villus architecture was accompanied by activated Wnt signalling (Sansom et al., 2004) and this phenotype was rescued with reversed Wnt signalling activity in *Apc Myc* double null mutants (Sansom et al., 2007). Cited1 is a myc-dependent Wnt target. In the *Apc Cited1* double null mice, the enhanced architecture alteration together with the increased proliferation and the elevated apoptosis may also associate with the Wnt signalling pathway regulations.

6.7.1 Loss of Cited1 does not inhibit nuclear β-catenin translocation in the double null (*Apc* $^{fl/fl}$ *Cited1* $^{-/-}$) mouse small intestinal epithelium

Nuclear β-catenin translocation is a critical event in activated Wnt signalling, which was tested for in all 4 cohorts by immuno-histochemistry assay. In the wild type mice, β-catenin does not translocate into nucleus (figure 6.11). When Apc was deleted, β-catenin translocated into nucleus in the crypts, indicating activated Wnt signalling in this cohort, which has been shown previously (Sansom et al., 2004). There was no nuclear β-catenin observed in the *Cited1* knock-out mice, which is similar to the wild type mice. Loss of both Cited1 and Apc caused translocation of β-catenin into nucleus. This data suggests that knocking out Cited1 does not inhibit nuclear β-catenin translocation in Apc deletion strains.

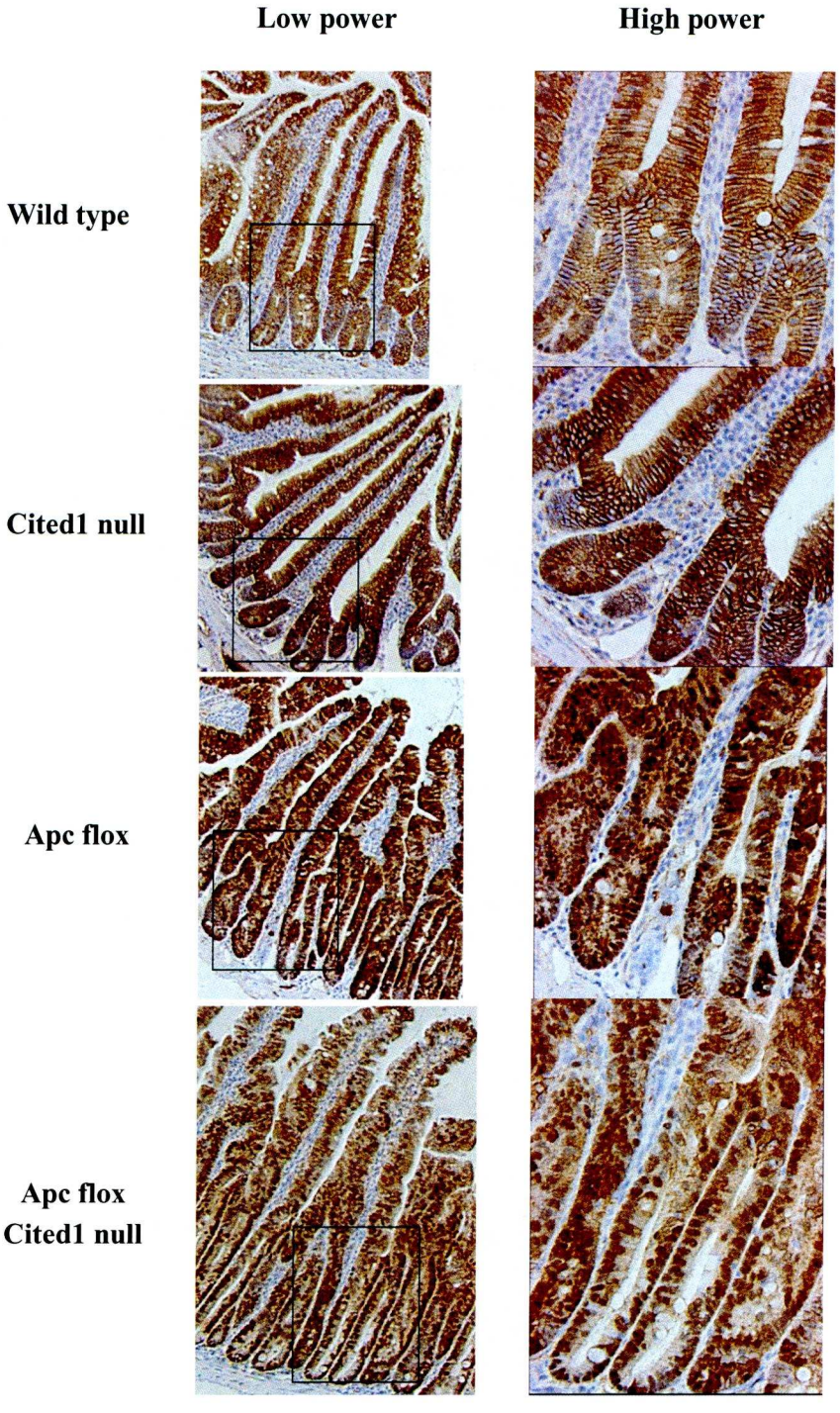

Figure 6.11 β-catenin translocation in Apc flox and Apcflox/Cited1 null mouse small intestinal epithelium. There are 3 mice in each cohort.

6.7.2 Detection of Wnt signalling regulated gene transcription in double null (*Apc* $^{fl/fl}$ *Cited1* $^{-/-}$) mouse small intestinal epithelium

Axin2, *CD44* and *Myc* mRNA expression levels were then measured by relative quantitative PCR. Fold changes of 3 target genes in *Apc* flox, *Apc Cited1* double null and *Cited1* null cohorts were all normalised to the wild type samples. All pairwise comparisons were made following Kruskal-Wallis ANOVA.

Three known Wnt targets were slightly up-regulated in the Cited1 null mice compared with wild type mice, however, not as much as in the Apc flox intestinal epithelium cells. In the *Apc Cited1* double null cohort, *Axin2*, *CD44* and *Myc* all showed same extend of the increased level of up-regulations as in the Apc flox cohort compared with wild type cohort. *Axin2* and *CD44* were significantly over-expressed ($P<0.05$, Kruskal-Wallis), however the increased expression of Myc was not statistically significant ($P>0.2$, Kruskal-Wallis) (Figure 6.12). The later result may be because there were only 3 mice being tested in this preliminary study of the *Apc Cited1* double null cohort.

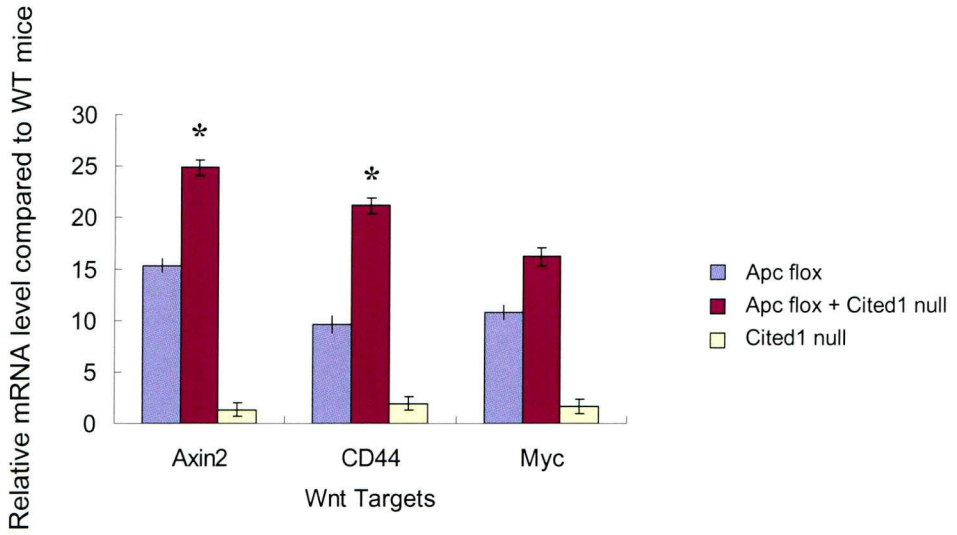

Figure 6.12 Wnt targets regulation in double null mouse small intestinal epithelium. Axin2 and CD44 were significantly up-regulated in the double null mouse small intestinal epithelium. Error bars stand for the standard error of the mean. There are 3 mice in each cohort.

The preliminary data suggests that Wnt signalling regulated gene transcription level may increase after losing Cited1 in addition of Apc deletion. However, Axin2 and CD44 may not be the best candidates for measuring the effects of knocking out Cited1 on Wnt signalling regulated gene transcription activity. CD44 has been identified to be Myc independent. Although being Myc dependent, Axin2 could possibly bring complexity into data interpretation as being both Wnt down stream target and recruited as part of the β-catenin degradation complex in upstream. Therefore, a series of Myc dependent Wnt target gene expression would need to be detected, to confirm the effects of Cited1 loss on the Wnt signalling regulated gene transcription. As Cited1 was a Myc dependent Wnt regulated target, knocking out Cited1 more likely regulate part of the Myc-dependent Wnt signalling activity.

6.8 Discussion

This immediate inducible model of Apc loss provided the opportunity to investigate the early stages of intestinal tumourigenesis. However, the limited time did not allow a comprehensive analysis enabling an understanding of the immediate alterations in the small intestinal epithelium of the *Apc Cited1* double null mice. Preliminary investigations were carried out to gain a general picture of the underlying process.

Data from the preliminary studies on this *Cited1* null *Apc* flox mouse model shows that knocking out Cited1 induced more altered crypt-villus architecture with increased proliferation and elevated apoptosis. Although the crypt-villus architecture was more altered with higher level of proliferation, only the remaining Apc deficient proliferative cells would be able to develop tumours in the intestine. The higher level of apoptosis in double null mice may tend to allow the Apc deficient cells die away in this early stage model, which can possibly reduce later tumourigenic events. If this is the case, this hypothesis would be consistent with the observation in *Cited1* null Min mouse model. However, 48 hours BrdU labelling in the β-napthoflavone induced mice would be needed to investigate the migration speed of proliferative cells to test whether Apc deficient cell would migrate quicker through the villus axis.

In the cohort with the additional loss of Cited1 on Apc flox background, β-catenin was observed to translocate into nucleus as was observed in the Apc flox mice. This suggests that knocking out Cited1 is not sufficient to inhibit Wnt signalling activity

at the point of nuclear β-catenin translocation. As Cited1 is a Myc dependent Wnt target, Axin2 and CD44 are not the best candidates to be tested. In order to detect the effect of losing Cited1 on Wnt signalling activity, a set of Myc dependent Wnt targets need to be tested.

So far, data suggested that some mechanisms are possibly involved with Cited1 loss to modulate Wnt signalling in downstream of β-catenin, in turn regulate intestinal tumourigenesis. In order to determine the potentially mechanisms involved, a comprehensive DNA microarray analysis needs to be performed.

Chapter 7 Conclusion

The Clarke group developed the intestinal tissue specific conditional Cre-*lox*P *Apc* knock-out mouse model using Cyp1A1 promoter. This model resolved the difficulty of *Apc* knock-out mice dying *in utero* and provided the possibility of investigating the effects of immediate loss of functional Apc in the intestine *in vivo*, allowing the identification of early phenotypic changes of Apc loss. An array analysis of this model identified dysregulated genes by activated Wnt signalling pathway in small intestine (Sansom et al., 2004). Using the same inducible deletion system, a double knock-out of *Apc* and *Myc* appeared to have 'wild type-like' intestinal architecture. The array analysis from this new cross identified 59% (27/46) of Wnt target genes became normally expressed following loss of c-Myc (Sansom et al., 2007). A subset of these changes (*Axin2*, *Musashi*, *Sox17*, *Fzd6*) were confirmed by real time quantitative reverse PCR. Therefore Myc-dependent Wnt signalling regulated genes are largely responsible for the Apc loss imposed intestinal architecture alteration.

To access the translational value of the observation from the mouse model, matching paired normal mucosa and colorectal tumour tissues from colorectal cancer patient were used. Data from homologous human gene expressions show that most of the Wnt targets deregulated in the inducible Apc knock-out mouse model are also deregulated in human colon cancer tissues, demonstrating the validity of this strategy. Unfortunately, due to the project scale and time, there were not sufficient data to allow sub-grouping linking the specific gene over-expression with the clinical

data, such as the location of colorectal carcinogenesis event on intestine, the staging, patient gender and age. From this data set, Cited1 was found to be one of the genes that are both up-regulated in mouse model and human colorectal cancers. It has been previously unrecognized as being involved with colorectal carcinogenesis.

Altered expression of Cited1 has previously been studied in melanoma, thyroid, and breast cancers (Li et al., 1998; Nair et al., 2001; Scognamiglio et al., 2006). In my project, the preliminary investigation on involvement of Cited1 in colorectal carcinogenesis was carried out using siRNA treated human colon cancer cell lines. Following *Cited1* expression reduction, decreased cell survival and proliferation was observed in HCT116 cells. This was also confirmed in HT29 cells. The inhibition of *Cited1* data demonstrates an inhibitory effect on cell proliferation implicating its possible role in carcinogenesis. Although *Axin2* and *CD44* expression were measured after reducing *Cited1* expression in cells, it was difficult to draw conclusion from this data on the underlying molecular mechanisms.

Two transgenic mouse models were then employed to investigate the inhibitory role of deficient Cited1 and to elucidate the underlying molecular mechanisms in the *in vivo* setting. When crossing *Cited1* null mice with *Apc* heterozygote Min mice, loss of Cited1 significantly extended the life span of the Min mice by another ~250 days, which almost double the latency in these animals. Tumour number was also significantly reduced in *Cited1* null Min mice, whose life span was predominantly

determined by the tumour number in small intestine and large intestine rather than the absolute tumour size. The increased tumour size in these mutants may be the result of longer time frame for the tumour development in the longer surviving animals. Therefore, Cited1 deficiency plays the inhibitory role in intestinal tumourgenesis in the min mice intestine. In the Min *Cited1* null model, deficient Cited1 is probably preventing the normal epithelium from transforming into tumour in Min mouse intestine, rather than killing cancerous cells and limiting those cells to proliferate in human colon cancel lines, data from the studies of Min *Cited1* null and *Apc Cited1* double null models are quite consistent in terms of the inhibitory role of deficient Cited1 in intestinal tumourigenesis.

The above studies support involvement of Cited1 in colorectal carcinogenesis. However, the results were only observed as the end point event. In the *Apc Cited1* double null model, loss of Cited1 triggered more alerted crypt/villus architecture with increased proliferation and apoptosis. This phenotype was observed 4 days after deleting Apc in the mice, this model mimics the initiation of the process of colorectal carcinogenesis. The high level of apoptosis may tend to allow the proliferative cells die away at early points, which makes the severe phenotype beneficial to the mutants, leading to the longer life span as found in Min mice. The similar phenomenon has been previously observed in limb morphogenesis, in which apoptosis is a prominent feature, resulting in the inter-digital tissue repression (Zuzarte-Luis and Hurle, 2002). In this process, the pattern of apoptosis determines

the cell fate in the inter-digital area, leaving the correct structure and number of digits (Zuzarte-Luis and Hurle, 2002). However, in the intestine of the mouse model, the underlying mechanisms need investigating to support this preliminary conclusion.

The immuno-histochemistry assay of β-catenin showed the nuclear translocation in Min adenomas and in intestinal epithelium of *Apc/Cited1* double null mice. As being down stream of Myc, losing Cited1 is not sufficient to reverse the nuclear β-catenin translocation as loss of *Myc* does in *Apc* null mice. DNA array analysis identified the Myc Max interaction as a potential underlying mechanism and similar observation was described by Mariadason in regard of the intestinal epithelial cell maturation along the crypt-villus axis (Mariadason et al., 2005). Wnt signalling activity was confirmed to be maximal in the proliferative compartment and Myc protein expression levels decrease from crypt to the top of the villus whilst MAX protein expression level increases, which predominantly regulate the Myc targets (Mariadason et al., 2005). This study implicates the relationships between proliferation activity, Myc-MAX antagonising mechanism and Myc target genes in the intestinal epithelium. Cited1 activates Smad4-dependent transcription involved in TGF-β signalling in kidney (Plisov et al., 2005) and Myc-Max, Mad-Max regulations repress mammary epithelial cell growth are regulated by TGF-β (Siegel et al., 2003b) As Cited1 is a Myc target, loss of Cited1 may disturb the Myc-related

regulations. This could be a potentially hypothetical mechanism modulating the perturbed epithelial proliferation in the *Cited1* knock-out *Apc* null mice.

So far, from the data already generated *in vitro* and *in vivo*, I conclude that deficient Cited1 inhibits the colorectal cancinogenesis, however the underlying mechanisms are still elusive. In the future, I shall validate our cell line data on cell growth using other colon cancer-derived cell lines with defective Wnt pathways, SW620 and DLD1 cells. The effects of Cited1 on cell cycle and apoptosis also need to be determined by FACS-based analysis. To determine whether deficient Cited1 is able to modulate Wnt signalling directly, luciferase assays will be performed using the Wnt responsive TOP-FLASH system. siRNA will be co-transfected with TOP-FLASH and one of the four known Wnt pathway transducers (ΔN-LRP6; FlagAx, ΔN beta-catenin or TCF4-VP16) (Brennan et al., 2004; Munemitsu et al., 1996; Smalley et al., 1999; Wakita et al., 2001). The four transducers will represent the Wnt pathway from the receptor (LRP) through to the degradation complex (Axin2), β-catenin and finally the transcription factor TCF-4. For the immediate *Apc* knock-out model, 24 hours BrdU incorporation will be able to detect the proliferative cell migration along the crypt/villus axis to define the fate of the proliferative cells. A series of immuno-histochemistry of differentiation and apoptosis markers shall be carried out to accomplish the characterisation of the phenotypic changes. A comprehensive DNA microarray would be able to help elucidate underlying molecular mechanism investigation.

Taken together, this data demonstrates the validity of the Cre-*loxP-Apc* strategy as an early colorectal cancer model and Cited1 is part of the colorectal carcinogenesis process.

Chapter 8 References

Ahlquist, D. A. (1995). Aggressive polyps in hereditary nonpolyposis colorectal cancer: targets for screening. Gastroenterology *108*, 1590-1592.

Al-Tassan, N., Chmiel, N. H., Maynard, J., Fleming, N., Livingston, A. L., Williams, G. T., Hodges, A. K., Davies, D. R., David, S. S., Sampson, J. R., and Cheadle, J. P. (2002). Inherited variants of MYH associated with somatic G:C-->T:A mutations in colorectal tumors. Nat Genet *30*, 227-232.

Anderson, C. B., Neufeld, K. L., and White, R. L. (2002). Subcellular distribution of Wnt pathway proteins in normal and neoplastic colon. Proc Natl Acad Sci U S A *99*, 8683-8688.

Ashton-Rickardt, P. G., Dunlop, M. G., Nakamura, Y., Morris, R. G., Purdie, C. A., Steel, C. M., Evans, H. J., Bird, C. C., and Wyllie, A. H. (1989). High frequency of APC loss in sporadic colorectal carcinoma due to breaks clustered in 5q21-22. Oncogene *4*, 1169-1174.

Attisano, L., and Labbe, E. (2004). TGFbeta and Wnt pathway cross-talk. Cancer Metastasis Rev *23*, 53-61.

Ayer, D. E., and Eisenman, R. N. (1993). A switch from Myc:Max to Mad:Max heterocomplexes accompanies monocyte/macrophage differentiation. Genes Dev *7*, 2110-2119.

Ayer, D. E., Kretzner, L., and Eisenman, R. N. (1993). Mad: a heterodimeric partner for Max that antagonizes Myc transcriptional activity. Cell *72*, 211-222.

Bachman, K. E., and Park, B. H. (2005). Duel nature of TGF-beta signaling: tumor suppressor vs. tumor promoter. Curr Opin Oncol *17*, 49-54.

Barker, C. R., McNamara, A. V., Rackstraw, S. A., Nelson, D. E., White, M. R., Watson, A. J., and Jenkins, J. R. (2006). Inhibition of Hsp90 acts synergistically with topoisomerase II poisons to increase the apoptotic killing of cells due to an increase in topoisomerase II mediated DNA damage. Nucleic Acids Res *34*, 1148-1157.

Barker, N., van Es, J. H., Kuipers, J., Kujala, P., van den Born, M., Cozijnsen, M., Haegebarth, A., Korving, J., Begthel, H., Peters, P. J., and Clevers, H. (2007). Identification of stem cells in small intestine and colon by marker gene Lgr5. Nature *449*, 1003-1007.

Barrios-Rodiles, M., Brown, K. R., Ozdamar, B., Bose, R., Liu, Z., Donovan, R. S., Shinjo, F., Liu, Y., Dembowy, J., Taylor, I. W., Luga V., Przulj N., Robinson M., Suzuki H., Hayashizaki Y., Jurisica I., Wrana J. L. (2005). High-throughput mapping of a dynamic signaling network in mammalian cells. Science *307*, 1621-1625.

Batlle, E., Bacani, J., Begthel, H., Jonkheer, S., Gregorieff, A., van de Born, M., Malats, N., Sancho, E., Boon, E., Pawson, T., Gallinger S., Pals S., Clevers H. (2005). EphB receptor activity suppresses colorectal cancer progression. Nature *435*, 1126-1130.

Batlle, E., Henderson, J. T., Beghtel, H., van den Born, M. M., Sancho, E., Huls, G., Meeldijk, J., Robertson, J., van de Wetering, M., Pawson, T., and Clevers, H. (2002). Beta-catenin and TCF mediate cell positioning in the intestinal epithelium by controlling the expression of EphB/ephrinB. Cell *111*, 251-263.

Bauer, A., Huber, O., and Kemler, R. (1998). Pontin52, an interaction partner of beta-catenin, binds to the TATA box binding protein. Proc Natl Acad Sci U S A *95*, 14787-14792.

Behrens, J. (2005). The role of the Wnt signalling pathway in colorectal tumorigenesis. Biochem Soc Trans *33*, 672-675.

Behrens, J., von Kries, J. P., Kuhl, M., Bruhn, L., Wedlich, D., Grosschedl, R., and Birchmeier, W. (1996). Functional interaction of beta-catenin with the transcription factor LEF-1. Nature *382*, 638-642.

Benito, M., and Diaz-Rubio, E. (2006). Molecular biology in colorectal cancer. Clin Transl Oncol *8*, 391-398.

Bernstein, E., Caudy, A. A., Hammond, S. M., and Hannon, G. J. (2001). Role for a bidentate ribonuclease in the initiation step of RNA interference. Nature *409*, 363-366.

Beroud, C., and Soussi, T. (1996). APC gene: database of germline and somatic mutations in human tumors and cell lines. Nucleic Acids Res *24*, 121-124.

Bertholon, J., Wang, Q., Galmarini, C. M., and Puisieux, A. (2006). Mutational targets in colorectal cancer cells with microsatellite instability. Fam Cancer *5*, 29-34.

Bettess, M. D., Dubois, N., Murphy, M. J., Dubey, C., Roger, C., Robine, S., and Trumpp, A. (2005). c-Myc is required for the formation of intestinal crypts but dispensable for homeostasis of the adult intestinal epithelium. Mol Cell Biol *25*, 7868-7878.

Bienz, M., and Clevers, H. (2000). Linking colorectal cancer to Wnt signaling. Cell *103*, 311-320.

Bierie, B., and Moses, H. L. (2006). Tumour microenvironment: TGFbeta: the molecular Jekyll and Hyde of cancer. Nat Rev Cancer *6*, 506-520.

Bodmer, W. F. (2006). Cancer genetics: colorectal cancer as a model. J Hum Genet *51*, 391-396.

Bondi, J., Bukholm, G., Nesland, J. M., and Bukholm, I. R. (2004). Expression of non-membranous beta-catenin and gamma-catenin, c-Myc and cyclin D1 in relation to patient outcome in human colon adenocarcinomas. APMIS *112*, 49-56.

Boyle, S., Shioda, T., Perantoni, A. O., and de Caestecker, M. (2007). Cited1 and Cited2 are differentially expressed in the developing kidney but are not required for nephrogenesis. Dev Dyn *236*, 2321-2330.

Brabletz, T., Jung, A., Hermann, K., Gunther, K., Hohenberger, W., and Kirchner, T. (1998). Nuclear overexpression of the oncoprotein beta-catenin in colorectal cancer is localized predominantly at the invasion front. Pathol Res Pract *194*, 701-704.

Brennan, K., Gonzalez-Sancho, J. M., Castelo-Soccio, L. A., Howe, L. R., and Brown, A. M. (2004). Truncated mutants of the putative Wnt receptor LRP6/Arrow can stabilize beta-catenin independently of Frizzled proteins. Oncogene *23*, 4873-4884.

Buermeyer, A. B., Deschenes, S. M., Baker, S. M., and Liskay, R. M. (1999). Mammalian DNA mismatch repair. Annu Rev Genet *33*, 533-564.

Burt, R. W., Bishop, D. T., Lynch, H. T., Rozen, P., and Winawer, S. J. (1990). Risk and surveillance of individuals with heritable factors for colorectal cancer. WHO Collaborating Centre for the Prevention of Colorectal Cancer. Bull World Health Organ *68*, 655-665.

Cadigan, K. M., and Nusse, R. (1997). Wnt signaling: a common theme in animal development. Genes Dev *11*, 3286-3305.

Campbell, P. M., and Der, C. J. (2004). Oncogenic Ras and its role in tumor cell invasion and metastasis. Semin Cancer Biol *14*, 105-114.

Capella, G., Cronauer-Mitra, S., Pienado, M. A., and Perucho, M. (1991). Frequency and spectrum of mutations at codons 12 and 13 of the c-K-ras gene in human tumors. Environ Health Perspect *93*, 125-131.

Cho, K. H., Baek, S., and Sung, M. H. (2006). Wnt pathway mutations selected by optimal beta-catenin signaling for tumorigenesis. FEBS Lett *580*, 3665-3670.

Chomczynski, P. (1993). A reagent for the single-step simultaneous isolation of RNA, DNA and proteins from cell and tissue samples. Biotechniques *15*, 532-534, 536-537.

Chung, D. C. (2000). The genetic basis of colorectal cancer: insights into critical pathways of tumorigenesis. Gastroenterology *119*, 854-865.

Clarke, A. R. (2005). Studying the consequences of immediate loss of gene function in the intestine: APC. Biochem Soc Trans *33*, 665-666.

Clarke, A. R. (2007). Cancer genetics: mouse models of intestinal cancer. Biochem Soc Trans *35*, 1338-1341.

Clarke, A. R., Cummings, M. C., and Harrison, D. J. (1995). Interaction between murine germline mutations in p53 and APC predisposes to pancreatic neoplasia but not to increased intestinal malignancy. Oncogene *11*, 1913-1920.

Clevers, H. (2004). Wnt breakers in colon cancer. Cancer Cell *5*, 5-6.

Clevers, H., and Batlle, E. (2006). EphB/EphrinB receptors and Wnt signaling in colorectal cancer. Cancer Res *66*, 2-5.

Corpet, D. E., and Pierre, F. (2005). How good are rodent models of carcinogenesis in predicting efficacy in humans? A systematic review and meta-analysis of colon chemoprevention in rats, mice and men. Eur J Cancer *41*, 1911-1922.

Crabtree, M., Sieber, O. M., Lipton, L., Hodgson, S. V., Lamlum, H., Thomas, H. J., Neale, K., Phillips, R. K., Heinimann, K., and Tomlinson, I. P. (2003). Refining the relation between 'first hits' and 'second hits' at the APC locus: the 'loose fit' model and evidence for differences in somatic mutation spectra among patients. Oncogene *22*, 4257-4265.

Cruz-Correa, M., and Giardiello, F. M. (2002). Diagnosis and management of hereditary colon cancer. Gastroenterol Clin North Am *31*, 537-549, x.

D'Orazio, D., Muller, P. Y., Heinimann, K., Albrecht, C., Bendik, I., Herzog, U., Tondelli, P., Bauerfeind, P., Muller, H., and Dobbie, Z. (2002). Overexpression of Wnt target genes in adenomas of familial adenomatous polyposis patients. Anticancer Res *22*, 3409-3414.

Dale, T. C. (1998). Signal transduction by the Wnt family of ligands. Biochem J *329 (Pt 2)*, 209-223.

Davis, A. C., Wims, M., Spotts, G. D., Hann, S. R., and Bradley, A. (1993). A null c-myc mutation causes lethality before 10.5 days of gestation in homozygotes and reduced fertility in heterozygous female mice. Genes Dev *7*, 671-682.

De Paula, D., Bentley, M. V., and Mahato, R. I. (2007). Hydrophobization and bioconjugation for enhanced siRNA delivery and targeting. RNA *13*, 431-456.

Debinski, H. S., Love, S., Spigelman, A. D., and Phillips, R. K. (1996). Colorectal polyp counts and cancer risk in familial adenomatous polyposis. Gastroenterology *110*, 1028-1030.

Derynck, R., and Zhang, Y. E. (2003). Smad-dependent and Smad-independent pathways in TGF-beta family signalling. Nature *425*, 577-584.

Dillon, R. L., Brown, S. T., Ling, C., Shioda, T., and Muller, W. J. (2007). An EGR2/CITED1 transcription factor complex and the 14-3-3sigma tumor suppressor are involved in regulating ErbB2 expression in a transgenic-mouse model of human breast cancer. Mol Cell Biol *27*, 8648-8657.

Din, F. V., Dunlop, M. G., and Stark, L. A. (2004). Evidence for colorectal cancer cell specificity of aspirin effects on NF kappa B signalling and apoptosis. Br J Cancer *91*, 381-388.

Dohi, T., Borodovsky, A., Wu, P., Shearstone, J. R., Kawashima, R., Runkel, L., Rajman, L., Dong, X., Scott, M. L., Michaelson, J. S., Jakubowski A., Burkly L. C. (2009). TWEAK/Fn14 pathway: a nonredundant role in intestinal damage in mice through a TWEAK/intestinal epithelial cell axis. Gastroenterology *136*, 912-923.

Doucas, H., Garcea, G., Neal, C. P., Manson, M. M., and Berry, D. P. (2005). Changes in the Wnt signalling pathway in gastrointestinal cancers and their prognostic significance. Eur J Cancer *41*, 365-379.

Dukes, C. E., and Bussey, H. J. (1958). The spread of rectal cancer and its effect on prognosis. Br J Cancer *12*, 309-320.

Eilers, M., and Eisenman, R. N. (2008). Myc's broad reach. Genes Dev *22*, 2755-2766.

Elbashir, S. M., Lendeckel, W., and Tuschl, T. (2001). RNA interference is mediated by 21- and 22-nucleotide RNAs. Genes Dev *15*, 188-200.

Elliott, R. L., and Blobe, G. C. (2005). Role of transforming growth factor Beta in human cancer. J Clin Oncol *23*, 2078-2093.

Eshleman, J. R., and Markowitz, S. D. (1995). Microsatellite instability in inherited and sporadic neoplasms. Curr Opin Oncol *7*, 83-89.

Fearnhead, N. S., Britton, M. P., and Bodmer, W. F. (2001). The ABC of APC. Hum Mol Genet *10*, 721-733.

Fearnhead, N. S., Wilding, J. L., and Bodmer, W. F. (2002). Genetics of colorectal cancer: hereditary aspects and overview of colorectal tumorigenesis. Br Med Bull *64*, 27-43.

Fearon, E. R., and Vogelstein, B. (1990). A genetic model for colorectal tumorigenesis. Cell *61*, 759-767.

Fenner, M. H., Parrish, J. E., Boyd, Y., Reed, V., MacDonald, M., Nelson, D. L., Isselbacher, K. J., and Shioda, T. (1998). MSG1 (melanocyte-specific gene 1): mapping to chromosome Xq13.1, genomic organization, and promoter analysis. Genomics *51*, 401-407.

Fernandez, J. C., Vizoso, F. J., Corte, M. D., Gava, R. R., Corte, M. G., Suarez, J. P., Garcia-Muniz, J. L., and Garcia-Moran, M. (2004). CD44s expression in resectable colorectal carcinomas and surrounding mucosa. Cancer Invest *22*, 878-885.

Fire, A., Xu, S., Montgomery, M. K., Kostas, S. A., Driver, S. E., and Mello, C. C. (1998). Potent and specific genetic interference by double-stranded RNA in Caenorhabditis elegans. Nature *391*, 806-811.

Fodde, R. (2002). The APC gene in colorectal cancer. Eur J Cancer *38*, 867-871.

Fodde, R., Edelmann, W., Yang, K., van Leeuwen, C., Carlson, C., Renault, B., Breukel, C., Alt, E., Lipkin, M., Khan, P. M., and Kucherlapati R. (1994). A targeted chain-termination mutation in the mouse Apc gene results in multiple intestinal tumors. Proc Natl Acad Sci U S A *91*, 8969-8973.

Fodde, R., Kuipers, J., Rosenberg, C., Smits, R., Kielman, M., Gaspar, C., van Es, J. H., Breukel, C., Wiegant, J., Giles, R. H., and Clevers, H. (2001). Mutations in the APC tumour suppressor gene cause chromosomal instability. Nat Cell Biol *3*, 433-438.

Freedman, S. J., Sun, Z. Y., Kung, A. L., France, D. S., Wagner, G., and Eck, M. J. (2003). Structural basis for negative regulation of hypoxia-inducible factor-1alpha by CITED2. Nat Struct Biol *10*, 504-512.

Galiatsatos, P., and Foulkes, W. D. (2006). Familial adenomatous polyposis. Am J Gastroenterol *101*, 385-398.

Gardner, E. J. (1962). Follow-up study of a family group exhibiting dominant inheritance for a syndrome including intestinal polyps, osteomas, fibromas and epidermal cysts. Am J Hum Genet *14*, 376-390.

Ghosh, K., and Van Duyne, G. D. (2002). Cre-loxP biochemistry. Methods *28*, 374-383.

Giles, R. H., van Es, J. H., and Clevers, H. (2003). Caught up in a Wnt storm: Wnt signaling in cancer. Biochim Biophys Acta *1653*, 1-24.

Gilmore, I. R., Fox, S. P., Hollins, A. J., Sohail, M., and Akhtar, S. (2004). The design and exogenous delivery of siRNA for post-transcriptional gene silencing. J Drug Target *12*, 315-340.

Golan, T., Yaniv, A., Bafico, A., Liu, G., and Gazit, A. (2004). The human Frizzled 6 (HFz6) acts as a negative regulator of the canonical Wnt. beta-catenin signaling cascade. J Biol Chem *279*, 14879-14888.

Grady, W. M., and Markowitz, S. D. (2002). Genetic and epigenetic alterations in colon cancer. Annu Rev Genomics Hum Genet *3*, 101-128.

Grandori, C., Cowley, S. M., James, L. P., and Eisenman, R. N. (2000). The Myc/Max/Mad network and the transcriptional control of cell behavior. Annu Rev Cell Dev Biol *16*, 653-699.

Green, D. W., Roh, H., Pippin, J. A., and Drebin, J. A. (2001). Beta-catenin antisense treatment decreases beta-catenin expression and tumor growth rate in colon carcinoma xenografts. J Surg Res *101*, 16-20.

Greene, F. L. (2006). Staging of colon and rectal cancer: from endoscopy to molecular markers. Surg Endosc *20 Suppl 2*, S475-478.
Gregorieff, A., and Clevers, H. (2005). Wnt signaling in the intestinal epithelium: from endoderm to cancer. Genes Dev *19*, 877-890.

Groden, J., Thliveris, A., Samowitz, W., Carlson, M., Gelbert, L., Albertsen, H., Joslyn, G., Stevens, J., Spirio, L., Robertson, M., Sargeant L., Krapchob K., Wolff E., Burt R., Hughes J. P., Warringtonf J., McPhersonf J., Wasmuthf J., Le Paslier D., Abderrahim H., Cohen D., Leppert M., and White R. (1991). Identification and characterization of the familial adenomatous polyposis coli gene. Cell *66*, 589-600.

Gryfe, R., Swallow, C., Bapat, B., Redston, M., Gallinger, S., and Couture, J. (1997). Molecular biology of colorectal cancer. Curr Probl Cancer *21*, 233-300.

Guerra, C., Mijimolle, N., Dhawahir, A., Dubus, P., Barradas, M., Serrano, M., Campuzano, V., and Barbacid, M. (2003). Tumor induction by an endogenous K-ras oncogene is highly dependent on cellular context. Cancer Cell *4*, 111-120.

Halberg, R. B., Katzung, D. S., Hoff, P. D., Moser, A. R., Cole, C. E., Lubet, R. A., Donehower, L. A., Jacoby, R. F., and Dove, W. F. (2000). Tumorigenesis in the multiple intestinal neoplasia mouse: redundancy of negative regulators and specificity of modifiers. Proc Natl Acad Sci U S A *97*, 3461-3466.

Hamilton, S. R., Liu, B., Parsons, R. E., Papadopoulos, N., Jen, J., Powell, S. M., Krush, A. J., Berk, T., Cohen, Z., Tetu, B., Burger P. C., Wood P. A., Taqi F., Booker S. V., Petersen G. M., Offerhaus G. J. A., Tersmette A. C., Giardiello F. M., Vogelstein B., and Kinzler K. W., (1995). The molecular basis of Turcot's syndrome. N Engl J Med *332*, 839-847.

Hannon, G. J. (2002). RNA interference. Nature *418*, 244-251.

Hao, X. P., Pretlow, T. G., Rao, J. S., and Pretlow, T. P. (2001). Beta-catenin expression is altered in human colonic aberrant crypt foci. Cancer Res *61*, 8085-8088.

Hauck, A. L., Swanson, K. S., Kenis, P. J., Leckband, D. E., Gaskins, H. R., and Schook, L. B. (2005). Twists and turns in the development and maintenance of the mammalian small intestine epithelium. Birth Defects Res C Embryo Today *75*, 58-71.

He, T. C., Sparks, A. B., Rago, C., Hermeking, H., Zawel, L., da Costa, L. T., Morin, P. J., Vogelstein, B., and Kinzler, K. W. (1998). Identification of c-MYC as a target of the APC pathway. Science *281*, 1509-1512.

He, X., Semenov, M., Tamai, K., and Zeng, X. (2004). LDL receptor-related proteins 5 and 6 in Wnt/beta-catenin signaling: arrows point the way. Development *131*, 1663-1677.

Heard, E., and Disteche, C. M. (2006). Dosage compensation in mammals: fine-tuning the expression of the X chromosome. Genes Dev *20*, 1848-1867.

Heasman, J. (1997). Patterning the Xenopus blastula. Development *124*, 4179-4191.
Heijstek, M. W., Kranenburg, O., and Borel Rinkes, I. H. M. (2005). Mouse models of colorectal cancer and liver metastases. Dig Surg *22*, 16-25.

Helleman, J., van Staveren, I. L., Dinjens, W. N., van Kuijk, P. F., Ritstier, K., Ewing, P. C., van der Burg, M. E., Stoter, G., and Berns, E. M. (2006). Mismatch repair and treatment resistance in ovarian cancer. BMC Cancer *6*, 201.

Henderson, B. R., and Fagotto, F. (2002). The ins and outs of APC and beta-catenin nuclear transport. EMBO Rep *3*, 834-839.

Hisamuddin, I. M., and Yang, V. W. (2004). Genetics of colorectal cancer. MedGenMed *6*, 13.

Howlin, J., McBryan, J., Napoletano, S., Lambe, T., McArdle, E., Shioda, T., and Martin, F. (2006). CITED1 homozygous null mice display aberrant pubertal mammary ductal morphogenesis. Oncogene *25*, 1532-1542.

Huang, J., Papadopoulos, N., McKinley, A. J., Farrington, S. M., Curtis, L. J., Wyllie, A. H., Zheng, S., Willson, J. K., Markowitz, S. D., Morin, P., Kinzler K. W., Vogelstein B., Dunlop M. G. (1996). APC mutations in colorectal tumors with mismatch repair deficiency. Proc Natl Acad Sci U S A *93*, 9049-9054.

Hughes, T. A., and Brady, H. J. (2006). Regulation of axin2 expression at the levels of transcription, translation and protein stability in lung and colon cancer. Cancer Lett *233*, 338-347.

Huls, G., Koornstra, J. J., and Kleibeuker, J. H. (2003). Non-steroidal anti-inflammatory drugs and molecular carcinogenesis of colorectal carcinomas. Lancet *362*, 230-232.

Iacopetta, B. (2003). TP53 mutation in colorectal cancer. Hum Mutat *21*, 271-276.

Ignatenko, N. A., Holubec, H., Besselsen, D. G., Blohm-Mangone, K. A., Padilla-Torres, J. L., Nagle, R. B., de Alboranc, I. M., Guillen, R. J., and Gerner, E. W. (2006). Role of c-Myc in intestinal tumorigenesis of the ApcMin/+ mouse. Cancer Biol Ther *5*, 1658-1664.

Ireland, H., Kemp, R., Houghton, C., Howard, L., Clarke, A. R., Sansom, O. J., and Winton, D. J. (2004). Inducible Cre-mediated control of gene expression in the murine gastrointestinal tract: effect of loss of beta-catenin. Gastroenterology *126*, 1236-1246.

Jackson, A. L., Burchard, J., Leake, D., Reynolds, A., Schelter, J., Guo, J., Johnson, J. M., Lim, L., Karpilow, J., Nichols, K., Marshall W., Khvorova A., Linsley P. S. (2006). Position-specific chemical modification of siRNAs reduces "off-target" transcript silencing. RNA *12*, 1197-1205.

Jacob, S., and Praz, F. (2002). DNA mismatch repair defects: role in colorectal carcinogenesis. Biochimie *84*, 27-47.

Janssen, K. P., el-Marjou, F., Pinto, D., Sastre, X., Rouillard, D., Fouquet, C., Soussi, T., Louvard, D., and Robine, S. (2002). Targeted expression of oncogenic K-ras in intestinal epithelium causes spontaneous tumorigenesis in mice. Gastroenterology *123*, 492-504.

Jeter, J. M., Kohlmann, W., and Gruber, S. B. (2006). Genetics of colorectal cancer. Oncology (Williston Park) *20*, 269-276; discussion 285-266, 288-269.

Jho, E. H., Zhang, T., Domon, C., Joo, C. K., Freund, J. N., and Costantini, F. (2002). Wnt/beta-catenin/Tcf signaling induces the transcription of Axin2, a negative regulator of the signaling pathway. Mol Cell Biol *22*, 1172-1183.

Johnson, L., Mercer, K., Greenbaum, D., Bronson, R. T., Crowley, D., Tuveson, D. A., and Jacks, T. (2001). Somatic activation of the K-ras oncogene causes early onset lung cancer in mice. Nature *410*, 1111-1116.

Kaplan, K. B., Burds, A. A., Swedlow, J. R., Bekir, S. S., Sorger, P. K., and Nathke, I. S. (2001). A role for the Adenomatous Polyposis Coli protein in chromosome segregation. Nat Cell Biol *3*, 429-432.

Kawabata, M., Imamura, T., Inoue, H., Hanai, J., Nishihara, A., Hanyu, A., Takase, M., Ishidou, Y., Udagawa, Y., Oeda, E., Goto D., Yagi K., Kato M., Miyazono K. (1999). Intracellular signaling of the TGF-beta superfamily by Smad proteins. Ann N Y Acad Sci *886*, 73-82.

Kawasaki, Y., Senda, T., Ishidate, T., Koyama, R., Morishita, T., Iwayama, Y., Higuchi, O., and Akiyama, T. (2000). Asef, a link between the tumor suppressor APC and G-protein signaling. Science *289*, 1194-1197.

Kim, H., Yang, X. L., Rosada, C., Hamilton, S. R., and August, J. T. (1994). CD44 expression in colorectal adenomas is an early event occurring prior to K-ras and p53 gene mutation. Arch Biochem Biophys *310*, 504-507.

Kinzler, K. W., and Vogelstein, B. (1996). Lessons from hereditary colorectal cancer. Cell *87*, 159-170.

Kleine-Kohlbrecher, D., Adhikary, S., and Eilers, M. (2006). Mechanisms of transcriptional repression by Myc. Curr Top Microbiol Immunol *302*, 51-62.

Knudsen, A. L., Bisgaard, M. L., and Bulow, S. (2003). Attenuated familial adenomatous polyposis (AFAP). A review of the literature. Fam Cancer *2*, 43-55.

Knudson, A. G., Jr. (1971). Mutation and cancer: statistical study of retinoblastoma. Proc Natl Acad Sci U S A *68*, 820-823.

Ko, L. J., and Prives, C. (1996). p53: puzzle and paradigm. Genes Dev *10*, 1054-1072.

Kolligs, F. T., Bommer, G., and Goke, B. (2002). Wnt/beta-catenin/tcf signaling: a critical pathway in gastrointestinal tumorigenesis. Digestion *66*, 131-144.

Kuhn, R., and Torres, R. M. (2002). Cre/loxP recombination system and gene targeting. Methods Mol Biol *180*, 175-204.

Kumar, L. D., and Clarke, A. R. (2007). Gene manipulation through the use of small interfering RNA (siRNA): from in vitro to in vivo applications. Adv Drug Deliv Rev *59*, 87-100.

Kuncova, J., Kostrouch, Z., Viale, M., Revoltella, R., and Mandys, V. (2005). Expression of CD44v6 correlates with cell proliferation and cellular atypia in urothelial carcinoma cell lines 5637 and HT1197. Folia Biol (Praha) *51*, 3-11.

Labbe, E., Lock, L., Letamendia, A., Gorska, A. E., Gryfe, R., Gallinger, S., Moses, H. L., and Attisano, L. (2007). Transcriptional cooperation between the transforming growth factor-beta and Wnt pathways in mammary and intestinal tumorigenesis. Cancer Res *67*, 75-84.

Lamlum, H., Ilyas, M., Rowan, A., Clark, S., Johnson, V., Bell, J., Frayling, I., Efstathiou, J., Pack, K., Payne, S., Roylance R., Gorman P., Sheer D., Neale K., Phillips R., Talbot I., Bodmer W., Tomlinson I. (1999). The type of somatic mutation at APC in familial adenomatous polyposis is determined by the site of the germline mutation: a new facet to Knudson's 'two-hit' hypothesis. Nat Med *5*, 1071-1075.

Lee, Y. S., Nakahara, K., Pham, J. W., Kim, K., He, Z., Sontheimer, E. J., and Carthew, R. W. (2004). Distinct roles for Drosophila Dicer-1 and Dicer-2 in the siRNA/miRNA silencing pathways. Cell *117*, 69-81.

Leung, J. Y., Kolligs, F. T., Wu, R., Zhai, Y., Kuick, R., Hanash, S., Cho, K. R., and Fearon, E. R. (2002). Activation of AXIN2 expression by beta-catenin-T cell factor. A feedback repressor pathway regulating Wnt signaling. J Biol Chem *277*, 21657-21665.

Li, F., Cao, Y., Townsend, C. M., Jr., and Ko, T. C. (2005). TGF-beta signaling in colon cancer cells. World J Surg *29*, 306-311.

Li, H., Ahmed, N. U., Fenner, M. H., Ueda, M., Isselbacher, K. J., and Shioda, T. (1998). Regulation of expression of MSG1 melanocyte-specific nuclear protein in human melanocytes and melanoma cells. Exp Cell Res *242*, 478-486.

Lipton, L., and Tomlinson, I. (2004). The multiple colorectal adenoma phenotype and MYH, a base excision repair gene. Clin Gastroenterol Hepatol *2*, 633-638.

Lipton, L., and Tomlinson, I. (2006). The genetics of FAP and FAP-like syndromes. Fam Cancer *5*, 221-226.

Liu, J. D., Carmell, M. A., Rivas, F. V., Marsden, C. G., Thomson, J. M., Song, J. J., Hammond, S. M., Joshua-Tor, L., and Hannon, G. J. (2004). Argonaute2 is the catalytic engine of mammalian RNAi. Science *305*, 1437-1441.

Lockhart-Mummery, A. (1952). Cancer and Heredity. Lancet *1*, 427-429.

Logan, C. Y., and Nusse, R. (2004). The Wnt signaling pathway in development and disease. Annu Rev Cell Dev Biol *20*, 781-810.

Lovvorn, H. N., 3rd, Boyle, S., Shi, G., Shyr, Y., Wills, M. L., Perantoni, A. O., and de Caestecker, M. (2007a). Wilms' tumorigenesis is altered by misexpression of the transcriptional co-activator, CITED1. J Pediatr Surg *42*, 474-481.

Lovvorn, H. N., Westrup, J., Opperman, S., Boyle, S., Shi, G., Anderson, J., Perlman, E. J., Perantoni, A. O., Wills, M., and de Caestecker, M. (2007b). CITED1 expression in Wilms' tumor and embryonic kidney. Neoplasia *9*, 589-600.

Luchtenborg, M., Weijenberg, M. P., Roemen, G. M., de Bruine, A. P., van den Brandt, P. A., Lentjes, M. H., Brink, M., van Engeland, M., Goldbohm, R. A., and de Goeij, A. F. (2004). APC mutations in sporadic colorectal carcinomas from The Netherlands Cohort Study. Carcinogenesis *25*, 1219-1226.

Lustig, B., Jerchow, B., Sachs, M., Weiler, S., Pietsch, T., Karsten, U., van de Wetering, M., Clevers, H., Schlag, P. M., Birchmeier, W., and Behrens, J. (2002). Negative feedback loop of Wnt signaling through upregulation of conductin/axin2 in colorectal and liver tumors. Mol Cell Biol *22*, 1184-1193.

Lynch, H. T., and de la Chapelle, A. (1999). Genetic susceptibility to non-polyposis colorectal cancer. J Med Genet *36*, 801-818.

Lynch, H. T., and de la Chapelle, A. (2003). Hereditary colorectal cancer. N Engl J Med *348*, 919-932.

Maddison, K., and Clarke, A. R. (2005). New approaches for modelling cancer mechanisms in the mouse. J Pathol *205*, 181-193.

Maltzman, T., Whittington, J., Driggers, L., Stephens, J., and Ahnen, D. (1997). AOM-induced mouse colon tumors do not express full-length APC protein. Carcinogenesis *18*, 2435-2439.

Malumbres, M., and Barbacid, M. (2003). RAS oncogenes: the first 30 years. Nat Rev Cancer *3*, 459-465.

Mariadason, J. M., Nicholas, C., L'Italien, K. E., Zhuang, M., Smartt, H. J., Heerdt, B. G., Yang, W., Corner, G. A., Wilson, A. J., Klampfer, L., Arango D., Augenlicht L. H. (2005). Gene expression profiling of intestinal epithelial cell maturation along the crypt-villus axis. Gastroenterology *128*, 1081-1088.

Marti, T. M., Kunz, C., and Fleck, O. (2002). DNA mismatch repair and mutation avoidance pathways. J Cell Physiol *191*, 28-41.

Martin, S. E., and Caplen, N. J. (2007). Applications of RNA interference in mammalian systems. Annu Rev Genomics Hum Genet *8*, 81-108.

Massague, J., Blain, S. W., and Lo, R. S. (2000). TGFbeta signaling in growth control, cancer, and heritable disorders. Cell *103*, 295-309.

McBryan, J., Howlin, J., Kenny, P. A., Shioda, T., and Martin, F. (2007). ERalpha-CITED1 co-regulated genes expressed during pubertal mammary gland development: implications for breast cancer prognosis. Oncogene *26*, 6406-6419.

McManus, M. T., and Sharp, P. A. (2002). Gene silencing in mammals by small interfering RNAs. Nat Rev Genet *3*, 737-747.

Meister, G., Landthaler, M., Patkaniowska, A., Dorsett, Y., Teng, G., and Tuschl, T. (2004). Human Argonaute2 mediates RNA cleavage targeted by miRNAs and siRNAs. Mol Cell *15*, 185-197.

Meister, G., and Tuschl, T. (2004). Mechanisms of gene silencing by double-stranded RNA. Nature *431*, 343-349.

Michor, F. (2005). Chromosomal instability and human cancer. Philos Trans R Soc Lond B Biol Sci *360*, 631-635.

Miller, J. R., and Moon, R. T. (1996). Signal transduction through beta-catenin and specification of cell fate during embryogenesis. Genes Dev *10*, 2527-2539.

Mishra, J. P., Mishra, S., Gee, K., and Kumar, A. (2005). Differential involvement of calmodulin-dependent protein kinase II-activated AP-1 and c-Jun N-terminal kinase-activated EGR-1 signaling pathways in tumor necrosis factor-alpha and lipopolysaccharide-induced CD44 expression in human monocytic cells. J Biol Chem *280*, 26825-26837.

Miyaki, M., Tanaka, K., Kikuchi-Yanoshita, R., Muraoka, M., and Konishi, M. (1995). Familial polyposis: recent advances. Crit Rev Oncol Hematol *19*, 1-31.

Miyoshi, Y., Nagase, H., Ando, H., Horii, A., Ichii, S., Nakatsuru, S., Aoki, T., Miki, Y., Mori, T., and Nakamura, Y. (1992). Somatic mutations of the APC gene in colorectal tumors: mutation cluster region in the APC gene. Hum Mol Genet *1*, 229-233.

Montera, M., Resta, N., Simone, C., Guanti, G., Marchese, C., Civitelli, S., Mancini, A., Pozzi, S., De Salvo, L., Bruzzone, D., Donadini A., Romio L., Mareni C. (2000). Mutational germline analysis of hMSH2 and hMLH1 genes in early onset colorectal cancer patients. J Med Genet *37*, E7.

Morin, P. J. (1999). beta-catenin signaling and cancer. Bioessays *21*, 1021-1030.

Moser, A. R., Pitot, H. C., and Dove, W. F. (1990). A dominant mutation that predisposes to multiple intestinal neoplasia in the mouse. Science *247*, 322-324.

Moustakas, A., and Heldin, C. H. (2005). Non-Smad TGF-beta signals. J Cell Sci *118*, 3573-3584.

Muncan, V., Sansom, O. J., Tertoolen, L., Phesse, T. J., Begthel, H., Sancho, E., Cole, A. M., Gregorieff, A., de Alboran, I. M., Clevers, H., and Clarke, A. R. (2006). Rapid loss of intestinal crypts upon conditional deletion of the Wnt/Tcf-4 target gene c-Myc. Mol Cell Biol *26*, 8418-8426.

Munemitsu, S., Albert, I., Rubinfeld, B., and Polakis, P. (1996). Deletion of an amino-terminal sequence beta-catenin in vivo and promotes hyperphosporylation of the adenomatous polyposis coli tumor suppressor protein. Mol Cell Biol *16*, 4088-4094.

Munoz, N. M., Upton, M., Rojas, A., Washington, M. K., Lin, L., Chytil, A., Sozmen, E. G., Madison, B. B., Pozzi, A., Moon, R. T., Moses H. L., Grady W. M. (2006). Transforming growth factor beta receptor type II inactivation induces the malignant transformation of intestinal neoplasms initiated by Apc mutation. Cancer Res *66*, 9837-9844.

Muraoka-Cook, R. S., Kurokawa, H., Koh, Y., Forbes, J. T., Roebuck, L. R., Barcellos-Hoff, M. H., Moody, S. E., Chodosh, L. A., Arteaga, C. L. (2004). Conditional overexpression of active transforming growth factor beta1 in vivo accelerates metastases of transgenic mammary tumors. Cancer Res *64*, 9002-9011.

Nagase, H., Miyoshi, Y., Horii, A., Aoki, T., Ogawa, M., Utsunomiya, J., Baba, S., Sasazuki, T., and Nakamura, Y. (1992). Correlation between the location of germ-line mutations in the APC gene and the number of colorectal polyps in familial adenomatous polyposis patients. Cancer Res *52*, 4055-4057.

Nagase, H., and Nakamura, Y. (1993). Mutations of the APC (adenomatous polyposis coli) gene. Hum Mutat *2*, 425-434.

Nair, S. S., Chaubal, V. A., Shioda, T., Coser, K. R., and Mojamdar, M. (2001). Over-expression of MSG1 transcriptional co-activator increases melanin in B16 melanoma cells: a possible role for MSG1 in melanogenesis. Pigment Cell Res *14*, 206-209.

Nakamura, Y. (1993). The role of the adenomatous polyposis coli (APC) gene in human cancers. Adv Cancer Res *62*, 65-87.

Nakayashiki, H., Kadotani, N., and Mayama, S. (2006). Evolution and diversification of RNA silencing proteins in fungi. J Mol Evol *63*, 127-135.

Napoli, C., Lemieux, C., and Jorgensen, R. (1990). Introduction of a Chimeric Chalcone Synthase Gene into Petunia Results in Reversible Co-Suppression of Homologous Genes in trans. Plant Cell *2*, 279-289.

Narayan, S., and Roy, D. (2003). Role of APC and DNA mismatch repair genes in the development of colorectal cancers. Mol Cancer *2*, 41.

Nathke, I. (2004). APC at a glance. J Cell Sci *117*, 4873-4875.

Nelson, W. J., and Nusse, R. (2004). Convergence of Wnt, beta-catenin, and cadherin pathways. Science *303*, 1483-1487.

Nowak, M. A., Komarova, N. L., Sengupta, A., Jallepalli, P. V., Shih Ie, M., Vogelstein, B., and Lengauer, C. (2002). The role of chromosomal instability in tumor initiation. Proc Natl Acad Sci U S A *99*, 16226-16231.

Nugent, K. P., Phillips, R. K., Hodgson, S. V., Cottrell, S., Smith-Ravin, J., Pack, K., and Bodmer, W. F. (1994). Phenotypic expression in familial adenomatous polyposis: partial prediction by mutation analysis. Gut *35*, 1622-1623.

Oft, M., Heider, K. H., and Beug, H. (1998). TGFbeta signaling is necessary for carcinoma cell invasiveness and metastasis. Curr Biol *8*, 1243-1252.

Okada, F., Rak, J. W., Croix, B. S., Lieubeau, B., Kaya, M., Roncari, L., Shirasawa, S., Sasazuki, T., and Kerbel, R. S. (1998). Impact of oncogenes in tumor angiogenesis: mutant K-ras up-regulation of vascular endothelial growth factor/vascular permeability factor is necessary, but not sufficient for tumorigenicity of human colorectal carcinoma cells. Proc Natl Acad Sci U S A *95*, 3609-3614.

Oliveira, S., van Rooy, I., Kranenburg, O., Storm, G., and Schiffelers, R. M. (2007). Fusogenic peptides enhance endosomal escape improving siRNA-induced silencing of oncogenes. Int J Pharm *331*, 211-214.

Oshima, H., Oshima, M., Kobayashi, M., Tsutsumi, M., and Taketo, M. M. (1997). Morphological and molecular processes of polyp formation in Apc(delta716) knockout mice. Cancer Res *57*, 1644-1649.

Oudejans, J. J., Slebos, R. J., Zoetmulder, F. A., J.Mooi, W., and S.Rodenhuis (1999). Differential activation of ras genes by point mutation in human colon cancer with metastases to either lung or liver. Int J Cancer *49*, 875-879.

Palombo, F., Iaccarino, I., Nakajima, E., Ikejima, M., Shimada, T., and Jiricny, J. (1996). hMutSbeta, a heterodimer of hMSH2 and hMSH3, binds to insertion/deletion loops in DNA. Curr Biol *6*, 1181-1184.

Pardali, K., and Moustakas, A. (2007). Actions of TGF-beta as tumor suppressor and pro-metastatic factor in human cancer. Biochim Biophys Acta *1775*, 21-62.

Parkin, D. M., Pisani, P., and Ferlay, J. (1999). Global cancer statistics. CA Cancer J Clin *49*, 33-64, 31.

Patek, C. E., Arends, M. J., Rose, L., Luo, F., Walker, M., Devenney, P. S., Berry, R. L., Lawrence, N. J., Ridgway, R. A., Sansom, O. J., and Hooper, M. L. (2008). The pro-apoptotic K-Ras 4A proto-oncoprotein does not affect tumorigenesis in the ApcMin/+ mouse small intestine. BMC Gastroenterol *8*, 24.

Patra, S. K. (2008). Ras regulation of DNA-methylation and cancer. Exp Cell Res *314*, 1193-1201.

Peltomaki, P. (1997). DNA mismatch repair gene mutations in human cancer. Environ Health Perspect *105 Suppl 4*, 775-780.

Peltomaki, P. (2001a). Deficient DNA mismatch repair: a common etiologic factor for colon cancer. Hum Mol Genet *10*, 735-740.

Peltomaki, P. (2001b). DNA mismatch repair and cancer. Mutat Res *488*, 77-85.

Pinto, D., and Clevers, H. (2005a). Wnt control of stem cells and differentiation in the intestinal epithelium. Exp Cell Res *306*, 357-363.

Pinto, D., and Clevers, H. (2005b). Wnt, stem cells and cancer in the intestine. Biol Cell *97*, 185-196.

Pinto, D., Gregorieff, A., Begthel, H., and Clevers, H. (2003). Canonical Wnt signals are essential for homeostasis of the intestinal epithelium. Gene Dev *17*, 1709-1713.

Plisov, S., Tsang, M., Shi, G., Boyle, S., Yoshino, K., Dunwoodie, S. L., Dawid, I. B., Shioda, T., Perantoni, A. O., and de Caestecker, M. P. (2005). Cited1 is a bifunctional transcriptional cofactor that regulates early nephronic patterning. J Am Soc Nephrol *16*, 1632-1644.

Powell, S. M., Petersen, G. M., Krush, A. J., Booker, S., Jen, J., Giardiello, F. M., Hamilton, S. R., Vogelstein, B., and Kinzler, K. W. (1993). Molecular diagnosis of familial adenomatous polyposis. N Engl J Med *329*, 1982-1987.

Prasad, M. L., Pellegata, N. S., Kloos, R. T., Barbacioru, C., Huang, Y., and de la Chapelle, A. (2004). CITED1 protein expression suggests Papillary Thyroid Carcinoma in high throughput tissue microarray-based study. Thyroid *14*, 169-175.

Prives, C. (1998). Signaling to p53: breaking the MDM2-p53 circuit. Cell *95*, 5-8.

Prolla, T. A., Abuin, A., and Bradley, A. (1996). DNA mismatch repair deficient mice in cancer research. Semin Cancer Biol *7*, 241-247.

Reed, K. R., Meniel, V. S., Marsh, V., Cole, A., Sansom, O. J., Clarke, A. R., (2008). A limited role for p53 in modulating the immediate phenotype of Apc loss in the intestine. BMC Cancer *8*, 162.

Reya, T., and Clevers, H. (2005). Wnt signalling in stem cells and cancer. Nature *434*, 843-850.

Rijsewijk, F., Schuermann, M., Wagenaar, E., Parren, P., Weigel, D., and Nusse, R. (1987). The Drosophila homolog of the mouse mammary oncogene int-1 is identical to the segment polarity gene wingless. Cell *50*, 649-657.

Rodriguez, T. A., Sparrow, D. B., Scott, A. N., Withington, S. L., Preis, J. I., Michalicek, J., Clements, M., Tsang, T. E., Shioda, T., Beddington, R. S., and Dunwoodie, S. L. (2004). Cited1 is required in trophoblasts for placental development and for embryo growth and survival. Mol Cell Biol *24*, 228-244.

Ross, J. S., and Fletcher, J. A. (1999). HER-2/neu (c-erb-B2) gene and protein in breast cancer. Am J Clin Pathol *112*, S53-67.

Ross, J. S., Slodkowska, E. A., Symmans, W. F., Pusztai, L., Ravdin, P. M., and Hortobagyi, G. N. (2009). The HER-2 receptor and breast cancer: ten years of targeted anti-HER-2 therapy and personalized medicine. Oncologist *14*, 320-368.

Rowan, A. J., Lamlum, H., Ilyas, M., Wheeler, J., Straub, J., Papadopoulou, A., Bicknell, D., Bodmer, W. F., and Tomlinson, I. P. (2000). APC mutations in sporadic colorectal tumors: A mutational "hotspot" and interdependence of the "two hits". Proc Natl Acad Sci U S A *97*, 3352-3357.

Rubinfeld, B., Albert, I., Porfiri, E., Fiol, C., Munemitsu, S., and Polakis, P. (1996). Binding of GSK3beta to the APC-beta-catenin complex and regulation of complex assembly. Science *272*, 1023-1026.

Salahshor, S., and Woodgett, J. R. (2005). The links between axin and carcinogenesis.[erratum appears in J Clin Pathol. 2005 Dec;58(12):1344]. J Clin Pathol *58*, 225-236.

Saletti, P., Edwin, I. D., Pack, K., Cavalli, F., and Atkin, W. S. (2001). Microsatellite instability: application in hereditary non-polyposis colorectal cancer. Ann Oncol *12*, 151-160.

Sancho, E., Batlle, E., and Clevers, H. (2004). Signaling pathways in intestinal development and cancer. Annu Rev Cell Dev Biol *20*, 695-723.

Sansom, O. J., Meniel, V., Wilkins, J. A., Cole, A. M., Oien, K. A., Marsh, V., Jamieson, T. J., Guerra, C., Ashton, G. H., Barbacid, M., *et al.* (2006). Loss of Apc allows phenotypic manifestation of the transforming properties of an endogenous K-ras oncogene in vivo. Proc Natl Acad Sci U S A *103*, 14122-14127.

Sansom, O. J., Meniel, V. S., Muncan, V., Phesse, T. J., Wilkins, J. A., Reed, K. R., Vass, J. K., Athineos, D., Clevers, H., Clarke, A. R. (2007). Myc deletion rescues Apc deficiency in the small intestine. Nature *446*, 676-679.

Sansom, O. J., Reed, K. R., Hayes, A. J., Ireland, H., Brinkmann, H., Newton, I. P., Batlle, E., Simon-Assmann, P., Clevers, H., Nathke, I. S., *et al.* (2004). Loss of Apc in vivo immediately perturbs Wnt signaling, differentiation, and migration. Genes Dev *18*, 1385-1390.

Sansom, O. J., Reed, K. R., van de Wetering, M., Muncan, V., Winton, D. J., Clevers, H., Clarke, A. R., Sansom, O. J., Reed, K. R., van de Wetering, M., *et al.* (2005). Cyclin D1 is not an immediate target of beta-catenin following Apc loss in the intestine. J Biol Chem *280*, 28463-28467.

Scognamiglio, T., Hyjek, E., Kao, J., and Chen, Y. T. (2006). Diagnostic usefulness of HBME1, galectin-3, CK19, and CITED1 and evaluation of their expression in encapsulated lesions with questionable features of papillary thyroid carcinoma. Am J Clin Pathol *126*, 700-708.

Shi, G., Boyle, S. C., Sparrow, D. B., Dunwoodie, S. L., Shioda, T., and de Caestecker, M. P. (2006). The transcriptional activity of CITED1 is regulated by phosphorylation in a cell cycle-dependent manner. J Biol Chem *281*, 27426-27435.

Shibata, H., Toyama, K., Shioya, H., Ito, M., Hirota, M., Hasegawa, S., Matsumoto, H., Takano, H., Akiyama, T., Toyoshima, K., Kanamaru R., Kanegae Y., Saito I., Nakamura Y., Shiba K., and Noda T. (1997). Rapid colorectal adenoma formation initiated by conditional targeting of the Apc gene. Science *278*, 120-123.

Shioda, T., Fenner, M. H., and Isselbacher, K. J. (1996). msg1, a novel melanocyte-specific gene, encodes a nuclear protein and is associated with pigmentation. Proc Natl Acad Sci U S A *93*, 12298-12303.

Shioda, T., Fenner, M. H., and Isselbacher, K. J. (1997). MSG1 and its related protein MRG1 share a transcription activating domain. Gene *204*, 235-241.

Shtutman, M., Zhurinsky, J., Simcha, I., Albanese, C., D'Amico, M., Pestell, R., and Ben-Ze'ev, A. (1999). The cyclin D1 gene is a target of the beta-catenin/LEF-1 pathway. Proc Natl Acad Sci U S A *96*, 5522-5527.

Sieber, O. M., Lipton, L., Crabtree, M., Heinimann, K., Fidalgo, P., Phillips, R. K., Bisgaard, M. L., Orntoft, T. F., Aaltonen, L. A., Hodgson, S. V., Thomas H. J., Tomlinson I. P. (2003). Multiple colorectal adenomas, classic adenomatous polyposis, and germ-line mutations in MYH. N Engl J Med *348*, 791-799.

Sieber, O. M., Segditsas, S., Knudsen, A. L., Zhang, J., Luz, J., Rowan, A. J., Spain, S. L., Thirlwell, C., Howarth, K. M., Jaeger, E. E., Robinson J., Volikos E., Silver A., Kelly G., Aretz S., Frayling I., Hutter P., Dunlop M., Guenther T., Neale K., Phillips R., Heinimann K., Tomlinson I. P. (2006). Disease severity and genetic pathways in attenuated familial adenomatous polyposis vary greatly but depend on the site of the germline mutation. Gut *55*, 1440-1448.

Siegel, P. M., Massague, J., Siegel, P. M., and Massague, J. (2003a). Cytostatic and apoptotic actions of TGF-beta in homeostasis and cancer. Nature Reviews Cancer *3*, 807-821.

Siegel, P. M., Shu, W., and Massague, J. (2003b). Mad upregulation and Id2 repression accompany transforming growth factor (TGF)-beta-mediated epithelial cell growth suppression. J Biol Chem *278*, 35444-35450.

Smakman, N., Borel Rinkes, I. H., Voest, E. E., and Kranenburg, O. (2005). Control of colorectal metastasis formation by K-Ras. Biochim Biophys Acta *1756*, 103-114.

Smalley, M. J., Sara, E., Paterson, H., Naylor, S., Cook, D., Jayatilake, H., Fryer, L. G., Hutchinson, L., Fry, M. J., and Dale, T. C. (1999). Interaction of axin and Dvl-2 proteins regulates Dvl-2-stimulated TCF-dependent transcription. EMBO J *18*, 2823-2835.

Smith, D. R., Myint, T., and Goh, H. S. (1993). Over-expression of the c-myc proto-oncogene in colorectal carcinoma. Br J Cancer *68*, 407-413.

Smits, R., Kielman, M. F., Breukel, C., Zurcher, C., Neufeld, K., Jagmohan-Changur, S., Hofland, N., van Dijk, J., White, R., Edelmann, W., Kucherlapati R., Khan P. M., and Fodde R. (1999). Apc1638T: a mouse model delineating critical domains of the adenomatous polyposis coli protein involved in tumorigenesis and development. Genes Dev *13*, 1309-1321.

Sodir, N. M., Chen, X., Park, R., Nickel, A. E., Conti, P. S., Moats, R., Bading, J. R., Shibata, D., and Laird, P. W. (2006). Smad3 deficiency promotes tumorigenesis in the distal colon of ApcMin/+ mice. Cancer Res *66*, 8430-8438.

Sokal, R. R., and Rohl, F.J. (1981). Thhe principles and practice in biological research. Second edition; W.H. Freeman and Company, San Francisco

Soreide, K., Janssen, E. A., Soiland, H., Korner, H., and Baak, J. P. (2006). Microsatellite instability in colorectal cancer. Br J Surg *93*, 395-406.

Sparks, A. B., Morin, P. J., Vogelstein, B., and Kinzler, K. W. (1998). Mutational analysis of the APC/beta-catenin/Tcf pathway in colorectal cancer. Cancer Res *58*, 1130-1134.

Strate, L. L., and Syngal, S. (2005). Hereditary colorectal cancer syndromes. Cancer Causes Control *16*, 201-213.

Su, L. K., Kinzler, K. W., Vogelstein, B., Preisinger, A. C., Moser, A. R., Luongo, C., Gould, K. A., and Dove, W. F. (1992). Multiple intestinal neoplasia caused by a mutation in the murine homolog of the APC gene. Science *256*, 668-670.

Su, L. K., Vogelstein, B., and Kinzler, K. W. (1993). Association of the APC tumor suppressor protein with catenins. Science *262*, 1734-1737.

Takahashi, M., Nakatsugi, S., Sugimura, T., and Wakabayashi, K. (2000). Frequent mutations of the beta-catenin gene in mouse colon tumors induced by azoxymethane. Carcinogenesis *21*, 1117-1120.

Takahashi, M., and Wakabayashi, K. (2004). Gene mutations and altered gene expression in azoxymethane-induced colon carcinogenesis in rodents. Cancer Sci *95*, 475-480.

Takaku, K., Oshima, M., Miyoshi, H., Matsui, M., Seldin, M. F., and Taketo, M. M. (1998). Intestinal tumorigenesis in compound mutant mice of both Dpc4 (Smad4) and Apc genes.[see comment]. Cell *92*, 645-656.

Takayama, T., Miyanishi, K., Hayashi, T., Sato, Y., and Niitsu, Y. (2006). Colorectal cancer: genetics of development and metastasis. J Gastroenterol *41*, 185-192.
Taketo, M. M. (2006a). Mouse models of gastrointestinal tumors. Cancer Sci *97*, 355-361.

Taketo, M. M. (2006b). Wnt signaling and gastrointestinal tumorigenesis in mouse models. Oncogene *25*, 7522-7530.

Taketo, M. M., and Edelmann, W. (2009). Mouse models of colon cancer. Gastroenterology *136*, 780-798.

Tetsu, O., and McCormick, F. (1999). Beta-catenin regulates expression of cyclin D1 in colon carcinoma cells. Nature *398*, 422-426.

Thibodeau, S. N., Bren, G., and Schaid, D. (1993). Microsatellite instability in cancer of the proximal colon. Science *260*, 816-819.

Thliveris, A., Albertsen, H., Tuohy, T., Carlson, M., Groden, J., Joslyn, G., Gelbert, L., Samowitz, W., Spirio, L., and White, R. (1996). Long-range physical map and deletion characterization of the 1100-kb NotI restriction fragment harboring the APC gene. Genomics *34*, 268-270.

Thomas, D. A., Massague, J., Thomas, D. A., and Massague, J. (2005). TGF-beta directly targets cytotoxic T cell functions during tumor evasion of immune surveillance.[see comment]. Cancer Cell *8*, 369-380.

Toyooka, S., Tsukuda, K., Ouchida, M., Tanino, M., Inaki, Y., Kobayashi, K., Yano, M., Soh, J., Kobatake, T., Shimizu, N., and Shimizu, K. (2003). Detection of codon 61 point mutations of the K-ras gene in lung and colorectal cancers by enriched PCR. Oncol Rep *10*, 1455-1459.

Turcot, J., Despres, J. P., and St Pierre, F. (1959). Malignant tumors of the central nervous system associated with familial polyposis of the colon: report of two cases. Dis Colon Rectum *2*, 465-468.

Tuschl, T. (2001). RNA interference and small interfering RNAs. Chembiochem *2*, 239-245.

Tuveson, D. A., Shaw, A. T., Willis, N. A., Silver, D. P., Jackson, E. L., Chang, S., Mercer, K. L., Grochow, R., Hock, H., Crowley, D., Hingorani S. R., Zaks T., King C., Jacobetz M. A., Wang L., Bronson R. T., Orkin S. H., DePinho R. A. and Jacks T. (2004). Endogenous oncogenic K-ras(G12D) stimulates proliferation and widespread neoplastic and developmental defects. Cancer Cell *5*, 375-387.

Utomo, A. R., Nikitin, A. Y., and Lee, W. H. (1999). Temporal, spatial, and cell type-specific control of Cre-mediated DNA recombination in transgenic mice. Nat Biotechnol *17*, 1091-1096.

Varesco, L. (2004). Familial adenomatous polyposis: genetics and epidemiology. Tech Coloproctol *8 Suppl 2*, s305-308.

Vaucheret, H. (2006). Post-transcriptional small RNA pathways in plants: mechanisms and regulations. Genes Dev *20*, 759-771.

Vivona, A. A., Shpitz, B., Medline, A., Bruce, W. R., Hay, K., Ward, M. A., Stern, H. S., and Gallinger, S. (1993). K-ras mutations in aberrant crypt foci, adenomas and adenocarcinomas during azoxymethane-induced colon carcinogenesis. Carcinogenesis *14*, 1777-1781.

Wakita, K., Tetsu, O., and McCormick, F. (2001). A mammalian two-hybrid system for adenomatous polyposis coli-mutated colon cancer therapeutics. Cancer Res *61*, 854-858.

Watson, A. J. (2006). An overview of apoptosis and the prevention of colorectal cancer. Crit Rev Oncol Hematol *57*, 107-121.

Wehrli, M., Dougan, S. T., Caldwell, K., O'Keefe, L., Schwartz, S., Vaizel-Ohayon, D., Schejter, E., Tomlinson, A., and DiNardo, S. (2000). arrow encodes an LDL-receptor-related protein essential for Wingless signalling. Nature *407*, 527-530.

Weitz, J., Koch, M., Debus, J., Hohler, T., Galle, P. R., and Buchler, M. W. (2005). Colorectal cancer. Lancet *365*, 153-165.

Wielenga, V. J., Heider, K. H., Offerhaus, G. J., Adolf, G. R., van den Berg, F. M., Ponta, H., Herrlich, P., and Pals, S. T. (1993). Expression of CD44 variant proteins in human colorectal cancer is related to tumor progression. Cancer Res *53*, 4754-4756.

Wielenga, V. J., Smits, R., Korinek, V., Smit, L., Kielman, M., Fodde, R., Clevers, H., and Pals, S. T. (1999). Expression of CD44 in Apc and Tcf mutant mice implies regulation by the WNT pathway. Am J Pathol *154*, 515-523.

Wiley, S. R., and Winkles, J. A. (2003). TWEAK, a member of the TNF superfamily, is a multifunctional cytokine that binds the TweakR/Fn14 receptor. Cytokine Growth Factor Rev *14*, 241-249.

Wilkins, J. A., and Sansom, O. J. (2008). C-Myc is a critical mediator of the phenotypes of Apc loss in the intestine. Cancer Res *68*, 4963-4966.

Winkles, J. A., Tran, N. L., and Berens, M. E. (2006). TWEAK and Fn14: new molecular targets for cancer therapy? Cancer Lett *235*, 11-17.

Winkles, J. A., Tran, N. L., Brown, S. A., Stains, N., Cunliffe, H. E., and Berens, M. E. (2007). Role of TWEAK and Fn14 in tumor biology. Front Biosci *12*, 2761-2771.

Wu, W., Hodges, E., Redelius, J., and Hoog, C. (2004). A novel approach for evaluating the efficiency of siRNAs on protein levels in cultured cells. Nucleic Acids Res *32*, e17.

Xu, L., Wallen, R., Patel, V., and DePinho, R. A. (1993). Role of first exon/intron sequences in the regulation of myc family oncogenic potency. Oncogene *8*, 2547-2553.

Xu, Y., and Pasche, B. (2007). TGF-beta signaling alterations and susceptibility to colorectal cancer. Hum Mol Genet *16 Spec No 1*, R14-20.

Yahata, T., de Caestecker, M. P., Lechleider, R. J., Andriole, S., Roberts, A. B., Isselbacher, K. J., and Shioda, T. (2000). The MSG1 non-DNA-binding transactivator binds to the p300/CBP coactivators, enhancing their functional link to the Smad transcription factors. J Biol Chem *275*, 8825-8834.

Yamada, Y., Itano, N., Narimatsu, H., Kudo, T., Hirohashi, S., Ochiai, A., Tohnai, I., Ueda, M., and Kimata, K. (2003). CD44 variant exon 6 expressions in colon cancer assessed by quantitative analysis using real time reverse transcriptase-polymerase chain reaction. Oncol Rep *10*, 1919-1924.

Yamada, Y., Yoshimi, N., Hirose, Y., Matsunaga, K., Katayama, M., Sakata, K., Shimizu, M., Kuno, T., and Mori, H. (2001). Sequential analysis of morphological and biological properties of beta-catenin-accumulated crypts, provable premalignant lesions independent of aberrant crypt foci in rat colon carcinogenesis. Cancer Res *61*, 1874-1878.

Yamaguchi, S., Shinmura, K., Saitoh, T., Takenoshita, S., Kuwano, H., and Yokota, J. (2002). A single nucleotide polymorphism at the splice donor site of the human MYH base excision repair genes results in reduced translation efficiency of its transcripts. Genes Cells *7*, 461-474.

Yan, D., Wiesmann, M., Rohan, M., Chan, V., Jefferson, A. B., Guo, L., Sakamoto, D., Caothien, R. H., Fuller, J. H., Reinhard, C., Garcia P. D., Randazzo F. M., Escobedo J., Fantl W. J., Williams L. T. (2001). Elevated expression of axin2 and hnkd mRNA provides evidence that Wnt/beta -catenin signaling is activated in human colon tumors. Proc Natl Acad Sci U S A *98*, 14973-14978.

Yasuda, M., Nakano, K., Yasumoto, K., and Tanaka, Y. (2002). CD44: functional relevance to inflammation and malignancy. Histol Histopathol *17*, 945-950.
Yokoya, F., Imamoto, N., Tachibana, T., and Yoneda, Y. (1999). beta-catenin can be transported into the nucleus in a Ran-unassisted manner. Mol Biol Cell *10*, 1119-1131.

Yost, C., Torres, M., Miller, J. R., Huang, E., Kimelman, D., and Moon, R. T. (1996). The axis-inducing activity, stability, and subcellular distribution of beta-catenin is regulated in Xenopus embryos by glycogen synthase kinase 3. Genes Dev *10*, 1443-1454.

Zaidi, N. H., Pretlow, T. P., O'Riordan, M. A., Dumenco, L. L., Allay, E., and Gerson, S. L. (1995). Transgenic expression of human MGMT protects against azoxymethane-induced aberrant crypt foci and G to A mutations in the K-ras oncogene of mouse colon. Carcinogenesis *16*, 451-456.

Zamore, P. D. (2001). RNA interference: listening to the sound of silence. Nat Struct Biol *8*, 746-750.

Zeilstra, J., Joosten, S. P., Dokter, M., Verwiel, E., Spaargaren, M., and Pals, S. T. (2008). Deletion of the WNT target and cancer stem cell marker CD44 in Apc(Min/+) mice attenuates intestinal tumorigenesis. Cancer Res *68*, 3655-3661.

Zuzarte-Luis, V., and Hurle, J. M. (2002). Programmed cell death in the developing limb. Int J Dev Biol *46*, 871-876.

Chapter 9 Published Abstracts

F. Song, J. R. Jenkins, A. L. Jorgensen, A. R. Clarke, A. J. M. Watson (2007) Colorectal cancer: mapping expression studies from murine models onto human disease. Gut; 56: Suppl II, A54

F. Song, O. J. Sansom, J. R. Jenkins, A. L. Jorgensen, A. R. Clarke, A. J. M. Watson (2007) Colorectal cancer: mapping expression studies from murine models onto human disease. Gastroenterology; 132: Suppl 2, T2183

F. Song, T. J. Phesse, J. R. Jenkins, A. R. Clarke, A. J. M. Watson (2009) Cited 1 is a novel colorectal cancer gene whose deficiency inhibits the growth of colorectal cancer. Gut; 58, Suppl 1, A3

F. Song, T. J. Phesse, A. R. Clarke, A. J. M. Watson. (2009) Cited 1 Knockout Mice Have Reduced Growth of Intestinal Tumours. Gastroenterology; 136, Suppl1, A6